Plant & Food RESEARCH
RANGAHAU AHUMĀRA KAI

PFR SPTS No. 11980

Novel poplars and willow adapted to climate change – Final Report

McIvor I, Jones T

August 2015

Confidential report for:

Ministry for Primary Industries
PFR30815

PUBLICATION DATA

McIvor I, Jones T. April 2015. Final Report. A Plant & Food Research report prepared for: Ministry for Primary Industries. Milestone No. 52227. Contract No. 29108. Job code: P/442050/01. SPTS No. 11980.

Report approved by:

Ian McIvor
Scientist, Production Footprints
August 2015

Brent Clothier
Science Group Leader, Sustainable Production – Production Footprints & Biometrics
August 2015

CONTENTS

SLMACC CONTRACT PFR30815

PROJECT: Novel poplars and willow adapted to climate change

Final Report

McIvor I, Jones T
Plant & Food Research, Palmerston North

August 2015

Milestones

	Milestone title	Description	Date delivered	$ to be invoiced (excl. GST)
1	Year 1 Controlled environment (CE) trials planned	Report on framework of final report including detailed methodology within one month of signing. Research team has met and planned controlled environment trials. Environmental conditions required have been identified.	20 Dec 2012	$50,000
2	Modelling and rust monitoring.	Modelling and rust monitoring protocols determined.	28 Feb 2013	$50,000
3	Controlled environment trials concluded Field trials planned	Preliminary conclusions of CE trials reported. First year progress report and initiation of modelling. Research team has met and planned field trials. Annual progress report provided.	20 June 2013	$50,000
4	Year 2 progress report	Review of previous year field, controlled environment activities Research team has met and planned willow water stress experiment	30 Sep 2013	$37,500
5	Water stress	Willow water stress progress report. Rust monitoring protocols established and a monitoring plan decided. Field trial sites have been identified.	20 Dec 2013	$37,500
6	Rust monitoring progress report	Progress and notable issues arising. Draft recommendations to NZPWRT for adoption.	30 April 2014	$37,500
7	Year 2 report	Update on field trials, modelling and drought tolerant poplars from IPC network Draft report on willow water stress trial Annual progress report provided.	20 June 2014	$37,500
8	Year 3 Progress report	Update on field trials and rust monitoring. Research team has met and planned poplar water stress experiment.	30 Sep 2014	$37,500
9	Interim draft reporting	Poplar water stress progress report. Finalising observations and trial analyses towards generating the final report.	20 Dec 2014	$37,500

	Milestone title	Description	Date delivered	$ to be invoiced (excl. GST)
10	Draft reporting generated for feedback	Draft report and guidelines to MPI and NZPWRT for feedback and generation of communications to stakeholders planned. Independently peer reviewed.	30 April 2015	$37,500
11	Final report.	Final report to MPI and NZPWRT. Popular Information sheet on results.	14 August 2015	$37,500
Total				$450,000

The report is a collation of several different sub-reports, each sub-report containing its own independent figures, tables and references. These sub-reports are:

- Effect of elevated temperature and carbon dioxide concentration on growth of selected poplar and willow clones
- Drought tolerance of five hybrid poplar clones to different watering regimes
- Establishing long-term national field trials to evaluate the adaptive capability of novel poplar and willow clones
- Identification of *Melampsora* spp. present on *Populus* spp. in New Zealand – a survey carried out at national monitoring sites in 2014
- Drought tolerance of five hybrid willow clones to different watering regimes
- Modelling survival, growth and disease risk of poplars under current and future climate
- Communications to stakeholders.

For further information please contact:

Ian McIvor
Plant & Food Research Palmerston North
Private Bag 11600
Palmerston North 4442
NEW ZEALAND
Tel: +64 6 953 7700
DDI: +64 6 953 7673
Fax: +64 6 351 7050
Email: ian.mcivor@plantandfood.co.nz

1 EFFECT OF ELEVATED TEMPERATURE AND CARBON DIOXIDE CONCENTRATION ON GROWTH OF SELECTED POPLAR AND WILLOW CLONES

Ian McIvor and Jonathan Crawford, Plant & Food Research.

1.1 Introduction

Poplars and willows are expected to continue to be the key tree species used to stabilise soil on pastoral hill country in New Zealand. Pastoral hill country is extensive across most regions of New Zealand, and particularly across regions of the North Island of New Zealand. Pastoral hill country erosion is more severe in the North Island, which tends to experience more intense rain storms. Hence the extensive planting of poplars and willows for hill slope stabilisation is more typical in the North Island than in the South Island.

Future climate scenarios for New Zealand (http://www.niwa.co.nz/our-science/climate/information-and-resources/clivar/scenarios) depict a climate with elevated temperature (~2.5°C annual mean increase by 2090) and atmospheric CO_2 (550 ppm). In summer and autumn, the North Island and northwest of the South Island are predicted to show the greatest warming, whereas in winter the South Island will have the greatest warming. These scenarios further predict that eastern parts of New Zealand already prone to summer drought will experience more frequent and more intense droughts.

Drought stress affects water retention in plants at the cellular, tissue and organ levels, causing both specific and unspecific reactions as well as potentially damaging tissues and inducing adaptive responses (Beck et al. 2007). Plants cope with droughts by activating defence mechanisms against water deficits, including stomatal closure (which reduces the rate of transpiration and photosynthesis); the synthesis of new proteins; and the accumulation of osmolytes (Cvikrova et al. 2013, Bray 1990). Plants interactions with the environment are mediated, at least in part, by phytohormones, of which the most important in dehydration responses is abscissic acid (ABA), a hormone responsible for leaf fall.

Poplars and willows utilise this unseasonal leaf drop as part of their coping mechanisms against drought. For this reason managing these trees by pollarding both reduces their water requirement during drought and maintains a stock fodder source becomes imperative. This may become an important management tool for assisting tree survival during severe droughts particularly droughts occurring in successive years or droughts following a warmer winter with lower than normal rainfall.

An experiment was carried out in a controlled environment to evaluate the growth response of selected willow and poplar clones to future climate change (elevated CO_2 and temperature). Since these environmental changes are predicted to rise together and are recognised as being interdependent, the experiment did not separate the effect of temperature from the effect of CO_2.

1.2 Methods

An experiment was carried out at the Controlled Environment facility at The New Zealand Institute for Plant & Food Research Limited, Palmerston North, to evaluate the response of *Populus* and *Salix* species to predicted climate change induced conditions of enhanced carbon dioxide and temperature. Two commercial poplar clones, 'Fraser' (*P. deltoides* × *nigra*) and 'Geyles' (*P. maximowiczii* × *nigra*) were used as representative of *Populus* clones, and two willow clones 'Hiwinui' (*S. matsudana* × *alba*) and ML1 (*S. matsudana* × *lasiandra*) were used as representative of *Salix* clones. 'Hiwinui' is a commercial clone and ML1 is being trialled for release as a commercial clone.

The controlled environment conditions are detailed in Table 1. The separate effects of enhanced temperature and enhanced CO_2 concentration were not able to be evaluated because of the additional costs involved. Instead, the approach was taken to separate the effects of each variable from published data.

Table 1. Controlled environment conditions.

	CO_2 ppm	Temp. °C	Humidity (±5%RH)	PPFD µmol $m^{-2}s^{-1}$	Daylength hr	Irrigation and nutrient regime	
						Normal	Drought
Normal	370	23/14	70/72	700	11	90%	30%
Enhanced	550	25.5/16.5	70/72	700	11	90%	30%

The trees were grown from 1-year-old cuttings 25 cm in length planted in 20-L bags, into a mix of peat (35%), sand (30%) and bark fines (35%), to which 3 month and 9 month slow release fertiliser was added. The bagged cuttings were sprouted in ambient conditions before moving them in to the controlled environment rooms.

The drought regime was introduced after 8 weeks of growth in the climate rooms. Plants were randomly selected for drought treatment. The treatment method was by reduction of irrigation delivery by removal of irrigation drippers. When plants were selected for drought, three drippers were removed from the planter bag. This allowed water delivery to one dripper only, i.e. one dripper instead of four to the plant. Three plants from each respective clone in both climates were selected for drought treatment.

Immediately prior to the imposition of drought conditions a measurement of production in each environment was obtained for both species. For the willows half the stems with their leaves were removed, and the measurements in Table 2 were taken. This amount of material removal was necessary because the willow stem growth was much faster than the poplar growth and some control was needed to retain light penetration and prevent leaf termination on some shoots. As far as possible, care was taken to match the cross-sectional areas at the collar of stems removed with the stems retained. For the poplars, half the foliage only was removed since the poplars had only one dominant stem. Leaf area and leaf dry mass (DM) were measured for each sample. The height and collar diameter were recorded for the tallest stem retained for each tree. The leaf area remaining was assumed to be equal to the leaf area removed. Likewise, for the willows, the stem mass retained was assumed to equal the stem mass removed.

Measures were analysed with analysis of variance (Genstat 16, VSNi Ltd, UK, 2013), fitting a model which tested for differences between species, CO_2 and temperature status ('status') and water availability ('treatment') and their interactions, and then within each species tested differences between the clones, overall and in how they reacted to the CO_2/temperature status and water availability. For all measures residuals were inspected to ensure the assumptions of ANOVA were met, and where necessary data were log- transformed to stabilise variability.

Since the CO_2/temperature status was not replicated (one climate room with standard temperature and CO_2, one with higher $CO_2$and temperature), it is possible that effects of 'status' actually reflect other differences between the rooms.

1.3 Results

The various treatments have been given codes (Table 2) to ease reporting.

Table 2. Codes for Treatments as used in the report.

Climate	Water treatment	Code
Normal	normal	NN
Enhanced	normal	EN
Normal	drought	ND
Enhanced	drought	ED

The data are considered as (1) growth response in the normal and enhanced climate, (2) growth response to the imposition of drought, (3) growth response during the complete growing season (non-drought and drought phases).

(1) Shoot growth response to the enhanced climate

Willows had significantly more leaf mass than poplars ($P < 0.001$), and the willows in the enhanced climate had more leaf mass than those in the control climate ($P < 0.001$). There were no significant differences between the poplar clones. 'Hiwinui' willows had more leaf mass than ML1 willows ($P = 0.022$).

Willows had significantly more leaf area than poplars ($P < 0.001$), and the trees in the enhanced climate had more leaf area than the trees in the control climate ($P < 0.001$). 'Fraser' poplars and 'Geyles' poplars in the enhanced climate had significantly higher leaf area than 'Geyles' in the control climate ($P = 0.008$ clone effect and $P = 0.012$ for clone x status interaction). There were no significant differences between willow clones.

Poplars showed a significant increase in mean leaf mass per unit leaf area ($P < 0.001$) in the enhanced climate, but the difference for willows was not significant.

The trees in the enhanced climate had more stem dry mass than the control trees ($P < 0.001$). There is a near-significant willow clone x temperature/CO_2 status interaction ($P = 0.057$) – 'Hiwinui' in the enhanced temperature/CO_2 status is similar to ML1 (either status), but 'Hiwinui' in the control climate is significantly lower.

Table 3. Response of the willow and poplar clones to enhanced climate prior to the application of drought (PDH) conditions.

	Mean PDH Leaf DM g	Mean PDH Total Leaf Area cm^2 (x1000)	Mean PDH Stem DM g	Mean Leaf DM per unit leaf area g/m^2
Poplar	**21**	**9**		
'Fraser'	**22**	**11.3**		**45**
Control	15 ± 9	11.4 ± 6.5		39 ± 10
Enhanced	30 ± 14	11.1 ± 3.1		52 ± 15
'Geyles'	**22**	**6.9**		**57**
Control	12 ± 11	2.9 ± 4.8		49 ± 9
Enhanced	33 ± 14	10.9 ± 3.7		66 ± 12
Willow	**47**	**12.4**	**77**	
'Hiwinui'	**53**	**11.7**	**73**	
Control	43 ± 10	8.9 ± 2.0	59 ± 13	95 ± 11
Enhanced	63 ± 16	14.5 ± 3.6	88 ± 22	86 ± 4
ML1	**41**	**13.1**	**80**	
Control	39 ± 7	11.4 ± 2.0	78 ± 15	68 ± 4
Enhanced	44 ± 6	14.8 ± 2.6	82 ± 9	60 ± 6
LSD	**13**	**4.5**	**18**	**11.1**

(2) Plant growth response to the enhanced environment conditions during drought

1.4 Shoot biomass

During the time drought conditions were imposed, differences in shoot biomass production (Table 5) between control and enhanced environmental conditions were small compared with the differences resulting from the drought treatment. Biomass production of above ground tissue was lower for willow plants subjected to drought treatment (Table 4). The effect of drought appeared to be less severe in those willow plants experiencing elevated day/night temperature and CO_2. The difference in % DM produced during the period in which some willow plants experienced drought treatment was less for the elevated environment than the normal environment. This difference was greater for 'Hiwinui', than for ML1 which was almost the same. There was more variation in the shoot biomass data for poplar plants during the drought period.

Table 4. Shoot biomass (g) of poplar and willow during the drought phase grown in varying environmental conditions of CO_2, temperature and water availability. LSD = 255.

	Control	Enhanced
Poplar		
'Fraser'		
Drought	338 ± 175	290 ± 151
Normal	420 ± 175	162 ± 140
'Geyles'		
Drought	114 ± 18	639 ± 406
Normal	245 ± 198	427 ± 188
Willow		
'Hiwinui'		
Drought	198 ± 54	188 ± 52
Normal	452 ± 106	371 ± 74
ML1		
Drought	216 ± 54	291 ± 23
Normal	456 ± 23	430 ± 82

There was a significant species x water availability interaction (P = 0.012 – poplars show no significant difference between normal and drought conditions, willows grow more shoots under normal conditions, but significantly less under drought conditions), and a significant temperature/CO_2 status x water availability interaction (P = 0.049 – drought significantly reduces shoot growth under control temperature/CO_2 conditions, but under higher temperature/CO_2 conditions water availability has no significant effect).

There was a significant difference in the way the two poplar clones reacted to temperature/CO_2 status (P < 0.001 – as with leaves, stems and total shoots, 'Fraser' showed no significant difference, but 'Geyles' gained more shoot mass in the enhanced temperature/CO_2 condition). There were no significant differences among the willow clones.

1.5 Leaf biomass

Leaf biomass production during the drought period is shown in Table 5. There was a significant species effect (P = 0.012), water availability effect (P = 0.019) and species x water availability interaction (P = 0.022 – poplars showed no significant difference between normal and drought conditions; willows grew similar amount of leaves under normal conditions, but significantly less under drought conditions), and a significant temperature/CO_2 status x water availability interaction (P = 0.040 – drought significantly reduced leaf growth under control temperature/CO_2 conditions, but under higher temperature/CO_2 conditions water availability had no significant effect).

There was a significant difference in the way the two poplar clones reacted to temperature/CO_2 status (P < 0.001 – 'Fraser' grew fewer leaves under enhanced temperature/CO_2 than the control, but 'Geyles' grew more in the enhanced temperature/CO_2 condition). There were no significant differences among the willow clones.

Table 5. Leaf biomass (g) production of poplar and willow during the drought phase grown in varying environmental conditions of [CO_2], temperature and water availability. LSD =71.

	Control	Enhanced
Poplar		
'Fraser'		
Drought	94 ± 29	98 ± 51
Normal	162 ± 24	54 ± 47
'Geyles'		
Drought	63 ± 4	203 ± 113
Normal	97 ± 42	149 ± 70
Willow		
'Hiwinui'		
Drought	63 ± 14	33 ± 29
Normal	130 ± 30	105 ± 20
ML1		
Drought	52 ± 10	63 ± 9
Normal	111 ± 6	104 ± 28

1.6 Shoot height

There was a significant species effect ($P < 0.001$), temperature/CO_2 status effect ($P < 0.001$) and a near-significant species x temperature/CO_2 status interaction ($P = 0.051$ – shoots were longer under enhanced temperature/CO_2, and the effect was larger for poplar than willow (Table 6)).

There was a significant difference in the way the two poplar clones reacted to temperature/CO_2 status ($P < 0.001$ – 'Fraser' showed no significant difference, but 'Geyles' grew taller in the enhanced temperature/CO_2 condition). There were no significant differences among the willow clones.

There were significant species ($P = 0.049$), climate ($P = 0.016$) and water availability ($P = 0.037$) effects, and also a significant species x climate interaction ($P < 0.001$ – poplar grew taller under enhanced temperature/ CO_2 but willow did not differ) and climate x water availability interaction ($P = 0.049$ – drought significantly reduced growth under control temperature/CO_2 conditions, but under higher temperature/CO_2 conditions water availability had no significant effect).

At final harvest there was a significant difference in the way the two poplar clones reacted to temperature/CO_2 status ($P = 0.019$ – 'Fraser' showed no significant difference, but 'Geyles' grew taller in the enhanced temperature/CO_2 condition). There were no significant differences among the willow clones.

Table 6. Mean shoot height (cm) for the tallest shoot measured prior to imposition of drought treatment (P) and at final harvest (F). LSD (pre-drought) = 76, LSD (final harvest) = 76.

	Control		Enhanced	
	P	F	P	F
Poplar	**103**	**186**	**187**	**270**
'Fraser'	**141**	**221**	**175**	**258**
Drought	157	206	159	263
Normal	125	237	199	251
'Geyles'	**64**	**152**	**197**	**280**
Drought	45	133	183	300
Normal	83	170	210	260
Willow	**210**	**262**	**241**	**247**
'Hiwinui'	**219**	**254**	**240**	**239**
Drought	226	208	220	210
Normal	213	300	261	268
ML1	**200**	**270**	**242**	**255**
Drought	197	238	238	255
Normal	202	302	246	255

(3) Growth response during the complete growing season

1.7 Root mass

In the enhanced climate of [CO_2] and temperature, root biomass was lower in both species (Table 7) and under both normal and drought conditions. However, there were no significant differences between the species, the temperature/CO_2 status, or water availability (*P* values ranged from 0.083 to 0.746). There was a significant difference between the two poplar clones (*P* = 0.022 – 'Fraser' had larger root systems) but no significant interactions with temperature or water. There were no significant differences between the willow clones (*P* values range from 0.460 to 0.902).

Table 7. Root mass (g) of poplar and willow clones grown under varying environmental conditions of [CO_2], temperature and water availability. LSD = 89.

	Control	Enhanced
Poplar	**Root mass g**	**Root mass g**
'Fraser'		
Drought	99 ± 51	41 ± 25
Normal	168 ± 152	86 ± 43
'Geyles'		
Drought	18 ± 6	54 ± 40
Normal	69 ± 95	43 ± 29
Willow		
'Hiwinui'		
Drought	101 ± 34	70 ± 5
Normal	127 ± 14	81 ± 28
ML1		
Drought	99 ± 18	95 ± 21
Normal	112 ± 30	104 ± 40
LSD	69	191

1.7.1 Shoot biomass

Leaf and stem biomass (Table 8) data suggest that under enhanced environmental conditions leaf DM production will be reduced and, when subjected to drought, the % reduction in leaf DM production will not be as great. The inference from these data is that enhanced CO_2 and temperature acting together will reduce leaf biomass production, possibly because the increased photosynthate production is compensated by a reduction in photosynthetic material.

(i) Leaf DM

There was a significant difference between the drought and normal water treatments (P = 0.009), with less leaf mass produced in the drought condition. LSD = 79 (for clone x temp/CO_2 status x water treatment means)

The two poplar clones had significantly different responses to the enhanced temperature/CO_2 status (p = <0.001); 'Fraser' produced similar leaf mass as in the control condition, but 'Geyles' produced more leaf mass in the enhanced temperature/CO_2 condition. However, there were no significant differences among the willow clones.

(ii) Stem DM

There was a significant difference in total stem DM produced between poplars and willows (P = 0.005), but also a significant species x water treatment interaction (P = 0.019); in unstressed conditions, willows produced more stem mass than poplars, while in drought conditions willows produced about the same stem mass as poplars in either drought or normal conditions (for poplars there is no significant difference between the two conditions).

Table 8. Leaf, stem and shoot biomass (g) of poplar and willow grown under varying environmental conditions of CO_2, temperature and water availability.

	Control			Enhanced		
	Total Leaf DM g	Total Stem DM g	Total Shoot DM g	Total Leaf DM g	Total Stem DM g	Total Shoot DM g
Poplar	**125**	**175**	**300**	**170**	**276**	**446**
'Fraser'	**159**	**251**	**409**	**122**	**180**	**302**
Drought	131 ± 46	243 ± 160	374 ± 191	120 ± 56	192 ± 100	311 ± 155
Normal	186 ± 44	258 ± 153	444 ± 195	125 ± 20	161 ± 7	287 ± 13
'Geyles'	92	99	191	209	357	566
Drought	68 ± 6	50 ± 15	118 ± 17	236 ± 128	436 ± 293	672 ± 421
Normal	117 ± 68	148 ± 68	264 ± 228	183 ± 75	278 ± 118	460 ± 192
Willow	**129**	**310**	**439**	**129**	**329**	**458**
'Hiwinui'	**139**	**287**	**426**	**131**	**298**	**430**
Drought	111 ± 20	203 ± 36	314 ± 57	83 ± 23	232 ± 17	315 ± 35
Normal	166 ± 38	372 ± 78	538 ± 116	179 ± 10	365 ± 35	544 ± 42
ML1	**120**	**333**	**453**	**127**	**359**	**486**
Drought	91 ± 18	242 ± 59	332 ± 76	106 ± 3	313 ± 10	419 ± 11
Normal	149 ± 8	424 ± 29	573 ± 23	148 ± 31	405 ± 601	553 ± 92

As with leaf mass, the two poplar clones had significantly different responses to the enhanced temperature/CO_2 status; 'Fraser' produced similar leaf mass as in the control condition, but 'Geyles' produced more leaf mass in the enhanced temperature/CO_2 condition. There were no significant differences among the willow clones. LSD = 190.

1.8 Shoot DM

There was a significant water treatment effect (P = 0.035), but also a significant species x water treatment interaction (P = 0.026); as with stems, in unstressed conditions, willows produced more mass than poplars, while in drought conditions willows produced about the same mass as poplars in either drought or normal conditions (for poplars there is no significant difference between the two conditions).

As with leaf and stem mass, the two poplar clones had significantly different responses to the enhanced temperature/CO_2 status; 'Fraser' produced similar leaf mass as in the control condition, but 'Geyles' produced more leaf mass in the enhanced temperature/CO_2 condition. There were no significant differences among the willow clones. LSD = 263.

1.9 Shoot: root ratio

Table 9. Shoot: root ratio of poplar and willow grown under varying environmental conditions of [CO_2], temperature and water availability.

	Control	Enhanced
Poplar		
'Fraser'		
Drought	3.4 ± 0.5	9.6 ± 6.5
Normal	3.5 ± 1.9	3.8 ± 1.7
'Geyles'		
Drought	6.7 ± 2.2	16.5 ± 9.6
Normal	7.8 ± 4.9	12.6 ± 4.2
Willow		
'Hiwinui'		
Drought	2.8 ± 0.6	3.7 ± 0.2
Normal	4.0 ± 0.5	4.7 ± 1.5
ML1		
Drought	3.1 ± 0.5	3.9 ± 0.8
Normal	5.1 ± 1.3	4.0 ± 0.7

There were significant differences between species ($P < 0.001$), temperature/CO_2 status ($P = 0.003$), a significant species x status interaction ($P = 0.037$ – poplars in the high temperature/CO_2 condition had higher shoot: root ratios than in the control condition, whereas willows showed no difference) and a significant species x water availability interaction ($P = 0.023$ – in the drought condition shoot: root ratio for poplars increased, but for willows decreased).

There was a significant difference between the poplar clones ($P < 0.001$ – 'Fraser' had lower shoot: root ratio) but no significant differences among the willow clones.

The elevated shoot: root ratio in the enhanced climate was contributed more by a reduction in root biomass (Table 7, 8) than an increase in shoot biomass.

1.10 Discussion

Prediction of increased drought frequency is alarming, and its effect is clear in this experiment where availability of water at depths of 0–40 cm is severely restricted. This experiment differs from field experiments in the depth of soil where water can be accessed. The ability of willow and poplar trees to maintain production of new leaf material in contrast to pasture is due to access to water at greater depths. This capability can be further enhanced through reducing the tree internal requirements for water by pollarding (reducing the trunk and large branch components of the canopy). This is a strong indication that drought will continue to be a major deterrent of production and is unlikely to be offset by the beneficial effects of enhanced CO_2 and temperature.

Table 10. Levels of significance for effect on various interactions on plant biomass parameters.

Parameter	Interaction	p
Leaf DM	species	0.012
	Species x climate	0.022
	Water availability	0.019
	Climate x water availability	0.04
	Species x water availability	0.022
	Clone (poplar)	<0.001
	Clone (willow)	NS
Stem DM	species	0.053
	climate	NS
	Water availability	NS
	Climate x water availability	0.034
	Clone (poplar)	<0.001
	Clone (willow)	NS
Shoot DM	species	0.026
	climate	NS
	Water availability	0.035
	Climate x water availability	0.049
	Clone (poplar)	0.001
	Clone (willow)	NS
Root DM	species	NS
	climate	NS
	Water availability	NS
	Clone (poplar)	0.022
	Clone (willow)	NS
Shoot : root DM	species	0.003
	Species x climate	0.037
	Species x Water availability	0.023
	Clone (poplar)	<0.001
	Clone (willow)	NS
Shoot height	species	0.049
	climate	0.016
	Water availability	0.037
	Species x climate	<0.001
	Climate x water availability	0.049
	Clone (poplar)	0.019
	Clone (willow)	NS

For the two willow clones grown under well watered and drought conditions, drought resulted in large reductions in above ground biomass, but lesser reductions in below ground biomass. This suggests that drought conditions produce changes in where photosynthate is invested, with relative increases in root production and decreases in shoot production. In the natural environment the promotion of root growth would enable a greater volume of soil to be tapped for water.

Temperature was not treated as a separate variable to CO_2. Primarily this was because future climate predictions link assume increasing CO_2 (as cause) and increasing temperature (as effect) as occurring together and it will be the combined scenario that plants will experience if these scenarios prove correct. The purpose of this experiment was to investigate plant response to that combined scenario. Discussion of the variables treated separately will utilise other research findings.

Flanagan et al. (2013) conducted an experiment with grassland species where they measured biomass response to elevated temperature (2.5°C) and varying precipitation (-50%, 0%, +50%). They reported above ground biomass was not significantly affected by the experimental manipulations, but warmed soil (0.5–1.0°C) increased root biomass. However, no significant differences in shoot: root ratio occurred among treatments during the 2 years of the experiment. They suggested that experimental warming over a longer time period may be required before consistent, significant effects of the warming treatment on root biomass could be discerned. Morgan et al. (2011) noted that 4 years of exposure to elevated atmospheric CO_2 concentration were required before a significant effect on root biomass was noted in a mixed-grass prairie site in Wyoming. For comparison, a recent meta-analysis covering a wide range of species indicated that experimental warming increased aboveground biomass on average by 27%, but did not significantly affect belowground or total biomass (Wu et al. 2011). In addition, experimental reductions in precipitation decreased aboveground biomass by 15%, and increased precipitation stimulated aboveground biomass by 12% and belowground biomass by 11% (Wu et al. 2011). Nutrient deficiency as an uncontrolled variable may mask controlled effects in open land studies. In growth chambers nutrient limitations are easily managed, as are such other variables as wind or air movement. The early gains in seasonal growth from elevated temperatures and CO_2 extends the growing season for those plants also.

However, a modest shift of carbon allocation toward increased root biomass, mycorrhizal symbioses and root exudation could substantially increase soil microbial activity with subsequent significant effects on soil respiration rates. For example, several previous studies have documented an increase in microbial activity and associated soil nitrogen cycle processes after ecosystems increase carbon allocation to roots as a result of exposure to elevated atmospheric CO_2 concentrations (Dukes et al. 2004, Drake et al. 2011 and Phillips et al. 2011).

Frenck et al. (2013) reported that elevated CO_2 led to higher quantities of reproductive output over several generations of *Brassica napus* L. grown in a phytotron independent of the two temperature regimes (normal and elevated). In this experiment flowering was observed for ML1 under EN after 8 weeks but not NN.

To examine whether deciduous and evergreen tree species differ in their performance and plastic responses to elevated atmospheric CO_2 (700 ppm) and temperature (+2.5°C), Duan et al. (2013) investigated growth of *Populus yunnanensis* and *Abies faxoniana* grown in environment-controlled chambers. Based on plant biomass and leaf area measurements, they concluded that temperature stimulated growth more than did CO_2 in both species. The magnitude of temperature and CO_2 effects varied between the species, as greater stimulation was detected in *A. faxoniana* than in *P. yunnanensis*. They also observed that ET

and EC resulted in a greater growth relative to initial biomass in *A. faxoniana* (179% by temperature and 142% by CO_2) than in *P. yunnanensis* (156% by temperature and 129% by CO_2).

Xu *et al.* (2013) found for Tibetan Juniper that from 1975 to 2002, intrinsic water use efficiency (iWUE) increased rapidly at the study site (by 12.4% compared with the overall mean from 1850 to 2002), which is greater than the expected increase due only to an active response to atmospheric CO_2. Their analysis showed that decreased water availability caused by greater evaporation due to decreased precipitation and a warming growth environment from 1975 to 2002 may have reduced stomatal conductance, leading to a higher iWUE.

The effects of the interaction between high growth temperatures and water stress on gas-exchange properties of *Populus nigra* saplings were investigated by Centritto *et al.* (2010). Water stress was expressed as a function of soil water content (SWC) or fraction of transpirable soil water (FTSW). Isoprene emission appears to be a mechanism that trees use to combat abiotic stresses .In particular, isoprene has been shown to protect against moderate heat stresses (~40°C). Current thinking is that isoprene emission was specifically used by plants to protect against large fluctuations in leaf temperature. Such temperatures exceed the temperature fluctuations likely to be experienced by trees in New Zealand. Isoprene emission and photosynthesis did not acclimate in response to elevated temperature. There was no significant effect of high growth temperature on the responses of photosynthesis, stomatal conductance, or isoprene emission. High growth temperature resulted in a significant increase in the soil water content endpoint. Photosynthesis was limited mainly by CO_2 acquisition in water-stressed plants. Since respiration and isoprene sensitivity are much lower than photosynthesis sensitivity to water stress, temperature interactions with water stress may dominate poplar acclimatory capability and maintenance of carbon homeostasis under climate change scenarios. Furthermore, predicted temperature increases in arid environments may reduce the amount of soil water that can be extracted before plant gas exchange decreases, exacerbating the effects of water stress even if soil water availability is not directly affected (Centritto *et al.* 2010).

Over the range of day time growth temperatures (5–32°C), Ow et al. (2010) did not observe strong evidence of photosynthetic acclimation to temperature in *Populus deltoides*, and the long-term responses of photosynthetic parameters to ambient temperature were similar to previously published instantaneous responses. At present, most climate-carbon cycle models assume that rates of photosynthesis and respiration will increase with increasing temperature in a predictable way that will remain constant over time. Ow et al. (2010) suggested that acclimation is likely to occur in *Populus*.

The experimental warming (average 1.8°C at 20 cm above ground and 3.6°C soil temperature at 5 cm depth) of seedlings of *Picea asperata* and *Abies faxoniana* over a 4-year period in outdoor plots increased root biomass, shoot biomass, root/shoot mass ratio, decreased coarse root/ fine root mass ratio, and significantly increased fine root length (Yin *et al.* 2013). Soil water availability was the same for the warmed and control plots. These findings may be more of a consequence of the soil temperatures being more elevated than the air temperatures by their warming technique, a situation that may not be so accentuated for poplar trees in pastoral situations.

Populus tremuloides (trembling aspen) recently experienced extensive crown thinning, branch dieback and mortality across North America. To investigate the role of climate, Worrall et al. (2013) developed a range-wide bioclimate model that characterizes climatic factors controlling distribution of aspen. They also examined indices of moisture stress, insect defoliation and

other factors as potential causes of the decline. Historic climate records showed that most decline regions experienced exceptionally severe drought preceding the recent episodes. The bioclimate model, driven primarily by maximum summer temperatures and April–September precipitation, shows that decline tended to occur in marginally suitable habitat, and that climatic suitability decreased markedly in the period leading up to decline in almost all decline regions.

Other factors, notably multi-year defoliation by tent caterpillars (*Malacosoma* spp.) and stem damage by fungi and insects, also play a substantial role in decline episodes, and may amplify or prolong the impacts of moisture stress on aspen over large areas. Many severely affected stands have poor regeneration potential; raising concerns that increasing aridity could ultimately lead to widespread loss of aspen forest cover. The analysis indicates that exceptional droughts were a major cause of the decline episodes, especially in the drier regions, and that aspen is sensitive to drought in much of its range. Coupling the bioclimate model with climate projections suggests that there will be substantial loss of suitable habitat within the current distribution, especially in the USA and Mexico.

We conclude from these studies that both enhanced CO_2 and elevated temperature change the growth and resource allocation in a range of plant species, and that there is considerable variability in the responses. In general, growth is enhanced and for trees in their natural environment this increased flow of resources to roots may increase the contribution to soil carbon through exudates and higher fine root turnover. The greater limitation will be reduced water availability in those regions likely to experienced increased drought risk, which will increase difficulty of establishment of young trees and stress older trees increasing susceptibility to pests and diseases. At this stage New Zealand is relatively free of significant insect pests of poplar and willow and with *Melampsora* spp. (rusts) being the main disease threat.

1.11 Conclusions

Increased atmospheric CO_2 can be expected to lead to an increase in plant biomass whereas increased mean temperatures may have a greater impact on plant respiration than photosynthesis. Of all the parameters measured the root biomass was the least affected by the imposition of drought conditions, and the net reduction in growth in response to drought was less severe under the enhanced conditions than under the normal conditions.

The combined effect of increased atmospheric CO_2 and increased mean day/night temperature is expected to result in an increase in biomass production. Under future climate change responses are likely to vary between clones in both poplar and willow and the interim period should be used to evaluate the relative responses to drought stress in the range of commercial poplar and willow clones being currently used or in the developmental stage.

1.12 References

Beck EH, Fettig S, Knake C, Hartig K, Bhattarai T 2007. Specific and unspecific responses of plants to cold and drought stress. J Biosci 32: 501–510.

Bray EA 1990. Drought-stress-induced polypeptide accumulation in tomato leaves. Plant Cell Env 13: 531–538.

Centritto M, F Brilli, R Fodale, F Loreto and M Abrams 2010. Different sensitivity of isoprene emission, respiration and photosynthesis to high growth temperature coupled with drought stress in black poplar (*Populus nigra*) saplings. Tree Physiol 31: 275–286.

Cvikrová M, Gemperlová L, Martincová O, Vanková R 2013. Effect of drought and combined drought and heat stress on polyamine metabolism in proline-over-producing tobacco plants. Plant Physiology Biochemistry 73: 7–15.

Drake JE, Gallet-Budynek A, Hofmokel KS, Bernhardt ES, Billings SA, Jackson RB, Johnsen KS, Lichter J, McCarthy HR, McCormack ML, Moore DJ, Oren R, Palmroth S, Phillips RP, Pippen JS, Pritchard SG, Treseder KK, Schlesinger WH, DeLucia EH, Finz AC 2011. Increases in the flux of carbon belowground stimulate nitrogen uptake and sustain the long-term enhancement of forest productivity under elevated CO_2. Ecol Lett 14: 349–357.

Duan B, Zhang X, Li Y, Li L, Korpelainen H, Li C 2013. Plastic responses of *Populus yunnanensis* and *Abies faxoniana* to elevated atmospheric CO_2 and warming. For Ecol Man 296: 33–40.

Dukes JS, Finzi A, Hartwig U, Hungate B, McMurtrie RE, Oren R, Parton WJ, Pataki DE, Shaw MR, Zak DR, Field CB 2004. Progressive nitrogen limitation of ecosystem processes to rising atmospheric carbon dioxide. BioScience 54: 731–739.

Flanagan LB, Sharp EJ, Letts MG 2013. Response of plant biomass and soil respiration to experimental warming and precipitation manipulation in a Northern Great Plains grassland. Agricultural and Forest Meteorology 173: 40–52.

Frenck G, van der Linden L, Mikkelsen TN et al. 2013. Response to multi-generational selection under elevated [CO_2] in two temperature regimes suggests enhanced carbon assimilation and increased reproductive output in *Brassica napus* L. Ecology and Evolution 3: 1163–1172.

Morgan JA, LeCain DR, Pendall E, Blumenthal DM, Kimball BA, Carrillo Y, Williams DW, Heisler-White J, Dijkstra FA, West M 2011. C_4 grasses prosper as carbon dioxide eliminates desiccation in warmed semi-arid grassland. Nature 476: 202–205.

Ow LF, Whitheead D, Walcroft A, Turnbull MH 2010. Seasonal variation in foliar carbon exchange in *Pinus radiata* and *Populus deltoides*: respiration acclimates fully to changes in temperature but photosynthesis does not. Global Change Biology 16: 288–302.

Phillips RP, Finzi AC, Bernhardt ES 2011. Enhanced root exudation induces microbial feedbacks to N cycling in a pine forest under long-term CO_2 fumigation. Ecol Lett 14: 187–194.

2 DROUGHT TOLERANCE OF FIVE HYBRID POPLAR CLONES TO DIFFERENT WATERING REGIMES

Trevor Jones[1], Ian McIvor[1], and Michael McManus[2]
[1] Plant & Food Research, Palmerston North
[2] Massey University, Palmerston North

The soil water deficits that occur in drought conditions are a major factor limiting the survival and growth of poplar trees for soil conservation in New Zealand. Poplars are among the fastest growing trees under temperate latitudes, but their high productivity is associated with a dependency on water availability. There is wide variability in the water-use efficiency and drought tolerance of poplar species and hybrids, and potential for the selection of poplar clones with improved adaptability to drought conditions.

The physiological response of four new hybrid poplar clones and the 'Veronese' poplar clone to soil water deficits was evaluated in a greenhouse pot trial, with well-watered, moderate and severe (90, 60 and 40% of field capacity) soil water deficit treatments. The biomass growth and water-use efficiency of the poplar trees, leaf stomatal conductance and water potential, and leaf chlorophyll content and antioxidant enzyme activity were measured to determine the drought tolerance of the poplar clones.

The four new hybrid poplar clones were not as drought-tolerant as the 'Veronese' poplar clone, showing a less conservative response to the soil water deficits, and lower antioxidant enzyme activity in the leaves, but they had the advantage of better biomass growth and water-use efficiency under drought conditions.

The 'Veronese' clone appears well adapted for drought-prone areas, where the survival of the trees during periods of severe soil water deficits is a constraint. In contrast, the new hybrid poplar clones appear better adapted to moderately drought-prone areas, where there is an advantage in combining high productivity and high water-use efficiency to better utilise the available water during the growing season.

2.1 Introduction

Soil water deficits are a major factor limiting the survival and growth of plants in many environments. Pastoral hill country in New Zealand is subject to periodic summer drought conditions which can produce significant soil water deficits (Garnier 1958). This can reduce the survival and growth of poplar trees (Ceulemans & Deraedt 1999) and compromise the effectiveness of poplar (*Populus* spp.) trees for soil conservation.

The physiological response of poplar trees to water deficits differs among poplar species and hybrids (Kelliher & Tauer 1980; Pallardy & Kozlowski 1981; Blake et al. 1984; Hinckley et al. 1989; Gebre & Kuhns 1991; Braatne et al. 1992; Yang et al. 2010), with wide variability in the water-use efficiency and tolerance to drought conditions (Blake et al. 1984; Marron et al. 2005; Monclus et al. 2005, 2006; Strong & Hansen 1991; Yin et al. 2005; Zhang et al. 2004).

There are consistent genotypic differences in the water-use efficiency (WUE) of poplar species and hybrids, and a lack of correlation between the WUE and productivity of poplar clones (Marron et al. 2005; Monclus et al. 2005, 2006). This indicates there is potential for the selection

of poplar clones that combine high water-use efficiency and high productivity, which would be an advantage for the growth of poplar trees in moderately drought-prone areas (Bonhomme et al. 2008; Marron et al. 2005).

In this study, the physiological response of four new hybrid poplar clones to drought conditions was evaluated and compared with the drought-tolerant 'Veronese' poplar clone that is widely used for soil conservation in New Zealand (Table 1). The tree growth and water-use parameters of these poplar clones were evaluated in a greenhouse water-stress experiment, to characterize the drought tolerance, water-use efficiency, and the capacity for drought acclimation of the poplar clones.

Table 1. Hybrid poplar clones used in the experiment and the parent clones.

Poplar clones	Female parent	Male parent
'Veronese'	*Populus deltoides*	*P. nigra*
MT103 -07-05-103	*P. maximowiczii* 87-007-04	*P. trichocarpa*
MT304 -07-02-304	*P. maximowiczii* 87-007-01	*P. trichocarpa*
TN008 -07-03-008	*P. trichocarpa*	*P. nigra* PN866 PG22
TN014 -07-06-014	*P. trichocarpa*	*P. nigra* PN874 Blanc de Garonne

2.2 Methods

2.2.1 Experiment design

A completely randomized design was used in the experiment, with 5 poplar clones × 3 water regimes (total of 15 treatments). Four replicates were used for each treatment (total of 60 pots). The three water regimes were: well-watered (90% of field capacity), moderate soil water deficit (60% field capacity), and severe soil water deficit (40% field capacity), where the field capacity was defined as the soil water content of the pots after 24 h of drainage, following saturation of the soil.

2.2.2 Field capacity of soil

The field capacity (FC) of the soil (Daltons poplar water-stress mix, Table 2) was measured by watering the soil in a 30-L plastic pot with a hose, covering the surface of the soil with a plastic sheet and allowing to drain for 24 h, and then taking 10 × 300 g samples for measurement of the gravimetric water content of the soil using Australian Standard 1289.2.1.1 (2005). The soil samples had a high content of organic carbon and were oven-dried at 65°C to constant weight.

Table 2. Composition of the poplar water-stress mix.

Basic ingredients	Percentage	Fertiliser ingredients	kg m^{-3}
Bark fines (CAN) A grade	35	Dolomite	4.00
Daltons Prop (No. 2) sand	30	Growers Choice Granular WA	0.75
Hauraki Peat	35	Lime – Ag Grade	2.00
		Osmocote Exact 3/4 Standard	3.00
		Osmoform NXT 22N	0.50

2.2.3 Greenhouse environment

The poplar trees were grown from cuttings in 30-L green plastic pots in a greenhouse at The New Zealand Institute for Plant & Food Research Limited in Palmerston North (Figure 1). The roof and walls of the greenhouse were enclosed with clear plastic sheeting, with the exception of the lower walls. These were covered with cloth along the two long sides of the greenhouse, to provide good ventilation and exposure to the wind. The greenhouse was ventilated by two fans (Figure 1) that were activated when the air temperature of the greenhouse reached 22°C.

The air temperature and humidity, and light conditions inside the greenhouse (Figure 2), were measured using a Humitter 50Y integrated temperature and humidity sensor (Vaisala Oyj, Helsinki, Finland), and a LI-190SB quantum (PAR) sensor (Li-Cor Inc., Lincoln, Nebraska, USA), that were connected to a CR10X data logger (Campbell Scientific, Logan, Utah, USA).

2.2.4 Propagation of the poplar trees

The poplar trees were propagated from cuttings of 15 to 26 mm diameter and 40 cm length. The cuttings were cut from 1-year-old shoots from nursery stools. The diameter of each cutting at the mid-point (along the length) was measured prior to soaking in water for 5 days. The cuttings were selected to provide a similar distribution of mid-point diameter for each poplar clone.

The poplar cuttings were planted on 1 October 2013, with one cutting planted in each of the 30-L plastic pots. The cuttings were planted after the soil in the pots was saturated with water, and drained for 24 hours to field capacity. The pots were positioned in a randomised block design inside the greenhouse. The pots were placed in four rows along the length of the greenhouse (Figure 1), with one pot of each poplar clone randomly assigned to each of three blocks of five pots within each row.

The pots were weighed every 2 days, and the water transpired was measured and replaced to maintain the soil at 90% of field capacity (FC). The addition of water to the trees was adjusted for the growth in the fresh weight of the shoots. The evaporation of water from the soil surface was minimised by covering the surface with plastic sheeting. The poplar trees were grown at 90% of field capacity for 70 days (10 weeks), and then the moderate soil water deficit (60% FC) and severe soil water deficit (40% FC) treatments were applied.

Figure 1. Layout of the poplar trees in the greenhouse at Plant & Food Research in Palmerston North.

2.2.5 Application of the soil water deficits

The trees (pots) of each poplar clone were re-allocated to four blocks in the greenhouse based on the amount of shoot biomass (leaves + stems) after 10 weeks of growth. The three trees of each clone with the largest amount of shoot biomass were allocated to block one, and the process was repeated for blocks two, three, and four, with three trees of each clone with progressively smaller amounts of shoot biomass. The three trees of each clone, in each of the four blocks, were randomly allocated to the 90%, 60%, or 40% of field capacity treatments.

The water regimes were started on 10 December 2013 by allowing the pots to dry down to the required soil water content, and were applied to the poplar trees for 49 days (7 weeks). The water regimes were maintained by weighing each pot every 2 days, and the transpired water was measured and replaced to maintain the pots at 90%, 60%, or 40% of field capacity (FC). The addition of water to the trees was adjusted for the growth in the fresh weight of the shoots.

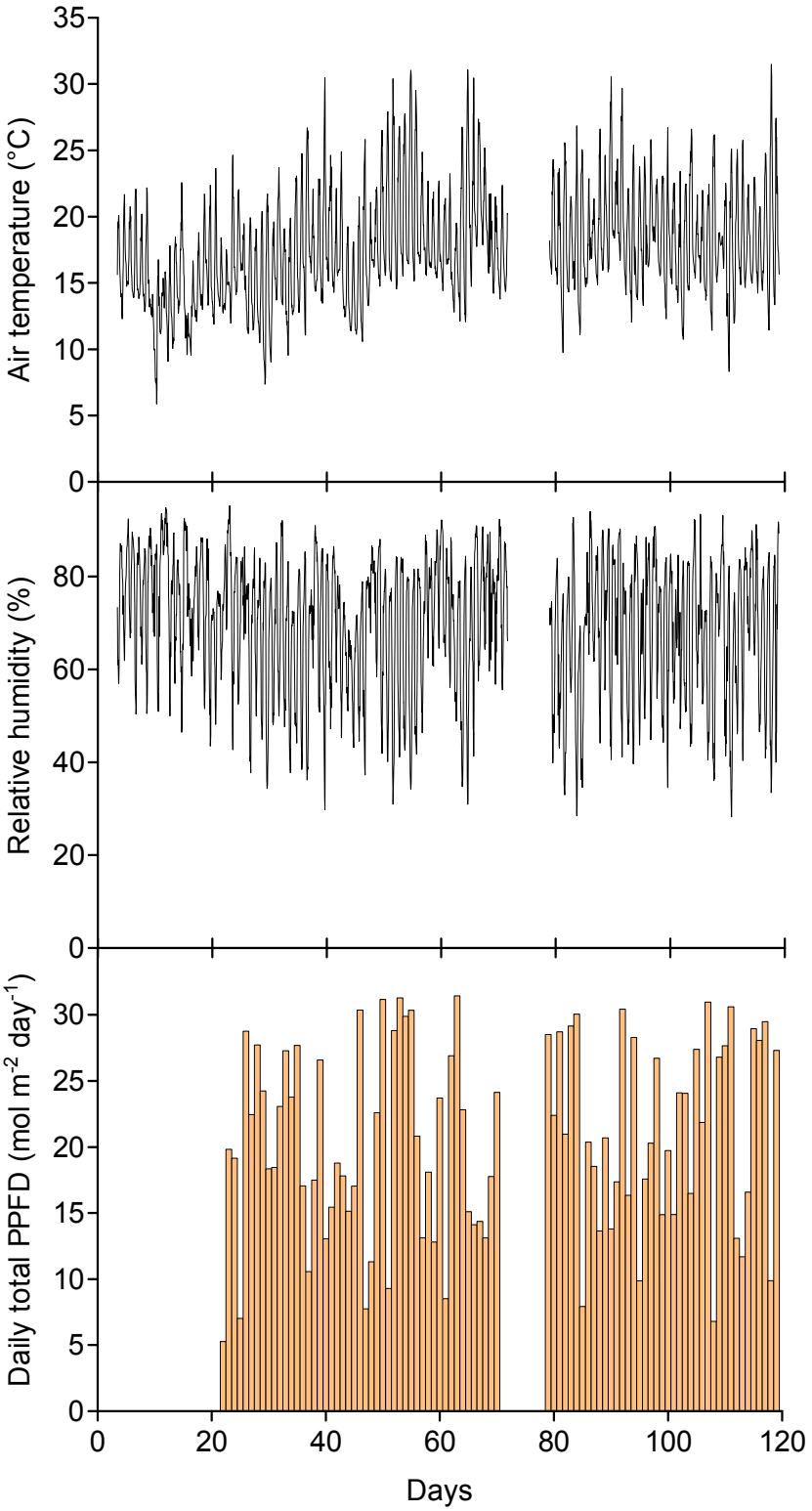

Figure 2. Hourly mean temperature and humidity, and daily photosynthetic photon flux density (PPFD) in the greenhouse during the experiment.

2.2.6 Monitoring the growth of the poplar trees

The basal diameter, number of leaves, and height of the shoots of each tree were measured weekly. The fresh weight of the shoots (leaves + stems) was estimated for each tree using the basal diameters and heights of the shoots in the linear regression equation:

$\text{Log}_{10}\, S = \log_{10} a + b \log_{10} B$ (1)
where S is the fresh weight of the shoot, and B is the basal diameter multiplied by the square of the shoot height. The equation was back-transformed to the power function:

$S = aB^b$ (2)
where the anti-log of the intercept was multiplied by a correction factor in order to account for bias inherent in fitting the model to the geometric mean rather than the arithmetic mean (Sprugel 1983). The correction factor was calculated as:

$$CF = 10^{(S^2_{y.x}/2)} \quad (3)$$
where $S_{y.x}$ is the standard error of the estimate (SEE) of the regression.

The regression coefficients in equation (1) were calculated using sample shoots with a wide range of basal diameter and height from nursery stools of the hybrid poplar clones. A single equation was found to give a good fit to the shoot data from all the poplar clones.

The leaf area of each tree was measured at the time the water regimes were started. A sample of 1 leaf in 20 was taken from each tree and measured for the fresh leaf weight, number of leaves, leaf area using a LI-3100 area meter (Li-Cor Inc., Lincoln, Nebraska, USA), and then oven-dried at 70°C to constant weight.

The diameter growth of the cuttings was measured at weekly intervals, from the start of the application of the water regimes. Two diameters were measured at right angles on the tree stems, using callipers and averaged.

2.2.7 Leaf stomatal conductance and water potential

The stomatal conductance of the leaves was measured using a cycling porometer (Delta-T porometer type AP4, Delta-T Devices Ltd, Cambridge, UK), and the water potential of the leaves was measured using a Scholander-type pressure chamber (Soil Moisture Equipment Co., Santa Barbara, California, USA).

The diurnal variation in the stomatal conductance of the leaves of the poplar trees was measured during the weeks following the application of the water regimes, on clear sunny days at 2-h intervals between 08:00 and 17:00. The measurements were made on the second day of the 2-day watering cycle. Two or three young fully expanded mature leaves, usually the sixth to tenth leaves from the apex of the shoot, were selected on each tree in block 1, and the stomatal conductance was measured twice on the abaxial (lower) surface of each leaf.

The variation in the stomatal conductance with leaf number along the length of the shoots was measured 1 and 5 weeks after the application of the water regimes. The measurements were made over a period of 5 days, between 13:00 and 17:30 on clear sunny days, and on the first day of the 2-day watering cycle. One dominant shoot was selected from each tree in block 1, and the stomatal conductance was measured twice on the abaxial (lower) surface of alternate leaf numbers from the apex to the base of the shoot.

The stomatal conductance and water potential of the leaves were measured on all the poplar trees (blocks 1 to 4) at 6–7 weeks after the application of the water regimes. The measurements were made over a period of 8 days, between 13:30 and 17:30 on clear sunny days. One young fully expanded mature leaf was measured on each tree, on the first and second days of the 2-day watering cycle (total of 2 leaves per tree) to provide a wide range of water potential. The stomatal conductance was measured two to four times on the abaxial (lower) surface of each leaf, and this was followed immediately by the measurement of the water potential.

2.2.8 Leaf stomatal density

The density of the stomata on the surface of the leaves was measured for poplar trees from each poplar clone and water regime treatment. Stomatal impressions were made by placing a drop of 'superglue' on the adaxial (upper) and abaxial surface of the leaf, covering with a glass microscope slide, and then removing the slide and taking the impression with it. The stomata were viewed and counted under an Olympus CX41 system microscope (Olympus Corp., Tokyo, Japan), and the stomatal density was calculated as the counted number divided by the area of the field of view.

2.2.9 Leaf chlorophyll, antioxidant enzymes, and free proline

The leaves of the poplar trees were sampled for measurements of the chlorophyll content, superoxide dismutase (SOD), ascorbate peroxidase (APX), and guaiacol peroxidase (GPX) activity, and free proline content at 78 and 119 days, 1 and 7 weeks after the application of the water regimes. One young fully expanded mature leaf was sampled from each tree in blocks 1 and 2, frozen immediately in dry ice, and stored at -80°C.

2.2.10 Chlorophyll content

The chlorophyll content was analysed as described by Evans et al. (2011) but with modification. Into a 0.2 mL Eppendorf tube, 0.5 mL of 96% (v/v) ethanol was pipetted and 50 mg of poplar leaf tissue (FW) was added. Briefly, the tube was subjected to 30 s 'pulse-spin' before being placed in the dark O/N at 4°C. The extract was then spun at 12,000 x g for 2 min and the resulting supernatant pipetted into fresh sterile Eppendorf tubes and kept at 4°C.

Immediately, 2 µL of the supernatant was quantified for chlorophyll content on a 'Nanodrop' spectrophotometer (Thermo Fisher Scientific Inc.) (UV-Vis option) at 649 nm and 665 nm. The total chlorophyll was calculated using the following equation:

$$\text{Chl a + b} = (6.1(A665) + 20.04(A649)) \quad (4)$$

Each sample was analysed in triplicate to gain a relative average. The results are expressed as total chlorophyll (µg mL^{-1}).

2.2.11 Antioxidant enzymes

Homogenised tissue (0.1 g) was added to 1 mL of extraction buffer solution comprising 50 mM K_2HPO_4 (pH 7.0), and 1 mM EDTA. Samples were then centrifuged at 4°C for 15 min at 12,000 x g and the supernatant used as a crude extract of cytoplasmic fractions for the determination of the APX and SOD activity. The resulting pellet was extracted prior to GPX determination.

As GPX is a cell-wall protein, the pellet was subjected to multiple clean-up steps (5 washes with 1 mM DTT, with centrifugation at 12,500 x g for 5 min at 4°C after each wash, followed by 5 washes with sterile MQ H_2O followed by centrifugation at 12,500 x g). A small volume of 1 M NaCl (containing a protease inhibitor, Sigma Aldrich) was used to cover the pellet and the suspension incubated O/N at 4°C. The following day, the extract was centrifuged at 12,500 x g for 10 min at 4°C, and the supernatant (the ionically-bound cell wall fraction) was collected. The remaining pellet was again suspended in enough 1 M NaCl (containing protease inhibitor) to cover the pellet and the slurry was incubated at 37°C for 1 h. After this, the extract was centrifuged at 12,500 x g for 10 min at 4°C and both supernatant fractions were pooled together for immediate GPX analysis.

For estimation of the SOD activity, the samples were assayed by measuring the photoreduction of nitroblue tetrazolium (NBT) at 560 nm (Beauchamp & Fridovich, 1971). Briefly, 25 µL of crude extract was added to an assay reaction mixture comprising 50 mM K_2HPO_4 (pH 7.8), containing final concentrations of 0.1 mM EDTA, 13 mM L-Methionine, 161 µM NBT and 22 µM riboflavin in a final volume of 2.8 mL.

The samples were prepared in standardised glass tubes of equal diameter and length and carried out in triplicate. To begin the reaction, the samples were prepared in the dark before initialising the reaction by illuminating the samples (representing T_0) with two 15 W fluorescent lights for 10 min (T_{10}) and terminating the reaction by switching the lights off. A sub-sample of the reduced reaction (100 µL) was pipetted into a microplate and the absorbance of each well read at 560 nm using a plate reader (Biotek) with Gen 5 software at 560 nm. One unit of SOD is considered to be the activity amount required to inhibit the photoreduction of NBT by 50% and is expressed in units (U) per mg^{-1} of protein.

The APX activity was measured through the oxidation of ascorbate to dehydroascorbate as described by Nakano & Asada (1981). Briefly, the reaction assay mixture comprised 50 mM K_2HPO_4 (pH 7.0), containing 0.25 mM ascorbic acid, and 1 mM H_2O_2. To initiate the reaction, 10 µL of undiluted sample was added to 3 mL assay mixture and the decrease in absorbance at 290 nm was measured every 20 s for 3 min. Results are expressed as mmol per µg protein using an extinction co-efficient of 2.8 mM^{-1} cm^{-1}. Each sample was assayed in triplicate.

The GPX activity was measured by the oxidation of guaiacol. The assay (1 mL) comprised 50 mm K_2HPO_4 (pH 6.0), 5 µL of H_2O_2 with 25 mM guaiacol, and a 10 µL sample of a 50-fold dilution of cell-wall extract was used. The reaction was started by the addition of guaiacol and followed spectrophotometrically as the increase of absorption at 470 nm. Readings were taken every 10 s for 3 min. The results are expressed as mmol per µg protein using an extinction co-efficient of 26.6 mM^{-1} cm^{-1}. Each sample was assayed in triplicate.

2.2.12 Harvesting the poplar trees

The poplar trees were harvested 49 days (7 weeks) after the application of the water regimes, on 28 January 2014. The biomass of the trees was divided for the leaves, stems, cuttings, and roots. The leaf area of each tree was measured and the number of leaves counted. The roots were separated from the soil by screening and washing with water the roots retained on a 2 mm size mesh. The oven-dried weight of the leaf, stem, cutting, and root biomass was measured for each tree after oven-drying at 70ºC to constant weight.

The water-use efficiency (WUE) of biomass production was determined for each tree. This was the ratio of the total biomass to the total amount of water used throughout the growing season (g biomass kg^{-1} water). The total biomass included the oven-dried leaf, stem and root weight, and the cutting weight minus the original cutting weight at the start of the experiment.

2.2.13 Statistical analysis

Analysis of variance (ANOVA) and covariance (ANCOVA) were used to assess the effects of the water regime, poplar clone and block (covariate), and the water regime × poplar clone interaction, on the various traits measured. The cutting diameter at the beginning of the experimental treatment period (70 days) was used as an additional covariate in the ANCOVA in order to statistically consider the effects of the initial plant size on the traits. Fisher's least-significant-difference LSD test was used to provide multiple comparisons of the poplar clone and water regime means. All the statistics were computed using the GenStat statistical software package (Version 14.2; VSN International Ltd, UK).

2.3 Results

2.3.1 Growth of the poplar trees prior to the soil water deficits

The poplar trees were grown at 90% of field capacity (FC) for 70 days, prior to the application of the soil water deficits of the 60% and 40% FC water regime treatments. During this period, the 'Veronese' clone had the fastest growth, with greater shoot biomass, shoot length, and leaf area (Table 3, Figure 3), while the TN008, TN014, and MT304 clones had slower growth, and the MT103 clone had the slowest growth. The number of leaves on the TN008 clone increased rapidly from 50 to 70 days (Figure 3), and it had a higher number of leaves than the other clones at 70 days. This could be attributed to the smaller size of the leaves, and to the large number of callus shoots that grew from the top of the cuttings of the TN008 clone.

2.3.2 Growth of the poplar trees after the application of soil water deficits

The application of the moderate and severe soil water deficits of the 60 and 40% FC water regime treatments, from 70 to 119 days, had a noticeable effect on the growth of the poplar trees and the number of leaves.

The 'Veronese', TN008 and TN014 clones showed leaf senescence on the lower parts of the stems within 8 days of the commencement of the water regime treatments (Figure 4). The number of leaves on the 'Veronese' 40 and 60% FC trees declined and remained at reduced levels on the 40% FC trees, and increased only slightly for the 60% FC trees, while the 'Veronese' 90% FC trees showed a large and continued increase in the number of leaves. The TN008 and TN014 clones showed a decline in the number of leaves on the 40% FC trees, but these and the 60% FC trees then showed a slow increase in the number of leaves that was less than for the 90% FC trees. The MT103 and MT304 clones showed no leaf senescence in response to the soil water deficits of the water regimes, but the number of leaves increased more slowly for the 60% and 40% FC trees, compared with 90% FC trees.

The height growth of the shoots was slower for the 60 and 40% FC water regime treatments ($P < 0.001$), compared with the 90% FC treatment (Figure 5). This was particularly noticeable

for the 'Veronese' and TN008 and TN014 clones, which had dropped their lower leaves in response to the moderate and severe soil water deficits. These clones had slower height growth than the MT103 and MT304 clones at 60 and 40% FC, and the 'Veronese' and TN008 clones also had slower height growth at 90% FC. The height growth of some of the 'Veronese' and TN014 clone trees stopped at 60% and 40% FC, and some shoot tip die-back was observed during the last 3 weeks.

The shoot tip die-back occurred in all the water regimes and poplar clones. The 60% FC water regime had a higher incidence of shoot tip die-back ($P < 0.001$), with 50% of the shoots affected at 112 days compared with 16 and 20% for the 40 and 90% FC treatments. The TN014 and MT103 poplar clones were the worst affected, with shoot tip die-back in 45 and 42% of the shoots at 112 days, compared with 30, 24, and 2% of the shoots for the MT304, 'Veronese', and TN008 clones ($P < 0.001$). The necrotic (dead) tissue from the shoot tips was placed onto bacterial isolating media and monitored for growth, but nothing grew, indicating that there was no bacterial or fungal infection associated with the shoot tip die-back.

The diameter growth of the cuttings of the poplar trees, from which the shoots had sprouted, was slower for the 60 and 40% FC water regime treatments ($P < 0.001$) than the 90% FC treatment (Figure 6). The diameter growth slowed progressively with the increasing severity of the soil water deficits for all the poplar clones, with the exception of the MT103 clone, where the diameter growth was slightly slower for the 60% FC water regime, and much slower for the 40% FC water regime than with the 90% FC trees.

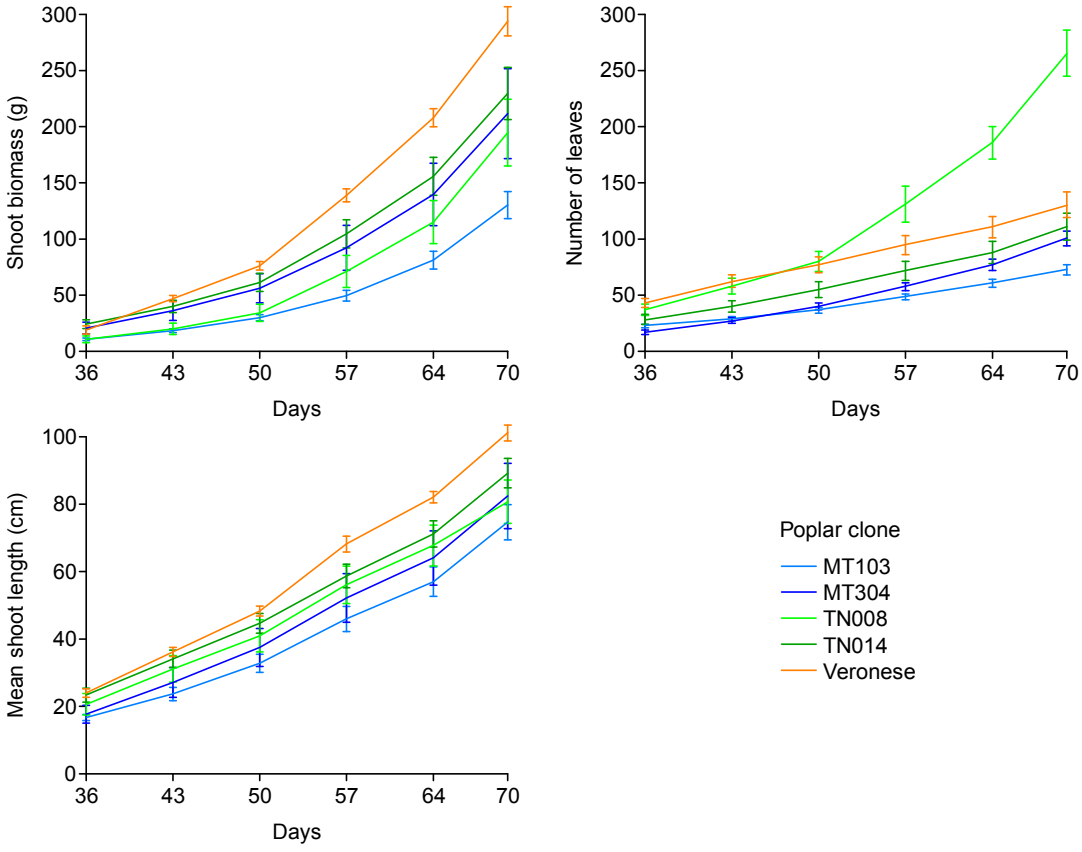

Figure 3. Growth to 70 days of the fresh shoot biomass (leaf + stem), number of leaves (per tree), and mean shoot height (for the tallest shoot per tree) of the poplar clones, prior to the application of the water regimes. The error bars are the standard errors of the means.

Table 3. Shoot biomass (fresh leaf + stem weight), leaf area, number of leaves, and mean shoot height for the tallest shoot per tree, of the poplar clones at 70 days from planting. Values are the mean ± standard error, and different letters represent significant differences among the water regimes within the same clone (*P* < 0.05).

Clone	Shoot biomass Leaf + stem g	Leaf area cm^2	Number of leaves	Mean shoot height cm
MT103	130 ± 12 a	265 ± 33 a	73 ± 4 a	75 ± 5 a
MT304	212 ± 40 b	387 ± 89 a	101 ± 7 ab	82 ± 10 a
TN008	195 ± 30 ab	397 ± 46 a	265 ± 20 c	81 ± 6 a
TN014	230 ± 23 bc	344 ± 30 a	111 ± 12 b	89 ± 4 ab
'Veronese'	294 ± 13 c	546 ± 32 b	130 ± 11 b	101 ± 2 b

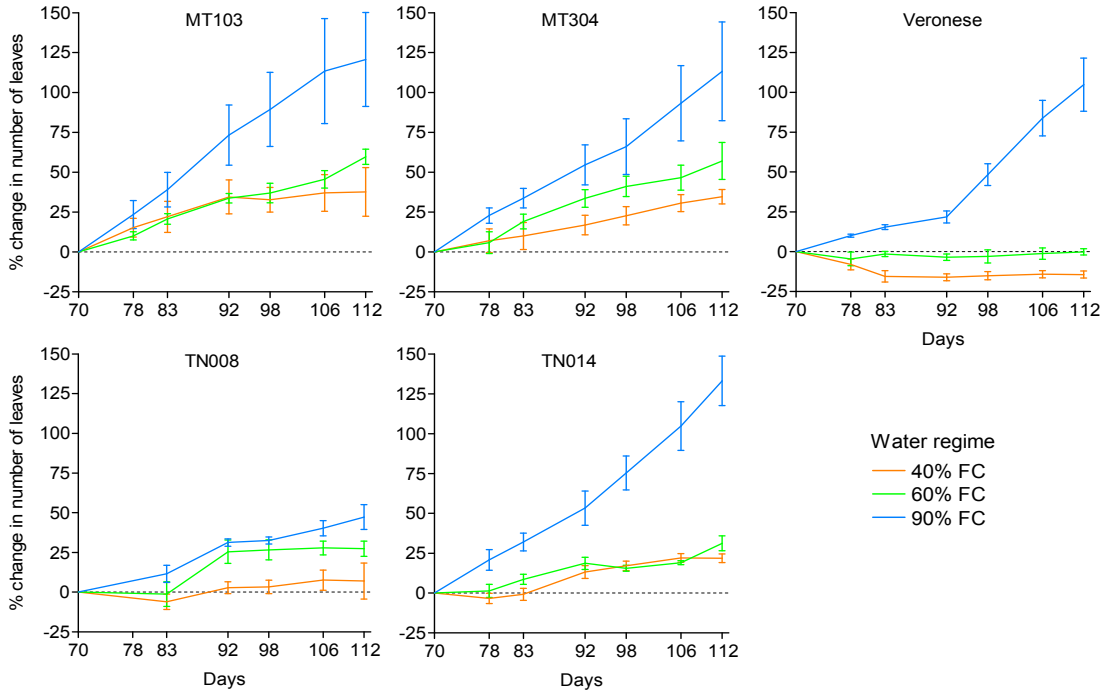

Figure 4. Change in the number of leaves on the trees of the poplar clones, following the application of the water regimes from 70 days. The water regimes were 40, 60, and 90% of field capacity (FC). The error bars are the standard errors of the means.

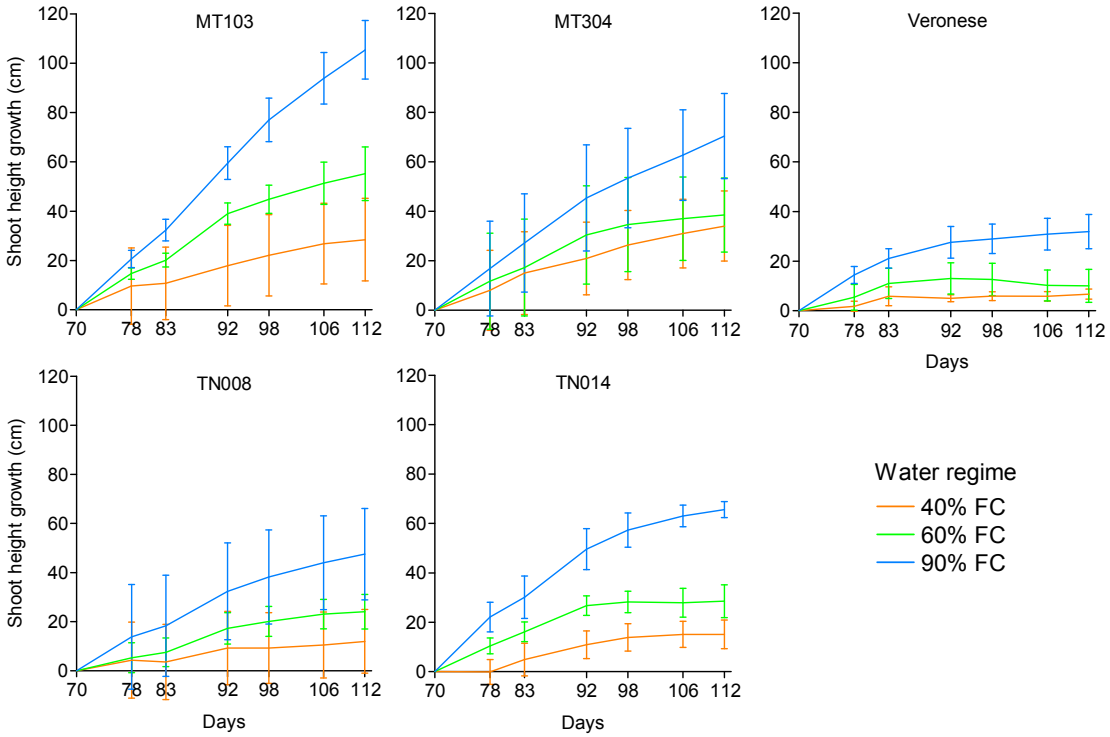

Figure 5. Mean growth of shoot height (tallest shoot per tree) of the poplar clones, following the application of the water regimes at 70 days. The water regimes were 40, 60, and 90% of field capacity (FC). The error bars are the standard errors of the means.

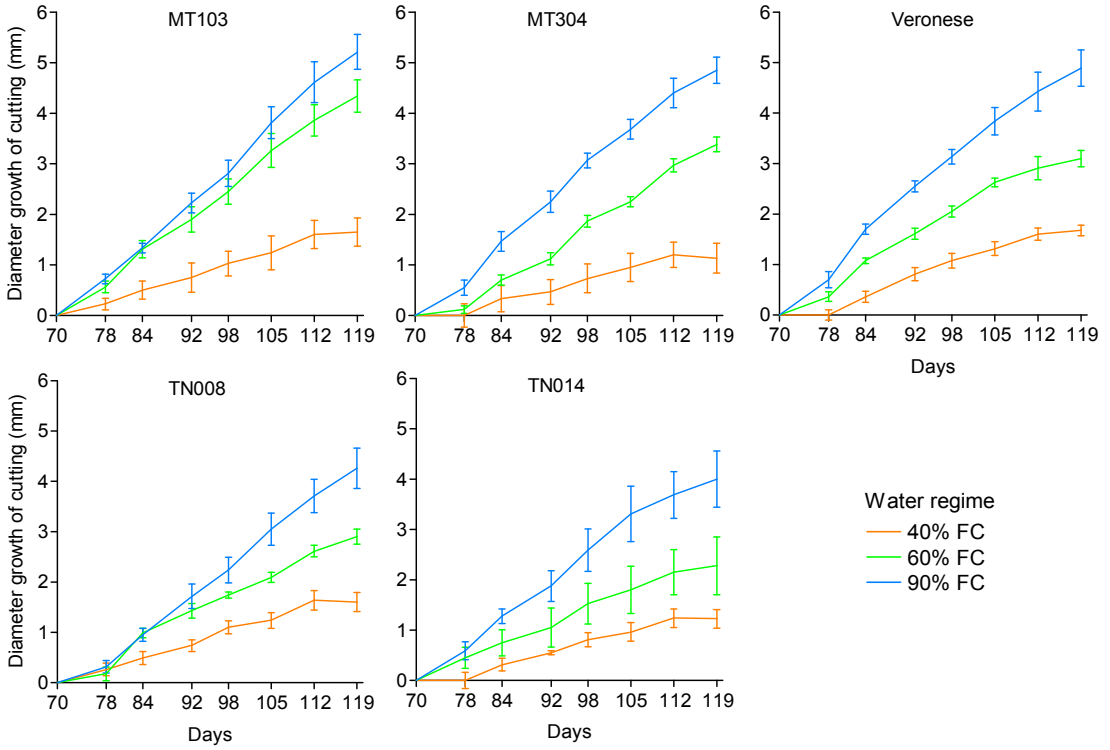

Figure 6. Mean growth in cutting diameter of the poplar clones, following the application of the water regimes at 70 days. The water regimes were 40, 60, and 90% of field capacity (FC). The error bars are the standard errors of the means.

2.3.3 Water content of the soil after the application of soil water deficits

The application of the moderate and severe soil water deficits of the 60 and 40% FC water regime treatments reduced the soil water content of the 30-L pots to lower levels ($P < 0.001$), compared with the 90% FC treatment (Figure 7). The reduction in the soil water content of the pots occurred within 10 days of the start of the water regimes for the 60% FC treatment, but more slowly for the 40% FC treatment, taking about 30 days for MT103 and MT304.

At 107 days there was no significant difference in the soil water content of the 40% FC water regime treatment for the poplar clones, but there were significant differences between the clones for the 90 and 60% FC treatments ($P = 0.007$). TN008, TN014, and 'Veronese' reduced the soil water content to lower levels, compared with MT103 and MT304 (Figure 8). The differences were larger for the 90% FC treatment than for the 60% FC treatment, with much of the difference occurring on the second day of the 2-day watering cycle.

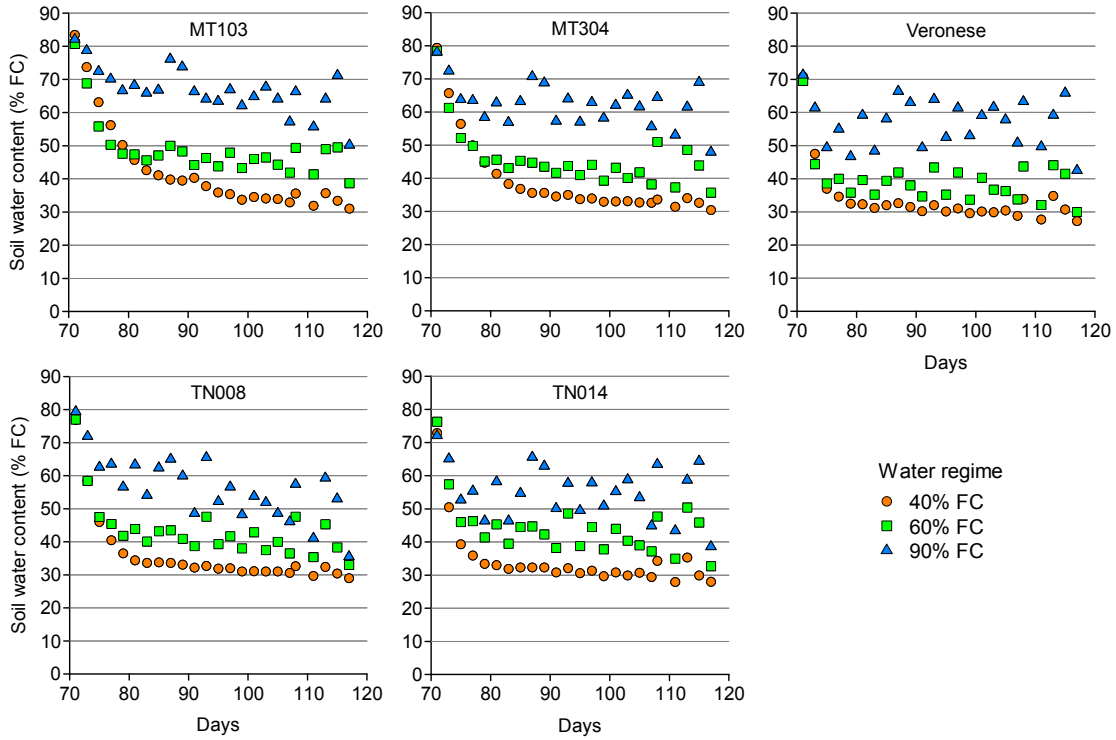

Figure 7. Water content of the soil of the poplar clones and water regimes from 70 to 119 days, after the application of the water regimes. Minimum values of soil water content during the 2-day watering cycle, as a percent of the field capacity. The water regimes were 40, 60, and 90% of field capacity (FC).

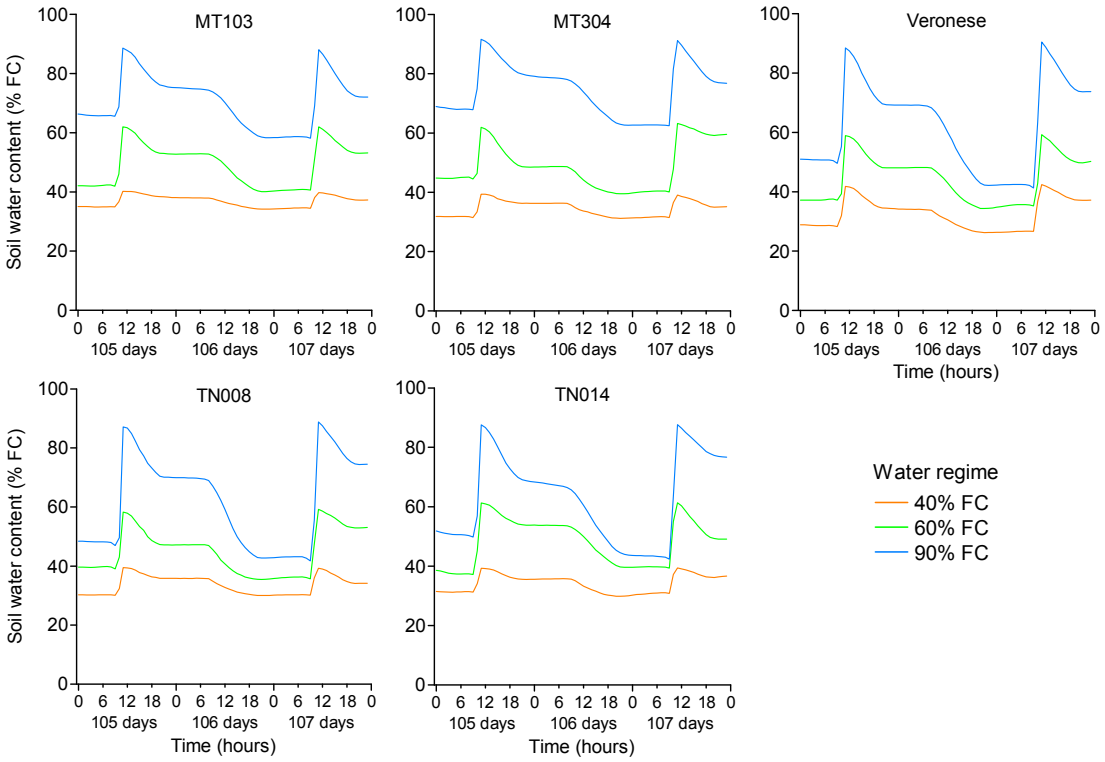

Figure 8. Water content of the soil of the poplar clones and water regimes, between watering cycles on days 105 to 107. Hourly average values of soil water content, as a percent of the field capacity. The water regimes were 40, 60, and 90% of field capacity (FC).

2.3.4 Biomass of the poplar trees at harvest

The soil water deficits of the water regime treatments and the poplar clones had a large effect on the leaf, stem and root biomass of the poplar trees at harvest, and on the water use efficiency of the trees, after 119 days of growth (Figure 9).

The leaf area and number of leaves on the trees was lower for the 60 and 40% FC water regime treatments than the 90% FC treatment for all the poplar clones (Tables 4 and 5). There were significant differences between the poplar clones, with the TN008 clone having a greater leaf area and number of leaves than the other clones. This clone had higher leaf specific area (leaf area per dry weight of leaf) and smaller size leaves than the other clones.

The leaf, stem and root biomass of the poplar trees at 119 days was lower for the 60 and 40% FC water regime treatments than the 90% FC treatment (Tables 6 and 7). There was a progressive decrease in the leaf and stem biomass of the trees with the increasing severity of the soil water deficits, but the root biomass showed a significant decrease only for the severe soil water deficit of the 40% FC treatment. When compared as a percentage of the total biomass, the allocation of the biomass to the stems decreased and the allocation to the roots increased with the application of the 60% and 40% FC water regime treatments.

The amount of water used and the dry weight (DW) gain of biomass by the poplar trees was lower and the water-use efficiency (WUE) and root-to-shoot ratio was higher for the 60 and 40% FC water regime treatments than the 90% FC treatment (Tables 8 & 9). There was a progressive decrease in the amount of water used and in the DW gained, and a progressive increase in the water-use efficiency (WUE) of the trees, with the increasing severity of the soil

water deficits. In contrast, the increase in the root-to-shoot ratio was similar for the 60 and 40% FC treatments.

The poplar clones showed significant differences in the water-use efficiency (WUE) of the water regime treatments (Tables 8 & 9). The differences were larger for the 60 and 40% FC water regime treatments, with the MT103, MT304, and TN008 clones having higher water-use efficiency (WUE) than the TN014 and 'Veronese' clones.

2.3.5 Leaf stomatal conductance and density, and water potential

The soil water deficits of the 60 and 40% FC water regimes had a large effect on the stomatal conductance and water potential of the leaves of the poplar trees (Tables 10 & 11). The stomatal conductance of the abaxial (lower) surface of the leaves, and the water potential of the leaves, decreased with the increasing severity of the soil water deficits. The leaves of the trees of the 60 and 40% FC water regime treatments had lower stomatal conductance and water potential than the 90% FC treatment. An exception was the TN008 clone, where the water potential of the trees did not decrease with lower stomatal conductance at 60% and 40% FC. The stomatal conductance of this clone was low, with the 60% and 40% FC treatments having the lowest stomatal conductance values of all the poplar clones.

The poplar clones showed significant differences in the stomatal conductance of the leaves, with the TN008 and 'Veronese' clones having lower stomatal conductance than the MT103, MT304, and TN014 clones at 90% FC (Tables 10 & 11). This might be attributed in part to the lower stomatal density of the abaxial surface of the leaves for the TN008 and 'Veronese' clones than the other poplar clones. The stomatal density on the adaxial surface of the leaves of the poplar clones was much lower than on the abaxial surface, with the 'Veronese' clone having the highest values of about half that of the abaxial (lower) surface of the leaves.

MT103

MT304

TN008

TN014

'Veronese'

Figure 9. Trees of the poplar clones and water regime treatments at 119 days. The trees of each clone are from left to right: well-watered (90% FC), moderate (60% FC), and severe (40% FC) soil water deficit treatments, with the three trees of each clone from block 1 or 2.

Table 4. Leaf area, number of leaves per tree, leaf size and specific leaf area of the poplar clones at harvest (119 days) as affected by the water regimes. Values are the mean ± standard error, and different letters represent significant differences among the water regimes within the same clone ($P < 0.05$).

Clone	Water regime	Leaf area m^2	Number of leaves	Leaf size cm^2	Specific leaf area $cm^2\ g^{-1}$
MT103	40% FC	0.54 ± 0.04 a	124 ± 40 a	60 ± 15 a	116 ± 10 a
	60% FC	0.69 ± 0.08 ab	119 ± 8 a	59 ± 5 a	98 ± 3 a
	90% FC	0.93 ± 0.05 b	141 ± 28 a	78 ± 14 a	109 ± 0 a
MT304	40% FC	0.68 ± 0.16 a	112 ± 29 a	76 ± 19 a	112 ± 3 a
	60% FC	1.02 ± 0.11 b	139 ± 23 a	76 ± 8 a	117 ± 3 a
	90% FC	1.36 ± 0.09 c	279 ± 55 b	56 ± 12 a	124 ± 10 a
TN008	40% FC	1.01 ± 0.10 a	498 ± 85 a	22 ± 3 a	158 ± 3 a
	60% FC	1.69 ± 0.09 b	667 ± 72 b	26 ± 2 a	186 ± 22 b
	90% FC	2.27 ± 0.13 c	690 ± 56 b	33 ± 1 a	170 ± 2 ab
TN014	40% FC	0.78 ± 0.03 a	127 ± 31 a	67 ± 11 a	119 ± 3 a
	60% FC	0.84 ± 0.13 a	170 ± 45 a	55 ± 11 a	120 ± 4 a
	90% FC	1.37 ± 0.10 b	319 ± 37 b	42 ± 4 a	115 ± 4 a
'Veronese'	40% FC	0.85 ± 0.10 a	111 ± 20 a	76 ± 5 a	120 ± 4 a
	60% FC	0.99 ± 0.10 ab	137 ± 17 a	70 ± 5 a	124 ± 3 a
	90% FC	1.15 ± 0.22 b	220 ± 15 a	51 ± 9 a	119 ± 5 a

Table 5. Analysis of covariance for the fixed effects of poplar clone and water regime, and the interactions between them, on the leaf area, number of leaves, leaf size and specific leaf area (SLA).

Source of variation	d.f.	Leaf area		No. of leaves		Leaf size		SLA	
		MS	P	MS	P	MS	P	MS	P
Block	3	0.04	0.327	3E+3	0.720	506	0.253	170	0.505
Initial cutting diameter	1	0.26	0.007	—	—	—	—	—	—
Clone	4	1.38	<.001	506E+3	<.001	3509	<.001	7463	<.001
Water regime	2	2.07	<.001	94E+3	<.001	306	0.433	63	0.745
Clone × water regime	8	0.15	<.001	9E+3	0.361	550	0.175	306	0.213
Error	41	0.03		8E+3		359		214	

Block and initial cutting diameter (mm) at the start of the water regimes (70 days) were used as covariates.
d.f., Degrees of freedom; MS, mean squares (variance); *P*, probability value

Table 6. Allocation of biomass to the leaves, stems and roots of the poplar clones at harvest (119 days) as affected by the water regimes. Values are the mean ± standard error, and different letters represent significant differences among the water regimes within the same clone ($P < 0.05$).

	Water	Biomass (g)			Biomass (%)		
Clone	regime	Leaf	Stem	Root	Leaf	Stem	Root
MT103	40% FC	48 ± 5 a	42 ± 7 a	20 ± 3 a	44	38	18
	60% FC	67 ± 7 b	73 ± 6 b	32 ± 3 b	39	42	19
	90% FC	85 ± 4 c	98 ± 5 c	30 ± 2 b	40	46	14
MT304	40% FC	59 ± 13 a	53 ± 14 a	24 ± 5 a	43	39	18
	60% FC	88 ± 11 b	91 ± 16 b	42 ± 7 b	40	41	19
	90% FC	111 ± 8 c	135 ± 22 c	37 ± 6 b	39	48	13
TN008	40% FC	63 ± 5 a	65 ± 9 a	25 ± 3 a	41	42	16
	60% FC	95 ± 13 b	99 ± 18 b	36 ± 6 b	41	43	16
	90% FC	133 ± 7 c	140 ± 20 c	40 ± 5 b	43	45	13
TN014	40% FC	66 ± 4 a	59 ± 3 a	28 ± 3 a	43	39	18
	60% FC	70 ± 9 a	81 ± 11 b	37 ± 5 b	37	43	20
	90% FC	119 ± 5 b	147 ± 10 c	38 ± 6 b	39	48	13
'Veronese'	40% FC	70 ± 6 a	65 ± 5 a	29 ± 4 a	43	40	17
	60% FC	80 ± 6 ab	84 ± 7 a	44 ± 3 b	38	41	21
	90% FC	96 ± 15 b	120 ± 16 b	47 ± 9 b	37	46	18

Table 7. Analysis of covariance for the fixed effects of poplar clone and water regime, and the interactions between them, on the leaf, stem and root biomass.

		Leaf biomass		Stem biomass		Root biomass	
Source of variation	d.f.	MS	P	MS	P	MS	P
Block	3	0.4E+3	0.063	2.5E+3	<.001	233	<.001
Initial cutting diameter	1	2.4E+3	<.001	3.6E+3	<.001	625	<.001
Clone	4	1.2E+3	<.001	1.2E+3	<.001	138	0.008
Water regime	2	11.4E+3	<.001	25.7E+3	<.001	1141	<.001
Clone × water regime	8	0.4E+3	0.009	0.4E+3	0.057	22	0.748
Error	41			0.2E+3		35	

Block and initial cutting diameter (mm) at the start of the water regimes (70 days) were used as covariates.
d.f., Degrees of freedom; MS, mean squares (variance); *P*, probability value

Table 8. Water usage, dry weight (DW) gain, and water use efficiency (WUE) from 0 to 119 days, and the root-to-shoot ratio of the poplar clones. Values are the mean ± standard error, and different letters represent significant differences among the water regimes within the same clone ($P < 0.05$)

Clone	Water regime	Water use kg	DW gain g	WUE g DW kg^{-1} water	Root-to-shoot ratio
MT103	40% FC	23 ± 4 a	124 ± 7 a	5.5 ± 0.3 c	0.22 ± 0.02 b
	60% FC	44 ± 3 b	201 ± 15 b	4.6 ± 0.1 b	0.24 ± 0.02 b
	90% FC	64 ± 4 c	246 ± 12 c	3.9 ± 0.2 a	0.16 ± 0.01 a
MT304	40% FC	29 ± 7 a	157 ± 43 a	5.3 ± 0.1 c	0.22 ± 0.02 b
	60% FC	52 ± 8 b	270 ± 6 b	4.8 ± 0.0 b	0.23 ± 0.01 b
	90% FC	77 ± 9 c	334 ± 21 c	4.1 ± 0.0 a	0.15 ± 0.01 a
TN008	40% FC	33 ± 4 a	173 ± 17 a	5.3 ± 0.3 c	0.20 ± 0.00 b
	60% FC	56 ± 7 b	261 ± 39 b	4.6 ± 0.2 b	0.19 ± 0.01 b
	90% FC	89 ± 9 c	351 ± 36 c	4.0 ± 0.1 a	0.14 ± 0.01 a
TN014	40% FC	38 ± 3 a	176 ± 11 a	4.6 ± 0.2 b	0.22 ± 0.02 b
	60% FC	55 ± 6 b	211 ± 28 a	3.7 ± 0.1 a	0.24 ± 0.01 b
	90% FC	98 ± 4 c	345 ± 25 b	3.5 ± 0.1 a	0.14 ± 0.01 a
'Veronese'	40% FC	49 ± 2 a	194 ± 15 a	3.9 ± 0.3 b	0.21 ± 0.01 a
	60% FC	72 ± 1 b	246 ± 17 b	3.4 ± 0.2 a	0.26 ± 0.01 b
	90% FC	99 ± 10 c	312 ± 46 c	3.1 ± 0.2 a	0.21 ± 0.01 a

Table 9. Analysis of covariance for the fixed effects of poplar clone and water regime, and the interactions between them, on the water used, dry weight (DW) gain, water use efficiency (WUE), and the root-to-shoot ratio (RSR).

Source of variation	d.f.	Water use		DW gain		WUE		RSR	
		MS	P	MS	P	MS	P	MS	P
Block	3	0.3E+3	<.001	9E+3	<.001	0.25	0.124	0.4E-3	0.610
Initial cutting diameter	1	0.6E+3	<.001	15E+3	<.001	0.53	0.043	—	—
Clone	4	0.9E+3	<.001	6E+3	<.001	2.82	<.001	4.4E-3	<.001
Water regime	2	13.2E+3	<.001	116E+3	<.001	7.51	<.001	27.0E-3	<.001
Clone × water regime	8	0.1E+3	0.080	2E+3	0.042	0.10	0.615	1.4E-3	0.032
Error	41	0.1E+3		1E+3		0.12		0.6E-3	

Block and initial cutting diameter (mm) at the start of the water regimes (70 days) were used as covariates.
d.f., Degrees of freedom; MS, mean squares (variance); P, probability value

The diurnal variation in the stomatal conductance of the leaves from 8:00 to 17:00 hours showed the stomatal conductance declined during the day, with large differences between the water regimes (Figure 10). The leaves of the 40% FC water regime trees had low values of stomatal conductance that declined very quickly in the morning and remained low through the day. The leaves of the 60% FC and 90% FC water regime trees had higher values in the

morning, with the stomatal conductance of the 60% FC trees declining to lower values during the day than the 90% FC trees.

The maturity and position of the leaves on the stems had a large effect on the stomatal conductance of the leaves, with contrasting trends between the poplar clones (Figure 11). The stomatal conductance increased with the maturity of the leaves, from the apex of the stems, and remained high to the base of the stem for the 'Veronese' clone. In contrast, the stomatal conductance of MT103, MT304, and TN014 clones increased with the maturity of the leaves, and then peaked and declined for the older leaves on the lower part of the stems. For the TN008 clone, the stomatal conductance of the leaves peaked close to the apex on the stems, on the young maturing leaves, and then declined and remained lower for the older leaves along the length of the stems.

2.3.6 Leaf chlorophyll, antioxidant enzymes, and free proline

The chlorophyll content of the leaves of the poplar trees was not affected by the soil water deficits of the water regimes, and there was only a slight reduction in the chlorophyll content from the first to seventh week of the water regime treatments (Tables 12 & 13). The main differences were between the poplar clones. The chlorophyll content of the leaves of the TN008 clone was higher at 78 days, but the differences diminished during the 7 weeks of the water regimes, with no significant difference between the clones at 119 days.

The superoxide dismutase (SOD) activity of the leaves increased from the first to seventh week, following the application of the water regime treatments, for all the poplar clones (Tables 12 & 13). The increase in the SOD activity was largest for the 90% FC water regime treatment, and least for the 40% FC treatment.

The ascorbate peroxidase (APX) and guaiacol peroxidase (GPX) activity of the leaves was much higher for the 'Veronese' clone (2 to 5 times higher) than the other poplar clones (Tables 12 & 13). The application of the soil water deficits of the water regime treatments had no effect on the APX activity of the leaves, but the GPX activity of the leaves increased from the first to seventh week of the water regimes for all the poplar clones. The leaves of the MT304, TN008 and TN014 clones showed an increase in the GPX activity for the 60 and 40% FC water regime treatments, but this was not observed for the MT103 and 'Veronese' clones.

The free proline content of the leaves showed no significant change during the 7 weeks of the water regimes, and no significant differences between the water regime treatments or the poplar clones (Tables 12 & 13).

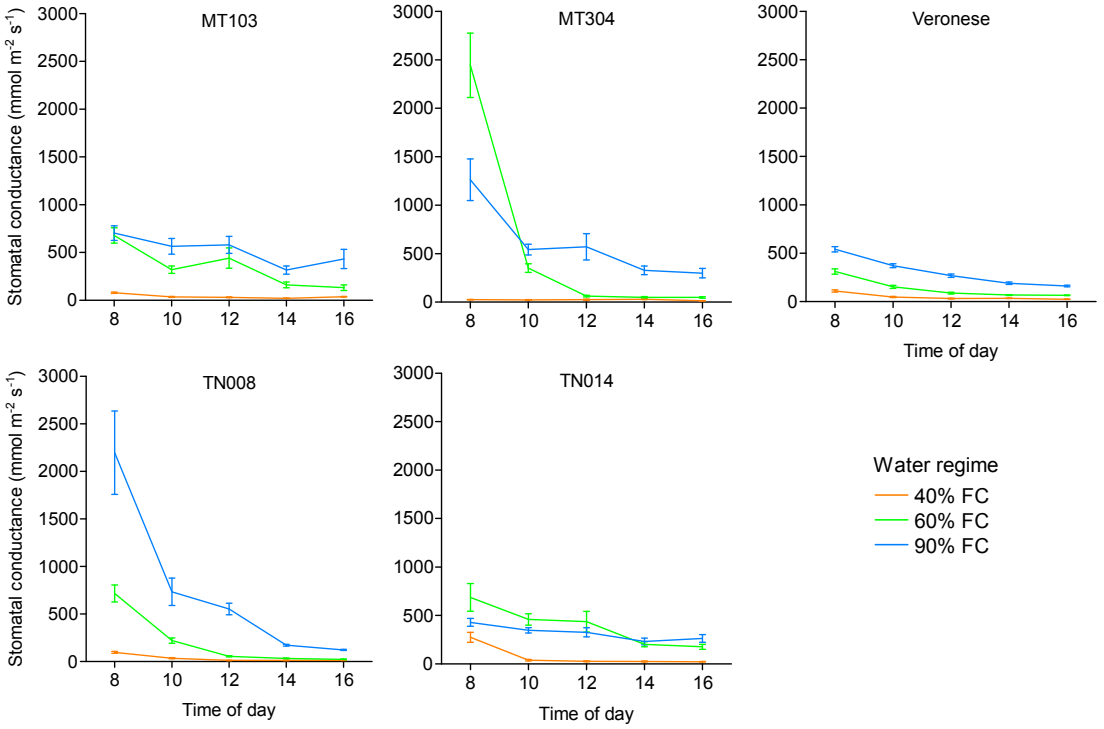

Figure 10. Diurnal variation in the leaf stomatal conductance (lower surface of the leaves) of the poplar trees, following the application of the water regimes (average of the diurnal measurements at 84, 94, 98, and 106 days). The water regimes were 40, 60, and 90% of field capacity (FC). The error bars are the standard errors of the means.

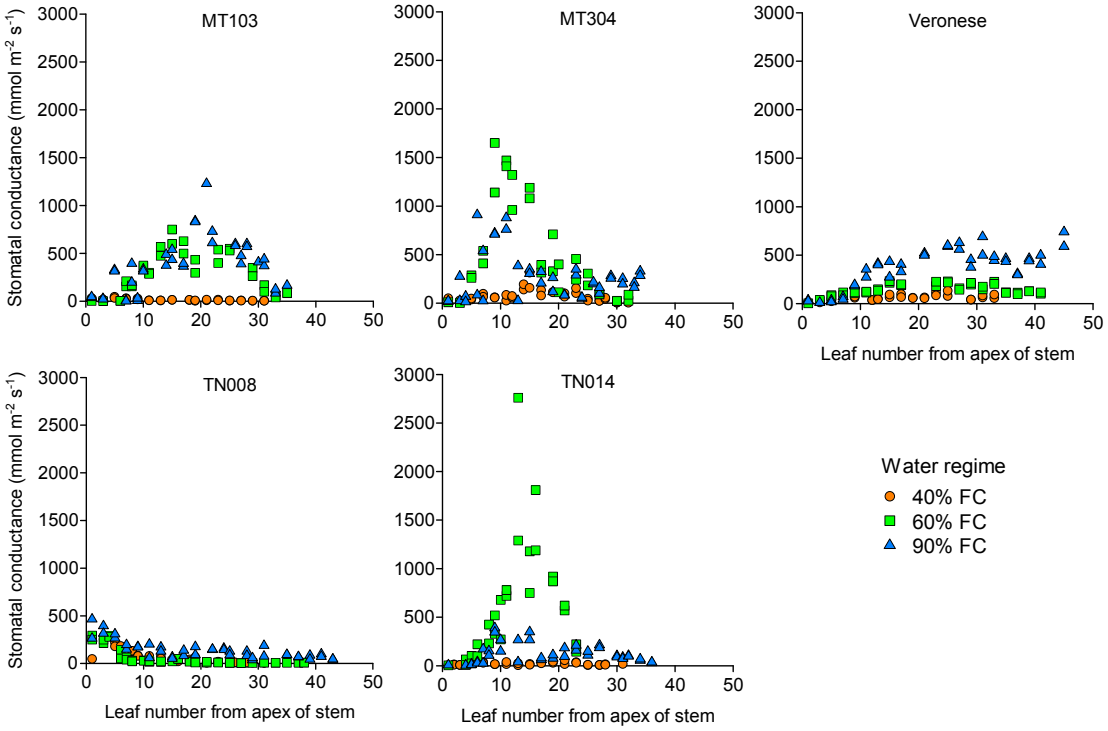

Figure 11. Stomatal conductance (lower surface of the leaves) for leaf number 6–10 from the apex of the stems of the poplar trees, following the application of the water regimes at 103 to 107 days. The water regimes were 40, 60, and 90% of field capacity (FC).

Table 10. Leaf stomatal conductance (lower leaf surface), stomatal density (upper and lower leaf surfaces), and water potential of the poplar clones at the different water regimes. Values are the mean ± standard error, and different letters represent significant differences among the water regimes within the same clone (*P* < 0.05).

Clone	Water regime	Stomatal conductance mmol m^{-2} s^{-1}	Stomatal density Adaxial mm^{-2}	Stomatal density Abaxial mm^{-2}	Water potential MPa
MT103	40% FC	164 ± 57 a	49 ± 7 b	339 ± 4 a	-1.03 ± 0.12 a
	60% FC	308 ± 61 a	33 ± 8 a	265 ± 40 a	-0.90 ± 0.10 a
	90% FC	1048 ± 173 b	43 ± 5 ab	265 ± 30 a	-0.71 ± 0.05 a
MT304	40% FC	129 ± 67 a	26 ± 10 a	348 ± 52 a	-1.15 ± 0.13 b
	60% FC	283 ± 99 a	26 ± 6 a	280 ± 59 a	-0.94 ± 0.13 ab
	90% FC	849 ± 240 b	23 ± 4 a	297 ± 14 a	-0.64 ± 0.07 a
TN008	40% FC	28 ± 9 a	27 ± 3 a	127 ± 11 a	-0.76 ± 0.18 a
	60% FC	90 ± 36 a	31 ± 3 a	180 ± 7 a	-0.64 ± 0.15 a
	90% FC	480 ± 238 b	31 ± 3 a	150 ± 6 a	-0.82 ± 0.11 a
TN014	40% FC	57 ± 16 a	26 ± 4 a	453 ± 119 b	-1.09 ± 0.19 b
	60% FC	332 ± 105 a	37 ± 3 a	285 ± 32 a	-0.94 ± 0.16 ab
	90% FC	797 ± 116 b	34 ± 3 a	307 ± 54 a	-0.74 ± 0.07 a
'Veronese'	40% FC	62 ± 18 a	89 ± 1 a	188 ± 13 a	-1.20 ± 0.15 b
	60% FC	155 ± 28 a	95 ± 14 a	194 ± 35 a	-0.96 ± 0.11 ab
	90% FC	219 ± 31 a	88 ± 10 a	158 ± 24 a	-0.72 ± 0.03 a

Table 11. Analysis of variance for the fixed effects of poplar clone and water regime, and the interactions between them, on the stomatal conductance and density (upper and lower surface of the leaves), and the water potential, of the leaves of the poplar clones.

		Stomatal conductance		Stomatal density Upper		Stomatal density Lower		Water potential	
Source of variation	d.f.	MS	P	MS	P	MS	P	MS	P
Block	3	2.3E+5	0.078	6.7E+2	0.001	14.6E+3	0.132	73.7	<.001
Clone	4	5.7E+5	<.001	86.0E+2	<.001	86.7E+3	<.001	16.7	0.190
Water regime	2	37.9E+5	<.001	0.0E+2	0.968	18.6E+3	0.092	101.8	<.001
Clone × water regime	8	2.0E+5	0.048	1.2E+2	0.345	7.7E+3	0.413	11.9	0.361
Error	102	1.0E+5		1.1E+2		7.3E+3		10.7	

The error degrees of freedom for stomatal density (upper and lower leaf surfaces) was 37.
d.f., Degrees of freedom; MS, mean squares (variance); *P*, probability value.

Table 12. Leaf chlorophyll, SOD, APX and GPX activity, and free proline content of the poplar clones and water regimes at 119 days. Values are the mean ± standard error, and different letters represent significant differences among the water regimes within the same clone (*P* < 0.05).

Clone	Water regime	Chlorophyll µg mL^{-1}	SOD activity units mg^{-1} protein	APX activity mmol min^{-1} µg^{-1} protein	GPX activity mmol min^{-1} µg^{-1} protein	Free proline µg g^{-1} FW
MT103	40% FC	19.6 ± 0.8 b	0.81 ± 0.16 a	0.21 ± 0.03 a	2.32 ± 0.74 a	42.5 ± 3.0 a
	60% FC	20.7 ± 2.9 b	1.12 ± 0.12 a	0.16 ± 0.04 a	2.34 ± 1.11 a	38.3 ± 14.6 a
	90% FC	15.0 ± 1.5 a	1.67 ± 0.30 a	0.11 ± 0.04 a	2.92 ± 1.24 a	39.5 ± 1.8 a
MT304	40% FC	18.3 ± 1.6 a	0.79 ± 0.12 a	0.17 ± 0.08 a	3.09 ± 1.05 a	18.2 ± 10.1 a
	60% FC	16.0 ± 0.3 a	1.08 ± 0.26 a	0.15 ± 0.04 a	1.99 ± 0.56 a	53.8 ± 11.2 b
	90% FC	14.0 ± 0.7 a	1.53 ± 0.24 a	0.12 ± 0.08 a	1.72 ± 0.64 a	30.2 ± 0.9 ab
TN008	40% FC	22.1 ± 1.9 b	0.71 ± 0.17 a	0.13 ± 0.02 a	2.17 ± 0.46 a	39.6 ± 3.7 a
	60% FC	18.9 ± 2.7 a	0.72 ± 0.27 a	0.30 ± 0.06 a	1.61 ± 0.22 a	54.3 ± 7.4 a
	90% FC	19.3 ± 2.7 a	1.48 ± 0.24 a	0.17 ± 0.07 a	1.54 ± 0.34 a	39.6 ± 18.4 a
TN014	40% FC	15.8 ± 1.1 a	0.98 ± 0.12 a	0.24 ± 0.02 a	3.08 ± 0.84 a	26.7 ± 18.0 a
	60% FC	16.6 ± 1.6 a	1.65 ± 0.75 a	0.37 ± 0.22 a	3.76 ± 1.18 a	34.1 ± 11.4 a
	90% FC	14.2 ± 1.4 a	1.71 ± 0.51 a	0.23 ± 0.03 a	1.91 ± 0.56 a	39.0 ± 21.6 a
Veronese	40% FC	16.7 ± 1.9 a	0.92 ± 0.13 a	0.48 ± 0.04 ab	14.95 ± 1.14 a	19.1 ± 7.4 a
	60% FC	19.3 ± 0.4 a	0.77 ± 0.27 a	0.72 ± 0.26 b	19.78 ± 3.98 b	27.9 ± 2.3 a
	90% FC	17.7 ± 0.9 a	0.91 ± 0.19 a	0.36 ± 0.08 a	17.55 ± 2.96 ab	21.6 ± 0.5 a

Table 13. Analysis of variance for fixed effects of poplar clone and water regime, and the interaction between them, on the leaf chlorophyll, SOD, APX and GPX activity, and free proline content.

Source of variation	d.f.	Chlorophyll		SOD activity		APX activity		GPX activity		Free proline	
		MS	P	MS	P	MS	P	MS	P	MS	P
Block	1	13.9	0.247	0.3	0.361	0.8E-2	0.637	0.5	0.743	0	1.000
Week	1	31.5	0.085	5.9	<.001	0.1E-2	0.886	153.7	<.001	165	0.682
Clone	4	41.3	0.007	0.6	0.184	28.3E-2	<.001	546.1	<.001	788	0.523
Week × clone	4	20.4	0.110	0.6	0.218	12.4E-2	0.013	18.1	0.009	614	0.640
Water regime	2	36.2	0.037	2.0	0.009	10.8E-2	0.052	4.0	0.427	1010	0.361
Clone × water regime	8	10.7	0.410	0.2	0.800	2.4E-2	0.689	6.5	0.220	782	0.598
Error	39	10.1		0.4		3.4E-2		4.6		966	

d.f., Degrees of freedom; MS, mean squares (variance); *P*, probability value.

2.4 Discussion

The physiological responses of the poplar clones to the soil water deficits of the water regimes differed for the poplar hybrids, and may reflect the inherited traits of the parent species.

The 'Veronese' clone is a *P. deltoides* × *P. nigra* hybrid, and had a conservative response to the soil water deficits, with the loss of leaves on the lower part of the stems to reduce the water transpiration and an abrupt reduction in the stem height and leaf growth for the 60 and 40% FC water regime treatments. This clone appeared to be particularly responsive to soil water deficits, with the 90% FC treatment trees having slower shoot growth and a higher allocation of biomass to the roots, similar to the 60 and 40% FC treatments. This was not seen in the other clones and may have contributed to the higher water use by the 90% FC trees, which experienced moderate to severe soil water deficits during the 2-day watering cycle. The 'Veronese' clone has good drought tolerance mechanisms, but these come at the expense of slower shoot growth and lower water-use efficiency (WUE).

The TN008 and TN014 clones were half-siblings, sharing the same *P. trichocarpa* female parent but having different *P. nigra* male parents. These two clones showed similar responses to the soil water deficits, with the loss of leaves on the lower part of the stems for the 40% FC treatment only; reduced shoot height and leaf growth, particularly for the 40% FC treatment; and high water use by the 90% FC trees, which experienced moderate to severe soil water deficits during the 2-day watering cycle. The responses were similar to the 'Veronese' clone, but the reduction in shoot height and leaf growth was less severe, and despite the moderate to severe soil water deficits experienced by the 90% FC trees, the allocation of biomass to the roots was less than for the 60 and 40% FC treatments. This suggests the TN008 and TN014 clones were less responsive to the soil water deficits than the 'Veronese' clone and would be more vulnerable to drought conditions. This would apply particularly to the TN014 clone, which had a higher use of water for the same dry weight gain and lower water-use efficiency (WUE) than the TN008 clone.

The MT103 and MT304 clones were half-siblings, sharing the same *P. trichocarpa* male parent, but having different *P. maximowiczii* female parents. These two clones showed similar responses to the soil water deficits, with no loss of leaves and better shoot height and leaf growth for the 60 and 40% FC treatments, and lower use of water than the other poplar clones. The 90% FC treatment trees used less water than the other clones and experienced less severe soil moisture deficits during the 2-day watering cycle, with less allocation of biomass to the roots than the 60 and 40% FC treatments. Of the two clones, the MT304 clone had a higher use of water, but also higher dry weight gain than the slower growing MT103 clone. Both clones had high water-use efficiency (WUE), and through a combination of lower water use and high water-use efficiency were able to maintain better shoot growth rates and avoid the severe soil water deficits experienced by the other clones for a longer period of time.

The increased allocation of biomass to the roots in response to soil water deficits has been reported in previous studies of poplar clones (Guo et al. 2010; Yin et al. 2005; Zang et al. 2004), and greater drought tolerance has been observed in poplar clones with a greater allocation of biomass to the roots during the early stages of drought (Tschaplinski et al. 1998). Drought tolerant clones of *P. deltoides* × *P. nigra* have shown greater uptake of water under soil water deficits, and greater shoot height and stem diameter growth, total dry biomass gain, root-to-shoot ratio, and water-use efficiency (WUE) (Guo et al. 2010; Tschaplinski et al. 1998).
The 'Veronese' clone demonstrated these drought tolerant traits, with the exception of shorter shoot height growth and lower WUE, taking instead a more conservative response to the soil

water deficits by allocating more of the biomass to the cutting diameter and root biomass growth and less to the shoot and leaf growth.

The stomatal conductance of the leaves of the poplar clones decreased sharply as the water potential of the leaves declined below -0.8 MPa in response to the soil water deficits. This pattern of stomatal regulation has been observed previously in poplar clones of *P. trichocarpa*, *P. deltoides*, and *P. trichocarpa* × *P. deltoides* as the stomata are closed to reduce the transpiration of water at low water potential (Pezeshki & Hinckley 1982; Bassman & Zwier 1991). The TN008 clone, however, maintained higher leaf water potentials at moderate to severe soil water deficits, which suggests that it had better stomatal control of water loss. The stomatal conductance of the TN008 clone was very low at moderate to severe soil water deficits, and this may have contributed to its lower water use and higher water-use efficiency than the TN014 clone. The maintenance of a favourable water balance by stomatal regulation is a water conservation strategy that can enhance the drought tolerance of poplar clones (Tschaplinski et al. 1998).

The guaiacol peroxidase (GPX) activity of the leaves of the poplar clones increased in response to the soil water deficits. This antioxidant enzyme is activated to avert the damage caused by reactive oxygen species (ROS), such as the superoxide radical (O_2^-), hydrogen peroxide (H_2O_2), and hydroxy radical (•OH). Drought stress triggers an increase in the ROS, which can attack the membrane lipids, inactivate metabolic enzymes, and damage the nucleic acids, leading to cell death (Bartosz 1997; Mittler 2002). The increase in the GPX activity of the leaves is a protective mechanism that has been found to increase in response to soil water deficits (Yang et al. 2010), and to the severity of soil water deficits (Guo et al. 2010). While the GPX activity of the leaves increased during the application of the soil water deficits in this study, the increase in the GPX activity was similar for the 90, 60, and 40% FC water regime treatments. This may reflect the moderate to severe soil water deficits that were experienced by all the water regime treatments during the 2-day watering cycle. However, there were large differences in the GPX activity of the poplar clones, with much higher levels of GPX activity in the 'Veronese' clone, which suggests it has a much more effective antioxidant system of protection under drought conditions.

2.5 Conclusions

The four new hybrid poplar clones were not as drought-tolerant as the 'Veronese' poplar clone, showing a less conservative response to the soil water deficits, and lower antioxidant enzyme activity in the leaves. However, they demonstrated better biomass growth and water-use efficiency under drought conditions.

The 'Veronese' clone had good biomass growth under favourable conditions and was very responsive to soil water deficits, with an abrupt reduction in shoot growth and high allocation of biomass to the stem and roots, and high activity of leaf antioxidant enzymes. However, its high water use and conservative response to soil water deficits lead to lower water-use efficiency.

The TN008 and TN014 clones had slower biomass growth under favourable conditions and were less responsive to soil water deficits, but had better shoot growth under drought conditions. The high water use of these clones makes them more vulnerable to drought, but the TN008 clone has good stomatal control of water loss, which gives it some drought tolerance and high water-use efficiency.

The MT103 and MT304 clones had slower biomass growth under favourable conditions, but the best shoot growth of all the clones under drought conditions. These clones have lower water use and high water-use efficiency, and experienced less severe soil water deficits through the more conservative use of available water.

The 'Veronese' clone appears well adapted for drought-prone areas, where periods of severe soil water deficits is a constraint on the survival of the trees. In contrast, the MT103, MT304, TN008, and TN014 clones appear better adapted to moderately drought-prone areas, where there is an advantage in combining high productivity and high water-use efficiency. Among these clones, the MT304 and TN008 clones had the best combination of high productivity and high water-use efficiency.

These findings need to be complemented by information on performance aspects, particularly survival, gathered from field trials of the clones in regions with high current and future drought risk.

2.6 Acknowledgements

We thank Emily Smith (Massey University) for help with the tree watering, leaf stomatal conductance and water potential measurements, and the tree harvest; Steve Green and Carlo van den Dijssel (Plant & Food Research) for the installation of the weather station and load cells and data logger; Jason Wargent and Chris Rawlingson (Massey University) for the use of the pressure bomb equipment; Mary Horner (Plant & Food Research) for the bacterial and fungal testing of the necrotic (dead) tissue from the shoot tips; Simon McIvor for help with the tree root washing; Sam Gregory (Massey University) for the measurement of the leaf chlorophyll content and antioxidant enzymes; Rachael Sheridan (Massey University) for the measurement of the leaf free proline content; and Duncan Hedderley (Plant & Food Research) for advice on the experimental design and statistical analysis of the data.

2.7 References

AS 1289.2.1.1 2005. Methods of testing soils for engineering purposes - Soil moisture content tests - Determination of the moisture content of a soil - Oven drying method (standard method). Standards Association of Australia.

Bartosz G 1997. Oxidative stress in plants. Acta Physiol Plant 19: 47–64.

Bassman JH, Zwier JC 1991. Gas exchange characteristics of *Populus trichocarpa*, *P deltoides*, and *P trichocarpa* × *P deltoides* clones. Tree Physiol 8: 145–159.

Beauchamp C, Fridovich I 1971. Superoxide dismutase: improved assays and an assay applicable to acrylamide gels. Analytical Biochemistry 44: 276–287.

Blake TJ, Tschaplinski TJ, Eastham A 1984. Stomatal control of water use efficiency in poplar clones and hybrids. Can J Bot 62: 1344–1351.

Bonhomme L, Barbaroux C, Monclus R, Morabito D, Berthelot A, Villar M, Dreyer E, Brignolas F 2008. Genetic variation in productivity, leaf traits and carbon isotope discrimination in hybrid poplars cultivated on contrasting sites. Ann For Sci 65: 503.

Braatne JH, Hinckley TM, Stettler RF 1992. Influence of soil water on the physiological and morphological components of plant water balance in *Populus trichocarpa*, *Populus deltoides* and their F1 hybrids. Tree Physiol 11: 325–339.

Evans T, Song J, Jameson, PE 2011. Micro-scale chlorophyll analysis and developmental expression of a cytokinin oxidase/dehydrogenase gene during leaf development and senescence. Plant Growth Regulation 66(1): 95–99.

Garnier BJ 1958. The climate of New Zealand. A Geographic Survey. Edward Arnold, London.

Gebre GM, Kuhns MR 1991. Seasonal and clonal variations in drought tolerance of *Populus deltoides*. Can J For Res 21: 910–916.

Guo XY, Zhang XS, Huang ZY 2010. Drought tolerance in three hybrid poplar clones submitted to different watering regimes. J Plant Ecology 3(2): 79–87.

Hinckley TM, Ceulemans R, Dunlap JM, Figliola A, Heilman PE, Isebrands JG, Scarascia-Mugnozza G, Schulte PJ, Smit B, Stettler RF, Van Volkenburgh E, Wiard B 1989. Physiological, morphological and anatomical components of hybrid vigor in *Populus*. In: Kreeb KH, Richter H, Hinckley TM eds. Structural and functional responses to environmental stresses. The Hague, The Netherlands, SPB Academic Publ. Pp. 199–217.

Kelliher FM, Tauer CG 1980. Stomatal resistance and growth of drought stressed eastern cottonwood from wet and dry site. Silvae Genet 29: 166–171.

Marron N, Villar M, Dreyer E, Delay D, Boudouresque E, Petit JM, Delmotte FM, Guehl JM, Brignolas F 2005. Diversity of leaf traits related to productivity in 31 *Populus deltoides* × *Populus nigra* clones. Tree Physiol 25: 425–435.

Mittler R 2002. Oxidative stress, antioxidants and stress tolerance. Trend Plant Sci 7: 405–410.

Monclus R, Dreyer E, Delmotte FM, Villar M, Delay D, Boudouresque E, Petit JM, Marron N, Bréchet C, Brignolas F 2005. Productivity, leaf traits and carbon isotope discrimination in 29 *Populus deltoides* × *P nigra* clones. New Phytol 167: 53–62.

Monclus R, Dreyer E, Villar M, Delmotte FM, Delay D, Petit JM, Barbaroux C, Le Thiec D, Bréchet C, Brignolas F 2006. Impact of drought on productivity and water use efficiency in 29 genotypes of *Populus deltoides* × *Populus nigra*. New Phytol 169: 765–777.

Nakano Y, Asada K 1981. Hydrogen peroxide is scavenged by ascorbate-specific peroxidase in spinach chloroplasts. Plant and Cell Physiology 22(5): 867–880.

Pallardy SG, Kozlowski TT 1981. Water relations in *Populus* clones. Ecology 62: 159–169.

Pezeshki SR, Hinckley TM 1982. The stomatal response of red alder and black cottonwood to changing water status. Can J For Res 12: 761–771.

Sprugel DG 1983. Correcting for bias in log-transformed allometric equations. Ecology 64: 209–210.

Strong T, Hansen EA 1991. Response of three *Populus* species to drought. USDA-FS Research Paper NC-302, 9 p.

Tschaplinski TJ, Tuskan GA, Gebre GM, Todd DE 1998. Drought resistance of two hybrid *Populus* clones grown in a large-scale plantation. Tree Physiol 18: 653–658.

Worrall JJ, Rehfeldt GE, Hamann A, Hogg EH, Marchetti SB, Michaelian M, Gray LK 2013. Recent declines of *Populus tremuloides* in North America linked to climate. Forest Ecology and Management 299: 35–51.

Wu Z, Dijkstra P, Koch G, Penuelas J, Hungate BA 2011. Responses of terrestrial ecosystems to temperature and precipitation change: a meta-analysis of experimental manipulation. Global Change Biol 17: 927–942.

Xu G, Liu X, Qin D, Chen T, An WL, Wang WZ, Wu GJ, Zeng XM, Ren JW 2013. Climate warming and increasing atmospheric CO_2 have contributed to increased intrinsic water-use efficiency on the northeastern Tibetan Plateau since 1850. Trees-Structure and Function 27: 465–475.

Yang F, Wang Y, Miao LF 2010. Comparative physiological and proteomic responses to drought stress in two poplar species originating from different altitudes. Physiol Plant 139: 388–400.

Yin H, Xiao J, Li Y, Chen Z, Cheng X, Zhao C, Liu Q 2013. Warming effects on root morphological and physiological traits: The potential consequences on soil C dynamics as altered root exudation. Agricultural and Forest Meteorology 180(2013): 287– 296.

Yin C, Wang X, Duan B, Luo J, Li C 2005. Early growth, dry matter allocation and water use efficiency of two sympatric *Populus* species as affected by water stress. Environ Exp Bot 53: 315–322.

Zhang X, Zang R, Li C 2004. Population differences in physiological and morphological adaptations of *Populus davidiana* seedlings in response to progressive drought stress. Plant Sci 166: 791–797.

3 ESTABLISHING LONG-TERM NATIONAL FIELD TRIALS TO EVALUATE THE ADAPTIVE CAPABILITY OF NOVEL POPLAR AND WILLOW CLONES

3.1 Novel poplar clones for slope stabilisation

Novel poplar selections were planted in August 2014 at three field trial sites, on hill country pastoral farms in Taranaki, Horizons, and Waikato regions. The locations are given in Table 1, together with other details about the sites.

Table 1. Site information for the three trial sites.

	Trial site		
Variable	**Strathmore**	**Waituna West**	**Waikaretu**
Region	Taranaki	Horizons	Waikato
Climatic zone	Central North Island	South-western North Island	Northern New Zealand
Latitude	39°16’50	40°02’06	37°32’28
Longitude	174°33’30	175°40’13	174°48’55
Aspect	NE	S	E
Slope	Rolling to steep	steep	Rolling to steep
Altitude	188 m	380 m	95 m
Prevailing wind	NW	W	W
Climatic limiting factors	None recognised	Occasional snow, frost	Drought, salt spray
Erosion status	slight	marked	low
Soil type	Clay-loam	Clay-loam	Clay-loam

At each site, 3 m poles of five novel poplar clones and four commercial poplar clones were planted in a random block arrangement at 10 m x 10 m spacing (e.g. Figure 1).

Figure 1. Wide-spaced poplar selection trial in the Taranaki region, planted in September 2014. Photograph: Maureen Paterson.

.

Each site is sloping to steep, and vulnerable to shallow landslide erosion. The trial site was marked out using measuring tape, measuring wheel and fluorescent spray paint and the poles were planted into augured holes at the marked spots. The clones planted are listed in Table 2.

Table 2. Poplar clone number, name, colour code and trial sites where the clones were planted in September 2014.

Clone	Name	Colour code	Site planted
07-02-085	*Populus maximowiczii* × *trichocarpa*	White/Blue	All
07-02-086	*P. maximowiczii* × *trichocarpa*	White/Red	All
07-02-079	*P. maximowiczii* × *trichocarpa*	White/Yellow	All
07-05-304	*P. maximowiczii* × *trichocarpa*	White/Green	Taranaki, Horizons only
07-05-103	*P. maximowiczii* × *trichocarpa*	White/Orange	All
PN 870	*P. x euramericana* 'Veronese'	Blue	All
NZ 5006	*P. deltoides* x *yunnanensis* 'Kawa'	Red	All
NZ 5017	*P. x euramericana* ' 'Fraser'	Orange	All
NZ 5020	*P. x euramericana* 'Otahuao'	White	All
03-011-035	*P. deltoides* × *yunnanensis*	Green/Red	Waikato only

The novel poplar clones are identified by a number and parentage, whereas the commercial poplar clones are identified by registration number and a name (e.g. 'Veronese'). Clones 03-011-035 and 07-05-304 were not planted at every site (Table 1) because sufficient 3-m poles were not available.

Survival was high for the Taranaki and Waikato trials, and less so for the Horizons trial.
A second trial planting was marked out and planted at each of the above sites in July 2015. The first year trial was marked out at Methven in the Canterbury region, Mavora Lakes in Southland in the South Island and at Aramoana in Hawke's Bay.

3.2 Novel willow clones for slope and river bank stabilisation

A limited number (<30) of novel tree willow *Salix matsudana* 'Kew' PN 227 × *S. lasiandra* were planted in a riverbank trial in Hawke's Bay in September 2014. Field trials of *S. matsudana* 'Kew' PN 227 × *S. lasiandra,* together with *Salix lasiandra* × *S. pentandra* 'Dark French' PN 670*,* and *S. matsudana* 'Kew' PN 227 × *S. pentandra* 'Dark French' PN 670 willows will be expanded in 2015, when more poles will be available.

3.3 Novel poplar and willow clones developed for shelterbelt use

Orchard shelterbelt trial**.**

Table 3. Size and form of twelve novel poplar clones after 12 years cultured as shelterbelt trees.

Clone	Parentage	Diameter at 40 cm (cm)	Form (narrow N, medium M, wide W)	Response to trimming
NZ 98-001-005	(*Populus maximowiczii x P. nigra*) NZ 85-061-073 x *P. yunnanensis* PN 035	30.3	W	Full leaf cover
NZ 98-002-100	(*Populus maximowiczii x P. nigra*) NZ 85-061-073 x *P. nigra* Blanc de Garonne PN 874	27.2	N	Full leaf cover
NZ 98-002-108		26.8	M	Full leaf cover
NZ 98-003-029	(*Populus maximowiczii* x *P. nigra*) NZ 85-061-073 x *P. nigra* Italica PN 019	27.0	N	Full leaf cover
NZ 98-003-032		28.3	N	Full leaf cover
NZ 98-003-141		24.7	N	Full leaf cover
NZ 98-003-262		32.2	N	Full leaf cover
NZ 98-019-013	*Populus maximowiczii* NZ 73-011-078 *x P. nigra* Blanc de Garonne PN 874	28.1	W	Full leaf cover
NZ 98-019-015		23.8	M	Full leaf cover
NZ 98-019-033		27.1		Full leaf cover
NZ 98-019-062		31.3	N	Full leaf cover
NZ 98-019-076		32.5	M	Full leaf cover

An orchard novel poplar clone shelterbelt trial established at Riwaka Plant & Food Research Orchard in 2003 was evaluated in 2015 for trunk growth, response to trimming and form (Table 3). Twelve novel clones were planted in a single shelterbelt row at 2 m spacings, each clone being represented by five trees.

3.4 Farm shelterbelt trial

Novel poplar clones (Table 4) were planted in a farm shelterbelt trial at 240 Mavora Lakes Road near Te Anau in July 2014. These clones are characterised by a fastigiate form (Figure 2). Their growth rate is slower than those of present commercial clones, with the exception of 'Crowsnest', but very suitable for this purpose. The trees were planted at 2 m spacing and separate clones were planted together in the row to reduce competition from differing growth rates, and for ease of identification. In addition novel osier willow clones (*Salix lasiolepis* × *S. viminalis*), which only grow to ~8 m height, were supplied for the same project, to provide

information on alternative options for the future. The trial is designed to evaluate the trees' capability to provide shelter for winter 'feeding cells' for dairy cows and to reduce the nitrogen leaching from the cells. The cells are enclosed on three sides by shelterbelt trees and will contain silage tubes from which the cows will progressively feed for 1–2 weeks until moved to the next cell. It is hypothesised that this approach reduces soil compaction and improves efficiency in containing effluent nitrogen within the cell. Both the poplar trees and the dual use are novel.

Figure 2. Shelterbelt poplar clones being grown as poles at Plant & Food Research Clyde research centre showing fastigiate (narrow) form. Photograph: Bernadette

Survival of the poplar clones at 240 Mavora Lakes Road was assessed on 18.02.15. Of the 20 trees of each clone planted survival varied from 90% to 100% (Table 4).

Table 4. Novel poplar clones planted at 240 Mavora Lakes Road, Southland in winter 2014.

Clone no.	Parents (female x male)	Survival to 18.02.15
NZ98-002-069	(*Populus maximowiczii x P. nigra*) NZ 85-061-073 x *P. nigra* PN 874	95
NZ98-003-082	(*Populus maximowiczii x P. nigra*) NZ 85-061-073 x *P. nigra* Italica PN 019	90
NZ98-002-114	(*Populus maximowiczii x P. nigra*) NZ 85-061-073 x *P. nigra* PN 874	95
NZ98-003-114	(*Populus maximowiczii x P. nigra*) NZ 85-061-073 x *P. nigra* Italica PN 019	100
NZ98-003-116	(*Populus maximowiczii x P. nigra*) NZ 85-061-073 x *P. nigra* Italica PN 019	100
NZ98-003-119	(*Populus maximowiczii x P. nigra*) NZ 85-061-073 x *P. nigra* Italica PN 019	100
NZ98-025-914	*Populus deltoides* G48 PN 441 x *P. nigra* Italica PN 019	95
NZ98-025-902	*Populus deltoides* G48 PN 441 x *P. nigra* Italica PN 019	100
NZ98-800-028	*Populus* unknown	100

3.5 Novel poplar clones for river bank stabilisation

The novel poplar selections listed in Table 5 were planted in a river berm trial on the north bank of the Waimakariri River upstream from the Environment Canterbury poplar nursery in July 2014. The plantings were organised in randomised blocks with each block containing a single clone. This trial is to evaluate the resilience and suitability of these clones in a riverbank environment. The trial will be repeated in 2 years' time when further material is available.

Table 5. Clone number, parentage, colour coding and numbers supplied for novel *Populus* clones planted in the river berm trial on the Waimakariri River, Canterbury in July 2014.

Clone no.	Parents (female x male)	Poles supplied (2 m)
NZ 98-002-069	(*Populus maximowiczii x P. nigra*) NZ 85-061-073 x *P. nigra* Blanc de Garonne PN 874	20
NZ98-003-082	(*P. maximowiczii x P. nigra*) NZ 85-061-073 x *P. nigra* Italica PN 019	20
NZ98-002-114	(*P. maximowiczii x P. nigra*) NZ 85-061-073 x *P. nigra* Blanc de Garonne PN 874	20
NZ98-003-114	(*P. maximowiczii x P. nigra*) NZ 85-061-073 x *P. nigra* Italica PN 019	20
NZ98-003-116	(*P. maximowiczii x P. nigra*) NZ 85-061-073 x *P. nigra* Italica PN 019	20
NZ98-003-119	(*P. maximowiczii x P. nigra*) NZ 85-061-073 x *P. nigra* Italica PN 019	20
NZ98-800-028	*Populus* unknown	20
NZ98-025-914	*P. deltoides* G48 PN 441 x *P. nigra* Italica PN 019	20
NZ98-025-902	*P. deltoides* G48 PN 441 x *P. nigra* Italica PN 019	20

3.6 To identify drought-tolerant clones from IPC breeding network

Ian McIvor met with Dr Brian Stanton, Chief Science Officer, Greenwood Resources, in Portland, Oregon, USA, during July 2014, and with other researchers at an International Poplar Symposium in Vancouver in July 2014. Inquiries about drought-tolerant poplars did not yield any solutions for New Zealand. We did discuss our expansion of poplar germplasm to breed drought-tolerant poplars (e.g. *Populus fremontii* for the Southeast of the United States, and white poplar (*P. alba)* hybrid). We also discussed our trials to validate stable carbon isotope discrimination as a method for selecting for water-use efficient poplar varieties. Discussions with international colleagues revealed that poplars currently grown in dry regions in the United States, Canada, Spain and Argentina grown on flat land in drip-irrigated plantations were selected for water use efficiency not for drought tolerance. Chinese scientists have selected poplar clones for drought tolerance (*Populus canadensis* Moench, *P.* × *euroamericana, P. tremula, P. simonii*) (www.fao.org/docrep/008/a0026e/a0026e08.htm), but have reported high mortality of poplar clones grown in dry and desert regions (www.bjreview.com.cn/nation/txt/2013-11/18/content_578522_2.htm, http://usa.chinadaily.com.cn/business/2013-11/25/content_17128952_2.htm) despite very significant efforts to plant trees deep enough to reach the water table. Survival of young trees is enabled by planting them to the depth of the water table, but high mortality of older trees is attributed to drought stress. The situation in New Zealand, where wide-spaced trees are grown for soil stabilisation in summer-drought prone areas and depend upon natural rainfall and soil water storage, was not familiar to many of the international researchers, although some

researchers had visited New Zealand in March 2014, and previously (e.g. Dr Stanton) and had seen how wide-spaced poplars are used for slope stabilisation in Gisborne district. Drought tolerance of our novel poplar and willow clones is being measured in pot trials in this project and these studies are being complemented by field trials where survival and growth will be measured over a period of 15 years.

4 IDENTIFICATION OF *MELAMPSORA* SPP. PRESENT ON *POPULUS* SPP. IN NEW ZEALAND – A SURVEY CARRIED OUT AT NATIONAL MONITORING SITES IN 2014

Ian McIvor and Duncan Hedderley Plant & Food Research. (ian.mcivor@plantandfood.co.nz)

4.1 Abstract

Leaf samples bearing a variable rust load were collected from a range of infected poplar clones. Collections were made during March–April 2014. Identification of the rust species was made from 24 separate samples of poplar rust geographically apart. The urediniospores had a mean spore length of 27.0±1.8 mm and a mean spore diameter of 12.8±1.1 mm with an apex devoid of spines. Based on the external morphology of the urediniospores all rust samples were identified as belonging to *Melampsora larici-populina.* There was no evidence of hybridisation or species evolution based on the urediniospore appearance.

4.2 Introduction

The most significant poplar diseases in New Zealand are caused by the poplar leaf rust *Melampsora larici-populina* and the leaf spot or anthracnose fungus *Marssonina brunnea*. Both of these leaf diseases thrive in our cool, moist environments and cause early defoliation, reduced root and stem growth, and dieback in susceptible cultivars. The poplar leaf rust *Melampsora medusae* is less significant nationally because of its limited range as determined from previous national rust surveys (Sivakumaran & McIvor 2010). Rust fungi have complex life cycles involving up to five different spore stages, and often require two unrelated host plants to complete their life cycle (Sivakumaran & McIvor 2010). The secondary host in New Zealand for *M. larici-populina* is larch (*Larix* sp.).

Incorporating resistance to poplar leaf rusts is included as an objective in the national poplar and willow breeding programme carried out at Plant & Food Research.

Hybridisation between *Melampsora* species in New Zealand was reported by Spiers and Hopcroft (1994) but was not been observed in a subsequent survey (Sivakumaran & McIvor 2009). However, evolution in *Melampsora* races has been reported from Europe and similar evolution occurring in New Zealand could result in poplar clones bred for resistance to rust disease becoming more susceptible and subsequently more stressed. This is a matter of concern considering the additional environmental stresses expected due to climate change.

A further survey was carried out in 2014 with the purpose of identifying any external morphological changes of the spores in *Melampsora larici-populina* and monitoring changes in poplar clonal resistance to rust disease.

4.3 Methods

Some of the 2009–10 *Melampsora* sp. rust indicator sites (Sivakumaran & McIvor 2010) were revisited in 2014 (Table 1, Figure 1) and *Melampsora* sp. rust infected leaf samples were collected from indicator poplar clones. The indicator clones included clones currently susceptible to the present *Melampsora* rust strains (e.g. *Populus* × *euramericana* 'I214', 'Veronese', 'Weraiti', and 'Selwyn', *P. deltoides* × *ciliata* 'San Rosa') and clones currently resistant (e.g. *P. deltoides* × *yunnanensis* 'Kawa', *Populus* × *euramericana* × *yunnanensis* 'Toa', *P. maximowiczii* × *nigra* 'Geyles').

One sample (Hunter) was included because the landowner reported a 'new' rust on his *P. ciliata.*

Table 1. National poplar indicator sites for monitoring *Melampsora* spp. rust infection.

Location	Site	Latitude	Longitude	Description
Parakai	Poplar Trial site	36°40'	174°23'	Coastal, range of clones
Lower Kaimai	Poplar trial site	37°49'	176°00'	Inland, range of clones
Lepperton	Taranaki RC nursery	39°04'	174°11'	Coastal, range of clones
Aokautere	RST nursery	40°11'	175°23'	Inland, range of clones
Gentle Annie	Poplar trial site	38°40'	177°49'	Coastal, range of clones
Napier	Hawke's Bay RC nursery	39°33'	176°52'	Coastal, range of clones
Riwaka	Research site (shelterbelt)	41°04'	172°59'	Coastal, range of clones
Hunterville	Poplar farm repository	39°53'	175°30'	Inland, range of clones
Waimakariri	ECan nursery	43°26'	172°15'	Coastal, range of clones
Clyde	Poplar research site	45°12'	169°18'	Inland, range of clones
Makarewa	Shelterbelt sample site	46°19'	168°20'	Coastal

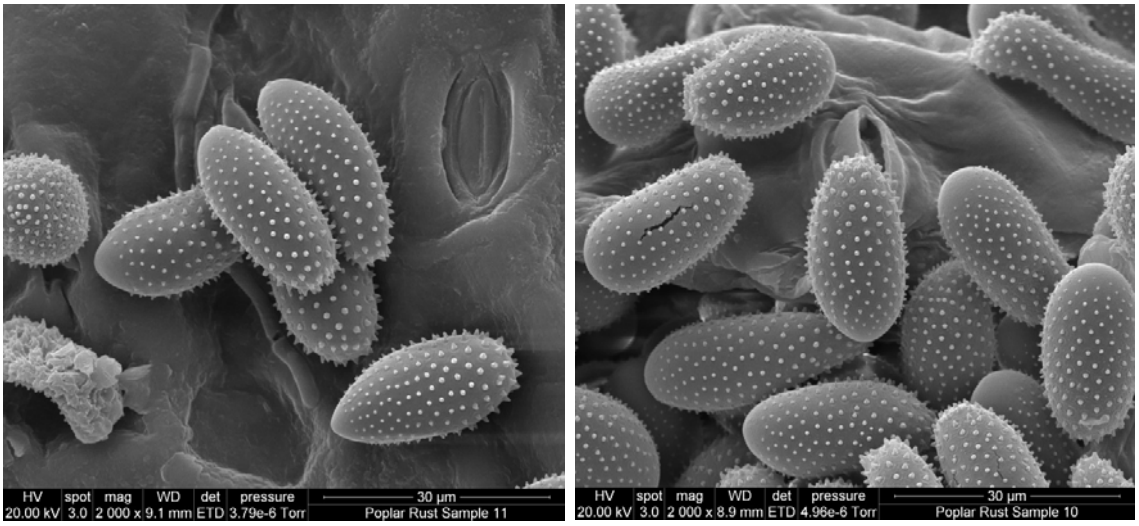

Figure 1. Urediniospores of *Melampsora larici-populina* sourced from underside of leaves of Populus × *euramericana* × *nigra* 'Crowsnest' from Gisborne shelterbelt (L), and *P. nigra* PN835 located at Clyde, Central Otago (R), during March 2014. Both photos x 2000.

The rust infected leaf samples were air dried. Dry samples were mounted on double-sided tape on aluminium specimen stubs; sputter coated with gold, and studied using an FEI Quanta 200 Scanning Electron Microscope at Massey University. The *Melampsora* sp. was identified from urediniospore characteristics (Pei & McCracken 2005; Speirs & Hopcroft 1985). The pathotype data was compared with 2010 data to quantify changes in relative frequency of *Melampsora* sp. and identify any new *Melampsora* sp. variants from external appearance of the urediniospores.

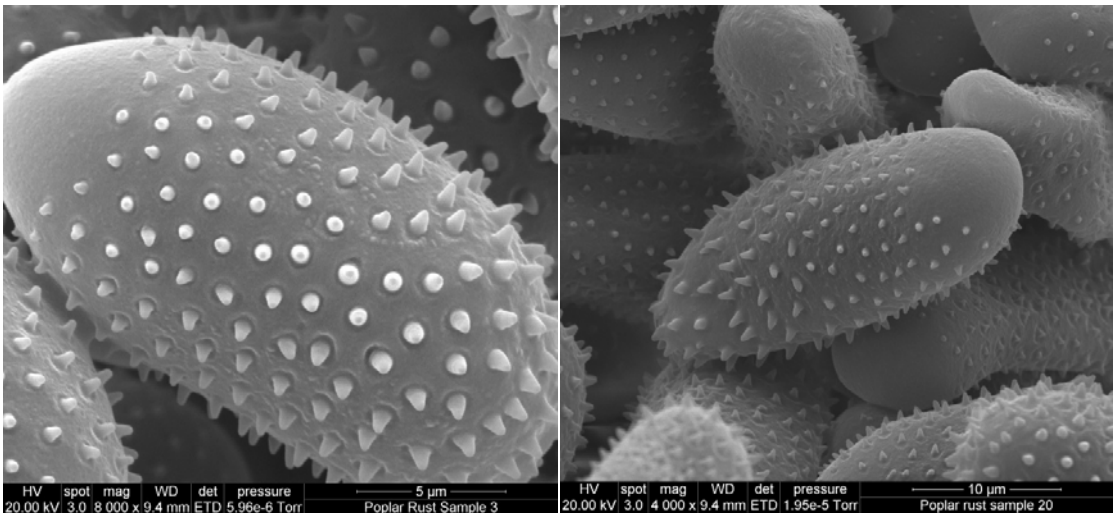

Figure 2. Urediniospores of *Melampsora larici-populina* showing apex bare of spikes and variable spike height over the external surface x 8000 (L), x 4000 (R).

4.4 Results

Table 1. Variation in length and diameter of *Melampsora sp.* urediniospores sampled from various locations around New Zealand, together with the poplar clone from which they were sampled. N = 10 for each sample. Mean (+ standard deviation sd) is given for all samples at the bottom of the table.

		Length µm		Diameter µm	
Location	Clone	mean	sd	mean	sd
Kaimai, Bay of Plenty	*P. deltoides x szechuanica*	24.7	2.3	11.8	1.0
Kaimai, Bay of Plenty	*P. x euramericana* 'Veronese'	24.2	1.4	13.1	1.1
Kaimai, Bay of Plenty	*P. deltoides* x *szechuanica*	24.9	1.7	12.1	0.8
Kaimai, Bay of Plenty	*P. deltoides x ciliata* 'Kaimai'	25.2	1.5	11.3	0.7
Kaimai, Bay of Plenty	*P. deltoides x ciliata* 'Kaimai'	25.9	1.2	11.0	0.7
Clyde, Central Otago	*P. koreana x nigra* PN878	25.5	1.7	11.0	1.6
Clyde, Central Otago	*P. x interamericana* PN473	25.5	1.5	11.4	1.0
Clyde, Central Otago	*P. nigra* PN866	23.7	1.0	13.0	0.6
Clyde, Central Otago	*P. nigra* PN835	24.9	1.2	12.6	0.5
Gisborne	*P. nigra* PN019 (Lombardy)	25.8	1.1	11.6	0.7
Riwaka, Tasman	*P. x euramericana*	25.2	1.7	12.1	0.5
Riwaka, Tasman	*P. x euramericana*	25.6	2.0	12.0	0.9

Location	Clone	Length µm		Diameter µm	
		mean	sd	mean	sd
Makarewa, Southland	*P. x euramericana* 'Tasman'	25.6	1.7	12.6	1.3
Makarewa, Southland	*P. x euramericana* 'Tasman'	24.6	1.4	11.6	1.3
Hunterville, Rangitikei	*P. trichocarpa*	33.2	2.0	15.7	1.2
Hunterville, Rangitikei	*P. ciliata*	31.6	1.5	14.1	1.2
Hunterville, Rangitikei	*P. trichocarpa*	32.1	2.0	15.5	1.6
Lincoln, Canterbury	*P. x euramericana* 'Tasman'	29.9	1.5	14.0	1.1
Lincoln, Canterbury	*P. x euramericana* 'Tasman'	31.4	4.1	14.3	1.3
Lepperton, Taranaki	*P. deltoides x yunnanensis* 'Kawa'	27.5	2.7	13.7	1.5
Lepperton, Taranaki	*P. deltoides x yunnanensis* 'Kawa'	28.1	3.2	12.2	2.1
Lepperton, Taranaki	*P. deltoides x yunnanensis* 'Kawa'	31.1	3.8	13.4	1.1
One Factor ANOVA					
Samples F (21, 195 df)		19.75		14.63	
P		<.001		<.001	
LSD		1.9		1.0	

The shapes of urediniospores varied from clavate to broadly ellipsoid observed under the scanning electron microscope. Some of them were oval to ovate (Figures 1, 2), and a few were obovate. Apices were rounded and bases were often truncate (Figure 2). Some spores had splits in the wall, possibly as an effect of the drying process. The wall surface of the urediniospore was echinulate (spiny) except for a smooth patch of 4–8 µm in width on the broad apex, or slightly to one side of the broad apex (Figure 2). The spines were largest toward the base (the apex opposite to the smooth patch) and progressively smaller toward the smooth patch.

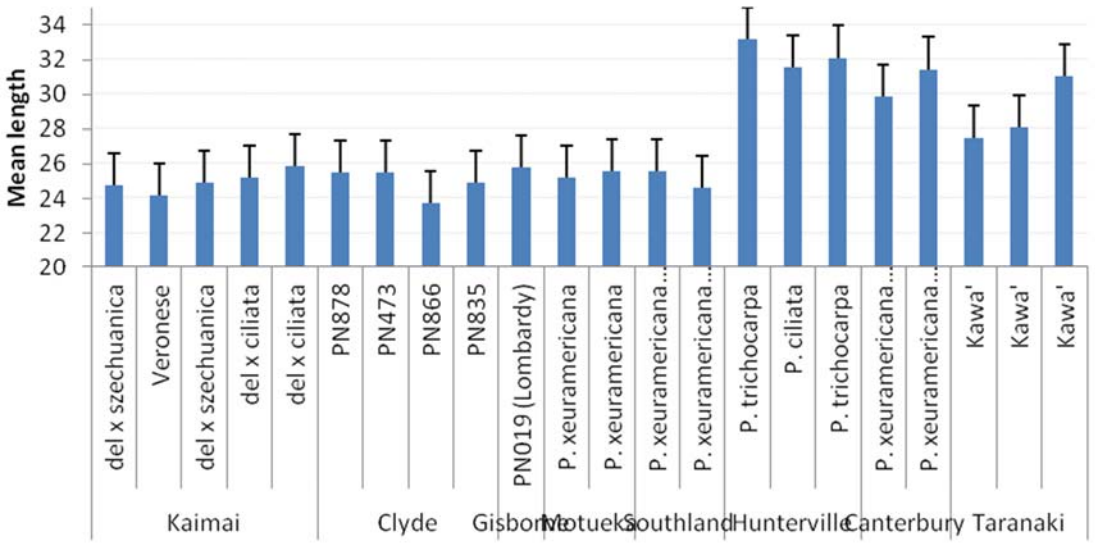

Figure 3. Mean urediniospore length (µm) for the 22 different samples plotted against both clone and location (bars indicate the LSD).

The above characteristics are very similar to that described for *M. larici-populina* (Pei & McCracken 2005). In contrast *to M. larici-populina*, the urediniospores of *M. occidentalis* are evenly echinulate without an obvious smooth patch (Newcombe & Chastagner 1993), whereas the urediniospores of *M. medusae* were echinulate with an equatorial smooth patch (Spiers & Hopcroft 1985). Urediniospores from the 2009–10 poplar rust samples (N = 17) had a mean spore length of 24.8 ± 1.7 µm and a mean spore diameter of 11.2 ± 1.0 µm. Urediniospores collected from the 2014 poplar rust samples (N = 22) had a mean spore length of 27.0 ± 1.8 µm and a mean spore diameter of 12.8 ± 1.1 µm (Table 1).

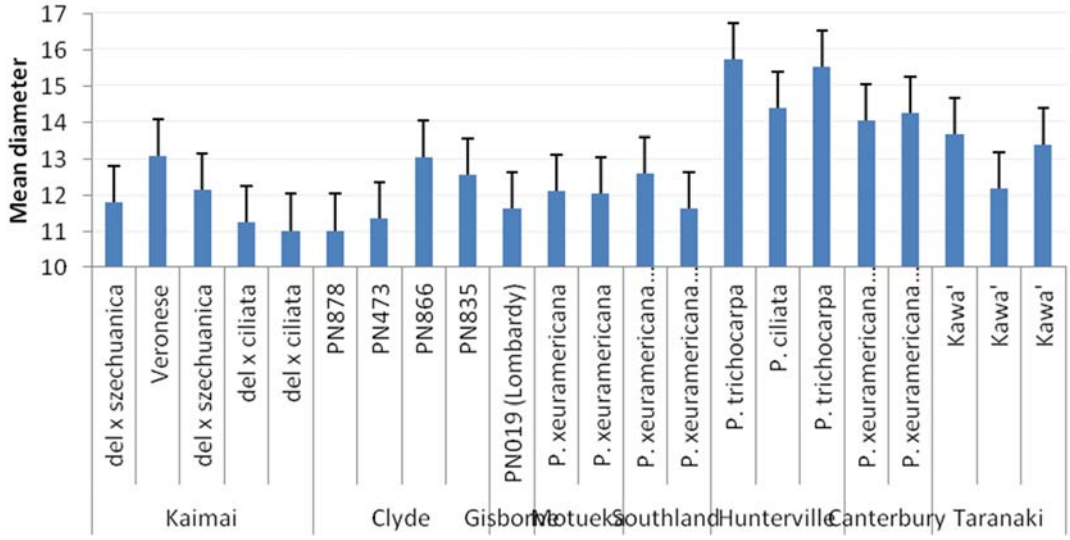

Figure 4. Mean urediniospore diameter (µm) for the 22 different samples plotted against both clone and location (bars indicate the LSD).

The Hunterville and Canterbury (and possibly Taranaki) samples appear to be larger than most others (Table 1, Figures 3 & 4); when the ANOVAs were run with two factors – region, and sample within region – region accounted for 92% of the variation between samples in length, and about 80% of the variation in diameter. In both cases the variation between regions is significantly higher than the variation between samples within a region, $P < 0.001$. Variation between samples within a region was still significantly higher than the variation between spores within a sample, $P = 0.007$ for length and $P < 0.001$ for diameter). Means for both urediniospore length and diameter varied significantly between locations (Figure 5).

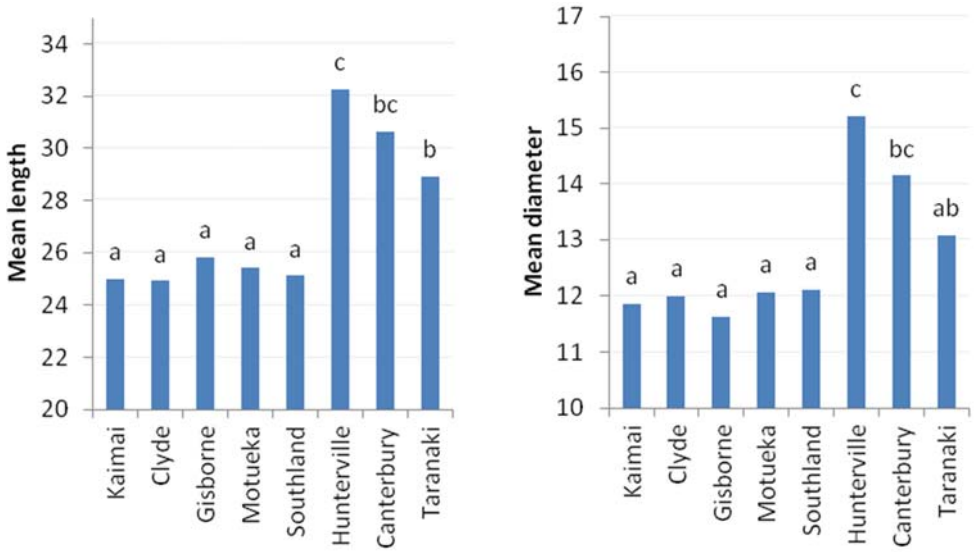

Figure 5. Mean urediniospore length (L) and mean urediniospore diameter (R) for the different locations (dimensions in µm). Means which share a letter are not significantly different based on a LSD test at *P* = 0.05 (because of the different number of samples from different regions, this is more accurate than trying to show a LSD bar).

We have similar data from 2010 (10 spores each from 16 samples). Comparing the means in the two years to the variation between samples within each year (using ANOVA), the 2014 mean length was significantly longer than the 2010 mean ($P = 0.005$ with 1, 36 df), and the 2014 diameter was significantly higher than the 2010 diameter ($P < 0.001$ with 1, 36 df). It is possible this could just be difference between the regions the 2010 and 2014 samples came from – the 2014 data had region information but the 2010 data did not.

4.5 Discussion

Melampsora rust disease causes premature leaf fall, reduces photosynthetic capacity and reduces wood volume in susceptible poplar clones. The damaging effects of rust disease can be minimised in breeding programmes through use of resistant parents and subsequent selection of resistant and less susceptible clones, and in the production nursery with fungicide applications.

Genetic diversity of *Melampsora* is recognised as contributing to a reduction in rust resistance in poplar clones (Borassa et al. 2007). For this reason it is important that a poplar breeding programme is continually evaluating any changes in the rust resistance of its current stable of clones through field and nursery observations of the degree of *Melampsora* rust infection, while at the same time measuring the genetic diversity of *Melampsora* across its range.

Rust infection becomes apparent when the first urediniospores (Figure 1) erupt from the leaf tissue. The urediniospores are capable of producing many cycles of the same form of spores during the growing season, causing disease epidemics on poplars. In this way new leaves become infected from spores dispersed from already infected leaves. Late in the growing season susceptible poplar trees can be observed to have a tuft of green leaves present at the extremities of the canopy, with all the other foliage shed as a result of rust infection. Those few remaining leaves are likely infected.

Melampsora larici-populina urediniospores are described as being mainly hypophyllous (located on the underside of the leaf), having dimensions of 30–50 x 14–22 µm and being smooth at the apex (Pei & McCracken 2005). The dimensions of *Melampsora sp.* urediniospores as measured during 2014 in New Zealand were consistent with 2009–10 New Zealand data (Sivakumaran & McIvor 2010) and similar to data reported from China (23.7 x 12.3 µm, Tian and Kakishima 2005; 22 x 11 µm, Wan et al. 2013). Considering the variability in morphological dimensions in other studies, our data suggest that the urediniospores of the pathotype or pathotypes are of *Melampsora larici-populina* and have not undergone any morphological change. There is no morphological evidence that a hybrid pathotype of *Melampsora larici-populina* and *M. medusae* has become more widespread than has been observed previously. The urediniospores for the samples collected at Hunterville were noticeably larger than those at all other sites. This may be significant since the landowner observed that rust on his *P. ciliata* trees appeared to be more virulent than in the past. There was heavy infection on *P. ciliata* leaves but the infection was very light on *P. trichocarpa* at the same location and was not accompanied by any defoliation.

Whether the significant differences in urediniospore dimensions identified at the different locations (Figure 5) are due to different pathotypes with varying virulence requires further investigation utilising both molecular and virulence techniques.

The main challenge for poplar breeding and cultivation is incorporation of durable resistance to rusts that are composed of diverse and changing populations. DNA fingerprinting capability enabling identification between *Melampsora larici-populina* has advanced and identification of the species, though not the pathotype, is by both morphology of the urediniospores and PCR amplification with a *Melampsora larici-populina* specific primer (Boyle et al. 2005; Wan et al. 2013). Although rust-resistant phenotypes can be selected early in a breeding programme, the visual selection of rust-free individuals in the field does not provide comprehensive information because field resistance is influenced by the environmental conditions (Hanley et al. 2011). To confirm their resistance, repetitive inoculation studies under controlled conditions are needed. The resistance survey conducted in this study needs to be complemented by regular research on rust resistance of the various commercial poplar clones released for commercial use at the sites where they are grown. It was noted that there was no rust present on any of the range of poplar clones visited in the national trial site at Parakai in Northland (listed in McIvor et al. 2011), and that though rust samples were collected from *P. trichocarpa* trees at Hunterville infection was slight. This survey was focussed on changes in rust presence and pathotype at the specified monitoring sites and not on changes in rust susceptibility of the various commercial clones all of which are not present at these sites.

Identification of a suspected new pathotype can be confirmed by exposing a range of poplar clones to pathotypes sourced from different locations and measuring the rate of infection and degree of virulence.

Recommendations to the New Zealand Poplar & Willow Research Trust:

- Initiate a project to search for the presence of different strains of *Melampsora larici-populina* using DNA fingerprinting techniques, complemented by the technique for identifying a suspected new pathotype described in the paragraph above.
- Repeat a national poplar rust survey in 2018.
- Monitor changes in *Melampsora* rust resistance of current commercial poplar clones biannually in specific field and nursery sites using the numerical assessment scale of Liesebach and Zaspel (in Mei & McCracken p. 77).
- Maintain communication with the International Poplar Commission Working Party on pests and diseases of poplar and willow.

4.6 Conclusion

The *Melampsora* pathotypes sourced from 11 sites across New Zealand were identified as being of *Melampsora larici-populina* as was the case in the 2009–10 survey. No evidence of new hybrid *Melampsora* pathotypes was found based on urediniospore morphology. There were significant regional differences in urediniospore dimensions. It is recommended that DNA fingerprinting technologies be developed in addition to urediniospore morphology for identifying *Melampsora* pathotypes.

4.7 Acknowledgements

Kevin Cash (Taranaki Regional Council), Nathan Cruikshank (Environment Southland), Bernadette Rout and Craig Tregurtha (both Plant & Food Research) collected leaf samples. Niki Minards and Doug Hopcroft (Massey University) prepared the rust samples for the scanning electron micrographs.

4.8 References

Bourassa M, Bernier L, Hamelin RC 2007. Genetic diversity in poplar leaf rust (*Melampsora medusae* f. sp. *deltoidae*) in the zones of host sympatry and allopatry. Phytopathology 97: 603–610.

Boyle B, Hamelin RC, Seguin A 2005. In vivo monitoring of obligate biotrophic pathogen growth by kinetic PCR. Applied and Environmental Microbiology 71: 1546–1552.

Hanley S, Pei MH, Powers SJ, Ruiz C, Mallott MD, et al. 2011. Genetic mapping of rust resistance loci in biomass willow. Tree Genetics & Genomes 7: 597–608.

McIvor IR, Hedderley DI, Hurst SE, Fung LE 2011. Survival and growth to age 8 of four *Populus maximowiczii* × *P. nigra* clones in field trials on pastoral hill slopes in six climatic zones of New Zealand. New Zealand Journal of Forestry Science 41(2011): 151–163.

Newcombe G, Chastagner GA 1993. First report of the Eurasian poplar leaf rust, *Melampsora larici-populina,* in North America. Plant Disease 77: 532–535.

Pei MH, McCracken AR 2005. Rust diseases of willow and poplar. CAB International 2005 264 p.

Sivakumaran S, McIvor IR 2010. National poplar rust disease survey 2009–10. PFR Client Report No. 30725, prepared for Ministry of Agriculture and Forestry.

Spiers AG, Hopcroft DH 1985. Ultrastructural studies of pathogenesis and uredinial development of *Melampsora larici-populina*, *M. medusae* on poplar, and *M. coleosporoides* and *M. epitea* on willow. New Zealand Journal of Botany 23: 117–133.

Spiers AG, Hopcroft DH 1994. Comparative studies of the poplar rusts *Melampsora medusae, M. larici-populina* and their interspecific hybrid *M. medusae-populina*. Mycol Res 98: 889–903.

Tian C-M, Kakishima M 2005. Current taxonomic status of *Melampsora* species on poplars in China. In: Pei MH, McCracken eds. Rust diseases of willow and poplar. CAB International 2005 264 p.

Wan Z, Li Y, Chen Y, Zhang X, Guan H and Yin T 2013. *Melampsora larici-populina,* the main rust pathogen, causes loss in biomass production of black cottonwood plantations in the south of China. Phytoparasitica 41: 337–344.

5 DROUGHT TOLERANCE OF FIVE HYBRID WILLOW CLONES TO DIFFERENT WATERING REGIMES

Trevor Jones and Ian McIvor, Plant & Food Research, Michael McManus, Massey University

5.1 Introduction

Willows (*Salix* spp.) are amongst the fastest growing tree species at temperate latitudes, and use large quantities of water because of their high rates of photosynthesis and transpiration, and large total leaf areas (Ögren & Sjöström1990; Persson & Lindroth 1994; Cienciala & Lindroth 1995; Wikberg & Ögren 2007). The water-use efficiency of willows is high compared with those of other tree species (Lindroth & Cienciala 1996; Lindroth et al. 1994), but they are sensitive to water stress during drought conditions (Rönnberg-Wästljung et al. 2005; Turtola et al. 2006; Wikberg & Ögren 2004, 2007). This occurs because willow trees are highly vulnerable to xylem cavitation and hydraulic failure, as the availability of water decreases with soil water deficits, and the water potential of the xylem declines in the stems and roots (Wikberg & Ögren 2007, 2004; Savage & Cavender-Bares 2011).

Drought conditions are likely to increase in both frequency and severity in the eastern lowlands of New Zealand, in response to a warming climate during the 21st century (Basher et al. 2012; Hollis 2015). The time spent in drought in eastern New Zealand is projected to double or triple by 2040, and large areas are likely to have less soil moisture (Hollis 2015). Changes in rainfall patterns, such as a projected decrease in the return periods of extreme rainfall events, could lead to erosion becoming a bigger problem on pastoral hill country (Basher et al. 2012). Shallow rapid landslides are triggered by intense storms or long periods of wet weather (Guzzetti et al. 2008), and these reduce the long-term productive capacity of pastoral hill country farms (Trustrum et al. 1984; Douglas et al. 1986; Derose et al. 1995).

Willow trees planted on pastoral hill country at low densities of 30 to 70 stems per hectare (sph) are effective in reducing shallow landslide occurrence by 95% compared with unplanted pasture (Douglas et al. 2013). The use of wide-spaced trees on pastoral hill country enables the continuation of livestock farming on these landscapes, rather than changing the vegetation to conservation or plantation forestry. Willow trees are also planted to protect land and property along rivers and smaller waterways, and are the best tree species to provide stability to river banks, with their fine-fibrous matted root systems holding river banks together and reducing the channel scouring of streams (Wilkinson 1999; Denyer 2015).

Currently the tree willows planted in New Zealand for erosion and river bank protection are clones of *Salix matsudana* and *S. matsudana* x *S. alba* (McIvor 2008), but new experimental hybrid clones of *S. matsudana*, *S. lasiandra*, and *S. pentandra* are being evaluated. These have been bred for resistance to browsing by possums (*Trichosurus vulpecula*), and the willow sawfly (*Nematus oligospilus*). *S. lasiandra*, and *S. pentandra* have bitter foliage, and *S. lasiandra* has a very long growing season, and very rough bark, which will be suitable for the abrasive river conditions in New Zealand. The use of these willow hybrids will broaden the genetic base of willow clones available for planting.

In this study, the physiological responses to drought conditions of four new experimental hybrid willow clones of *S. matsudana*, *S. lasiandra*, and *S. pentandra* were evaluated and compared

with the drought-tolerant *S. matsudana* x *S. alba* 'Tangoio' willow clone that is widely used for soil conservation in New Zealand (Table 1). The tree growth and water-use parameters of these willow clones were evaluated in a greenhouse water-stress experiment, to characterise the drought tolerance, water-use efficiency, and the capacity for drought acclimation of the willow clones.

Table 1. Hybrid willow clones used in the greenhouse water-stress experiment and the parent clones.

Willow clones	Female parent	Male parent
'Tangoio'	*Salix matsudana* PN 227 'Kew'	*S. alba* I4/59
ML089 - 07-01-089	*S. matsudana* PN 227 'Kew'	*S. lasiandra* 000/0-15
ML022 - 03-004-022	*S. matsudana* PN 227 'Kew'	*S. lasiandra* 113/1-13
MP002 - 03-012-002	*S. matsudana* PN 227 'Kew'	*S. pentandra* PN 670 'Dark French'
LP026 - 03-001-026	*S. lasiandra*	*S. pentandra* PN 670 'Dark French'

5.2 Methods

5.2.1 Experiment design

A completely randomised design was used in the experiment, with five willow clones × three water regimes (total of 15 treatments). Four replicates were used for each treatment (total of 60 pots). The three water regimes were: well-watered (90% of field capacity), moderate soil water deficit (60% field capacity), and severe soil water deficit (40% field capacity), where the field capacity was defined as the soil water content of the pots after 24 hours of drainage, following saturation of the soil.

5.2.2 Field capacity of soil

The field capacity (FC) of the soil (Daltons willow water-stress mix, Table 2) was measured by watering the soil in a 30-L plastic pot with a hose, covering the surface of the soil with a plastic sheet and allowing to drain for 24 hours, and then taking 10 × 300 g samples for measurement of the gravimetric water content of the soil using Australian Standard 1289.2.1.1 (2005). The soil samples had a high content of organic carbon and were oven-dried at 65°C to constant weight.

Table 2. Composition of the soil in the willow greenhouse water-stress experiment – Daltons willow water-stress mix.

Basic ingredients	Percentage	Fertiliser ingredients	kg m^{-3}
Bark fines (CAN) A grade	35	Dolomite	4.00
Daltons Prop (No. 2) sand	30	Growers Choice Granular WA	0.75
Hauraki Peat	35	Lime – Ag Grade	2.00
		Osmocote Exact 3/4 Standard	3.00
		Osmoform NXT 22N	0.50

5.2.3 Greenhouse environment

The willow trees were grown from cuttings in 30-L green plastic pots in a greenhouse at Plant & Food Research in Palmerston North (Figure 1). The roof and walls of the greenhouse were enclosed with clear plastic sheeting, with the exception of the lower walls. These were covered with cloth along the two long sides of the greenhouse, to provide good ventilation and exposure to the wind. The greenhouse was ventilated by two fans (Figure 1) that were activated when the air temperature of the greenhouse reached 22°C.

Figure 1. Layout of the willow trees in the greenhouse at Plant & Food Research in Palmerston North.

The air temperature and humidity, and light conditions inside the greenhouse (Figure 2) were measured using a Humitter 50Y integrated temperature and humidity sensor (Vaisala Oyj, Helsinki, Finland), and a LI-190SB quantum (PAR) sensor (Li-Cor Inc., Lincoln, Nebraska, USA), that were connected to a CR10X data logger (Campbell Scientific, Logan, Utah, USA).

5.2.4 Propagation of the willow trees

The willow trees were propagated from cuttings of 12 to 32 mm (average 20 mm) diameter and 40 cm length. The cuttings were cut from one-year-old shoots from one- or two-year-old plants in the Hawke's Bay Regional Council Nursery, Pakowhai, Napier. The diameter of each cutting at the mid-point (along the length) was measured after soaking in water for five days. The cuttings were selected to provide a similar distribution of mid-point diameter for each willow clone.

The willow cuttings were planted on 17 September 2014, with one cutting planted in each of the 30-L plastic pots. The cuttings were planted after the soil in the pots was saturated with water, and drained for 24 hours to field capacity. The pots were positioned in a randomised block design inside the greenhouse. The pots were placed in four rows orientated along the length of the greenhouse (Figure 1), with one pot of each willow clone randomly assigned to each of three blocks of five pots within each row.

The pots were weighed every two days, and the water transpired was measured and replaced to maintain the soil at 90% of field capacity (FC). The addition of water to the trees was adjusted for the growth in the fresh weight of the shoots. The evaporation of water from the soil surface was minimised by covering the surface with plastic sheeting. The willow trees were grown at 90% of field capacity for 70 days (10 weeks), and then the moderate soil water deficit (60% FC), and severe soil water deficit (40% FC) treatments were applied.

5.2.5 Application of the soil water deficits

The trees (pots) of each willow clone were re-allocated to four blocks in the greenhouse, based on the amount of shoot biomass (leaves + stems) after 10 weeks of growth. The three trees of each clone with the largest amount of shoot biomass were allocated to block 1, and the process was repeated for blocks 2, 3, and 4, with three trees of each clone with progressively smaller amounts of shoot biomass. The three trees of each clone, in each of the four blocks, were randomly allocated to the 90%, 60%, or 40% of field capacity treatments.

The water regimes were started on 26 November 2014, by allowing the pots to dry down to the required soil water content, and were applied to the willow trees for 49 days (7 weeks). The water regimes were maintained by weighing each pot every two days, and the transpired water was measured and replaced to maintain the pots at 90%, 60%, or 40% of field capacity (FC). The addition of water to the trees was adjusted for the growth in the fresh weight of the shoots.

5.2.6 Monitoring the growth of the willow trees

The basal diameter, number of leaves on selected shoots, and the height of the shoots of each tree were measured weekly. The fresh weight of the shoots (leaves + stems) and the leaf area of the shoots were estimated for each tree using the basal diameter and height of the shoots in the linear regression equation:

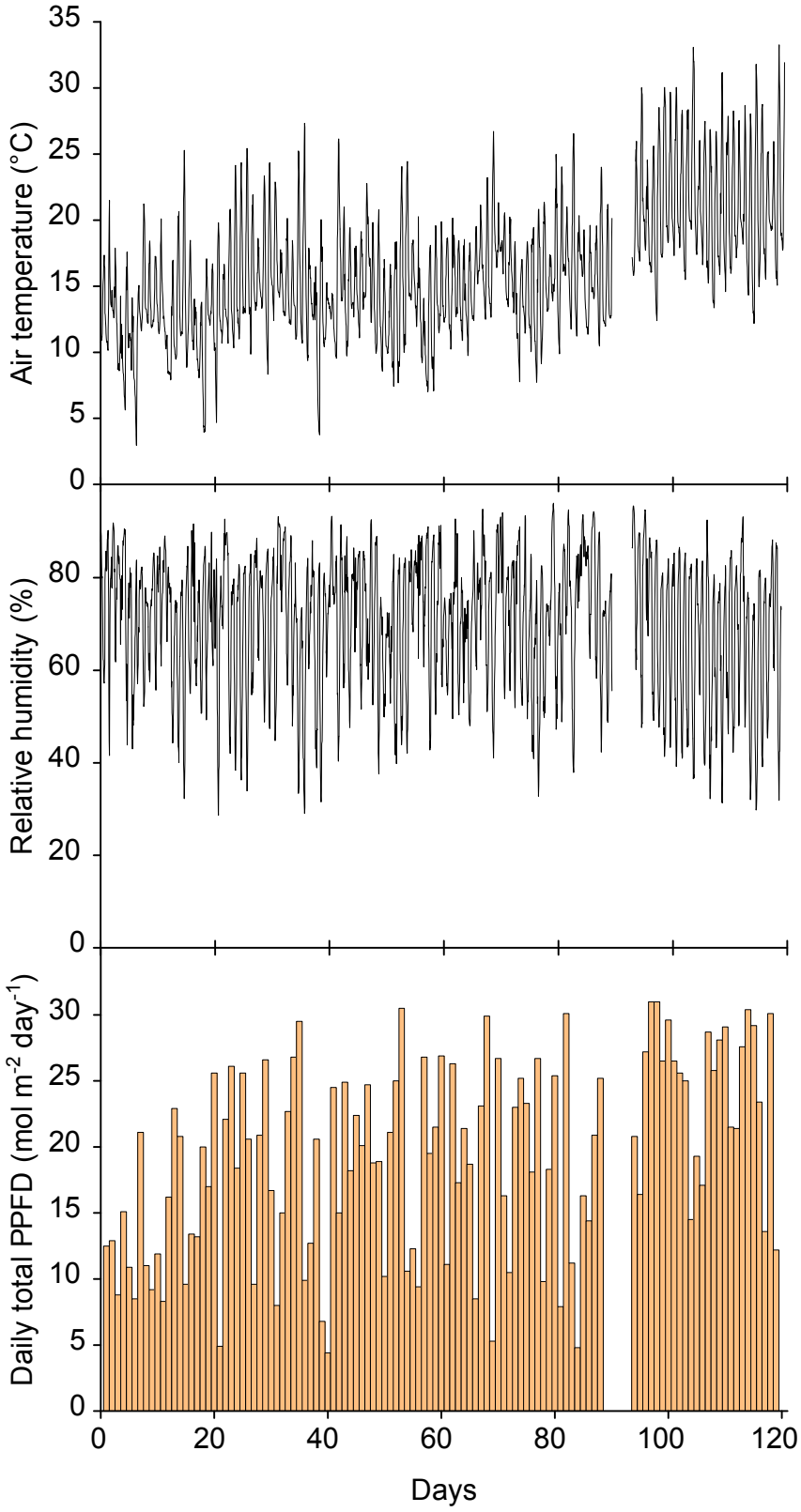

Figure 2. Hourly mean temperature and humidity, and daily photosynthetic photon flux density (PPFD) in the greenhouse during the willow water-stress experiment.

$$\text{Log}_{10}\, S = \log_{10} a + b \log_{10} B \quad (1)$$

where S is the fresh weight of the shoot, and B is the square of the basal diameter multiplied by the shoot height. The equation was back-transformed to the power function:

$$S = aB^b \quad (2)$$

where the anti-log of the intercept was multiplied by a correction factor to account for bias inherent in fitting the model to the geometric mean rather than the arithmetic mean (Sprugel 1983). The correction factor was calculated as:

$$CF = 10^{(S^2_{y.x}/2)} \quad (3)$$

where $S_{y.x}$ is the standard error of the estimate (SEE) of the regression.

The regression coefficients in equation (1) were calculated using sample shoots with a wide range of basal diameters and heights from nursery stools of the willow clones. The fresh biomass of the sample shoots was weighed, and the leaf area measured using a LI-3100 area meter (Li-Cor Inc., Lincoln, Nebraska, USA). A single equation was found to give a good fit to the shoot biomass weight for all the willow clones, but separate equations were used to estimate the shoot leaf area for each of the willow clones.

The diameter growth of the cuttings was measured at weekly intervals, from the start of the application of the water regimes at 70 days. Two diameters were measured at right angles on the tree stems, using callipers, and averaged.

5.2.7 Leaf stomatal conductance and water potential

The stomatal conductance of the leaves was measured using a cycling porometer (Delta-T porometer type AP4, Delta-T Devices Ltd, Cambridge, UK), and the water potential of the leaves was measured using a Scholander-type pressure chamber (Soil Moisture Equipment Co., Santa Barbara, California, USA).

The diurnal variation in the stomatal conductance of the leaves of the willow trees was measured after the application of the water regimes on day 115 (a clear sunny day) at one hour intervals between 06:00 and 21:00. The measurements were made on the second day of the two day watering cycle. Two or three young fully expanded mature leaves were selected on the same shoot on each tree in block 2, and the stomatal conductance was measured once on the abaxial (lower) surface of each leaf.

The variation in the stomatal conductance with leaf number along the length of the shoots was measured after the application of the water regimes on day 90 (a clear sunny day). The measurements were made between 13:00 and 16:30, on the first day of the two-day watering cycle. One dominant shoot was selected from each tree in block 2, and the stomatal conductance was measured once on the abaxial (lower) surface of each leaf from the apex to the base of the shoot.

The stomatal conductance and water potential of the leaves were measured on all the willow trees (blocks 1 to 4) after the application of the water regimes on days 110, 111, 112, 113, and 114. The measurements were made between 13:30 and 17:30 on the first and second days of the two-day watering cycle. One young fully expanded mature leaf was selected on each tree per day, and the stomatal conductance was measured once on the abaxial (lower) surface of the leaf, and this was followed immediately by the measurement of the water potential.

5.2.8 Leaf photosynthesis

The photosynthetic rate and transpiration rate of the leaves of the willow trees were measured on all the willow trees (blocks 1 to 4) after the application of the water regimes on days 111, 112, 113, and 114. The measurements were made between 10:00 and 13:00 on the first and second days of the two-day watering cycle. One young fully expanded mature leaf was selected on each tree per day. The photosynthesis was measured with saturating light (2000 µmol m^{-2} s^{-1}), ambient CO_2 concentration (400 µmol CO_2 mol^{-1} air), leaf temperature 20°C, and relative humidity 65–70%.

5.2.9 Harvesting the willow trees

The willow trees were harvested 49 days (7 weeks) after the application of the water regimes, on 14 January 2015. The biomass of the trees was divided for the leaves, stems, cuttings, and roots. The leaf area of each tree was measured and the number of leaves counted. The roots were separated from the soil by washing with water the roots retained on a 2 mm size mesh. The weights of the leaf, stem, cutting, and root biomass were measured for each tree after oven-drying at 70ºC to constant weight.

The water-use efficiency (WUE) of biomass production was determined for each tree. This was the ratio of the total biomass to the total amount of water used throughout the growing season (g biomass kg^{-1} water). The total biomass included the oven-dried leaf, stem and root weights, and the cutting weight minus the original cutting weight at the start of the experiment. The oven-dried weight of the original cutting was calculated as a proportion of the volume of the cutting at harvest.

5.2.10 Statistical analysis

Analysis of variance (ANOVA) and covariance (ANCOVA) were used to assess the effects of the water regime, willow clone and block (covariate), and the water regime × willow clone interaction, on the various traits measured. The cutting diameter at the beginning of the experimental treatment period (70 days) was used as an additional covariate in the ANCOVA in order to consider the effects of the initial plant size on the traits statistically. Fisher's Least Significant Difference (LSD) test was used post hoc, at the 5% level, to provide multiple comparisons of the willow clone and water regime means. All the statistics were computed using the GenStat statistical software package (Version 14.2; VSN International Ltd, UK).

5.3 Results

5.3.1 Growth of the willow trees prior to the soil water deficits

The willow trees were grown at 90% of field capacity (FC) for 70 days, before the application of the soil water deficits of the 60% and 40% FC water regime treatments. During this period, the *Salix matsudana* (M) x *S. pentandra* (P) clone MP002, and the *S. matsudana* (M) x *S. lasiandra* (L) clones ML022 and ML089 had greater shoot biomass (leaf + stem) growth (Table 3, Figure 3), while the *S. matsudana* x *S. alba* clone 'Tangoio' had slower growth, and the *S. lasiandra* (L) x *S. pentandra* (P) clone LP026 had the slowest growth. The shoots of the LP026 clone were slower in sprouting from the cuttings than the other clones, and the LP026 and 'Tangoio' clones had fewer shoots per cutting than the other clones. This contributed to the lower leaf area of the trees of the LP026 and 'Tangoio' clones, compared with those of the MP002, ML022, and ML089 clones. The height (tallest shoot per tree) growth was similar for the 'Tangoio', MP002, ML022, and ML089 clones, but was less for the LP026 clone.

5.3.2 Growth of the willow trees after the application of soil water deficits

The application of the moderate and severe soil water deficits of the 60 and 40% FC water regime treatments, from 70 to 119 days, had a noticeable effect on the growth of the willow trees and on the number of leaves.

All the willow clones showed leaf senescence on the lower parts of the stems from 7 to 15 days after the commencement of the 40% FC water regime treatment (Figure 4). The loss of leaves was greatest for the MP002 clone, and occurred to a lesser extent for the ML022, LP026 and ML089 clones, in that order. The 'Tangoio' clone was less affected, with the growth in the number of new leaves compensating for the loss of leaves on the lower parts of the stems. The MP002 clone also showed some leaf senescence for the 60% FC treatment from 7 days, but this was compensated for by the growth of new leaves. The plants in the 90% FC treatment showed some leaf senescence at 92 days, particularly for the MP002 and ML022 clones, which occurred in response to water stress as the rapid growth in the leaf area of the trees increased the soil water deficits during the two-day watering cycle.

The height growth of the shoots showed a strong response to the soil water deficits, and was slower for the plants in the 60 and 40% FC water regime treatments ($p < 0.001$) than for those in the 90% FC treatment (Figure 5). However, the responses varied widely for the willow clones. The LP026 and MP002 clones had the greatest height growth at 90% FC, and while the LP026 clone had good height growth at 60 and 40% FC, the MP002 clone had the slowest height growth (with some shoot tip die-back) at 40% FC. The MP002 clone had the largest differences in height growth between the 90, 60 and 40% FC treatments. The ML022, ML089, and 'Tangoio' clones had good height growth at 60 and 40% FC, but the additional height growth at 90% FC was smaller than for theLP026 and MP002 clones, and not significantly different from the 60% FC height growth for the ML089 and 'Tangoio' clones.

The diameter growth of the cuttings of the willow trees, from which the shoots had sprouted, was slower for the plants in the 60 and 40% FC water regime treatments ($p < 0.001$) than for those in the 90% FC treatment (Figure 6). The diameter growth slowed progressively with the increasing severity of the soil water deficits (from 90 to 40% FC). The cutting diameter growth was similar for all the clones at 40% FC, and greater for the 'Tangoio' and MP002 clones, and

slower for the LP026 clone, at 60 and 90% FC. The 'Tangoio' clone differed from the other clones in showing negative diameter growth during the first 8 days, after the commencement of the 40% FC treatment, as water was drawn from the cutting in response to the soil water deficit.

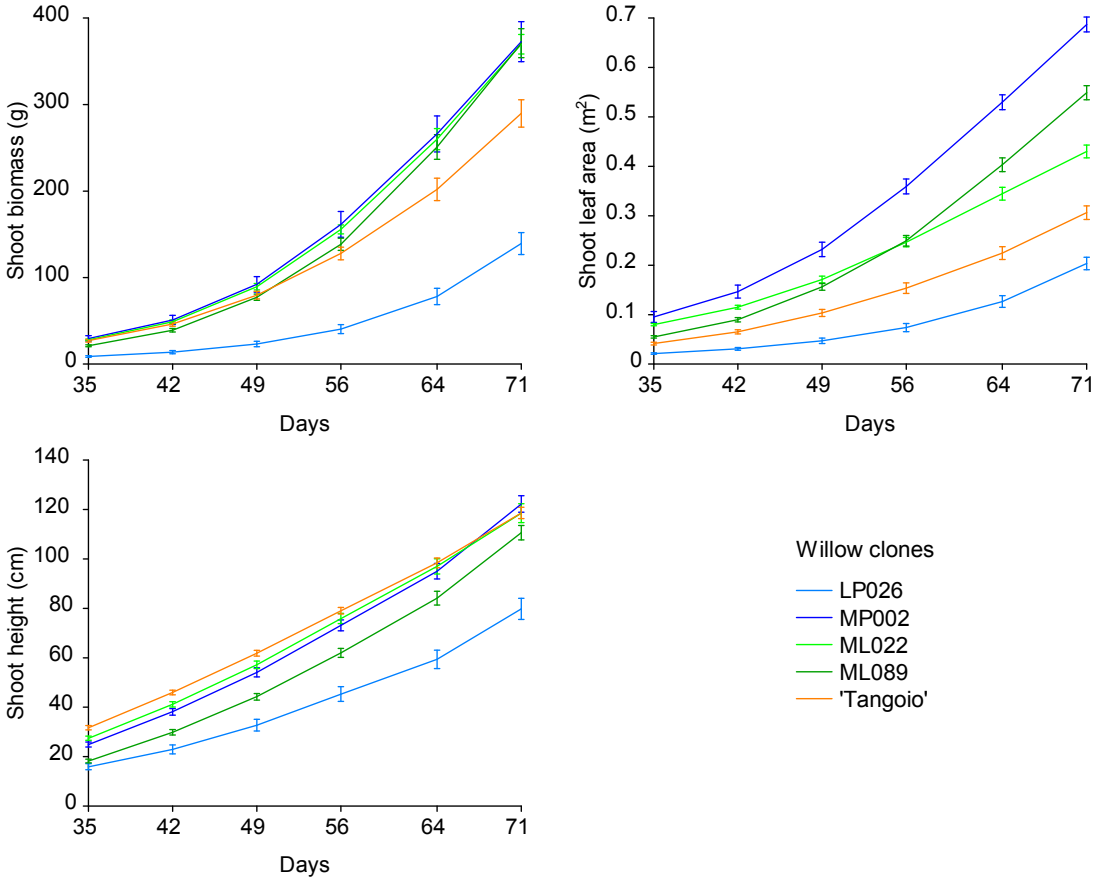

Figure 3. Growth to 70 days of the fresh shoot biomass (leaf + stem), shoot leaf area (per tree), and mean shoot height (for the tallest shoot per tree) of the willow clones, prior to the application of the water regimes. The error bars are the standard errors of the means.

Table 3. Shoot biomass (fresh leaf + stem weight), leaf area, number of shoots per tree, and mean shoot height for the tallest shoot per tree, of the willow clones at 70 days from planting. Values are the mean ± standard error, and different letters represent significant differences among the water regimes within the same clone ($P < 0.05$).

Clone	Shoot biomass Leaf + stem g	Leaf area cm²	Number of shoots	Mean shoot height cm
LP026	139 ± 13 a	2034 ± 125 a	9 ± 1 a	80 ± 4 a
MP002	373 ± 23 c	6869 ± 152 e	13 ± 1 b	122 ± 3 c
ML022	370 ± 11 c	4301 ± 131 c	13 ± 1 b	119 ± 4 bc
ML089	371 ± 17 c	5491 ± 143 d	15 ± 1 c	111 ± 3 b
'Tangoio'	290 ± 16 b	3062 ± 138 b	9 ± 0 a	119 ± 2 bc

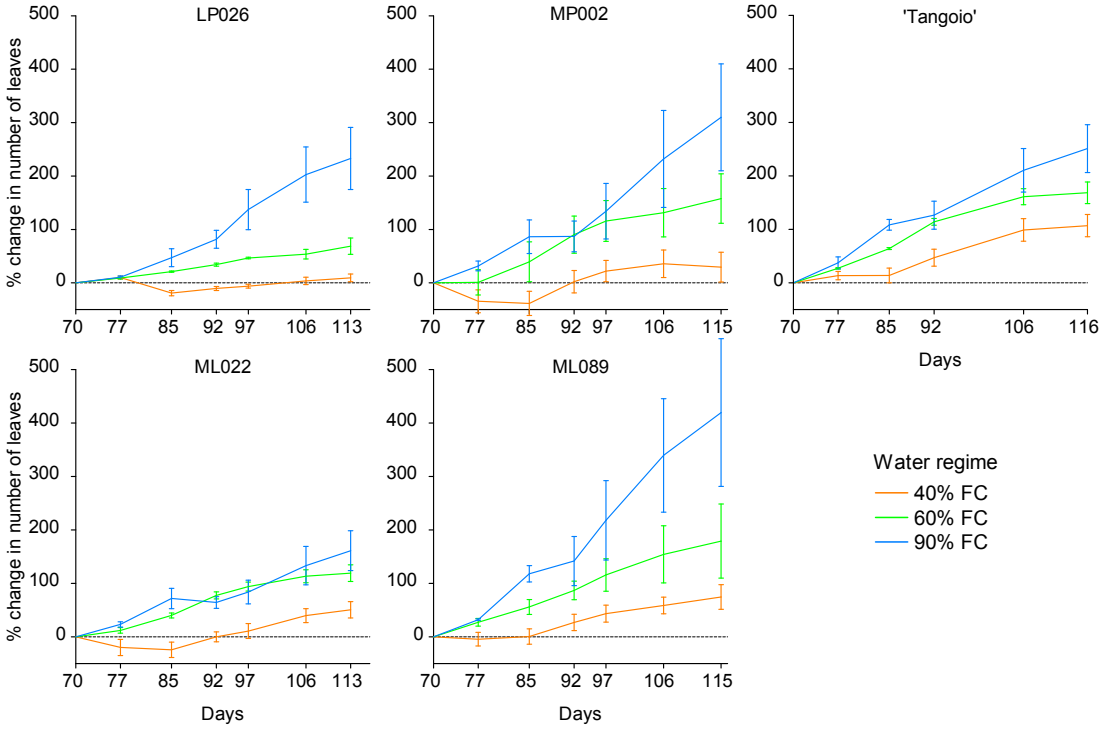

Figure 4. Change in the number of leaves on the trees of the willow clones, following the application of the water regimes from 70 days. The water regimes were 40, 60, and 90% of field capacity (FC). The error bars are the standard errors of the means.

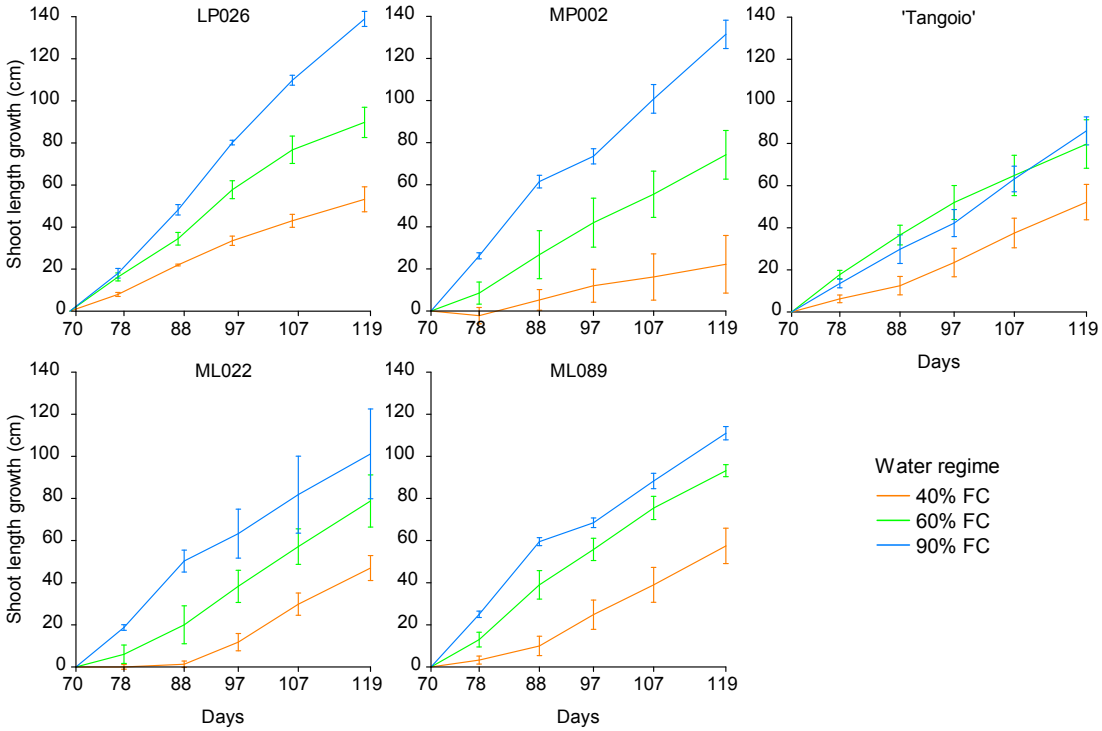

Figure 5. Growth of the mean shoot height (tallest shoot per tree) for the willow clones, following the application of the water regimes at 70 days. The water regimes were 40, 60, and 90% of field capacity (FC). The error bars are the standard errors of the means.

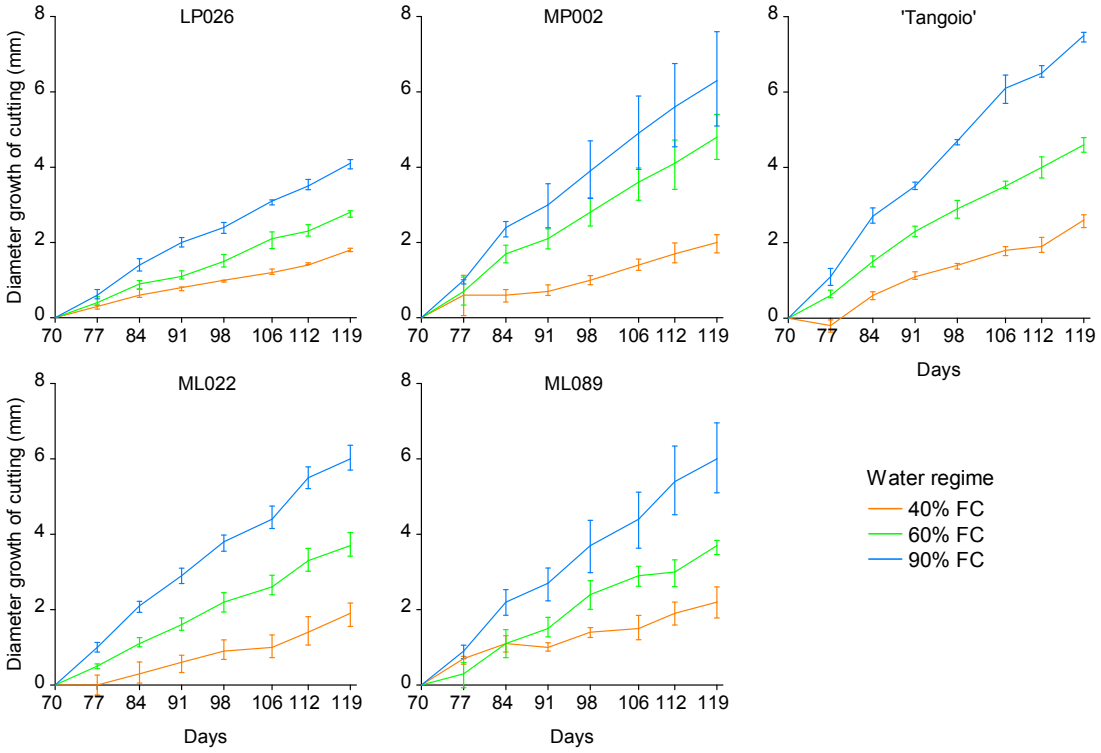

Figure 6. Growth of the cutting diameter for the willow trees, following the application of the water regimes at 70 days. The water regimes were 40, 60, and 90% of field capacity (FC). The error bars are the standard errors of the means.

5.3.3 Water content of the soil after the application of soil water deficits

The application of the moderate and severe soil water deficits of the 60 and 40% FC water regime treatments reduced the soil water content of the 30-L pots to lower levels ($p < 0.001$) than those in the 90% FC treatment (Figures 7 and 8). The reduction in the soil water content of the pots occurred within 10 days of the start of the water regimes for the 60 and 40% FC treatments. The soil water contents were similar for all the willow clones, and consistently lower for the 40% FC treatment, and highly variable for the 60 and 90% FC treatments, during the two-day watering cycles. This variability reflected the day-to-day variation of the environmental conditions, such as the sunlight, air temperature and humidity, in the greenhouse during the experiment (Figure 2).

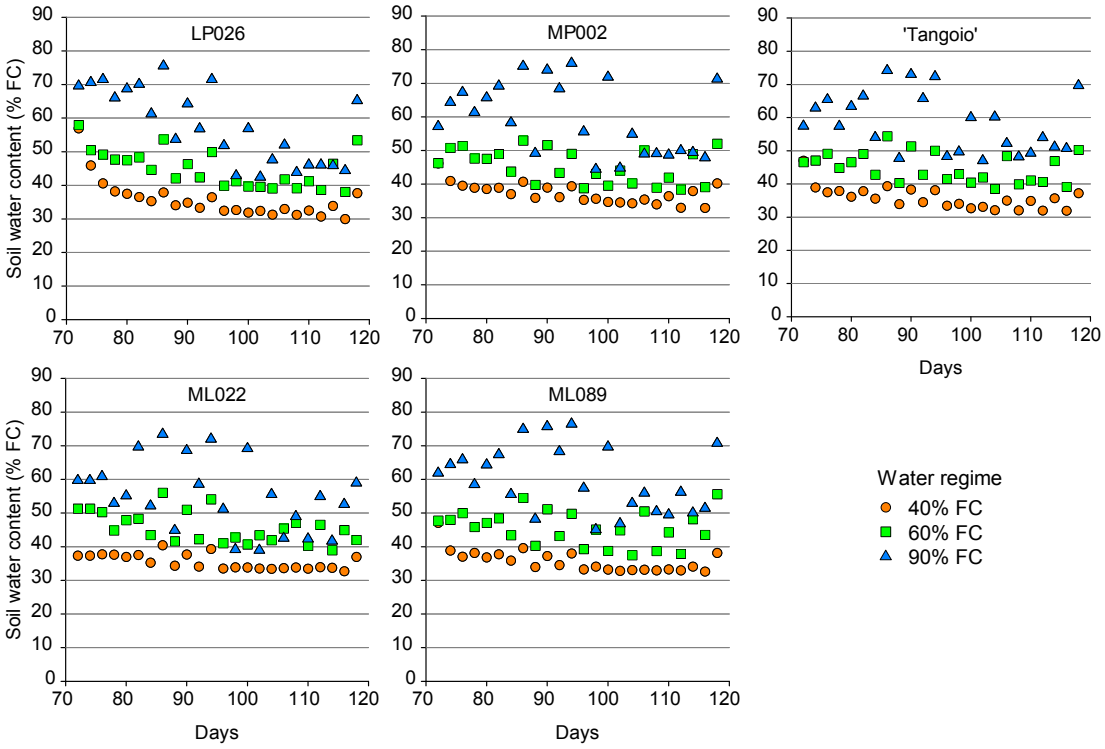

Figure 7. Water content of the soil for the willow clones and water regimes from 70 to 119 days, after the application of the water regimes. Minimum values of soil water content, during the two-day watering cycle, are given as a percentage of the field capacity. The water regimes were 40, 60, and 90% of field capacity (FC).

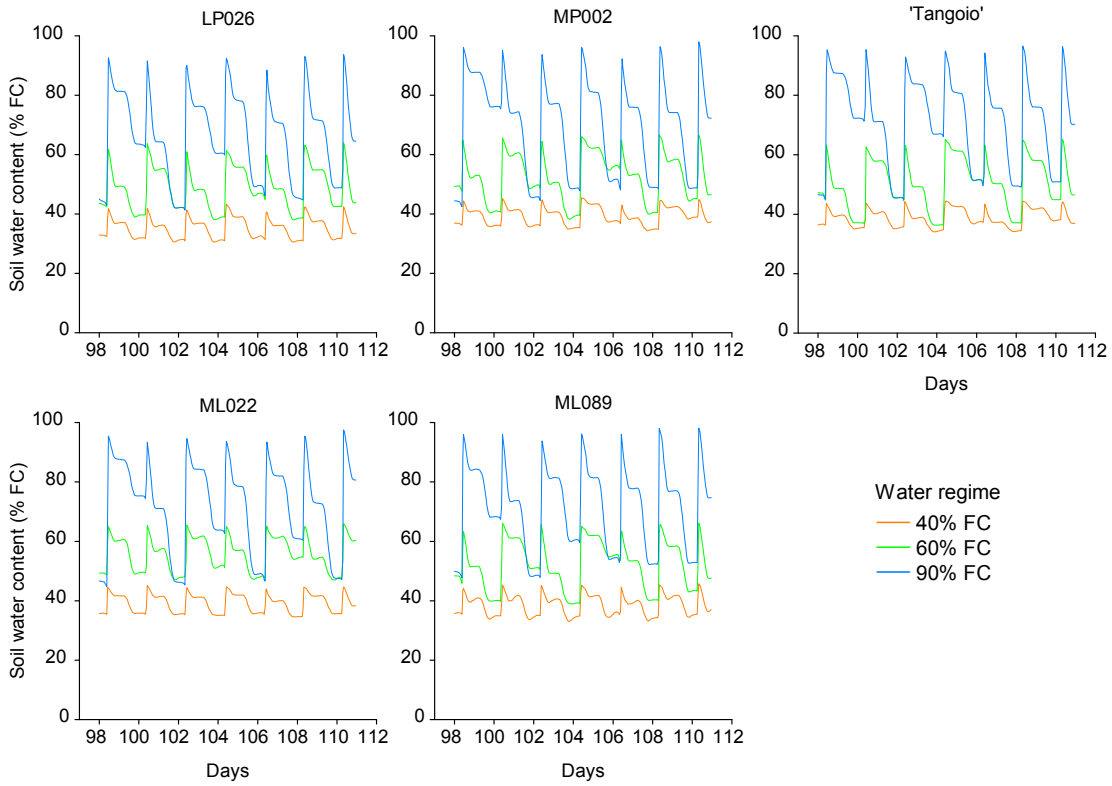

Figure 8. Water content of the soil of the willow clones and water regimes, between watering cycles on days 105 to 107. Hourly average values of soil water content, as a percentage of the field capacity. The water regimes were 40, 60, and 90% of field capacity (FC).

5.3.4 Biomass of the willow trees at harvest

The soil water deficits of the water regime treatments and the willow clones had a large effect on the leaf, stem, cutting and root biomass of the willow trees at harvest, and on the water use efficiency of the trees, during the 119 days of growth (Figure 9, Tables 4-11).

The leaf area and number of leaves on the trees were lower for the plants in the 60 and 40% FC water regime treatments than for those in the 90% FC treatment, for all the willow clones (Tables 4 and 5). The leaf area was similar for the willow clones in each treatment, but the LP026 clone had a smaller, and the ‘Tangoio’ clone a larger number of leaves, in inverse proportion to the larger and smaller size of the leaves of these clones, respectively. The leaf size declined for the 40% FC treatment, most notably for the MP002 clone. The leaf specific area (leaf area per dry weight of leaf) was lower for the ML022 and LP026 clones, and higher for the ‘Tangoio’ and MP002 clones, and generally increased with the severity of the soil water deficits (from 90 to 40% FC).

The diameter and basal area of the shoots, the ratio of the leaf area to basal area of the shoots, and the shoot height (tallest shoot per tree) at 119 days were lower for the plants in the 60 and 40% FC water regime treatments than those in the 90% FC treatment (Tables 6 and 7). There were differences among the willow clones, with the ML089 clone having higher, and the LP026 and ‘Tangoio’ clones lower basal area of the shoots, and the LP026 and ‘Tangoio’ clones having higher, and the ML089 clone lower ratios of leaf area to basal area of the shoots. The diameter and height (tallest shoot per tree) of the shoots were similar for the willow clones.

The leaf, stem, cutting and root biomass of the willow trees at 119 days were lower for the plants in the 60 and 40% FC water regime treatments than for those in the 90% FC treatment (Tables 8 and 9). There was a progressive decrease in the leaf, stem, cutting and root biomass of the trees with the increased severity of the soil water deficits (from 90 to 40% FC). With the application of the 60% and 40% FC water regime treatments, the allocation of the biomass to the leaves generally decreased, as a percentage of the total biomass, and the allocation to the stems and cuttings increased, with no change in the allocation of biomass to the roots. There were differences in biomass allocation among the willow clones, with the LP026 clone allocating more biomass to the roots, and less to the stems, and the ML089 clone allocating more biomass to the stems and less to the roots. The 'Tangoio' clone allocated more biomass to the cuttings than the other willow clones.

The amount of water used and the dry weight (DW) gained by the willow trees were lower, the water-use efficiency (WUE) of the trees was higher, and the root-to-shoot ratio was unchanged, for the plants in the 60 and 40% FC water regime treatments than for those in the 90% FC treatment (Tables 10 and 11). There was a progressive decrease in the amount of water used and in the DW gained, and a progressive increase in the WUE of the trees, with the increased severity of the soil water deficits (from 90 to 40% FC). There were differences among the willow clones in the water usage, DW gain, WUE, and root-to-shoot ratio. The LP026 clone had lower, and the ML022 clone higher water usage. The DW gains were lower for the LP026 clone, and higher for the 'Tangoio', ML089, and ML022 clones. The 'Tangoio', ML089, and LP026 clones had higher WUE than the MP002 and ML022 clones. The LP026 clone had higher root-to-shoot ratios, double those of the ML089 clone, which had the lowest root-to-shoot ratios.

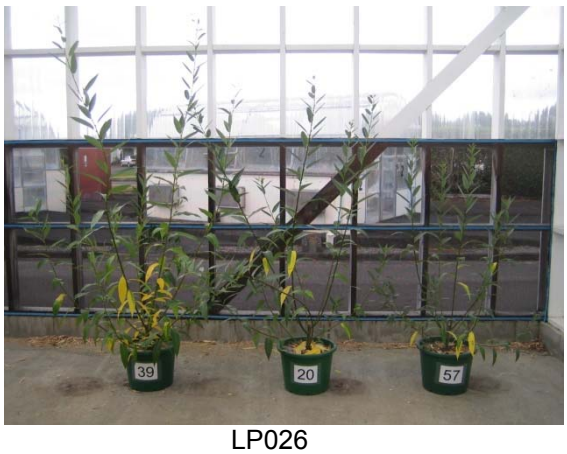

LP026

MP002

ML022

ML089

’Tangoio’

Figure 9. Representative trees of the willow clones and water regime treatments at 119 days. The trees of each clone are from left to right: well-watered (90% field capacity (FC)), moderate (60% FC), and severe (40% FC) soil water deficit treatments, with the three trees of each clone being from block 2 or 3.

Table 4. The leaf area and number of leaves per tree, and the leaf size and specific leaf area of the willow clones at harvest (119 days) as affected by the water regimes. Values are the mean ± standard error, and different letters represent significant differences among the water regimes within the same clone ($P < 0.05$).

Clone	Water regime	Leaf area m^2	Number of leaves	Leaf size cm^2	Specific leaf area $cm^2\ g^{-1}$
LP026	40% FC	0.57 ± 0.02 a	217 ± 17 a	26.4 ± 1.5 a	133 ± 2 a
	60% FC	0.98 ± 0.06 b	268 ± 26 a	37.5 ± 3.1 b	138 ± 5 a
	90% FC	1.43 ± 0.08 c	516 ± 45 a	28.3 ± 2.6 a	130 ± 12 a
MP002	40% FC	0.61 ± 0.04 a	1042 ± 137 a	6.1 ± 0.6 a	167 ± 10 a
	60% FC	1.04 ± 0.04 b	1377 ± 100 a	7.7 ± 0.7 ab	155 ± 1 a
	90% FC	1.57 ± 0.06 c	1583 ± 77 a	9.9 ± 0.3 b	156 ± 8 a
ML022	40% FC	0.71 ± 0.04 a	959 ± 103 a	7.8 ± 1.2 a	138 ± 3 a
	60% FC	1.06 ± 0.09 b	1175 ± 138 ab	9.2 ± 0.8 a	131 ± 2 a
	90% FC	1.66 ± 0.05 c	1712 ± 58 b	9.7 ± 0.4 a	131 ± 3 a
ML089	40% FC	0.68 ± 0.05 a	987 ± 55 a	6.9 ± 0.4 a	148 ± 2 a
	60% FC	0.99 ± 0.11 b	1248 ± 153 a	8.0 ± 0.2 a	146 ± 0 a
	90% FC	1.63 ± 0.11 c	2125 ± 403 b	8.2 ± 1.0 a	142 ± 5 a
'Tangoio'	40% FC	0.71 ± 0.07 a	1410 ± 323 a	5.9 ± 1.4 a	159 ± 14 b
	60% FC	1.27 ± 0.13 b	2607 ± 389 b	5.0 ± 0.3 a	158 ± 7 b
	90% FC	1.77 ± 0.07 c	2967 ± 192 b	6.0 ± 0.2 a	133 ± 4 a

FC = field capacity

Table 5. Analysis of covariance for the fixed effects of willow clone and water regime, and the interactions between them, on the leaf area, number of leaves, leaf size and specific leaf area (SLA).

Source of variation	d.f.	Leaf area		No. of leaves		Leaf size		SLA	
		MS	*P*	MS	*P*	MS	*P*	MS	*P*
Block	3	4.3E6	0.112	0.8E5	0.664	2.1	0.824	226	0.266
Initial cutting diameter	1	—	—	—	—	—	—	—	—
Clone	4	10.5E6	0.002	60.2E5	<.001	1309.2	<.001	1494	<.001
Water regime	2	456.4E6	<.001	36.8E5	<.001	41.0	0.006	583	0.038
Clone × water regime	8	1.3E6	0.746	3.5E5	0.038	30.0	<.001	159	0.480
Error	41	2.0E6		1.5E5		7.1		165	

Block and initial cutting diameter (mm) at the start of the water regimes (70 days) were used as covariates.
d.f., Degrees of freedom; MS, mean squares (variance); *P*, probability value

Table 6. The shoot diameter, basal area of the shoots, ratio of leaf area to basal area of shoots, and shoot height (tallest shoot per tree) of the willow clones at harvest (119 days) as affected by the water regimes. Values are the mean ± standard error, and different letters represent significant differences among the water regimes within the same clone ($P < 0.05$).

Clone	Water regime	Shoot diameter mm	Basal area of shoots cm^2	Leaf area / Basal area of shoots	Shoot height m
LP026	40% FC	7.3 ± 0.5 a	4.2 ± 0.5 a	1361 ± 119 a	1.3 ± 0.1 a
	60% FC	9.2 ± 0.3 b	6.0 ± 0.3 b	1623 ± 92 b	1.7 ± 0.1 b
	90% FC	10.3 ± 0.7 b	7.3 ± 0.4 c	1932 ± 119 c	2.2 ± 0.1 c
MP002	40% FC	7.9 ± 0.4 a	6.8 ± 1.1 a	983 ± 165 a	1.5 ± 0.1 a
	60% FC	9.7 ± 0.4 b	8.8 ± 1.1 b	1217 ± 167 a	1.9 ± 0.0 b
	90% FC	9.0 ± 0.4 ab	10.7 ± 1.4 c	1524 ± 165 b	2.6 ± 0.1 c
ML022	40% FC	7.8 ± 0.3 a	6.7 ± 0.2 a	1072 ± 77 a	1.6 ± 0.1 a
	60% FC	10.0 ± 0.7 b	8.9 ± 0.5 b	1227 ± 137 ab	2.0 ± 0.1 b
	90% FC	10.2 ± 0.5 b	11.5 ± 0.5 c	1449 ± 113 b	2.2 ± 0.2 b
ML089	40% FC	8.0 ± 0.3 a	7.9 ± 0.6 a	897 ± 86 a	1.6 ± 0.1 a
	60% FC	9.3 ± 0.6 b	10.3 ± 0.9 b	1004 ± 160 a	2.0 ± 0.0 b
	90% FC	10.0 ± 0.3 b	13.1 ± 0.7 c	1274 ± 136 b	2.2 ± 0.1 b
'Tangoio'	40% FC	9.0 ± 0.5 a	5.2 ± 0.4 a	1305 ± 159 a	1.7 ± 0.1 a
	60% FC	9.7 ± 0.4 a	7.6 ± 0.3 b	1620 ± 110 b	2.0 ± 0.2 a
	90% FC	11.7 ± 0.2 b	10.1 ± 0.5 c	1737 ± 123 b	2.1 ± 0.1 a

FC = field capacity

Table 7. Analysis of covariance for the fixed effects of willow clone and water regime, and the interactions between them, on the shoot diameter, basal area of the shoots, ratio of leaf area to basal area of shoots, and shoot height (tallest shoot per tree).

Source of variation	d.f.	Shoot diameter		Basal area of shoots		Leaf area / Basal area of shoots		Shoot height	
		MS	*P*	MS	*P*	MS	*P*	MS	*P*
Block	3	1.6	0.110	11.7	<.001	49.8E4	<.001	7.0E4	0.273
Initial cutting diameter	1	—	—	20.1	<.001	13.9E4	0.039	—	—
Clone	4	3.2	0.006	29.8	<.001	61.2E4	<.001	8.9E4	0.166
Water regime	2	27.2	<.001	96.7	<.001	105.6E4	<.001	299.3E4	<.001
Clone × water regime	8	1.3	0.116	0.8	0.135	1.5E4	0.867	11.3E4	0.052
Error	41	0.8		0.5		3.1E4		5.2E4	

Block and initial cutting diameter at the start of the water regimes (70 days) were used as covariates.
d.f., Degrees of freedom; MS, mean squares (variance); *P*, probability value

Table 8. Allocation of biomass to the leaves, stems, cutting, and roots of the willow clones at harvest (119 days) as affected by the water regimes. Values are the mean ± standard error, and different letters represent significant differences among the water regimes within the same clone (*P* < 0.05).

Clone	Water regime	Biomass (g)				Biomass (%)			
		Leaf	Stem	Cutting	Root	Leaf	Stem	Cutting	Root
LP026	40% FC	42 ± 2 a	65 ± 8 a	15 ± 2 a	35 ± 3 a	27	41	10	22
	60% FC	71 ± 4 b	121 ± 12 b	22 ± 1 a	62 ± 7 b	26	44	8	22
	90% FC	111 ± 8 c	185 ± 15 c	31 ± 1 b	86 ± 8 c	27	45	8	21
MP002	40% FC	37 ± 1 a	109 ± 12 a	23 ± 3 a	28 ± 2 a	19	55	12	14
	60% FC	65 ± 2 b	169 ± 9 b	24 ± 10 a	50 ± 1 b	21	55	8	16
	90% FC	101 ± 5 c	245 ± 16 c	40 ± 3 b	67 ± 5 c	22	54	9	15
ML022	40% FC	52 ± 3 a	106 ± 7 a	22 ± 1 a	30 ± 2 a	25	56	10	14
	60% FC	83 ± 7 b	167 ± 16 b	33 ± 2 b	54 ± 5 b	25	49	10	16
	90% FC	126 ± 1 c	234 ± 8 c	48 ± 2 c	84 ± 7 c	26	48	10	17
ML089	40% FC	48 ± 3 a	131 ± 4 a	22 ± 2 a	26 ± 1 a	21	58	10	12
	60% FC	70 ± 8 b	204 ± 5 b	33 ± 2 b	42 ± 2 b	20	59	9	12
	90% FC	118 ± 9 c	265 ± 6 c	43 ± 2 c	52 ± 3 c	25	55	9	11
‘Tangoio’	40% FC	43 ± 4 a	112 ± 4 a	27 ± 2 a	28 ± 3 a	21	54	13	13
	60% FC	79 ± 7 a	180 ± 8 b	40 ± 2 b	49 ± 3 b	23	52	12	14
	90% FC	131 ± 2 b	252 ± 6 c	59 ± 2 c	63 ± 2 c	26	50	12	12

FC = field capacity.

Table 9. Analysis of covariance for the fixed effects of willow clone and water regime, and the interactions between them, on the leaf, stem and root biomass.

Source of variation	d.f.	Leaf		Stem		Cutting		Root	
		MS	*P*	MS	*P*	MS	*P*	MS	*P*
Block	3	3.1E+2	0.018	24.1E+2	<.001	0.2E+2	0.648	3.4E+2	<.001
Initial cutting diameter	1	4.0E+2	0.033	16.4E+2	0.006	6.1E+2	<.001	—	—
Clone	4	7.0E+2	<.001	89.2E+2	<.001	25.6E+2	<.001	7.9E+2	<.001
Water regime	2	541.2E+2	<.001	864.2E+2	<.001	0.6E+2	0.165	83.8E+2	<.001
Clone × water regime	8	0.9E+2	0.362	1.0E+2	0.839	1.7E+2	0.038	1.4E+2	0.012
Error	41	0.8E+2		1.9E+2		0.4E+2		0.5E+2	

Block and initial cutting diameter at the start of the water regimes (70 days) were used as covariates.
d.f., Degrees of freedom; MS, mean squares (variance); *P*, probability value.

Table 10. Water usage, dry weight (DW) gain, and water use efficiency (WUE) from 0 to 119 days, and the root-to-shoot ratio of the willow clones under different water regimes. Values are the mean ± standard error, and different letters represent significant differences among the water regimes within the same clone ($P < 0.05$).

Clone	Water regime	Water use kg	DW gain g	WUE g DW kg^{-1} water	Root-to-shoot ratio
LP026	40% FC	29 ± 3 a	156 ± 14 a	5.5 ± 0.2 b	0.32 ± 0.01 a
	60% FC	50 ± 5 b	275 ± 24 b	5.5 ± 0.1 b	0.32 ± 0.02 a
	90% FC	87 ± 5 c	413 ± 28 c	4.7 ± 0.1 a	0.29 ± 0.03 a
MP002	40% FC	43 ± 6 a	198 ± 17 a	4.8 ± 0.3 a	0.19 ± 0.01 a
	60% FC	65 ± 7 b	307 ± 8 b	4.8 ± 0.4 a	0.21 ± 0.01 a
	90% FC	104 ± 9 c	453 ± 27 c	4.4 ± 0.1 a	0.19 ± 0.01 a
ML022	40% FC	46 ± 3 a	211 ± 11 a	4.6 ± 0.2 ab	0.19 ± 0.01 a
	60% FC	69 ± 6 b	338 ± 28 b	4.9 ± 0.2 b	0.22 ± 0.01 ab
	90% FC	115 ± 3 c	492 ± 12 c	4.3 ± 0.0 a	0.23 ± 0.02 b
ML089	40% FC	42 ± 2 a	228 ± 6 a	5.6 ± 0.2 b	0.15 ± 0.00 a
	60% FC	63 ± 3 b	351 ± 14 b	5.7 ± 0.2 b	0.16 ± 0.01 a
	90% FC	99 ± 5 c	480 ± 6 c	5.0 ± 0.2 a	0.14 ± 0.01 a
'Tangoio'	40% FC	35 ± 2 a	208 ± 10 a	5.7 ± 0.2 b	0.17 ± 0.01 a
	60% FC	60 ± 2 b	347 ± 20 b	5.7 ± 0.2 b	0.19 ± 0.01 a
	90% FC	98 ± 2 c	504 ± 10 c	5.1 ± 0.1 a	0.16 ± 0.00 a

FC = field capacity

Table 11. Analysis of covariance for the fixed effects of willow clone and water regime, and the interactions between them, on the water used, dry weight (DW) gain, water use efficiency (WUE), and the root-to-shoot ratio (RSR).

Source of variation	d.f.	Water use		DW gain		WUE		RSR	
		MS	*P*	MS	*P*	MS	*P*	MS	*P*
Block	3	4.4E+2	<.001	4.7E+3	<.001	11.2	<.001	0.8E-3	0.210
Initial cutting diameter	1	6.2E+2	<.001	6.8E+3	0.002	—	—	—	—
Clone	4	7.3E+2	<.001	11.1E+3	<.001	22.2	<.001	44.1E-3	<.001
Water regime	2	194.5E+2	<.001	359.0E+3	<.001	23.6	<.001	1.3E-3	0.093
Clone × water regime	8	0.3E+2	0.403	0.4E+3	0.718	0.4	0.907	0.8E-3	0.185
Error	41	0.3E+2		0.6E+3		1.0		0.5E-3	

Block and initial cutting diameter at the start of the water regimes (70 days) were used as covariates.
d.f., Degrees of freedom; MS, mean squares (variance); *P*, probability value.

5.3.5 Leaf stomatal conductance and water potential

The soil water deficits of the water regimes had a large effect on the stomatal conductance of the leaves of the willow trees. The stomatal conductance of the abaxial (lower) surface of the leaves decreased with the increasing severity of the soil water deficits, and was lower for the plants in the 60 and 40% FC water regime treatments than for those in the 90% FC treatment (Tables 12 and 13). The water regimes had no effect on the water potential of the leaves (Ψ_l), but the watering cycle had a significant effect, with the leaves having lower values of Ψ_l on the second day of the two-day watering cycle (-0.50 and -0.90 MPa, days 1 and 2). The stomatal conductance of the leaves was also lower on the second day of the watering cycle (373 and 211 mmol m^{-2} s^{-1}, days 1 and 2). There were differences among the willow clones in the stomatal conductance of the leaves, with the ML089 and 'Tangoio' clones having lower stomatal conductance at 90% FC, and the 'Tangoio' clone had the lowest stomatal conductance at 60 and 40% FC.

The diurnal variation in the stomatal conductance of the leaves from 6:00 to 21:00 hours showed the stomatal conductance increasing and peaking during the morning and then declining through the afternoon, with large differences between the water regimes (Figure 10). The leaves of the 40% FC water regime trees had low values of stomatal conductance that declined very quickly in the morning, and remained low through the day. The leaves of the 60% FC and 90% FC water regime trees had higher values in the morning, with the stomatal conductance of the 60% FC trees declining to lower values during the day than that of the 90% FC trees.

The maturity and position of the leaves on the tree stems had a large effect on the stomatal conductance of the leaves of the willow clones (Figure 11). The stomatal conductance increased with the maturity of the leaves from the apex on the upper part of the stems, and then generally declined to low values on the lower part of the stems.

5.3.6 Leaf photosynthesis

The soil water deficits of the water regimes had a large effect on the photosynthesis and transpiration rates of the leaves of the willow trees (Tables 12 and 13). The net photosynthetic rate and transpiration rate of the leaves decreased with the increasing severity of the soil water deficits (from 90 to 40% FC). There were differences among the willow clones in the net photosynthetic rate, with the LP026 having a higher photosynthetic rate, particularly at 40% FC, and the MP002 clone having a lower photosynthetic rate at 40% FC. The watering cycle did not have a noticeable effect on the net photosynthetic rate or the transpiration rate.

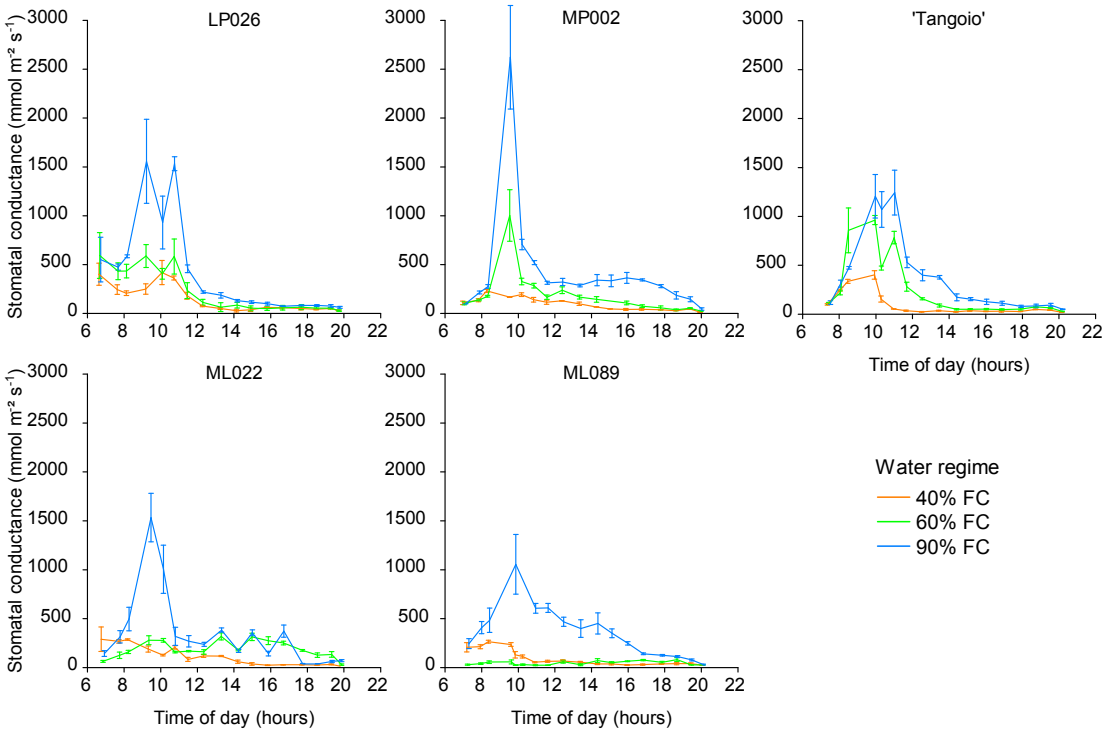

Figure 10. Diurnal variation in the leaf stomatal conductance (lower surface of the leaves) of the willow trees on day 115, the second day of the two-day watering cycle. The water regimes were 40, 60, and 90% of field capacity (FC). The error bars are the standard errors of the means.

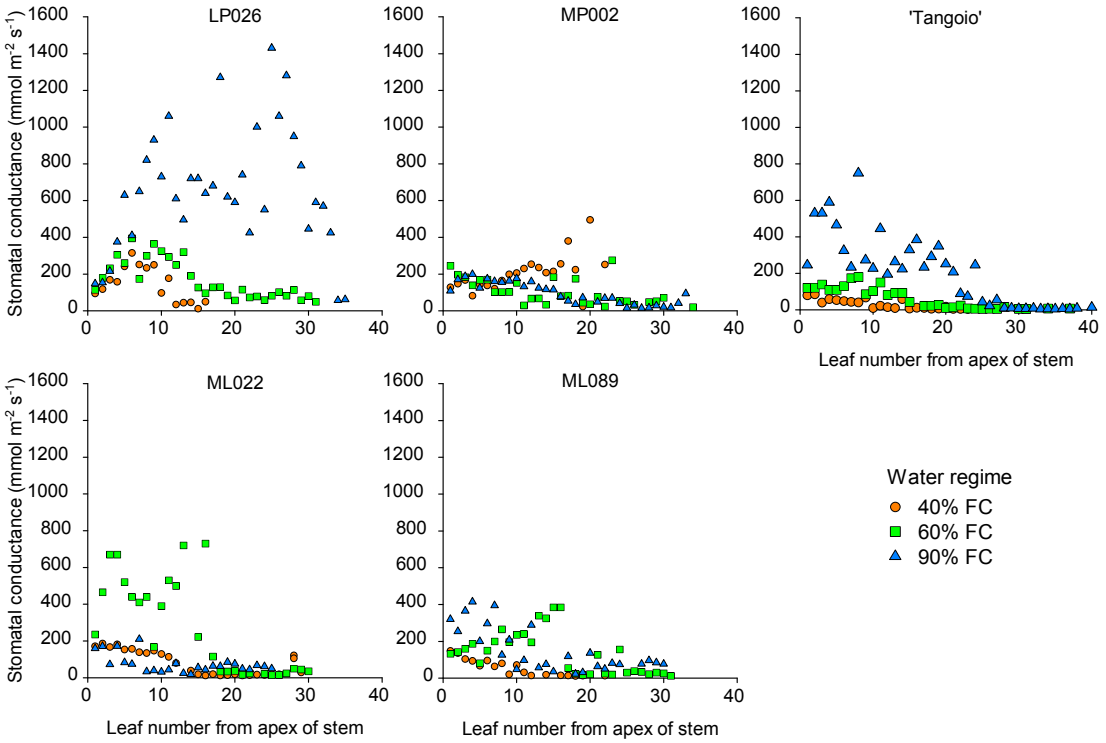

Figure 11. Stomatal conductance (lower surface of the leaves) for leaf number from the apex to base of the stems of the willow trees, between 13:00 and 16:30 on day 90, the first day of the two-day watering cycle. The water regimes were 40, 60, and 90% of field capacity (FC).

Table 12. Leaf net photosynthetic rate, transpiration rate, stomatal conductance, and water potential of the willow clones under different water regimes. Values are the mean ± standard error, and different letters represent significant differences among the water regimes within the same clone ($P < 0.05$).

Clone	Water regime	Photosynthetic rate µmol CO_2 m^{-2} s^{-1}	Transpiration rate mmol H_2O m^{-2} s^{-1}	Stomatal Conductance mmol m^{-2} s^{-1}	Water potential MPa
LP026	40% FC	15.1 ± 1.5 a	1.7 ± 0.2 a	226 ± 25 a	-0.86 ± 0.1 a
	60% FC	13.8 ± 1.6 a	1.8 ± 0.2 a	213 ± 23 a	-0.76 ± 0.1 a
	90% FC	17.0 ± 1.2 a	3.1 ± 0.4 b	583 ± 92 b	-0.89 ± 0.1 a
MP002	40% FC	6.7 ± 1.8 a	0.7 ± 0.2 a	115 ± 13 a	-0.64 ± 0.1 a
	60% FC	13.5 ± 1.9 b	1.4 ± 0.4 a	314 ± 64 b	-0.78 ± 0.1 a
	90% FC	14.7 ± 1.0 b	3.1 ± 0.4 b	659 ± 108 c	-0.75 ± 0.1 a
ML022	40% FC	11.5 ± 0.9 a	1.6 ± 0.3 a	150 ± 24 a	-0.80 ± 0.1 a
	60% FC	12.6 ± 1.7 a	2.1 ± 0.4 a	280 ± 60 a	-0.78 ± 0.1 a
	90% FC	13.6 ± 1.2 a	4.0 ± 0.5 b	557 ± 119 b	-0.70 ± 0.1 a
ML089	40% FC	9.8 ± 1.4 a	1.2 ± 0.3 a	143 ± 16 a	-0.70 ± 0.1 a
	60% FC	9.1 ± 1.8 a	1.3 ± 0.3 a	216 ± 44 a	-0.69 ± 0.1 a
	90% FC	15.4 ± 1.0 b	3.5 ± 0.2 b	294 ± 30 a	-0.78 ± 0.1 a
'Tangoio'	40% FC	9.2 ± 1.8 a	1.2 ± 0.3 a	92 ± 12 a	-0.85 ± 0.1 a
	60% FC	9.1 ± 2.1 a	1.9 ± 0.4 a	162 ± 28 ab	-0.68 ± 0.1 a
	90% FC	14.0 ± 0.4 b	4.2 ± 0.2 b	295 ± 37 b	-0.81 ± 0.1 a

FC = field capacity.

Table 13. Analysis of variance for the fixed effects of willow clone and water regime, and the interactions between them, on the leaf net photosynthetic rate, transpiration rate, stomatal conductance, and water potential.

Source of variation	d.f.	Photosynthetic rate		Transpiration rate		Stomatal conductance		Water potential	
		MS	*P*	MS	*P*	MS	*P*	MS	*P*
Block	3	40.8	0.245	2.5	0.087	4.4E5	0.033	47.0	0.009
Day	1	66.0	0.134	2.9	0.108	33.4E5	<.001	723.8	<.001
Clone	4	89.3	0.019	3.0	0.036	9.1E5	<.001	9.7	0.517
Water regime	2	282.8	<.001	82.8	<.001	58.3E5	<.001	3.6	0.737
Clone × water	8	36.9	0.265	1.0	0.520	3.1E5	0.033	6.9	0.791
Day × clone	4	29.0	0.412	1.3	0.323	4.0E5	0.030	39.0	0.013
Day × water	2	16.4	0.571	0.1	0.950	0.8E5	0.581	3.2	0.763
Error	139	29.1		1.1		1.5E5		11.9	

d.f., Degrees of freedom; MS, mean squares (variance); *P*, probability value.

5.4 Discussion

The willow clones varied in their growth characteristics and responses to the soil water deficits of the 90, 60 and 40% FC water regime treatments.

The MP002 clone was very sensitive to the soil water deficits, showing the greatest loss of leaves at the onset of the 60 and 40% FC water regime treatments, the most suppressed height growth (with shoot tip dieback), and the most significant decrease in leaf photosynthesis, transpiration and leaf size under the 40% FC treatment. In contrast, at 90% FC the MP002 clone had the tallest height growth, but the biomass growth of the trees was lower than for the ML022, ML089 and 'Tangoio' clones, which could be attributed to the lower water-use efficiency (WUE) of the MP002 clone.

The ML022 clone was also sensitive to the soil water deficits, showing leaf loss at the onset of the 40% FC water regime treatment, but the trees of this clone had a greater capacity for biomass growth than the MP002 clone under the 60 and 90% FC treatments. The ML022 clone had greater water usage than the other willow clones, which helped to compensate for the lower water-use efficiency (WUE) of this clone, which was similar to that of the MP002 clone.

The LP026 clone showed leaf loss similar to that of the ML022 clone at the onset of the 40% FC water regime treatment, and had a greater capacity for root biomass growth, allocating more of the biomass to the roots and less to the shoots, than the other willow clones. The LP026 clone had height growth that matched those of the other clones under 90, 60 and 40% FC, but slower biomass growth and lower water usage than the other clones. The water-use efficiency (WUE) was higher than those of the MP002 and ML022 clones.

The ML089 clone showed less leaf loss at the onset of the 40% FC water regime treatment than the MP002, ML022 and LP026 clones, and had a greater capacity for shoot biomass growth, producing more shoots per tree and allocating more of the biomass to the shoots and less to the roots, than the other willow clones. The water usage of the ML089 clone was similar to that of the MP002 clone, but the ML089 clone had higher water-use efficiency (WUE), similar to that of the LP026 clone, and greater biomass growth, similar to that of the ML022 clone.

The 'Tangoio' clone appeared more tolerant of the soil water deficits, with less leaf loss than the other clones, and it could sustain lower values of stem water potential (Ψ_s) during the onset of the 40% FC water regime treatment. The 'Tangoio' clone had lower leaf stomatal conductance and greater diameter growth of the cuttings, allocating more of the biomass to the cuttings, than the other clones. The biomass growth of the 'Tangoio' clone was similar to those of the ML022 and ML089 clones, with water usage similar to those of the MP002 and ML089 clones, and higher water-use efficiency (WUE) similar to those of the LP026 and ML089 clones.

The extent of the leaf loss or senescence reflects the severity of the water stress in the trees (Monclus et al. 2006; Giovannelli et al. 2007), and has been observed to increase significantly in poplar clones as the pre-dawn leaf water potential (Ψ_{pd}) declines with the onset of drought conditions (Pallardy & Rhoads 1997). Willow clones with a high vulnerability to xylem cavitation can prevent extensive hydraulic failure and tree death, by dropping their leaves early in drought (Savage & Cavender-Bares 2011). This drought avoidance strategy reduces water loss by transpiration, and improves the water balance in the trees. The MP002, ML022, LP026, ML089 and 'Tangoio' clones experienced a 38, 24, 19, 4 and 0% reduction in the number of leaves, respectively, after the onset of the 40% FC water regime treatment. The MP002, ML089 and LP026 clones appeared to be successful in maintaining a favourable water balance in the tree

stems, as shown by the continued cambial activity and diameter growth of the cuttings during the onset of the soil water deficits.

The 'Tangoio' clone did not experience a reduction in the number of leaves, and appeared to be less vulnerable to xylem cavitation and more tolerant of the drought conditions. The diameter of the cuttings of the 'Tangoio' clone showed measurable shrinkage with the onset of the 40% FC water regime treatment, in contrast to those of the other clones. This suggests that water was drawn from the bark phloem and xylem of the cuttings to maintain the water potential of the leaves (Ψ_l), and that the 'Tangoio' clone was able to sustain lower values of stem water potential (Ψ_s) than the other clones. Stem shrinkage has been associated with lower values of Ψ_s in plum (*Prunus salicina*) trees, because of the dehydration of the bark phloem and xylem (Intrigliolo & Castel 2005). The drought avoidance strategy of the 'Tangoio' clone differed from those of the other clones, as the cambial activity and diameter growth of the cuttings stopped, and a greater proportion of leaves was retained. When the watering resumed at the soil water content of 40%, the 'Tangoio' clone was able to resume and maintain faster diameter growth of the cuttings, while the diameter growth of the other clones slowed as they produced new leaves to recover from the leaf loss during the onset of the soil water deficits.

The transpiration rate of water through the stomata of the leaves has been found to contribute to the variation in the drought resistance of willow clones, with greater drought resistance associated with lower stomatal conductance (Wikberg & Ogren 2004; Savage & Cavender-Bares 2011). The 'Tangoio' and ML089 clones had lower stomatal conductance under 90% FC, and also under 60 and 40% FC for the 'Tangoio' clone, and much lower rates of leaf senescence during the onset of the soil water deficits than the other clones. It suggests that the lower stomatal conductance of the leaves has contributed to the lower drought stress shown by the 'Tangoio' and ML089 clones.

The allocation of biomass to the roots and the root-to-shoot ratio generally increase in plants in response to soil water deficits (Kozlowski & Pallardy 2002). However, there was no increase in the allocation of biomass to the roots and the root-to-shoot ratio of the willow clones under the 60 and 40% FC treatments in this study. Li et al. (2004) and McIvor et al. (2005) also found no increase in the root-to-shoot ratio of black willow (*Salix nigra*) and 'Tangoio' (*Salix matsudana* x *S. alba*) trees, respectively, but Martin & Stephens (2006) observed an increase in the root-to-shoot ratio of *Salix viminalis* trees in response to drought. The differences may reflect the severity of the soil water deficits, and the size of the containers, with 6-, 20- and 30-L pots used by Li et al. (2004), McIvor et al. (2005), and in this study, respectively, compared with 206–L lysimeters used by Martin & Stephens (2006).

Drought resistance has been associated with higher water-use efficiency in willow clones (Wikberg & Ogren 2007; Weih 2001), and in this study the more drought-tolerant 'Tangoio' and ML089 clones had a more conservative use of water and higher water-use efficiency. Willow species that occur in drier, more seasonally variable habitats tend to have higher water-use efficiency, lower stomatal conductance, and faster growth rates than species from wetter habitats (Savage & Cavender-Bares 2011). These were features of the 'Tangoio' and ML089 clones, which suggest they may be better adapted to the drier and more variable soil moisture conditions expected in the eastern lowlands of New Zealand during the 21st century.

5.5 Conclusions

The four new experimental hybrid willow clones and the 'Tangoio' willow clone varied in their drought tolerance, in the order: Tangoio > ML089 > LP026, ML022 > MP002, based on their physiological responses to the 90, 60 and 40% of field capacity (FC) soil water deficits. The drought tolerance of the 'Tangoio' and ML089 clones appeared to be associated with their higher water-use efficiency, lower stomata conductance, and their ability to minimise leaf senescence at the onset of drought conditions, indicative of lower water stress under the 60 and 40% FC soil water deficits. The MP002, ML022 and LP026 clones had higher rates of leaf senescence, and the MP002 and ML022 clones had lower water-use efficiency, which contributed to lower drought tolerance.

The growth characteristics of the willow clones differed. The LP026 clone was slower growing, and allocated more biomass to the roots and less to the shoots than the other clones. The 'Tangoio', ML089 and ML022 clones were faster growing, with the 'Tangoio' clone allocating more biomass to the cuttings, and the ML089 clone allocating more biomass to the shoots and less to the roots than the other clones. The biomass growth of the ML022 clone was similar to those of the 'Tangoio' and ML089 clones, as a result of the greater use of water, which compensated for its lower water-use efficiency.

5.6 Acknowledgements

We thank Steve Green and Carlo van den Dijssel (Plant & Food Research) for the use and monitoring of the weather station equipment and load cells and data logger; Jeff Tantrum at the Hawke's Bay Regional Council nursery for the willow cuttings and sample branches for the development of the allometric equations; Jason Wargent and Chris Rawlingson (Massey University) for support and advice with the photosynthesis measurements and the use of the pressure bomb equipment; and Duncan Hedderley (Plant & Food Research) for advice on the experimental design and statistical analysis of the data.

5.7 References

Australian Standard (AS) 1289.2.1.1 2005. Methods of testing soils for engineering purposes - Soil moisture content tests - Determination of the moisture content of a soil - Oven drying method (standard method). Standards Association of Australia.

Basher L, Elliot S, Hughes A, Tait A, Page M, Rosser B, McIvor I, Douglas G, Jones H 2012. Impacts of Climate Change on Erosion and Erosion Control Methods – A Critical Review. MPI Technical Paper No. 2012/45, Ministry for Primary Industries, Wellington, New Zealand, 208 pp.

Cienciala E, Lindroth A 1995. Gas-exchange and sap flow measurements of *Salix viminalis* trees in short-rotation forest. II. Diurnal and seasonal variations of stomatal response and water use efficiency. Trees 9: 295–301.

Denyer K 2015. Willows and alders. Your guide to managing these trees in Waikato wetlands and waterways. NZ Landcare Trust, Hamilton, New Zealand, 23 pp.

Derose RC, Trustrum NA, Thomson NA, Roberts AHC 1995. Effect of landslide erosion on Taranaki hill pasture production and composition. New Zeal. J. Agr. Res. 38: 457–471.

Douglas GB, McIvor IR, Manderson AK, Koolaard JP, Todd M, Braaksma S, Gray RA 2013. Reducing shallow landslide occurrence in pastoral hill country using wide-spaced trees. Land Degrad. Develop. 24: 103–114.

Douglas GB, Trustrum NA, Brown IC 1986. Effect of soil slip erosion on Wairoa hill pasture production and composition. New Zeal. J. Agr. Res. 29: 183-192.

Giovannelli A, Deslauriers A, Fragnelli G, Scaletti L, Castro G, Rossi S, Crivellaro A 2007. Evaluation of drought response of two poplar clones (*Populus* x *Canadensis* Mönch 'I-214' and *P. deltoides* Marsh. 'Dvina') through high resolution analysis of stem growth. J. Exp. Bot. 58(10): 2673–2683.

Guzzetti F, Peruccacci F, Rossi M, Stark CP 2008. The rainfall intensity-duration control of shallow landslides and debris flows: an update. Landslides 5: 3–17.

Hollis M 2015. Climate Change, IPCC Fifth Assessment Report New Zealand findings. New Zealand Climate Change Centre, NIWA, Wellington, New Zealand, 4 pp.

Intrigliolo DS, Castel JR 2005. Usefulness of diurnal trunk shrinkage as a water stress indicator in plum trees. Tree Physiol. 26: 303–311.

Kozlowski TT, Pallardy SG 2002. Acclimation and adaptive responses of wood plants to environmental stresses. Bot. Rev. 68(2): 270–334.

Li S, Pezeshki SR, Goodwin S, Shields FD 2004. Physiological responses of black willow (*Salix nigra*) cuttings to a range of soil moisture regimes. Photosynthetica 42(4): 585–590.

Lindroth A, Cienciala E 1996. Water use efficiency of short-rotation *Salix viminalis* at leaf, tree and stand scales. Tree Physiol. 16: 257–262.

Lindroth A, Verwijst T, Halldin S 1994. Water-use efficiency of willow: variation with season, humidity and biomass allocation. J. Hydrol. 156: 1–19.

Martin PJ, Stephens W 2006. Willow growth in response to nutrients and moisture on a clay landfill cap soil. I. Growth and biomass production. Bioresource Technol. 97: 437–448.

McIvor I 2008. Breeding poplars and willows. New Zealand Tree Grower, Feb. 27–28, 32.

McIvor I, Cumming H, Hurst S 2005. Response of four *Salix* species to soil water deficit. Agronomy NZ 35: 74–80.

Monclus R, Dreyer E, Delmotte FM, Villar M, Delay D, Boudouresque E, Petit JM, Marron N, Bréchet C, Brignolas F 2006. Impact of drought on productivity and water use efficiency in 29 genotypes of *Populus deltoides* x *Populus nigra*. New Phytol. 169: 765–777.

Ögren E, Sjöström M 1990. Estimation of the effect of photoinhibition on the carbon gain in leaves of a willow canopy. Planta 181: 560–567.

Pallardy SG, Rhoads JL 1997. Drought effects on leaf abscission and leaf production in *Populus* clones. In: Pallardy SG, Cecich RA, Garrett HE, Johnson PS, eds. Proceedings 11th central hardwood forest conference. North Central Forest Experiment Station, general technical report, NC-188. Washington, DC, USA: US Department of Agriculture, Forest Service, 374–384.

Persson G, Lindroth A 1994. Simulating evaporation from short-rotation forest - variations within and between seasons. J. Hydrol. 156: 21–45.

Rönnberg-Wästljung AC, Glynn C, Weih M 2005. QTL analyses of drought tolerance and growth for a *Salix dasyclados* x *Salix viminalis* hybrid in contrasting water regimes. Theor. Appl. Genet. 110: 537–549.

Savage JA, Cavender-Bares JM 2011. Contrasting drought survival strategies of sympatric willows (genus: *Salix*): consequences for coexistence and habitat specialization. Tree Physiol. 31: 604–614.

Sprugel DG 1983. Correcting for bias in log-transformed allometric equations. Ecology 64: 209–210.

Trustrum NA, Thomas VJ, Lambert MG 1984. Soil slip erosion as a constraint to hill country pasture production. Proceedings of the New Zealand Grassland Association 45: 66–76.

Turtola S, Rousi M, Pusenius J, Yamaji K, Heiska S, Tirkkonen V, Meier B, Julkunen-Tiitto R 2006. Genotypic variation in drought response of willows grown under ambient and enhanced UV-B radiation. Environ. Exp. Bot. 56: 80–86.

Weih M 2001. Evidence for increased sensitivity to nutrient and water stress in a fast-growing hybrid willow compared with a natural willow clone. Tree Physiol. 21: 1141–1148.

Wikberg J, Ögren E 2004. Interrelationships between water use and growth traits in biomass-producing willows. Trees 18: 70–76.

Wikberg J, Ögren E 2007. Variation in drought resistance, drought acclimation and water conservation in four willow cultivars used for biomass production. Tree Physiol. 27: 1339–1346.

Wilkinson AG 1999. Poplars and willows for soil erosion control in New Zealand. Biomass Bioenerg. 16: 263–274

6 MODELLING SURVIVAL, GROWTH AND DISEASE RISK OF POPLARS UNDER CURRENT AND FUTURE CLIMATE

Steve Green and Ian McIvor, Plant & Food Research.

6.1 Introduction

Simulating the effects of climate change on water stress, tree growth and likelihood of rust appearance on poplar trees in New Zealand

We consider three climate drivers for the impact on poplar trees: rising CO_2 levels, changing temperatures and changing patterns of rainfall. We address various impacts as a result of changes in these three drivers. The main focus of this desktop study is to examine the following three factors associated with poplar production:

- Survival rates of planted poles
- Disease risk from poplar rusts
- Tree productivity.

Our modelling was carried out using version 5 of SPASMO (Soil Plant Atmosphere System Model). SPASMO is a mechanistic model that operates on a daily time-step (Green et al. 2008). Current climate simulations use regional data over the time period 1972–2010. The future climate scenarios use data for the time period 2030–2070, so that we can assess temporal variability and consider extreme events. One future scenario has been considered, the IPCC A1B 'challenging' scenario. Model outputs from future climate simulations are compared with current conditions, being derived from our modelling of climate data from the past 40 years. The modelling allows us to assess the impacts in relation to the three climate drivers of CO_2 rise, the changing temperature, and changing patterns of rainfall.

6.2 The SPASMO modelling framework

Since SPASMO is a fully mechanistic model that accounts for all flows of water into and out of the root-zone soil, it is possible to assess the degree of water stress of both recently-planted poplar poles and developing poplar trees. As SPASMO also accounts for the carbon and nitrogen cycles, it is possible to predict the impact on growth and development of the trees. In addition, for this study we have added a statistical model to describe the likelihood of occurrence of two fungi, namely *Melampsora larici-populina* and *Melampsora medusae,* which are known to be causal agents of poplar rust (Pei & McCracken 2005).

All calculations presented here were carried out using The New Zealand Institute for Plant & Food Research Limited's SPASMO model (Green et al. 1999; Vanclooster et al. 2004). This model considers water, solute (e.g. nitrogen and phosphorus), pesticide, heavy metals, dissolved organic matter (i.e. dissolved organic carbon and dissolved organic nitrogen), as well as microbial (e.g. viruses and bacteria) transport through a 1-dimensional soil profile. The focus of this study was on assessing the soil water balance, plant growth and occurrence of fungi associated with poplar rust.

The soil water balance is calculated by considering the inputs (rainfall and irrigation) and losses (plant uptake, evaporation, runoff and drainage) of water from the soil profile. The model includes components to predict the carbon and nitrogen budget of the soil. These components allow for a calculation of plant growth and uptake of N; various exchange and transformation processes that occur in the soil and aerial environment; recycling of nutrients and organic material to the soil biomass; the addition of surface-applied fertilizer and/or effluent to the land; and the returns of dung and urine from grazing animals (Rosen et al. 2004). Some components of the model have been omitted from the calculations, e.g. irrigation and grazing animals, while other components, e.g. soil properties, have been simplified. Here we consider just one generic soil type, a free-draining silt loam, across all climate regions.

Model results for the water balance are expressed in terms of mm (= one litre of water per square metre of ground area). We use modelling to assess the water deficit (difference between field capacity or the soil's upper drained limit and the daily-averaged water content of the root zone soil). Model results for tree productivity are expressed in terms of dry matter allocation to various components of the tree structure (leaf branch, trunk, roots) in terms of kg/ha. All calculations run on a daily basis and the results are presented at the paddock scale. We assume an initial planting density of 40 stems/ha.

6.2.1 Climate inputs

SPASMO uses daily values of global radiation, air temperature (maximum and minimum), relative humidity (maximum and minimum), wind speed and rainfall. These climate variables are used to calculate a daily water balance and to grow each of the crops according to a defined set of allocation rules that determine dry matter production and allocation according to light interception (a function of the green-leaf area) and the availability of soil water and nutrients. Crop growth is curtailed if water and nitrogen are in short supply. Irrigation is supplied on the basis of need, although we have assumed no irrigation in all the simulations presented here. In the case of pastoral systems, the grazing management is dictated by animal feed requirements, production targets and pasture supply. Details of the model framework in SPASMO are presented in Rosen et al. (2004) and Green et al. (2008).

For the purpose of calculation, daily climate data (1972–2011) were downloaded from the NIWA database using the Cliflo search engine (www.cliflo.niwa.co.nz). We used data from the Virtual Climate Network (VCN). Future-climate data were supplied by NIWA, as part of a SLMACC study on Horticulture (Clothier et al. 2013).The location and names of each climate station are shown in Table 1. Daily values of climate variables were used to calculate a local value for the potential evapo-transpiration (ETO, mm/d) using the FAO-56 Penman-Monteith model (Allen et al. 1998).

Table 1. Data source from NIWA.

Region/District	Name of NIWA station	Agent Number	Latitude (dec.deg)	Longitude (dec.deg)
Northland	Far North District	27019	-35.175	173.925
Waikato*	Hamilton City	30277	-37.825	175.275
Bay of Plenty	Western Bay Of Plenty District	29974	-37.825	176.325
Gisborne	Gisborne District	29602	-38.675	177.925
Hawke's Bay*	Hastings District	29002	-39.625	176.825
Hawke's Bay	Southern Hawke's Bay District	29984	-39.925	176.425
Levin*	Horowhenua District	30825	-40.625	175.275
Martinborough	South Wairarapa District	30858	-41.225	175.425
Tasman	Tasman District	20302	-41.375	173.125
Marlborough*	Marlborough District	27539	-41.525	173.875
Canterbury	Hurunui District	21270	-42.775	172.875
Otago*	Central Otago District	15044	-45.225	169.325

For those stations marked with a '*' we have presented tabulated outputs only.

6.2.2 Calculation of crop water use

A standard crop-factor approach is used to relate crop water use to the prevailing weather and physiological time of development. The procedure is based on guidelines given by the Food and Agriculture Administration (FAO) of the United Nations (Allen et al. 1998). Daily values of global radiation, air temperature, relative humidity and wind speed are required for the calculation. These have been downloaded from the NIWA database using historical records. The reference evaporation rate, ET_0 [mm d^{-1}], is calculated as

$$\lambda ET_0 = \frac{s(R_N - G_H) + \rho_A c_P (e_s - e_a)/r_A}{s + \gamma(1 + r_S/r_A)} \qquad \text{[Eq. 1]}$$

where R_N [MJ m-2 d-1] is the net radiation, G_H [MJ m^{-2} d^{-1}] is the ground heat flux, T [ºC] is the mean air temperature, e_s [kPa] is the saturation vapour pressure at the mean air temperature, e_a [kPa] is the mean actual vapour pressure of the air, s [Pa $ºC^{-1}$] is the slope of the saturation vapour-pressure versus temperature curve, γ [66.1 Pa] is the psychometric constant, and λ [2.45 MJ kg^{-1}] is the latent heat of vaporisation for water, and the terms r_S and r_A refer to the (bulk) surface and aerodynamic resistances, respectively. The surface resistance for evaporation from the pasture is set equal to 70 s m^{-1} (Allen et al. 1998). Similarly, the surface resistance for evaporation from the pond is set equal to zero. The aerodynamic resistance for both the pasture and the pond has been set equal to $208/U_2$, where U_2 is the median wind speed at a height of 2 m.

ET_0 defines the potential rate of evaporation from an extensive surface of green grass cover, of a short, uniform height, that is actively growing, completely shading the ground, and not short of water or nutrients. The potential water use of the crops is then calculated

$$ET_C = K_C ET_0 \qquad \text{[Eq. 2]}$$

using a crop factor K_C derived from the amount of light intercepted by the leaf canopy. Light interception is a function of the leaf-area index, LAI [m^2 of leaf per m^2 of ground area] (Green et al. 2003a), and this is re-calculated each day. Coppicing the trees will reduce LAI and this impact on ET_C via a reduction in K_C.

When soil water and nutrients are non-limiting, water is extracted easily by the plant roots and transpiration proceeds at the potential rate ET_C. However, as the soil dries, water becomes more strongly bound by capillary and absorptive forces to the soil matrix. Plant roots then have to work much harder to extract water from 'dry' soil. Plants will tolerate a certain level of water deficit in their root-zone soil, yet they will eventually exhibit symptoms of water stress (i.e. reduced transpiration and loss of turgor) if the soil water content drops below a certain threshold value.

An empirical adjustment factor K_R [-] is used to represent the plant's tolerance to water stress. The total-available water *TAW* [mm], as defined by the difference between the water content at field capacity (-10 kPa matric potential) W_{FC} [mm] and wilting point (-1500 kPa matric potential) W_{WP} [mm], is calculated across the depth of the root-zone, z_R [mm]. The plant-available water *PAW* [mm] is then defined by a fraction *p* of *TAW* that a crop can extract from the root-zone without suffering water stress. Values of *p* are listed in Table 22 of Allen et al. (1998). The pattern of water and nutrient uptake from the root-zone soil is determined from the depth-wise pattern of root development (Green et al. 2002).

6.2.3 Modelling surface runoff

The surface runoff component of SPASMO is based on a daily rainfall total. The calculation uses the Soil Conservation Service (SCS) curve number approach (Williams 1991). The curve number approach was selected here because: (i) it is based on over 30 years of runoff studies on pasture, arable and forest sites in the USA, (ii) it is computationally simple and efficient, (iii) the required inputs are available, (iv) and the calculation relates runoff to soil type, land use and management practice.

Surface runoff is predicted from daily rainfall plus irrigation, using the SCS curve number equation:

$$Q = \frac{(R - 0.2S)^2}{R + 0.8S}, \qquad R > 0.2S$$
$$Q = 0, \qquad , \qquad R \le 0.2S \qquad \text{[Eq. 3]}$$

where *Q* [mm] is the daily runoff, *R* [mm] is the daily rainfall plus irrigation, and *S* [mm] is the retention parameter that reflects variations among soils, land use and management. The retention parameter, *S*, is related to the curve number, *CN*, using the SCS equation (Soil Conservation Service 1972)

$$S = 254\left(\frac{100}{CN} - 1\right) \qquad \text{[Eq. 4]}$$

where the constant, 254, gives *S* in millimetres. Moisture condition 2 (CN2) or the average curve number, can be obtained easily for any area of land use type from the SCS Hydrology

Table 2. SCS curve number for a grazed pasture (Soil Conservation Service 1972).

SCS CN number		Drainage Condition			
		Excessive	Good	Fair	Poor
Pasture Condition	Good	39	61	74	80
	Average	49	69	79	84
	Poor	68	79	86	89

Handbook (Soil Conservation Service 1972). An example of CN numbers is given below for a range of pasture and drainage conditions.

A pasture in good condition that is growing on a free draining soil will have a low *CN* value (39), while a pasture in poor condition and on a poorly drained soil will have a high *CN* value (89). A lower *CN* value implies a bigger retention parameter, *S*, and so a given soil/pasture combination will yield less runoff for the same daily rainfall total. The SCS runoff calculation also includes an additional adjustment to *S*, to express the effect of slope and soil water content (Williams 1991). In the calculations presented here, we have assumed the pasture slope is always less than 5% and have used a reference *CN* value for a pasture sward in average condition. The only other allowance that we have made, with respect to runoff, is to include any changes in S that are due to different soil water contents.

6.2.4 Nitrogen balance of the soil

The nitrogen component of SPASMO is based on a set of balance equations that account for nitrogen uptake by plants, exchange and transformation processes in the soil, losses of gaseous nitrogen to the atmosphere, additions of nitrogen in the effluent or fertilizer, and the leaching of nitrogen below the root zone. SPASMO considers both organic nitrogen (i.e. in the soil biomass) and the mineral nitrogen (i.e. urea, ammonium and nitrate). Dissolved urea and nitrate are considered to be mobile and to percolate freely through the profile, being carried along with the invading water. The movement of dissolved ammonium is retarded as it binds to the mineral clay particles of the soil. The soil can receive inputs of organic carbon and nitrogen from decaying plant residues, which is added to the litter layer of the topsoil, and inputs of ammonium and nitrate in the effluent applied to the soil surface. Details of the nitrogen component of SPASMO are published in Rosen et al. (2004).

6.2.5 Crop growth

The uptake of soil nutrients (i.e. nitrogen and phosphorus) by pasture and trees is determined largely by the growth of the above- and below-ground *DM*, multiplied by their respective nitrogen concentrations. Daily biomass production is modelled using a potential production rate per unit ground area, *G* (kg m^{-2} d^{-1}) that is related, via a conversion efficiency, ε (kg MJ^{-1}), to the amount of solar radiant energy, Φ (MJ m^{-2} d^{-1}), intercepted by the leaves

$$G = \varepsilon \Phi \; f_T \; f_N \; f_W \qquad \text{[Eq. 5]}$$

Here f_T, f_N and f_W are response functions that range between zero and unity depending on temperature, plant nitrogen and soil water status respectively (Eckersten & Jansson 1991). The value of *G* depends on the daily sunshine and temperature, plus the leaf-area index of the crop, and is moderated by the soil's water and nitrogen status (King 1993; Thornley et al. 1995). Crop growth is maximised only if soil water and soil nutrients are non-limiting.

A simple allometric relationship is used to partition the daily biomass production into the growth of the foliage, stem material and roots. Plant biomass is expressed in terms of the balance between growth and senescence of the plant organs. For each plant organ we write out a simple mass balance equation that considers inputs of *DM* due to carbon allocation, losses of *DM* as the plants senescence, and the removal of DM as the plants are harvested. The total mass of foliage, *F* [kg m^{-2}] is calculated from

$$\frac{dF}{dt} = \alpha_F G - \gamma_F F - H_F \qquad \text{[Eq. 6]}$$

the total mass of stem material, *S* [kg m^{-2}] is calculated from

$$\frac{dS}{dt} = \alpha_S G - \gamma_S F - H_S \qquad \text{[Eq. 7]}$$

and the total mass of roots, *R* [kg m^{-2}], is calculated from

$$\frac{dR}{dt} = \alpha_R G - \gamma_R R \qquad \text{[Eq. 8]}$$

Here α_F is the fraction of biomass partitioned to the foliage, α_S is the biomass partitioned to the stem, and α_R (=1-α_F-α_S) is the fraction of biomass allocated to the roots, and γ is the corresponding senescence rate for these plant components. The variable *H* is used to represent the amount of DM that is removed during harvest. In the case of fruiting crops, additional terms are included in each balance equation to represent an amount of DM transferred to fruit production.

Allocation of DM to the roots depends on the leaf nitrogen content $[N]_F$, having a minimum value $[\alpha_{R0}]$ at a maximum leaf concentration $[N]_{Fx}$, and increasing as N_L decreases (Eckersten & Jansson 1991)

$$\alpha_R = \alpha_{R0} + 1 - \left(1 - \left(\left([N]_{Fx} - [N]_F\right)/[N]_{Fx}\right)^2\right)^{0.5} \qquad \text{[Eq. 9]}$$

This formulation enables SPASMO to accommodate seasonal changes in DM allocation associated with a changing leaf nutrient status. For simplicity, any seasonal changes in senescence rates have been neglected in the model because we are concerned with the long-term consequences of DM allocation.

6.2.6 Climate change and disease risk

The SPASMO model was used to explore the possible effects of climate change on the activity of two key forest-pathogenic fungi, namely *Melampsora larici-populina* and *Melampsora medusae,* which are known to be causal agents of poplar rust (a reference).

We adopted a simple statistical model to describe the likelihood of occurrence of these two fungi, based on the work of Desprez-Loustau et al. (2007) who used a logistic regression approach to describe leaf data collected from 311 nurseries around France, between the years 1993 and 2003. Their analysis was restricted to nondescrimanant clones, i.e. susceptible to all rust species. In the absence of local data, we have adopted the same parameter values for this study.

The relative frequency of *Melampsora larici-populina* was modelled using:

$$\text{Logit}(p) = -10.34 + 0.471*Ts + 0.007*WDs \qquad \text{Eq. [10]}$$

where Ts (ºC) is the mean summer air temperature and WDs (mm)is the mean summer water deficit (potential ET minus rainfall). The relative frequency of *Melampsora medusae* was modelled using:

$$\text{Logit}(p) = -7.27 + 1.04*TMw \qquad \text{Eq. [11]}$$

where TW is the mean winter minimum temperature (ºC). The logit of a number *p* between 0 and 1 is given by the formula:

$$\text{Logit}(p) = \log(p/(1-p)) = -\log(1/p - 1) \qquad \text{Eq. [12]}$$

6.3 Model outputs

Model outputs were generated for 12 regions/districts: Northland, Waikato, Bay of Plenty, Gisborne, Central Hawke's Bay, Southern Hawke's Bay, Wairarapa, Horowhenua, Tasman, Marlborough, Canterbury, and Central Otago.

The model outputs are summarised in Figures 1–6 below. A more detailed series of figures and tables for each of the 12 regions/districts are given in Appendix 1.

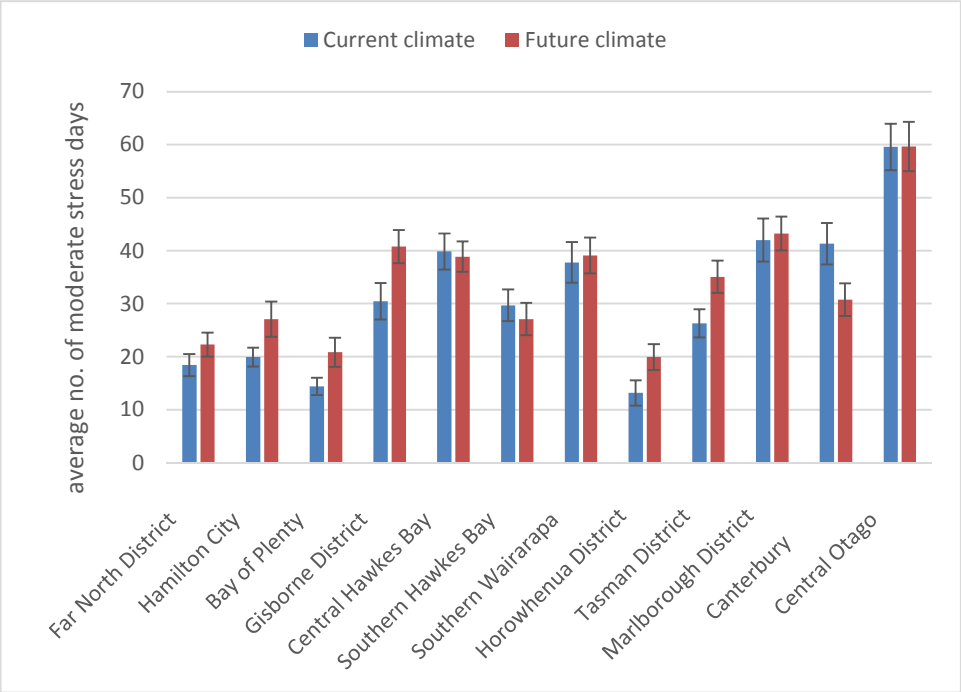

Figure 1. Model outputs used to assess the survivability of planted poplar poles growing under current (1972–2013) and future (2031–2070) climate regimes across New Zealand. This plot shows the average number of moderate-stress days that occur each growing season, as defined by days when the soil water content (SWC) is < 25% of the total available soil water (TAW) over the root zone depth (=0.4 m).

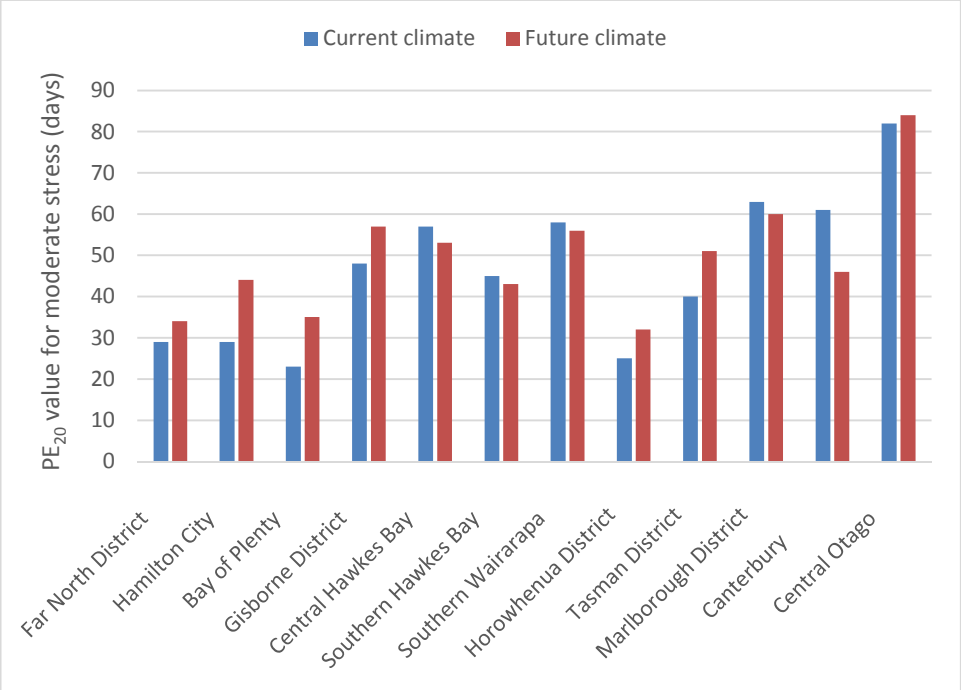

Figure 2. Model outputs used to assess the survivability of planted poplar poles growing under current (1972–2013) and future (2031–2070) climate regimes across New Zealand. This plot shows the average number of moderate-stress days that occur each growing season, as defined by days when the soil water content (SWC) is < 25% of the total available soil water (TAW) over the root zone depth (=0.4 m).

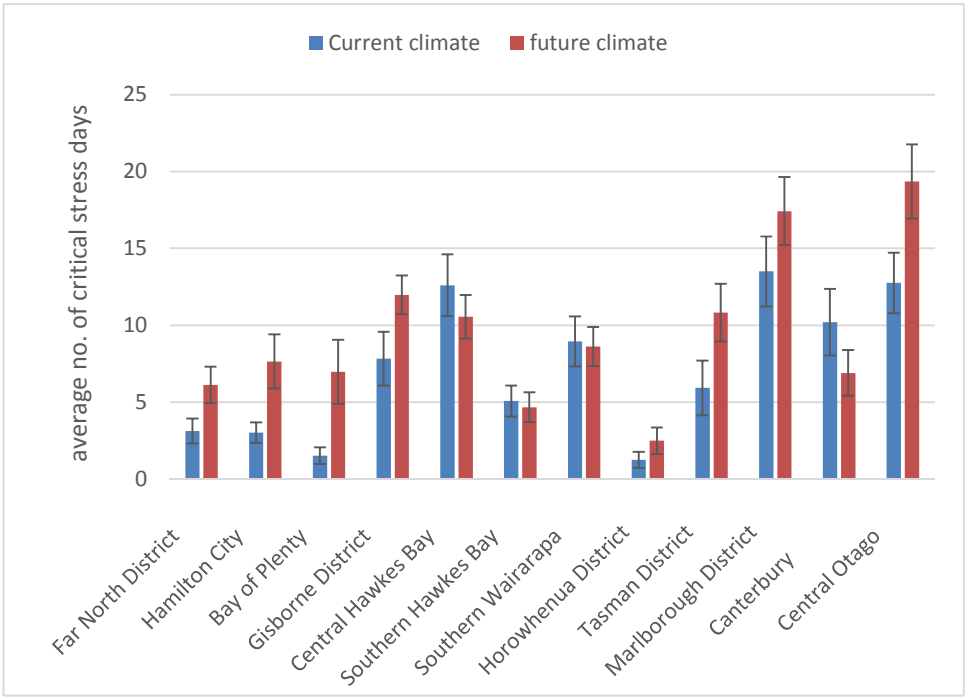

Figure 3. Model outputs used to assess the survivability of planted poplar poles growing under current (1972–2013) and future (2031–2070) climate regimes across New Zealand. This plot shows the average number of critical-stress days that occur each growing season, as defined by days when the soil water content (SWC) is < 5% of the total available soil water (TAW) over the root zone depth (=0.4 m).

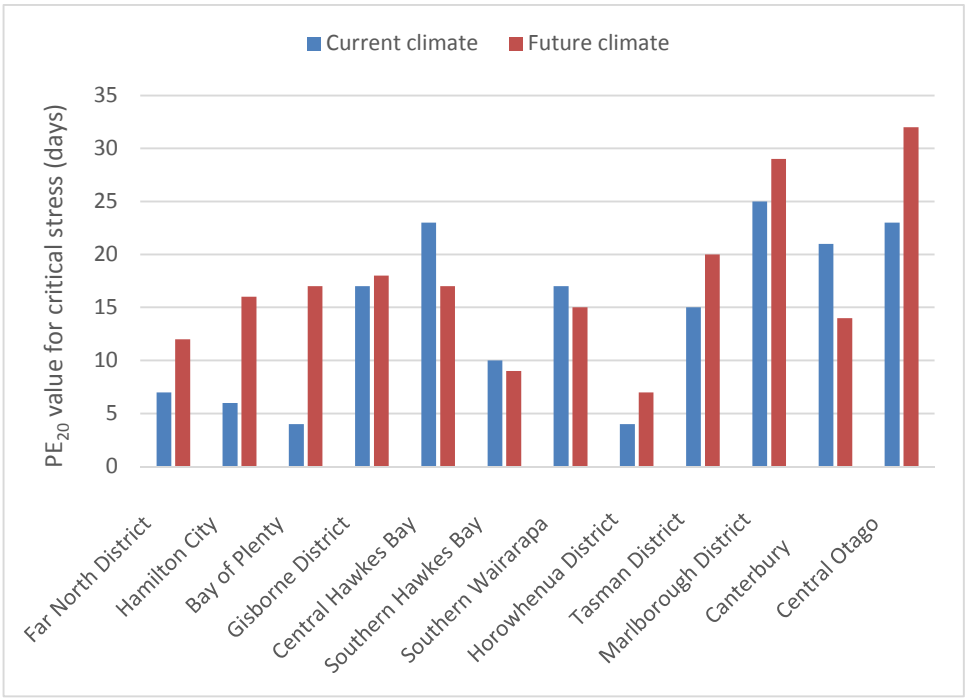

Figure 4. Model outputs used to assess the survivability of planted poplar trees growing under current (1972–2013) and future (2031–2070) climate regimes across New Zealand. This plot shows the average number of critical-stress days that occur each growing season, as defined by days when the soil water content (SWC) is < 5% of the total available soil water (TAW) over the root zone depth (=0.4 m).

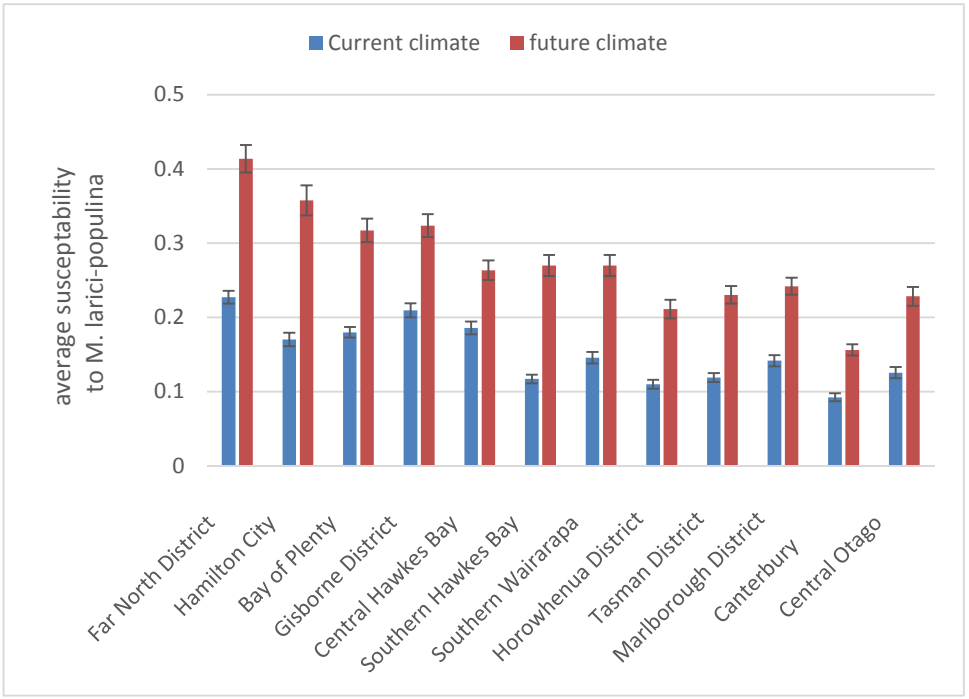

Figure 5. A regional plot of the average degree of susceptibility to *Melampsora larici-populina* for poplar poles growing under current (1972–2013) and future (2031–2070) climate regimes across New Zealand.

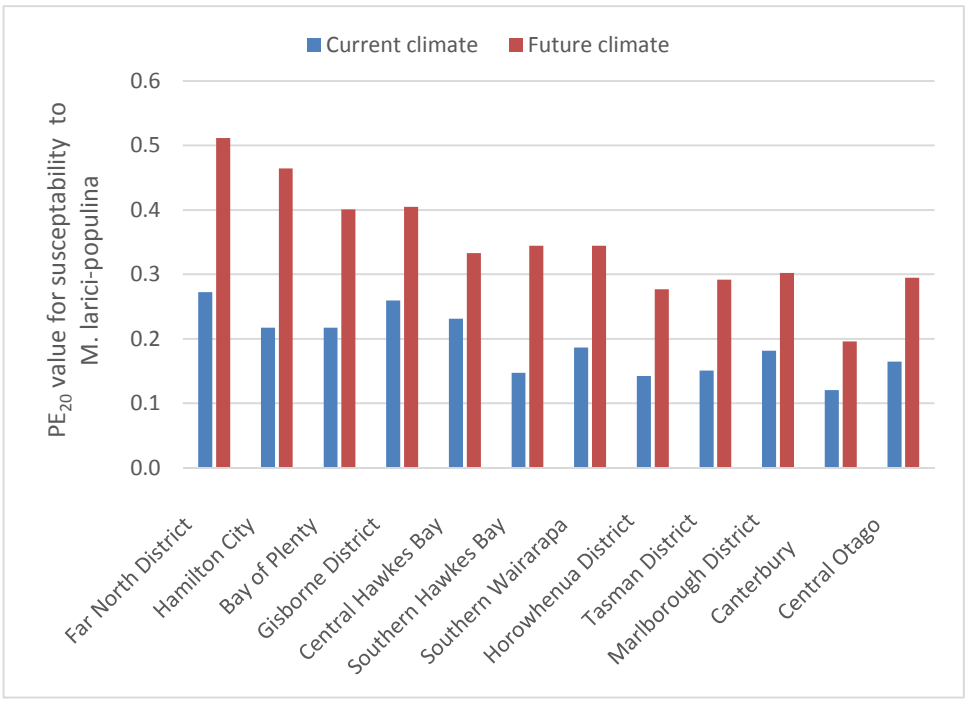

Figure 6. A regional plot of the susceptibility to *M. larici-populina* for poplar poles growing under current (1972–2013) and future (2031–2070) climate regimes across New Zealand.

6.4 Conclusions

Survivability and establishment of poplar poles is predicted to decrease in regions with increased susceptibility to prolonged drought, and remain unchanged in western regions where summer rainfall is predicted to increase.

While all regions are likely to experience drought periods, these will be more severe in the eastern regions and poplar poles (and all trees) will become increasingly harder to establish in the first 1–3 years. This makes it imperative to increase effort to plant erosion-prone pastoral hill country with urgency if the detrimental effects of climate change are to be mitigated.

Growth of established trees is predicted to change little from present rates. Disease risk from poplar fungal rusts is predicted to rise in all regions. Poplar clones bred in future should be selected for rust resistance and options for drought tolerance need to be part of the clonal mix available to landowners.

6.5 References

Allen RG, Pereira LS, Raes D, Smith M 1998. Crop Evapotranspiration. Guidelines for computing crop water requirements. FAO Irrigation and Drainage Paper No. 56. Food and Agriculture Organization of the United Nations, Rome, 301 p.

Clothier B, Hall A, Green S 2012. Chapter 6 Horticulture: Adapting the horticultural and vegetable industries to climate change. In: Clark AJ, Nottage RAC eds. Impacts of Climate Change on Land-based Sectors and Adaptation Options. Technical Report to the Sustainable Land Management and Climate Change Adaptation Technical Working Group, Ministry for Primary Industries. Pp. 237–292.

Desprez-Loustau M-L, Robin C, Reynaud G, Deque M, Badeau V, Piou D, Husson C, Marcais B 2007. Simulating the effects of a climate-change scenario on the geographical range and activity of forest-pathogenenic fungi. Can. J. Plant Pathology 29: 101–120.

Eckersten H, Jansson PE 1991. Modelling water flow, nitrogen uptake and production for wheat. Fertilizer Research 27: 313–330.

Green SR, Clothier BE, van den Dijssel C, Deurer M, Davidson P 2008. Measurement and modelling the stress response of grapevines to soil-water deficits in their rootzones. In: Ahuja et al. eds. Modeling the response of crops to limited water: Recent advances in understanding and modeling water stress effects on plant growth processes. Chapter 12, Soil Science Society America. Pp. 357–386.

Green S, Sivasivakumaran S, van den Dijssel C, Mills T, Blattmann P, Snelgar W 2007. A water and nitrogen budget for ‘Hort16A’ kiwifruit vines. Acta Horticulturae 753: 527–534.

King DA 2003. Allocation of above-ground growth is related to light in temperate deciduous saplings. Functional Ecology 17: 482–488.

McIvor IR, Hedderley DI, Hurst SE, Fung LE 2011b. Survival and growth to age 8 of four *Populus maximowiczii* × *P. nigra* clones in field trials on pastoral hill slopes in six climatic zones of New Zealand. New Zealand Journal of Forestry Science 41: 151–163.

Pei MH, McCracken AR 2005. Rust Diseases of Willow and Poplar. Publisher, CABI. 264 p.

Rosen MR, Reeves RR, Green SR, Clothier BE, Ironside N 2004. Prediction of groundwater nitrate contamination after closure of an unlined sheep feedlot in New Zealand. Vadose Zone Journal 3: 990–1006.

Soil Conservation Service 1972. Hydrology. 'SCS National Engineering Handbook.' Section 4. U.S. Govt Printing Office: Washington D.C.

Thornley JHM, Bergelson J, Parsons AJ 1995. Complex dynamics in a carbon-nitrogen model of a grass-legume pasture. Annals of Botany 75: 79–94.

Williams JR 1991. Runoff and water erosion. In: Hanks J, Ritchie JT eds. Modelling plant and soil systems. Agonomy No. 31 series, American Soc. Agronomy, Madison, USA.

Vanclooster M, Boesten J, Tiktak A, Jarvis N, Kroes JG, Muñoz-Carpena R, Clothier BE, Green SR 2004. On the use of unsaturated flow and transport models in nutrient and pesticide management. In: Feddes RA, Rooij GH, van Dam JC eds. Unsaturated zone modelling: Progress, Challenges and Applications. Kluwer. Pp. 331–361.

6.6 Appendix 1

Climate data summaries

This appendix provides model outputs for each region based on present climate data (1972–2013) and future (2031–2070 A1B) climate change simulations. These outputs are given separately for each region/district included in the table below and cover:

- growing degree days
- rainfall
- changing pattern of soil water content in the root zone
- survivability and disease risk of poplar poles
- survivability and disease risk of poplar trees
- risk of occurrence of an outbreak of rust on poplar trees.

Data are given in graphic and tabular form.

Data source from NIWA

Region/District	Name of NIWA station	Agent Number	Latitude (dec.deg)	Longitude (dec.deg)
Northland	Far North District	27019	-35.175	173.925
Waikato*	Hamilton City	30277	-37.825	175.275
Bay of Plenty	Western Bay Of Plenty District	29974	-37.825	176.325
Gisborne	Gisborne District	29602	-38.675	177.925
Hawke's Bay*	Hastings District	29002	-39.625	176.825
Hawke's Bay	Southern Hawkes Bay District	29984	-39.925	176.425
Levin*	Horowhenua District	30825	-40.625	175.275
Martinborough	South Wairarapa District	30858	-41.225	175.425
Tasman	Tasman District	20302	-41.375	173.125
Marlborough*	Marlborough District	27539	-41.525	173.875
Canterbury	Hurunui District	21270	-42.775	172.875
Otago*	Central Otago District	15044	-45.225	169.325

For those stations marked with a '*' we have presented tabulated outputs only.

6.6.1 Model Outputs: The Far North

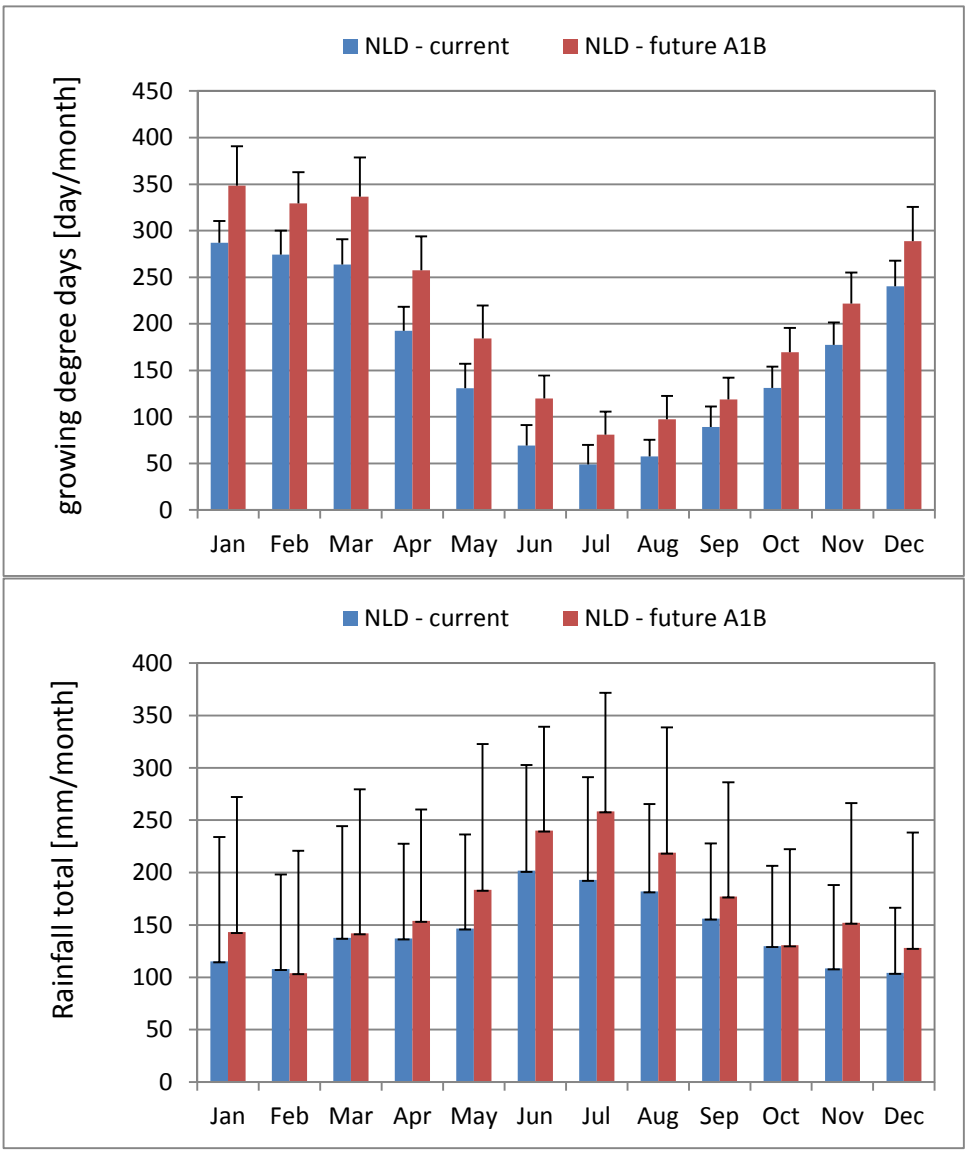

Figure 1.1.1. Summary of seasonal climate data for the Far North region (NLD, Northland) as represented by the number growing-degree days (base 10ºC) and monthly rainfall under current (1972–2013) and future (2031–2070 A1B) climate change simulations.

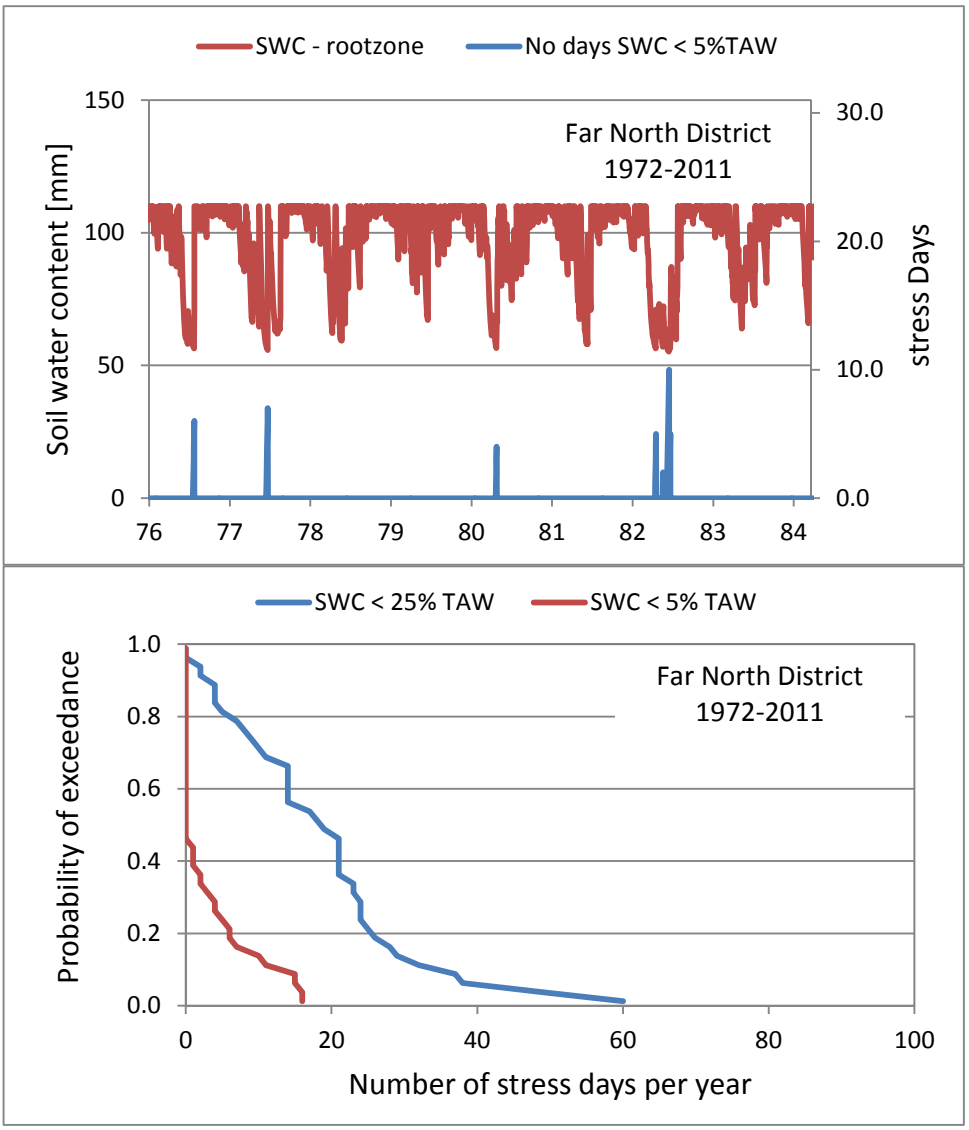

Figure 1.1.2. Model outputs used to assess the survivability of planted poplar poles growing under a current climate scenario (1972–2013) in the Far North district. The top panel shows a time series of soil water content (SWC) in the top 40 cm of the root-zone soil, and the cumulative number of high-stress days where SWC < 5% of total available water (TAW). The bottom panel shows the probabilities of exceedance associated with cumulative of high stress days (SWC<5%TAW) and mild-stress days (SWC < 25%TAW) that occur during each growing season.

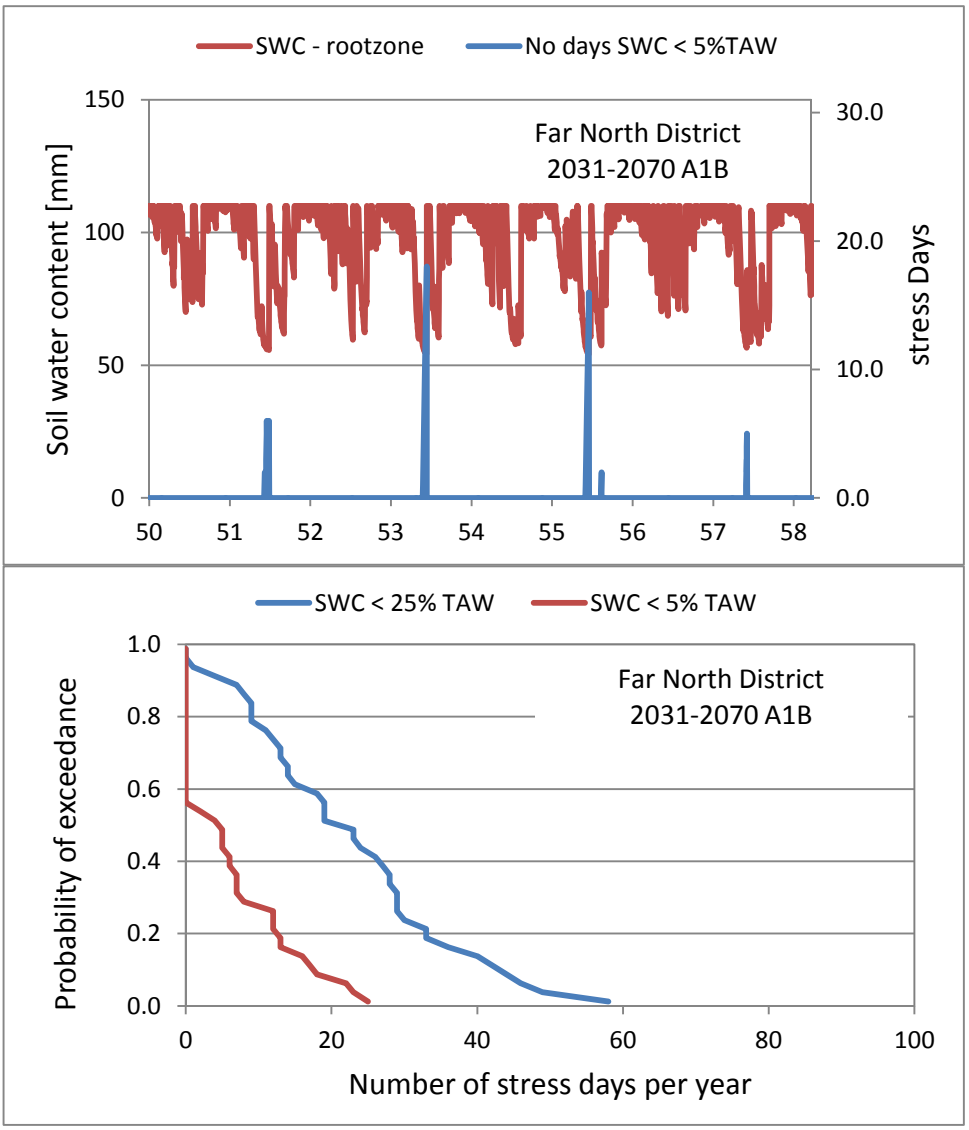

Figure 1.1.3. Model outputs used to assess the survivability of planted poplar poles growing under a future climate scenario (2031–2070 A1B) in the Far North region. The top panel shows a time series of soil water content (SWC) in the top 40 cm of the root-zone soil, and the cumulative number of high-stress days where SWC < 5% of total available water (TAW). The bottom panel shows the probabilities of exceedance associated with cumulative of high stress days (SWC<5%TAW) and mild-stress days (SWC < 25%TAW) that occur during each growing season.

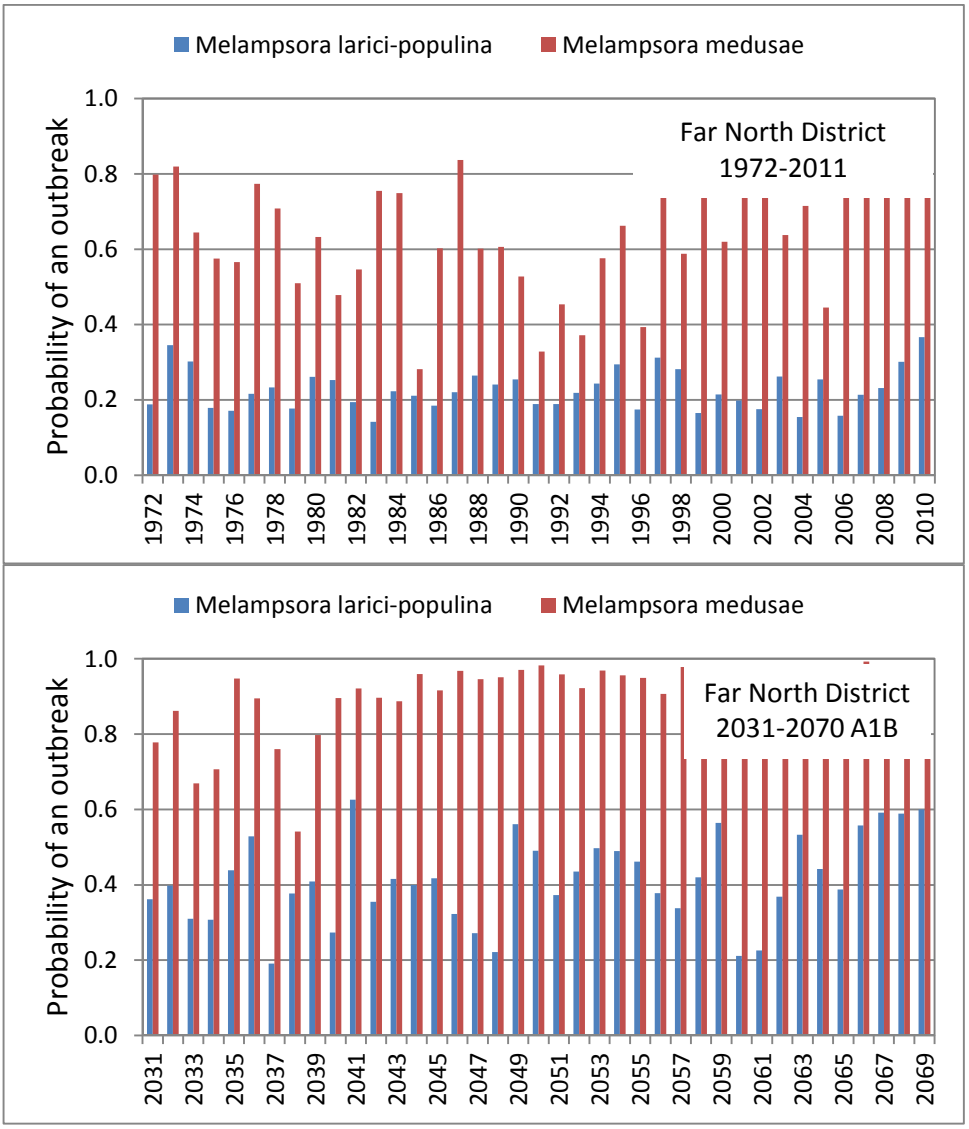

Figure 1.1.4. Model outputs used to assess the risk of occurrence of an outbreak of *Melampsora* rust on poplar trees growing in the Far North region under the current (1972–2010) and future (2031–2070 A1B) climate change scenarios.

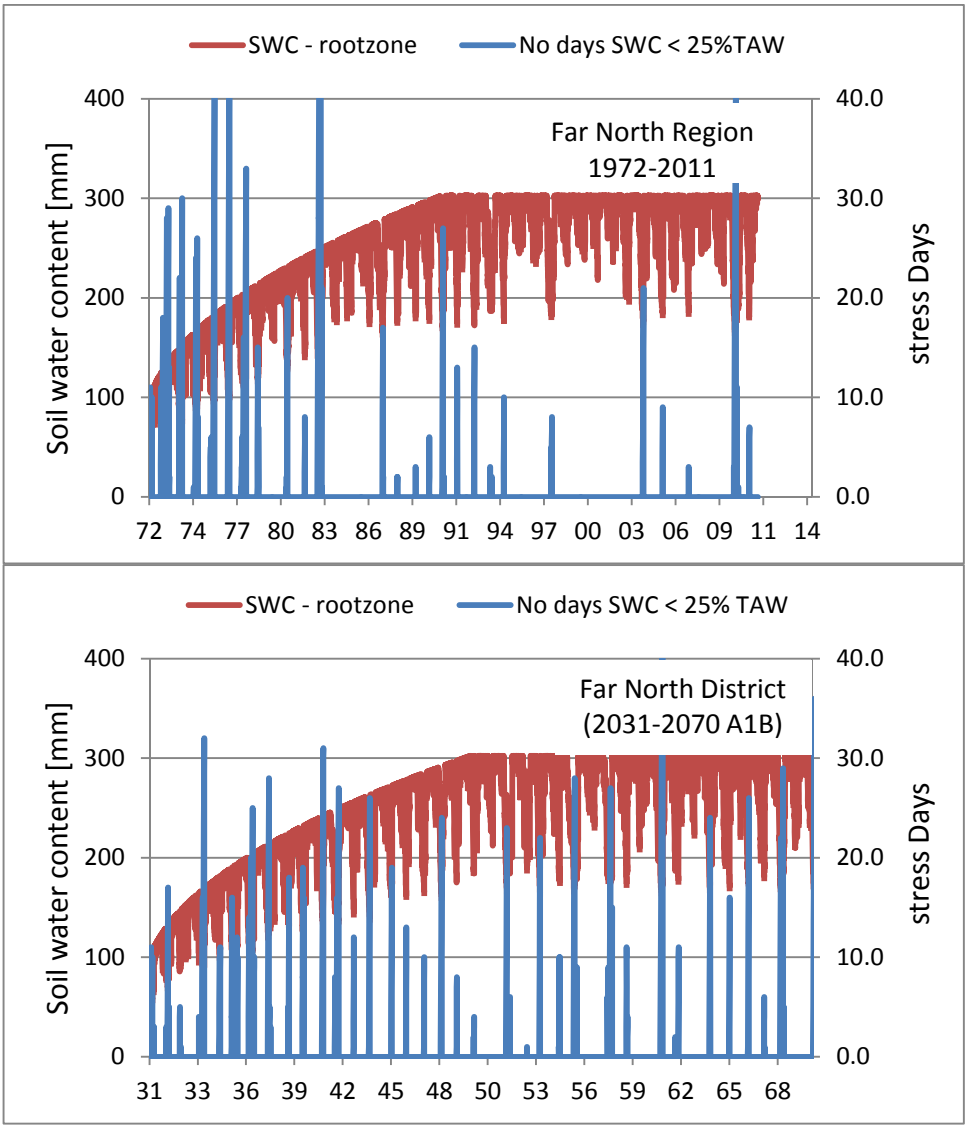

Figure 1.1.5. Model outputs for poplar trees growing under current (1972–2013) and future (2030–2070 A1B) climate change scenarios in the Far North region. These results depict the changing pattern of soil water content in the root zone (red line) and the corresponding cumulative number of mild-stress days (SWC < 25%TAW) that occur during each growing season.

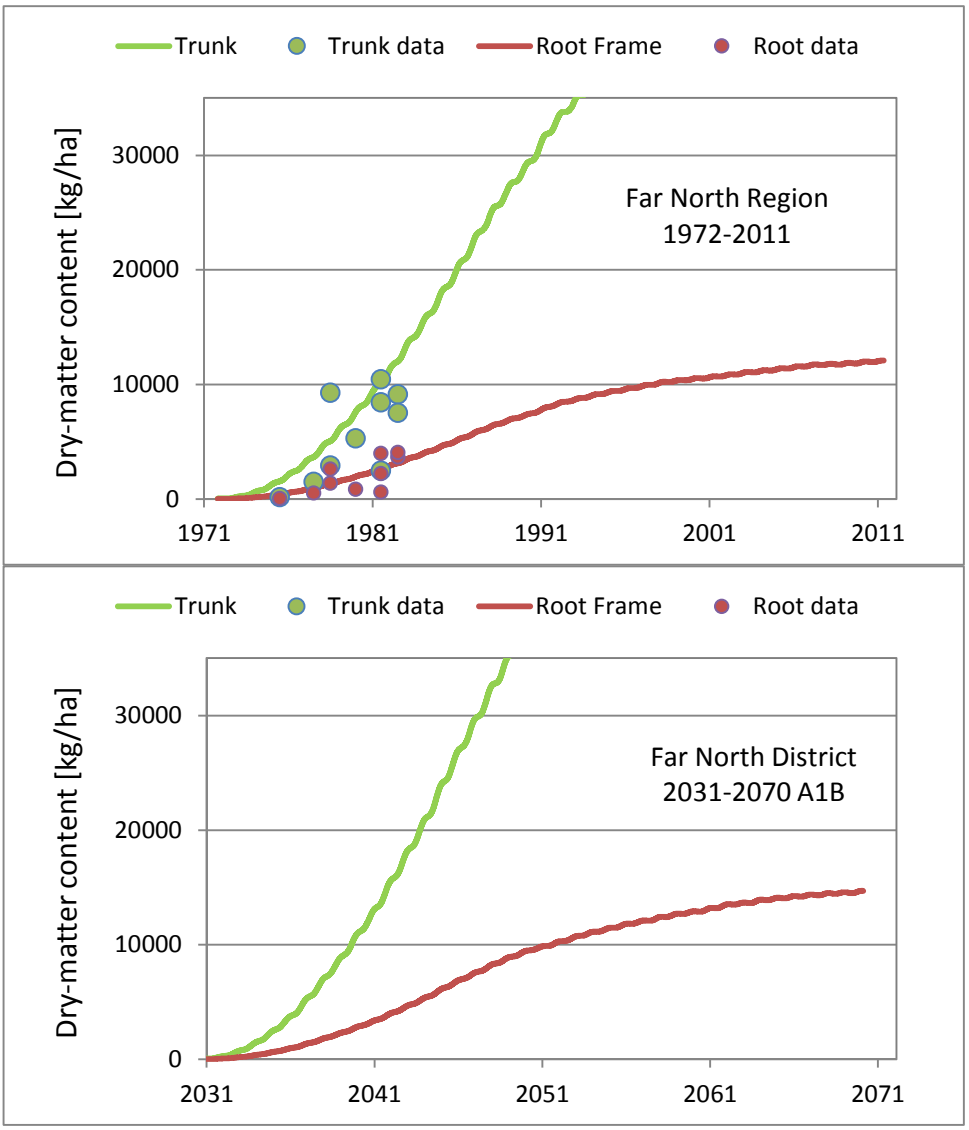

Figure 1.1.6. Model outputs for the dry-matter accumulation (i.e. growth) of poplar trees growing under current (1972–2013) and future (2030–2070 A1B) climate change scenarios in the Far North region. Data are from field trials near Woodville.

Table 1.1.1. A statistical analysis of model outputs used to assess survivability and disease risk of poplar poles growing in the Far North Region under current (1972–2011) and future (2031–2070 A1B) climate change scenarios. Here we have assumed a fixed root-zone depth of 0.40 m.

	statistic	no. moderate stress days	no. critical stress days	Disease risk *M. larici-populina*	Disease risk *M. medusae*
Far North District (1972-2011)	mean	18	3	0.23	0.65
	stdev	13	5	0.05	0.16
	PE20	29	7	0.27	0.78
	Prob (NSD>7)	0.79	0.16	na	na
	statistic	no. moderate stress days	no. critical stress days	Disease risk *M. larici-populina*	Disease risk *M. medusae*
Far North District (2031-2070 A1B)	mean	22	6	0.41	0.90
	stdev	14	7	0.12	0.10
	PE20	34	12	0.51	0.99
	Prob (NSD>7)	0.89	0.31	na	na

Table 1.1.2. A statistical analysis of model outputs used to assess survivability and disease risk of poplar trees growing in the Far North Region under current (1972–2011) and future (2031–2070 A1B) climate change scenarios. Trees have been 'grown' from poles planted at the start of the simulation period.

	statistic	no. moderate stress days	no. critical stress days	Disease risk *M. larici-populina*	Disease risk *M. medusae*
Far North Region (1972-2011)	mean	13	1	0.26	0.65
	stdev	18	3	0.07	0.16
	PE20	28	3	0.32	0.78
	Prob (NSD>7)	0.50	0.04	na	na
	statistic	no. moderate stress days	no. critical stress days	Disease risk *M. larici-populina*	Disease risk *M. medusae*
Far North District (2031-2070) A1B	mean	17	0	0.46	0.90
	stdev	12	1	0.12	0.10
	PE20	27	0	0.56	0.99
	Prob (NSD>7)	0.78	0.01	na	na

Table 1.1.3. Model outputs for the dry-matter accumulation (i.e. growth) of poplar trees growing under current (1972–2013) and future (2030–2070 A1B) climate change scenarios in the Far North region. $T_{50\%}$ and $T_{90\%}$ represent the amount of time (years) to reach 50% and 90% of the final value, respectively.

Far North Region (1972–2011)			Far North Region (2031–2070) A1B		
age	tree biomass [kg/ha]		age	tree biomass [kg/ha]	
	above ground	below ground		above ground	below ground
0	93	28	0	93	28
5	3322	918	5	3610	995
10	11621	3095	10	12995	3450
15	23270	6025	15	27601	7026
25	41127	10166	25	48839	12068
39	52495	12348	39	64073	15012
$T_{50\%}$	17	16	$T_{50\%}$	17	16
$T_{90\%}$	32	30	$T_{90\%}$	32	31

6.6.2 Model outputs: Waikato.

Table 1.2.1. A statistical analysis of model outputs used to assess survivability and disease risk of poplar poles growing in the Waikato Region under current (1972–2011) and future (2031–2070 A1B) climate change scenarios. Here we have assumed a fixed root-zone depth of 0.40 m.

	statistic	no. moderate stress days	no. critical stress days	Disease risk *M. larici-populina*	Disease risk *M. medusae*
Hamilton City (1972-2011)	mean	20	3	0.17	0.11
	stdev	11	4	0.06	0.09
	PE20	29	6	0.22	0.19
	Prob (NSD>7)	0.89	0.19	na	na
	statistic	no. moderate stress days	no. critical stress days	Disease risk *M. larici-populina*	Disease risk *M. medusae*
Hamilton City (2031-2070 A1B)	mean	27	8	0.36	0.27
	stdev	21	11	0.13	0.16
	PE20	44	16	0.46	0.41
	Prob (NSD>7)	0.91	0.36	na	na

Table 1.2.2. A statistical analysis of model outputs used to assess survivability and disease risk of poplar trees growing in the Waikato Region under current (1972–2011) and future (2031–2070 A1B) climate change scenarios. Trees have been 'grown' from poles planted at the start of the simulation period.

	statistic	no. moderate stress days	no. critical stress days	Disease risk *M. larici-populina*	Disease risk *M. medusae*
Hamilton City (1972-2011)	mean	14	1	0.20	0.11
	stdev	20	4	0.07	0.09
	PE20	30	4	0.26	0.19
	Prob (NSD>7)	0.50	0.09	na	na
	statistic	no. moderate stress days	no. critical stress days	Disease risk *M. larici-populina*	Disease risk *M. medusae*
Hamilton City (2031-2070) A1B	mean	24	2	0.42	0.27
	stdev	22	5	0.15	0.16
	PE20	42	6	0.55	0.41
	Prob (NSD>7)	0.78	0.09	na	na

Table 1.2.3. Model outputs for the dry-matter accumulation (i.e. growth) of poplar trees growing under current (1972–2013) and future (2030–2070 A1B) climate change scenarios in the Waikato region. $T_{50\%}$ and $T_{90\%}$ represent the amount of time (years) to reach 50% and 90% of the final value, respectively.

Hamilton City (1972–2011)			Hamilton City (2031–2070) A1B		
age	tree biomass [kg/ha]		age	tree biomass [kg/ha]	
	above ground	below ground		above ground	below ground
0	93	28	0	93	28
5	3127	864	5	3530	975
10	10718	2865	10	12652	3359
15	22116	5765	15	25773	6688
25	38601	9566	25	46154	11527
39	51154	12104	39	60722	14360
$T_{50\%}$	17	16	$T_{50\%}$	17	16
$T_{90\%}$	33	32	$T_{90\%}$	32	31

6.6.3 Model outputs: Bay of Plenty Region

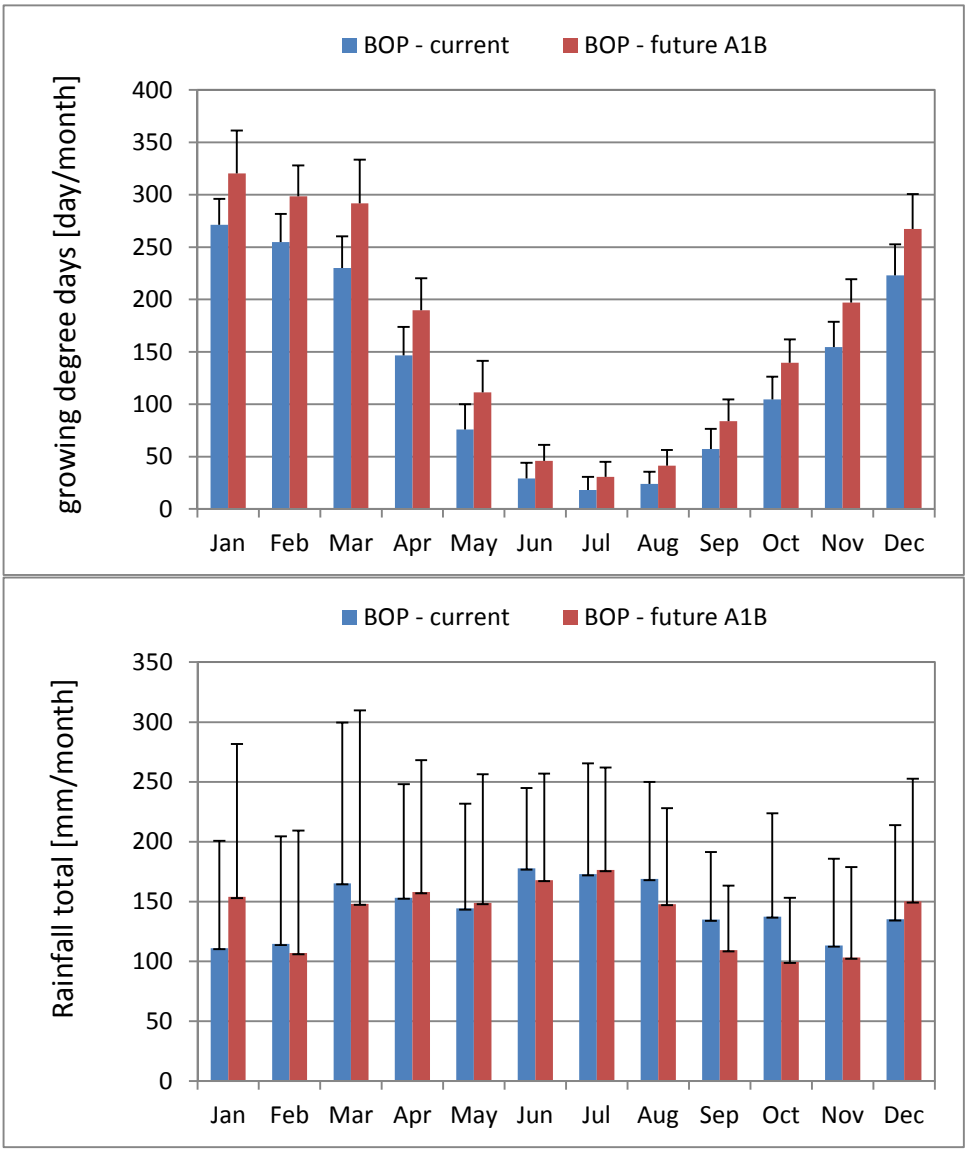

Figure 1.3.1. Summary of seasonal climate data for the Bay of Plenty region.as represented by the number growing-degree days (base 10˚C) and monthly rainfall under current (1972–2013) and future (2031–2070 A1B scenario) climate simulations.

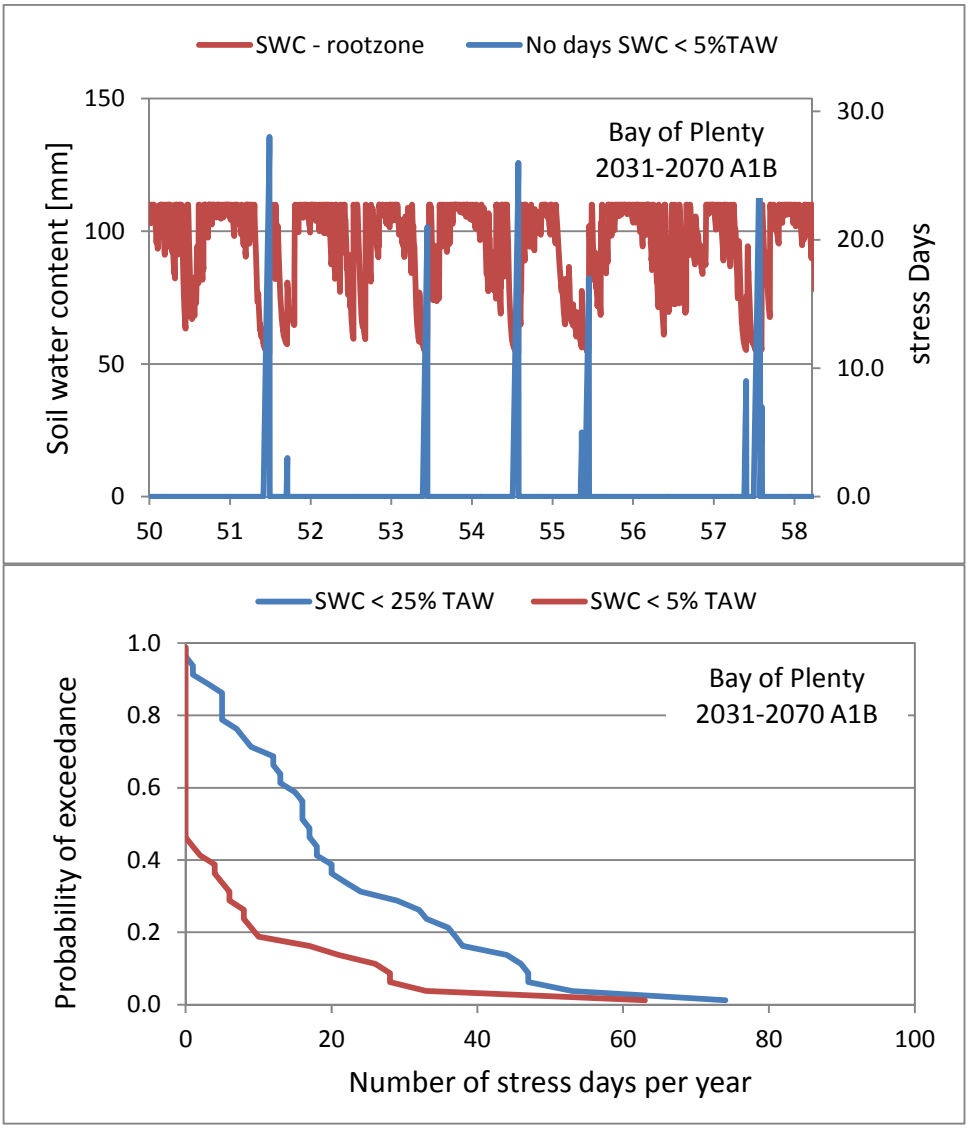

Figure 1.3.2. Model outputs used to assess the survivability of planted poplar poles growing under a future climate scenario (2031–2070 A1B) in the Bay of Plenty region. The top panel shows a time series of soil water content (SWC) in the top 40 cm of the root-zone soil, and the cumulative number of high-stress days where SWC < 5% of total available water (TAW). The bottom panel shows the probabilities of exceedance associated with cumulative of high stress days (SWC<5%TAW) and mild-stress days (SWC < 25%TAW) that occur during each growing season.

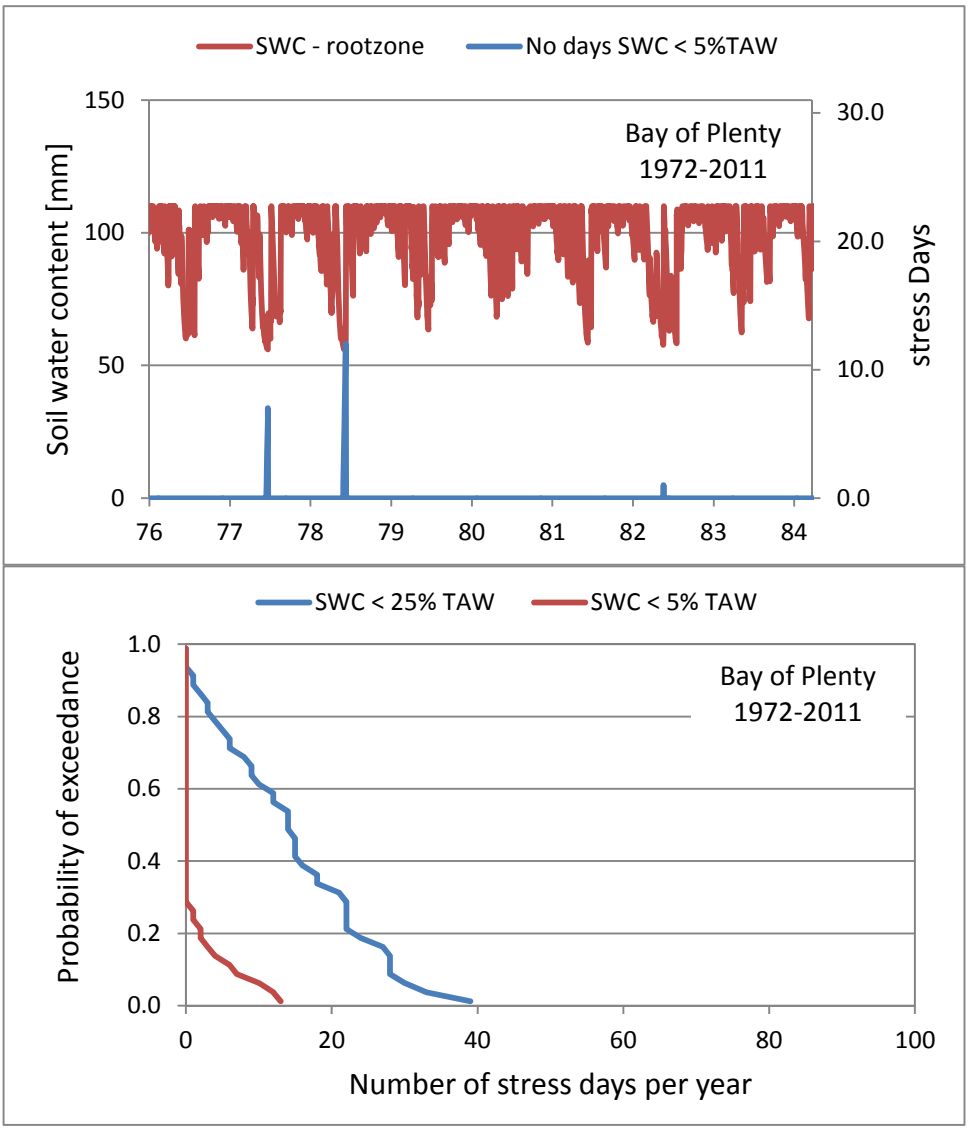

Figure 1.3.3. Model outputs used to assess the survivability of planted poplar poles growing under a current climate scenario (1972–2013) in the Bay of Plenty region. The top panel shows a time series of soil water content (SWC) in the top 40 cm of the root-zone soil, and the cumulative number of high-stress days where SWC < 5% of total available water (TAW). The bottom panel shows the probabilities of exceedance associated with cumulative of high stress days (SWC<5%TAW) and mild-stress days (SWC < 25%TAW) that occur during each growing season.

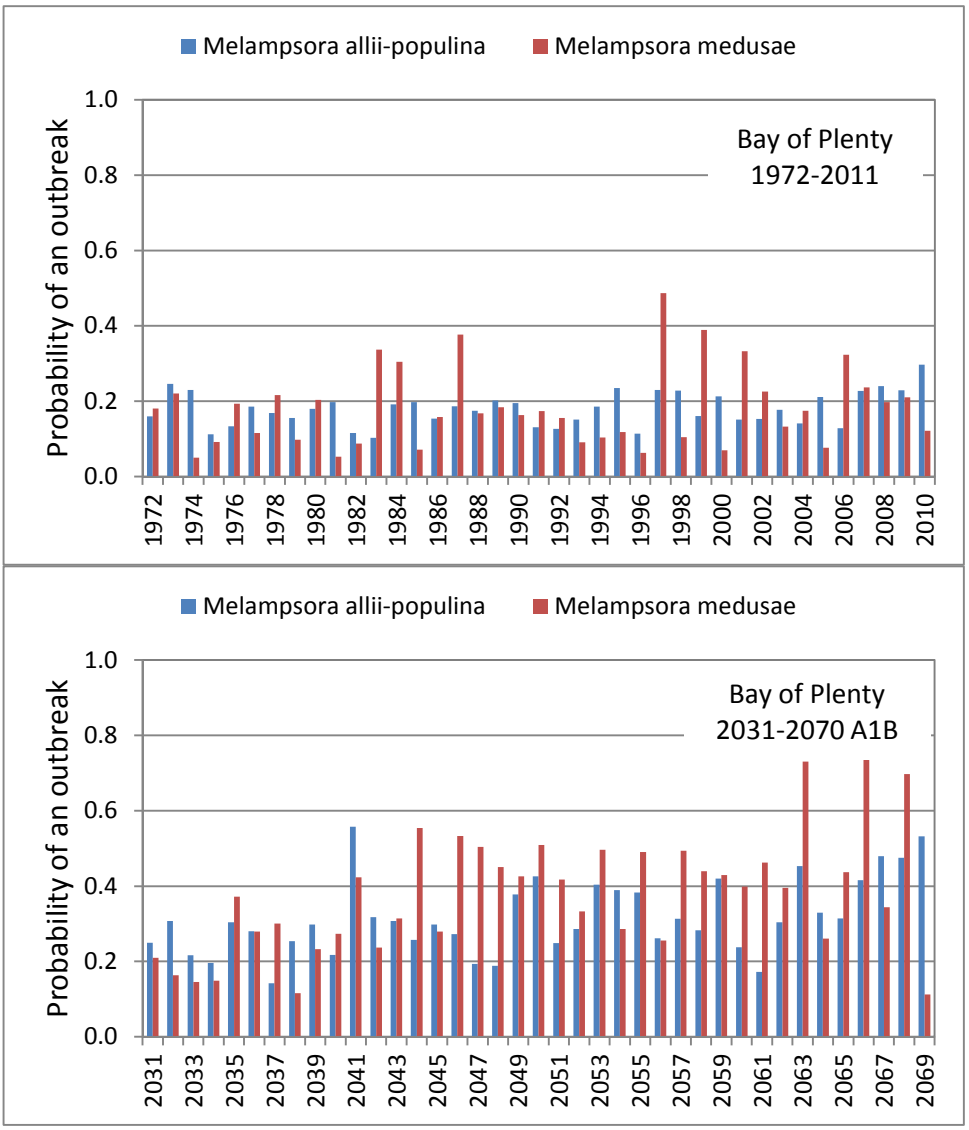

Figure 1.3.4. Model outputs used to assess the risk of occurrence of an outbreak of *Melampsora* rust on poplar trees growing in the Bay of Plenty region under the current (1972–2010) and future (2031–2070 A1B) climate change scenarios.

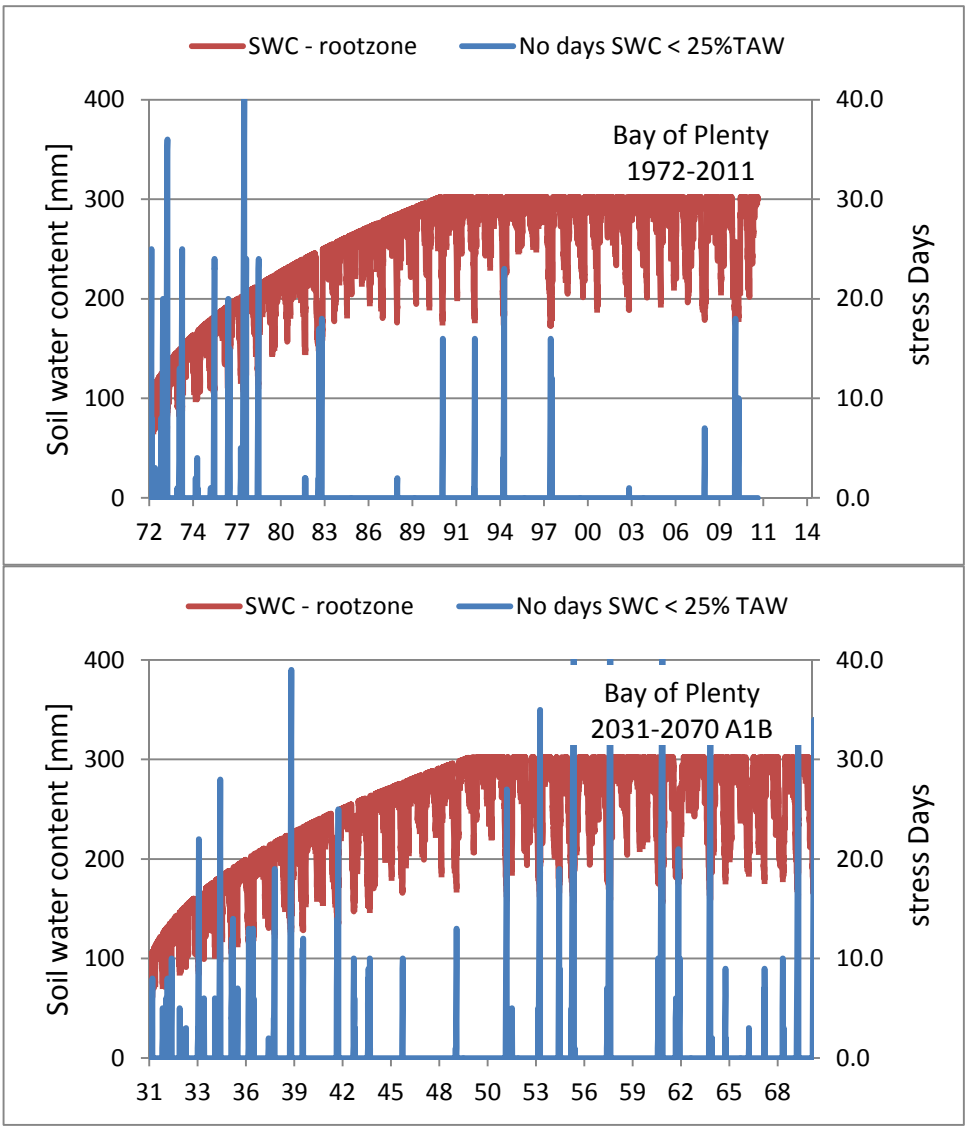

Figure 1.3.5. Model outputs for poplar trees growing under current (1972–2013) and future (2030–2070 A1B) climate change scenarios in the Bay of Plenty region. These results depict the changing pattern of soil water content in the root zone (red line) and the corresponding cumulative number of mild-stress days (SWC < 25%TAW) that occur during each growing season.

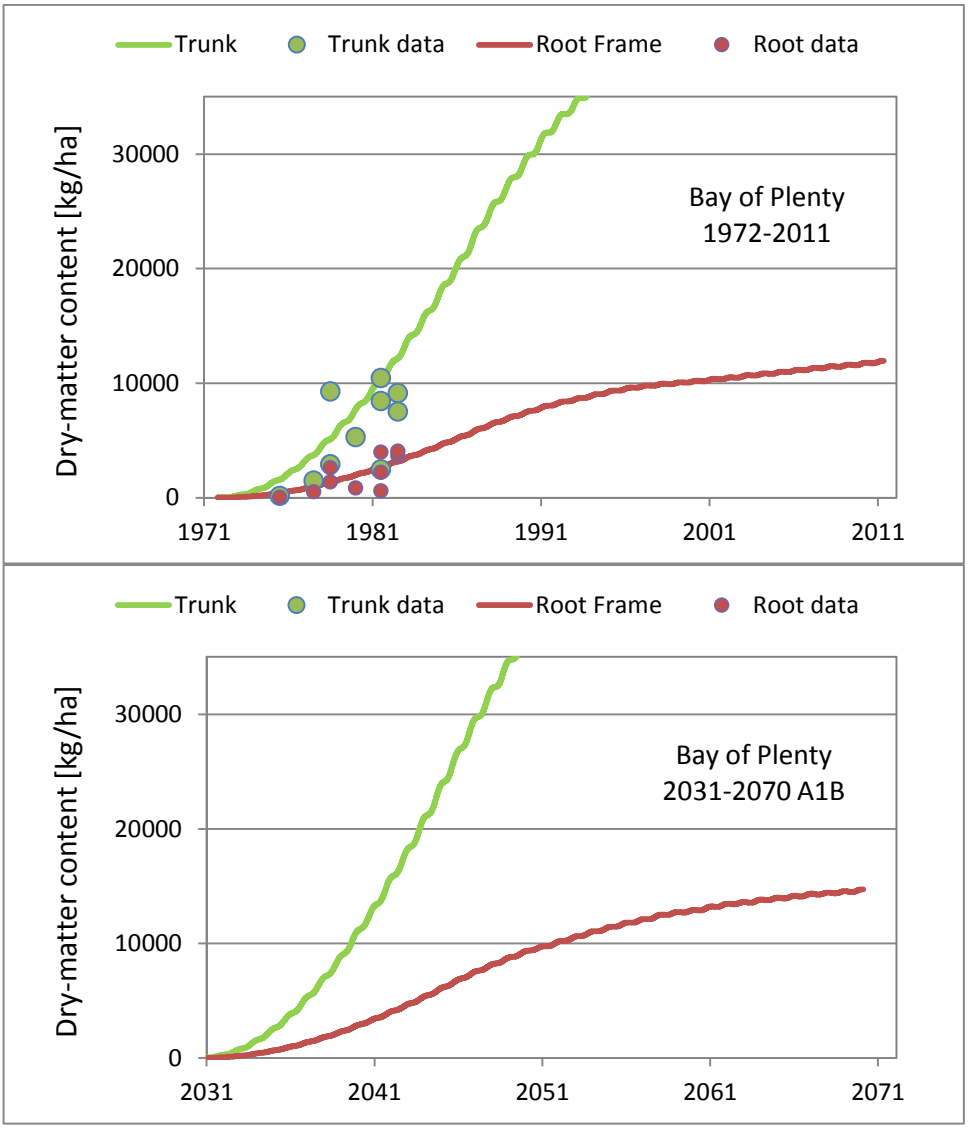

Figure 1.3.6. Model outputs for the dry-matter accumulation (i.e. growth) of poplar trees growing under current (1972–2013) and future (2030–2070 A1B) climate change scenarios in the Bay of Plenty region. Data are from field trials near Woodville.

Table 1.3.1. A statistical analysis of model outputs used to assess survivability and disease risk of poplar poles growing in the Bay of Region under current (1972–2011) and future (2031–2070 A1B) climate change scenarios. Here we have assumed a fixed root-zone depth of 0.40 m.

	statistic	no. mild stress days	no. critical stress days	Disease risk *M. larici-populina*	Disease risk *M. medusae*
Bay of Plenty (1972–2011)	mean	14	2	0.18	0.18
	Std dev	10	3	0.04	0.10
	PE20	23	4	0.22	0.27
	Prob (NSD>7)	0.71	0.09	-	-
	statistic	**no. moderate stress days**	**no. critical stress days**	**Disease risk *M. larici-populina***	**Disease risk *M. medusae***
Bay of Plenty (2031–2070 A1B)	mean	21	7	0.32	0.38
	stdev	17	13	0.10	0.16
	PE20	35	17	0.40	0.51
	Prob (NSD>7)	0.76	0.29	-	-

Table 1.3.2. A statistical analysis of model outputs used to assess survivability and disease risk of poplar trees growing in the Bay of Region under current (1972–2011) and future (2031–2070 A1B) climate change scenarios. Trees have been 'grown' from poles planted at the start of the simulation period.

	statistic	no. moderate stress days	no. critical stress days	Disease risk *M. larici-populina*	Disease risk *M. medusae*
Bay of Plenty (1972–2011)	mean	8	0	0.21	0.18
	stdev	11	1	0.06	0.10
	PE20	17	0	0.25	0.27
	Prob (NSD>7)	0.32	0.01	-	-
	statistic	**no. moderate stress days**	**no. critical stress days**	**Disease risk *M. larici-populina***	**Disease risk *M. medusae***
Bay of Plenty (2031–2070) A1B	mean	16	1	0.36	0.38
	stdev	16	2	0.12	0.16
	PE20	30	2	0.46	0.51
	Prob (NSD>7)	0.68	0.06	-	-

Table 1.3.3. Model outputs for the dry-matter accumulation (i.e. growth) of poplar trees growing under current (1972–2013) and future (2030–2070 A1B) climate change scenarios in the Bay of Plenty region. $T_{50\%}$ and $T_{90\%}$ represent the amount of time (years) to reach 50% and 90% of the final value, respectively.

Bay of Plenty (1972–2011)			Bay of Plenty (2031–2070) A1B		
age	tree biomass [kg/ha]		age	tree biomass [kg/ha]	
	above ground	below ground		above ground	below ground
0	93	28	0	93	28
5	3379	933	5	3676	1014
10	11772	3136	10	13172	3493
15	23538	6074	15	27238	6985
25	40394	10007	25	48391	12052
39	51860	12183	39	64018	15020
$T_{50\%}$	17	16	$T_{50\%}$	17	16
$T_{90\%}$	33	32	$T_{90\%}$	32	31

6.6.4 Model outputs: Gisborne District

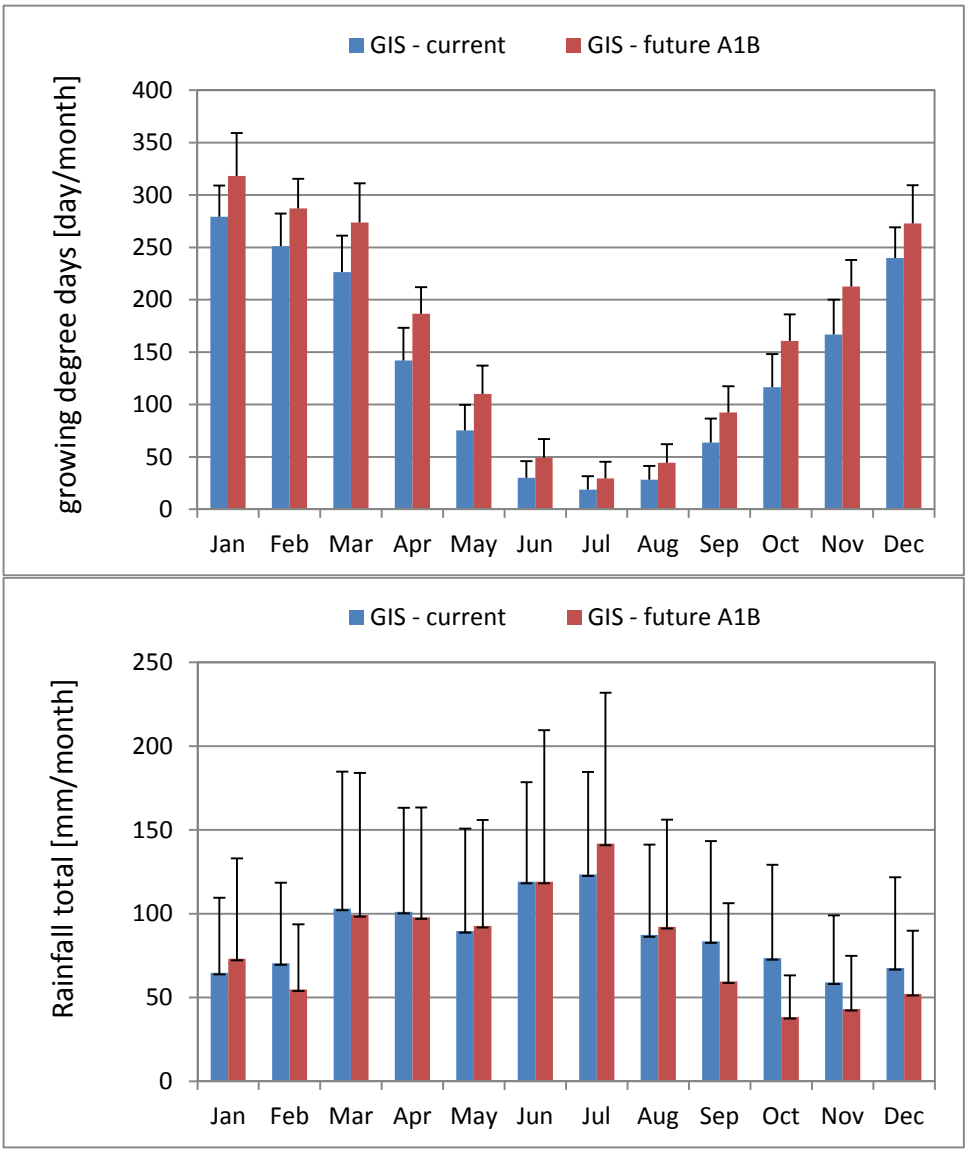

Figure 1.4.1. Summary of seasonal climate data for the Gisborne District (GIS) as represented by the number growing-degree days (base 10ºC) and monthly rainfall under current (1972–2013) and future (2031–2070 A1B) climate change simulations.

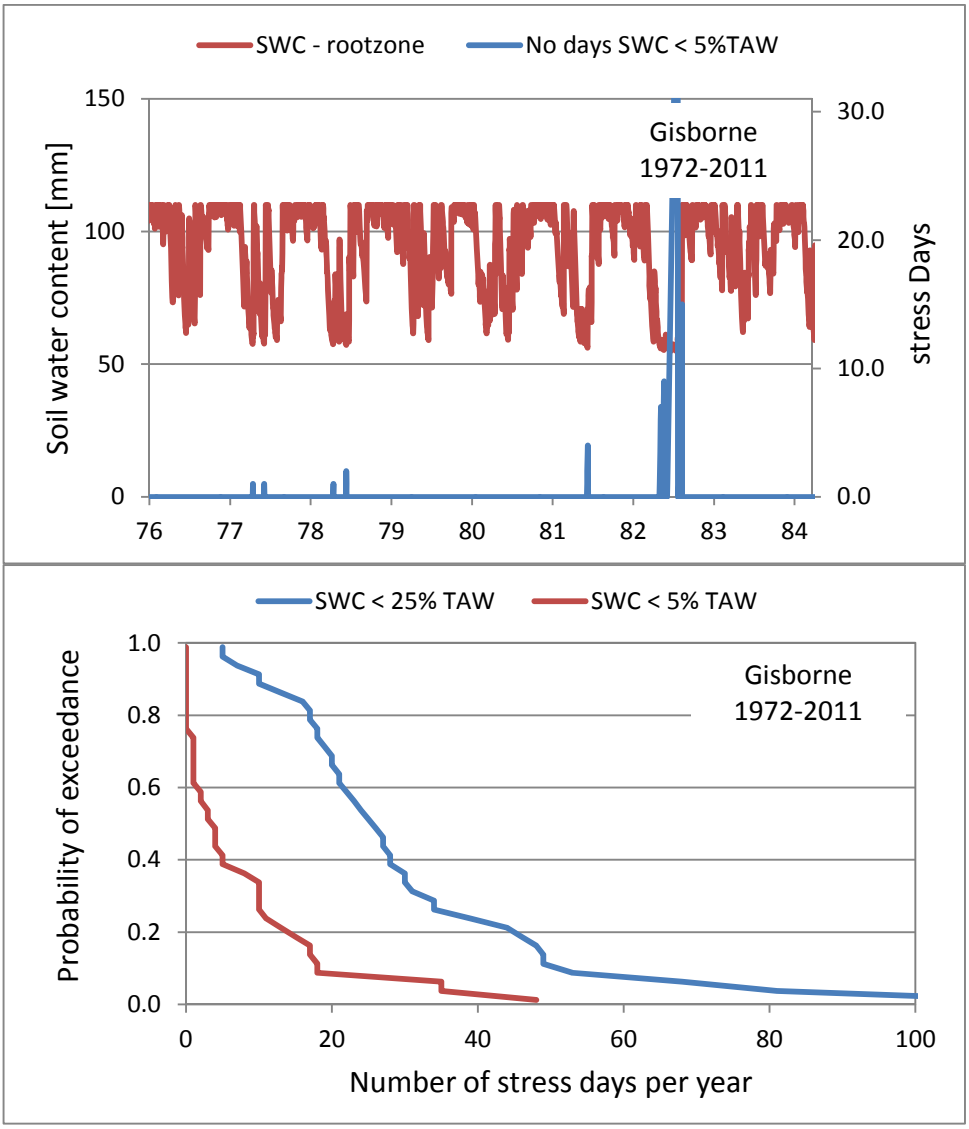

Figure 1.4.2. Model outputs used to assess the survivability of planted poplar poles growing under a current climate scenario (1972–2013) in the Gisborne district. The top panel shows a time series of soil water content (SWC) in the top 40 cm of the root-zone soil, and the cumulative number of high-stress days where SWC < 5% of total available water (TAW). The bottom panel shows the probabilities of exceedance associated with cumulative of high stress days (SWC<5%TAW) and mild-stress days (SWC < 25%TAW) that occur during each growing season.

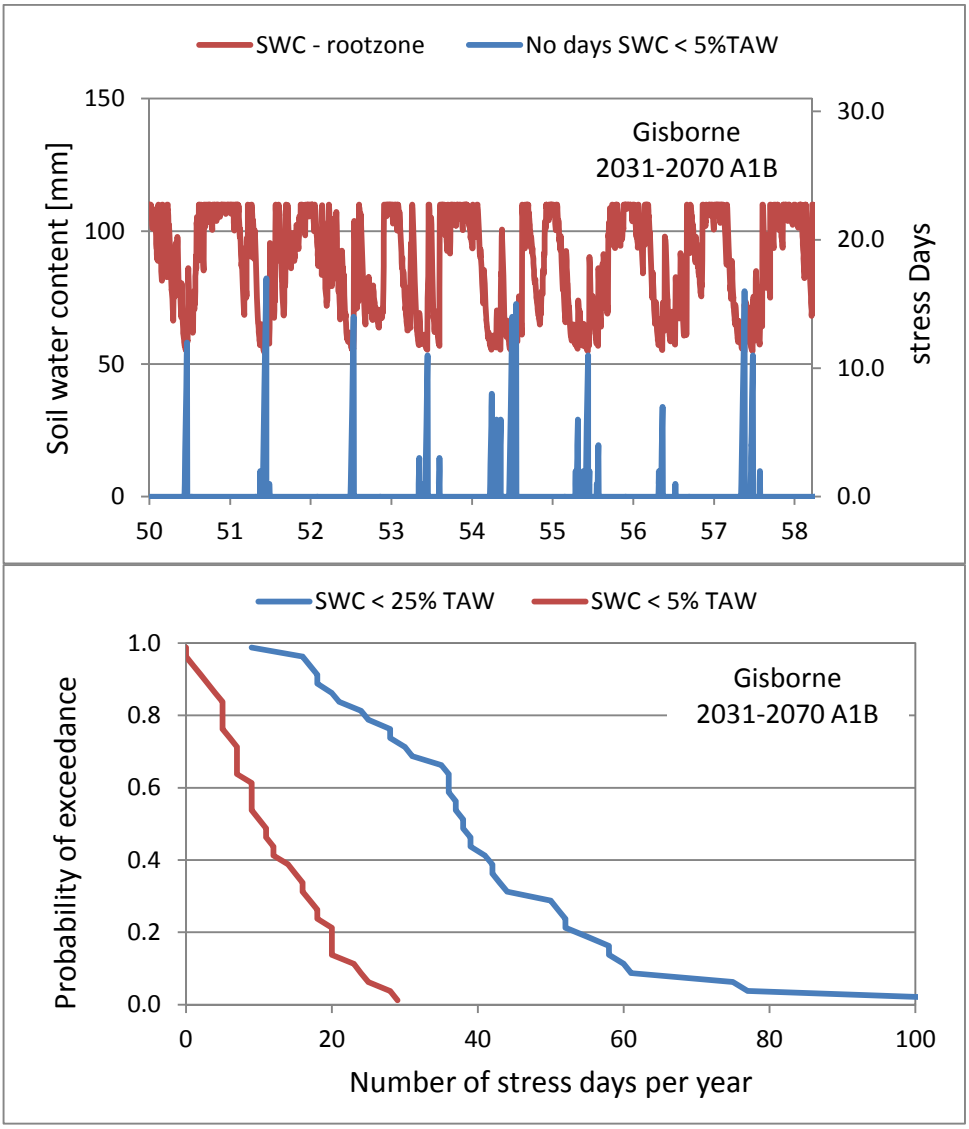

Figure 1.4.3. Model outputs used to assess the survivability of planted poplar poles growing under a future climate scenario (2031–2070 A1B) in the Gisborne District. The top panel shows a time series of soil water content (SWC) in the top 40 cm of the root-zone soil, and the cumulative number of high-stress days where SWC < 5% of total available water (TAW). The bottom panel shows the probabilities of exceedance associated with cumulative of high stress days (SWC<5%TAW) and mild-stress days (SWC < 25%TAW) that occur during each growing season.

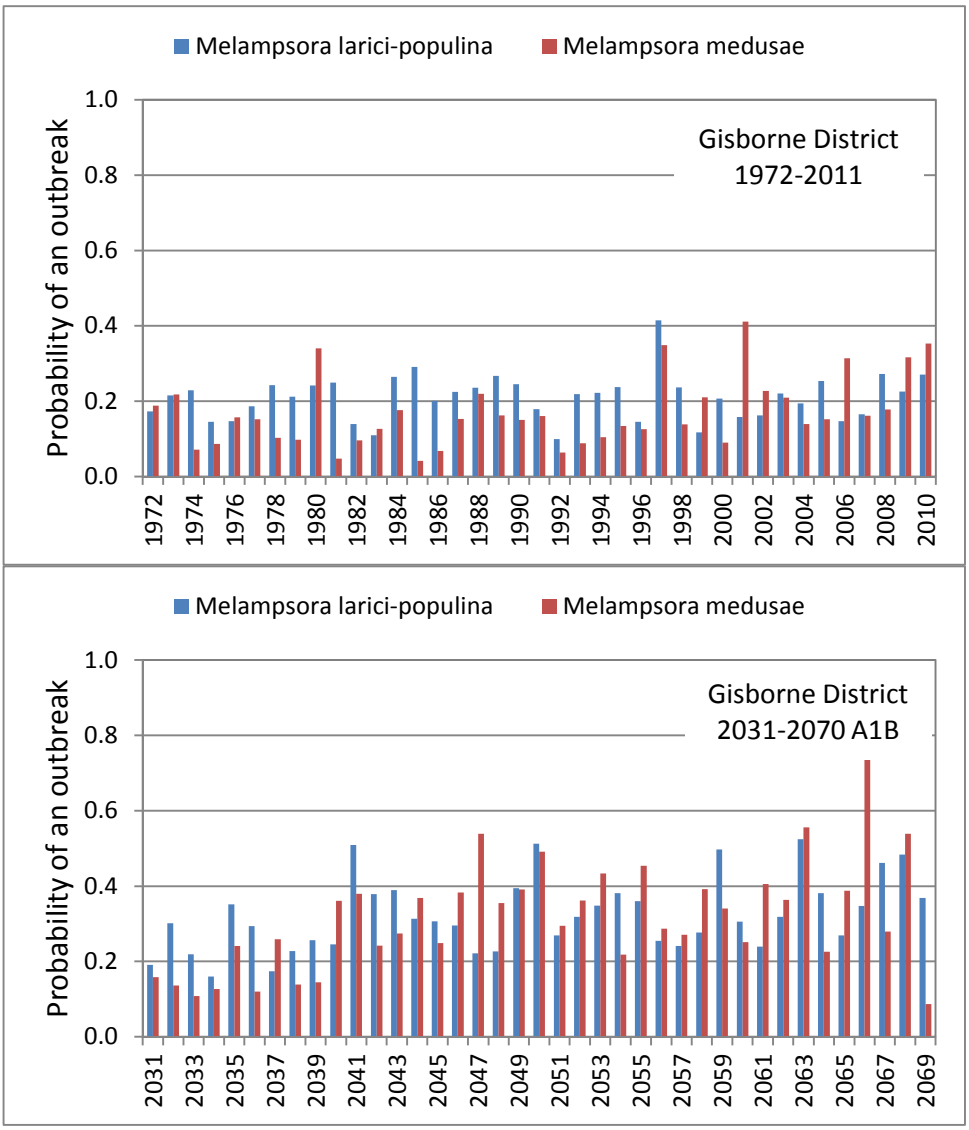

Figure 1.4.4. Model outputs used to assess the risk of occurrence of an outbreak of *Melampsora* rust on poplar trees growing in the Gisborne District under the current (1972–2010) and future (2031–2070 A1B) climate change scenarios.

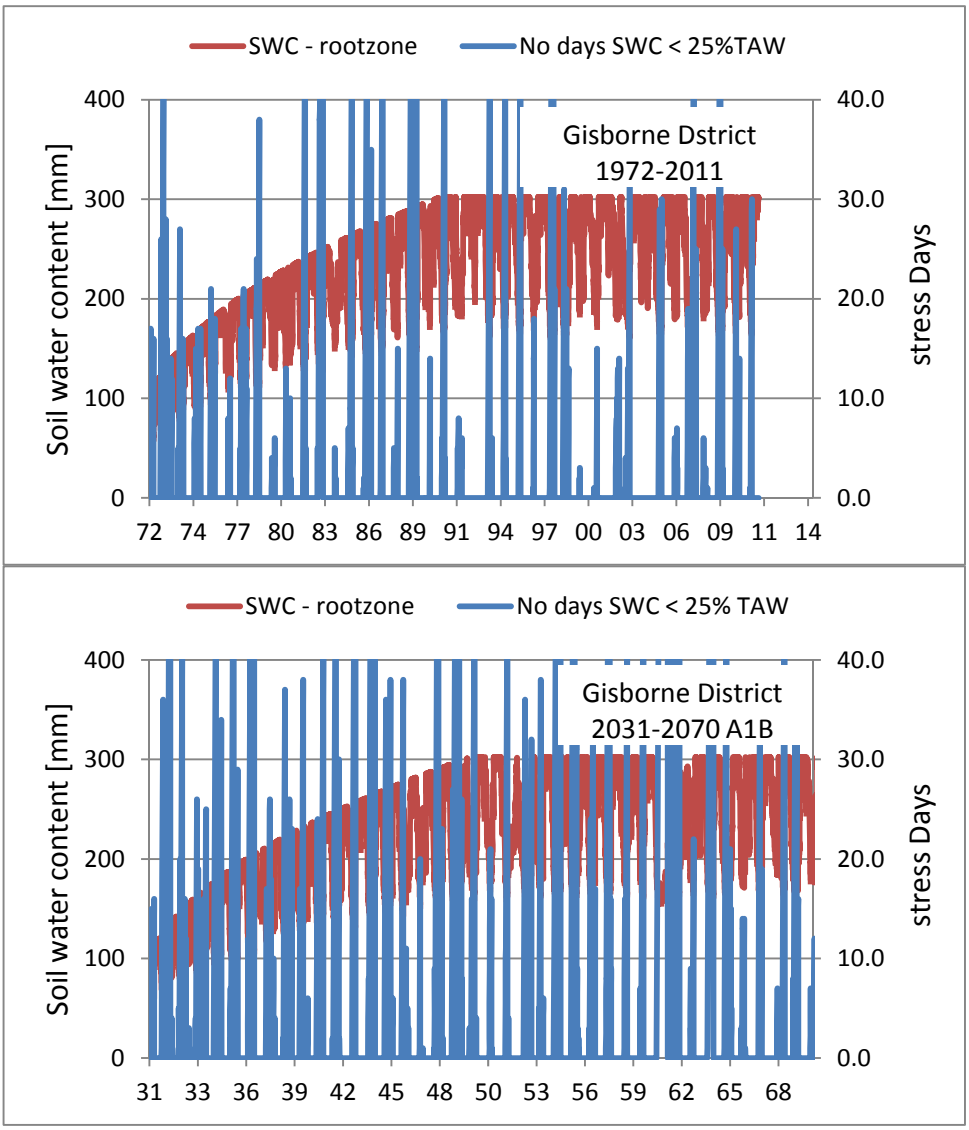

Figure 1.4.5. Model outputs for poplar trees growing under current (1972–2013) and future (2030–2070 A1B) climate change scenarios in the Gisborne District. These results depict the changing pattern of soil water content in the root zone (red line) and the corresponding cumulative number of mild-stress days (SWC < 25%TAW) that occur during each growing season.

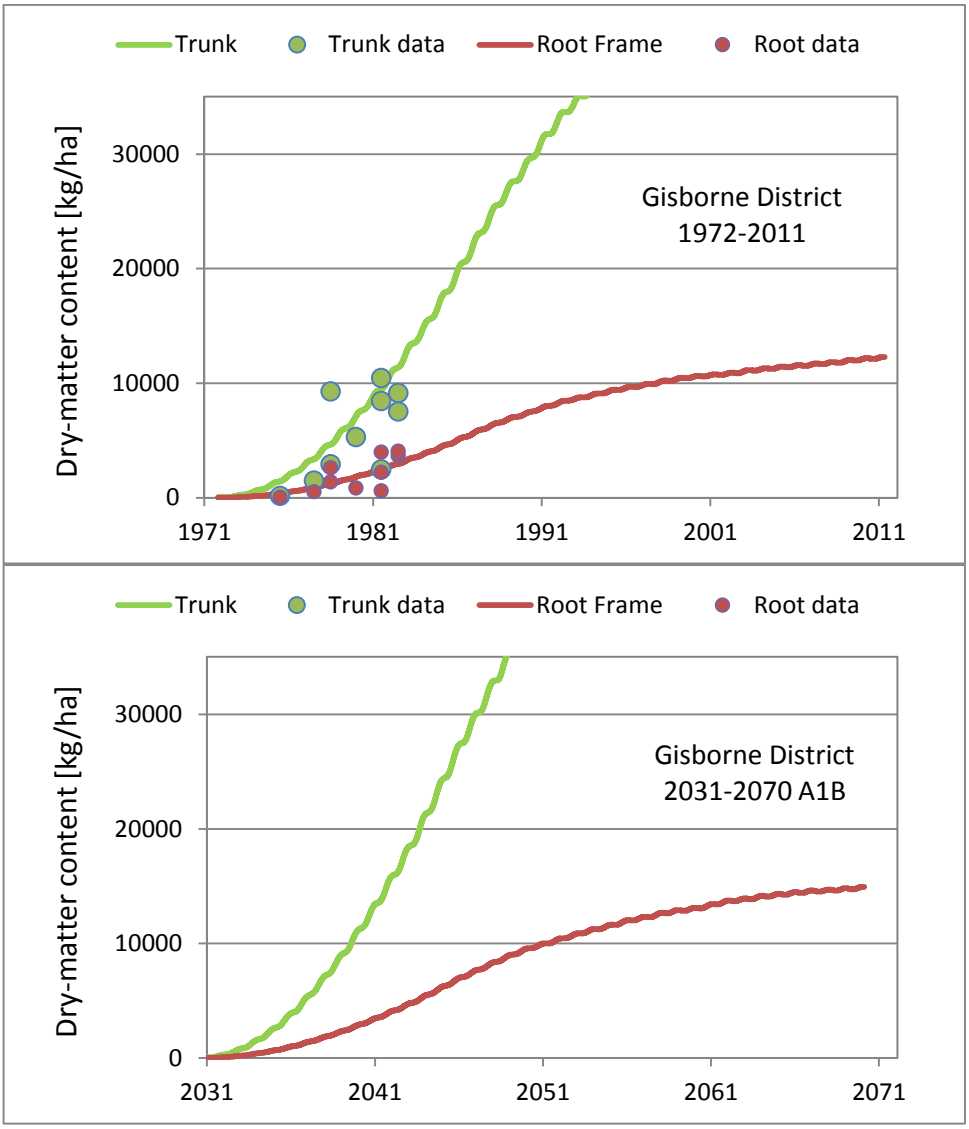

Figure 1.4.6. Model outputs for the dry-matter accumulation (i.e. growth) of poplar trees growing under current (1972–2013) and future (2030–2070 A1B) climate change scenarios in the Gisborne District. Data are from field trials near Woodville.

Table 1.4.1. A statistical analysis of model outputs used to assess survivability and disease risk of poplar poles growing in the Gisborne District under current (1972–2011) and future (2031–2070 A1B) climate change scenarios. Here we have assumed a fixed root-zone depth of 0.40 m.

	statistic	no. moderate stress days	no. critical stress days	Disease risk *M. larici-populina*	Disease risk *M. medusae*
Gisborne District (1972–2011)	mean	30	8	0.21	0.17
	stdev	21	11	0.06	0.09
	PE20	48	17	0.26	0.25
	Prob (NSD>7)	0.94	0.39	-	-
	statistic	no. moderate stress days	no. critical stress days	Disease risk *M. larici-populina*	Disease risk *M. medusae*
Gisborne District (2031–2070 A1B)	mean	41	12	0.32	0.32
	stdev	20	8	0.10	0.14
	PE20	57	18	0.40	0.44
	Prob (NSD>7)	> 0.99	0.64	-	-

Table 1.4.2. A statistical analysis of model outputs used to assess survivability and disease risk of poplar trees growing in the Gisborne District under current (1972–2011) and future (2031–2070 A1B) climate change scenarios. Trees have been 'grown' from poles planted at the start of the simulation period.

	statistic	no. moderate stress days	no. critical stress days	Disease risk *M. larici-populina*	Disease risk *M. medusae*
Gisborne District (1972–2011)	mean	33	3	0.27	0.17
	stdev	27	9	0.09	0.09
	PE20	55	10	0.35	0.25
	Prob (NSD>7)	0.83	0.12	-	-
	statistic	no. moderate stress days	no. critical stress days	Disease risk *M. larici-populina*	Disease risk *M. medusae*
Gisborne District (2031–2070) A1B	mean	54	4	0.42	0.32
	stdev	38	6	0.12	0.14
	PE20	86	8	0.52	0.44
	Prob (NSD>7)	0.99	0.24	-	-

Table 1.4.3. Model outputs for the dry-matter accumulation (i.e. growth) of poplar trees growing under current (1972–2013) and future (2030–2070 A1B) climate change scenarios in the Gisborne District. $T_{50\%}$ and $T_{90\%}$ represent the amount of time (years) for reach 50% and 90% of the final value, respectively.

Gisborne District (1972–2011)			Gisborne District (2031–2070) A1B		
age	tree biomass [kg/ha]		age	tree biomass [kg/ha]	
	above ground	below ground		above ground	below ground
0	93	28	0	93	28
5	3072	848	5	3681	1022
10	10939	2938	10	13118	3521
15	22765	5973	15	27197	7099
25	40760	10138	25	48931	12251
39	52953	12542	39	64872	15255
$T_{50\%}$	17	16	$T_{50\%}$	17	16
$T_{90\%}$	32	31	$T_{90\%}$	32	31

6.6.5 Model outputs: Central Hawke's Bay

Table 1.5.1. A statistical analysis of model outputs used to assess survivability and disease risk of poplar poles growing in the Central Hawke's Bay under current (1972–2011) and future (2031–2070 A1B) climate change scenarios. Here we have assumed a fixed root-zone depth of 0.40 m.

	statistic	no. moderate stress days	no. critical stress days	Disease risk *M. larici-populina*	Disease risk *M. medusae*
Central Hawkes Bay (1972–2011)	mean	40	13	0.19	0.06
	stdev	21	13	0.05	0.04
	PE20	57	23	0.23	0.09
	Prob (NSD>7)	>0.99	0.64	-	-
Central Hawkes Bay (2031–2070 A1B)	statistic	no. moderate stress days	no. critical stress days	Disease risk *M. larici-populina*	Disease risk *M. medusae*
	mean	39	11	0.26	0.13
	stdev	18	9	0.08	0.09
	PE20	53	17	0.33	0.21
	Prob (NSD>7)	>0.99	0.61	-	-

Table 1.5.2. A statistical analysis of model outputs used to assess survivability and disease risk of poplar trees growing in the Central Hawke's Bay under current (1972–2011) and future (2031–2070 A1B) climate scenarios. Trees have been 'grown' from poles planted at the start of the simulation period.

	statistic	no. moderate stress days	no. critical stress days	Disease risk *M. larici-populina*	Disease risk *M. medusae*
Central Hawkes Bay (1972–2011)	mean	54	6	0.26	0.06
	stdev	40	9	0.08	0.04
	PE20	87	13	0.32	0.09
	Prob (NSD>7)	0.96	0.29	-	-
Central Hawkes Bay (2031–2070) A1B	statistic	no. moderate stress days	no. critical stress days	Disease risk *M. larici-populina*	Disease risk *M. medusae*
	mean	56	4	0.35	0.13
	stdev	38	7	0.11	0.09
	PE20	88	9	0.45	0.21
	Prob (NSD>7)	0.99	0.22	-	-

Table 1.5.3. Model outputs for the dry-matter accumulation (i.e. growth) of poplar trees growing under current (1972–2013) and future (2030–2070 A1B) climate change scenarios in the Central Hawke's Bay. $T_{50\%}$ and $T_{90\%}$ represent the amount of time (years) to reach 50% and 90% of the final value, respectively.

Central Hawke's Bay (1972–2011)			Central Hawke's Bay (2031–2070) A1B		
age	tree biomass [kg/ha]		age	tree biomass [kg/ha]	
	above ground	below ground		above ground	below ground
0	93	28	0	93	28
5	3176	879	5	3606	1001
10	11056	2976	10	12819	3439
15	22542	5931	15	26387	6904
25	39255	9791	25	47523	11897
39	52513	12463	39	62806	14816
$T_{50\%}$	17	16	$T_{50\%}$	17	16
$T_{90\%}$	32	31	$T_{90\%}$	32	31

6.6.6 Model Outputs: Southern Hawke's Bay region

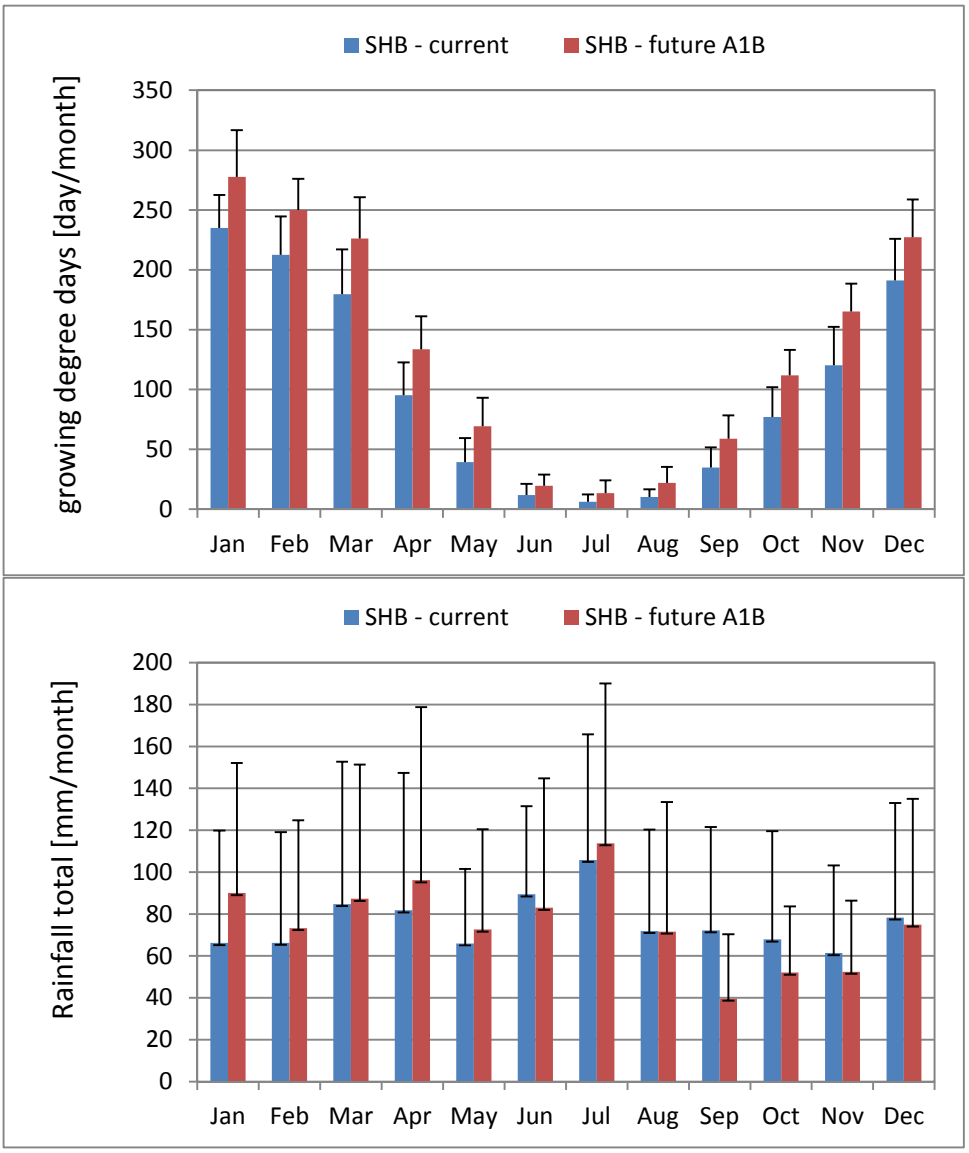

Figure 1.6.1. Summary of seasonal climate data for the Southern Hawke's Bay (SHB) as represented by the number growing-degree days (base 10ºC) and monthly rainfall under current (1972–2013) and future (2031–2070 A1B) climate change simulations.

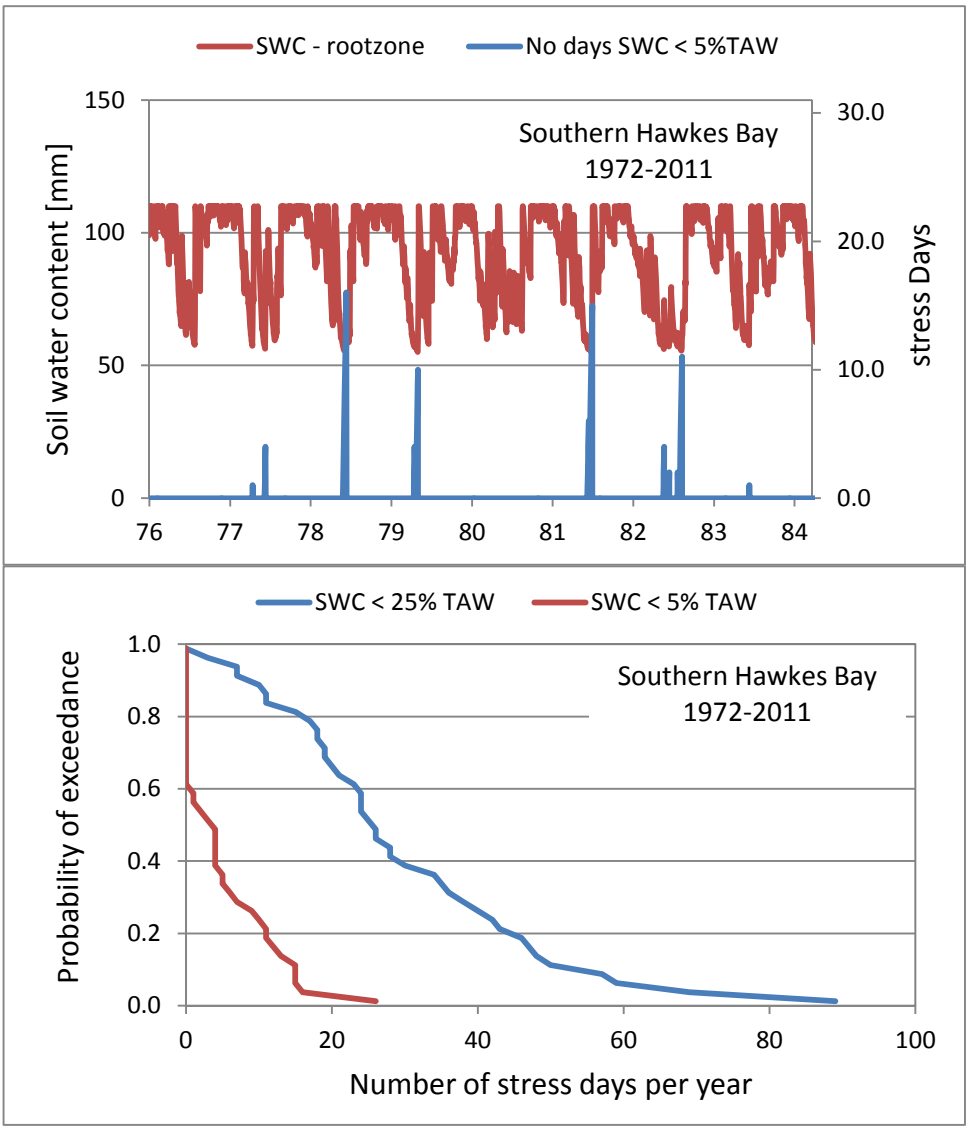

Figure 1.6.2. Model outputs used to assess the survivability of planted poplar poles growing under a current climate scenario (1972–2013) in the southern Hawke's Bay region. The top panel shows a time series of soil water content (SWC) in the top 40 cm of the root-zone soil, and the cumulative number of high-stress days where SWC < 5% of total available water (TAW). The bottom panel shows the probabilities of exceedance associated with cumulative of high stress days (SWC<5%TAW) and mild-stress days (SWC < 25%TAW) that occur during each growing season.

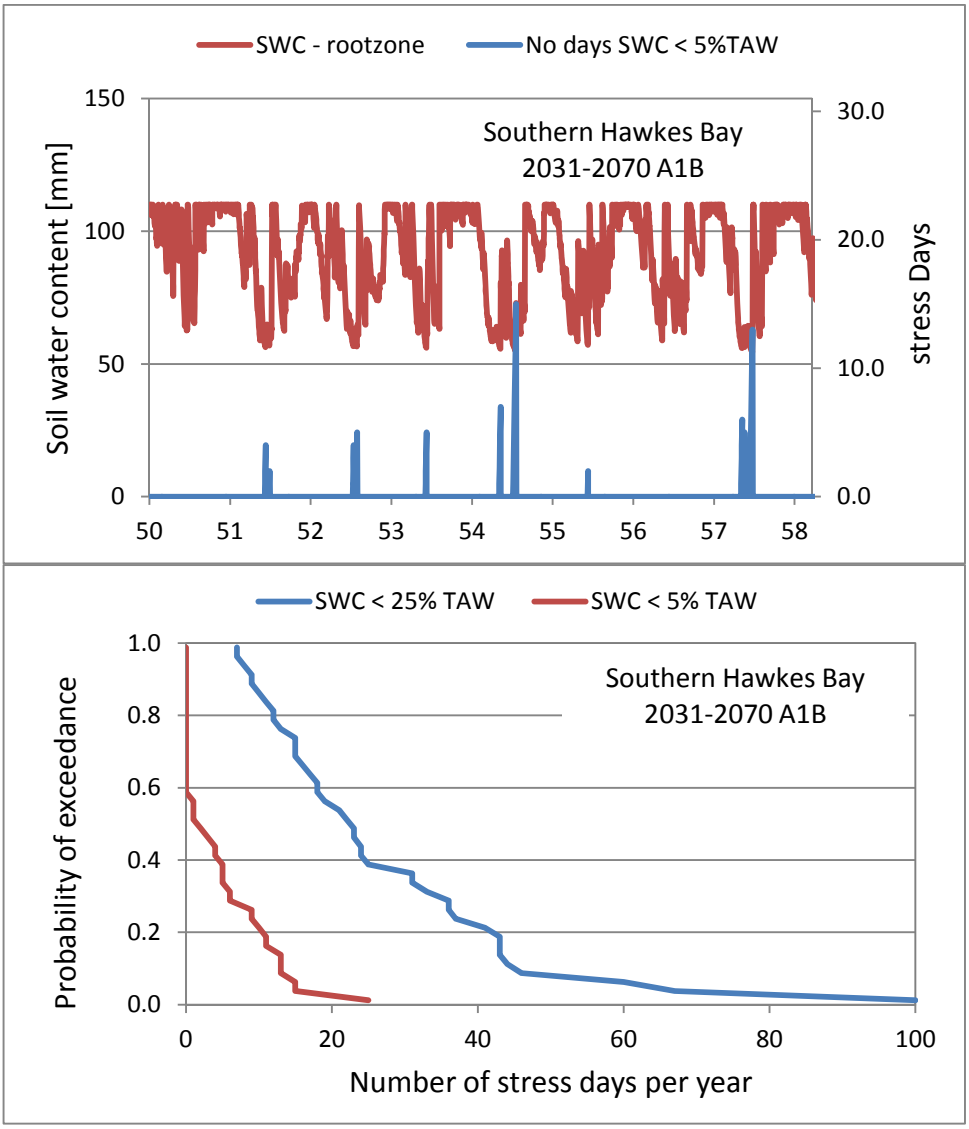

Figure 1.6.3. Model outputs used to assess the survivability of planted poplar poles growing under a future climate scenario (2031–2070 A1B) in the Southern Hawke's Bay region. The top panel shows a time series of soil water content (SWC) in the top 40 cm of the root-zone soil, and the cumulative number of high-stress days where SWC < 5% of total available water (TAW). The bottom panel shows the probabilities of exceedance associated with cumulative of high stress days (SWC<5%TAW) and mild-stress days (SWC < 25%TAW) that occur during each growing season.

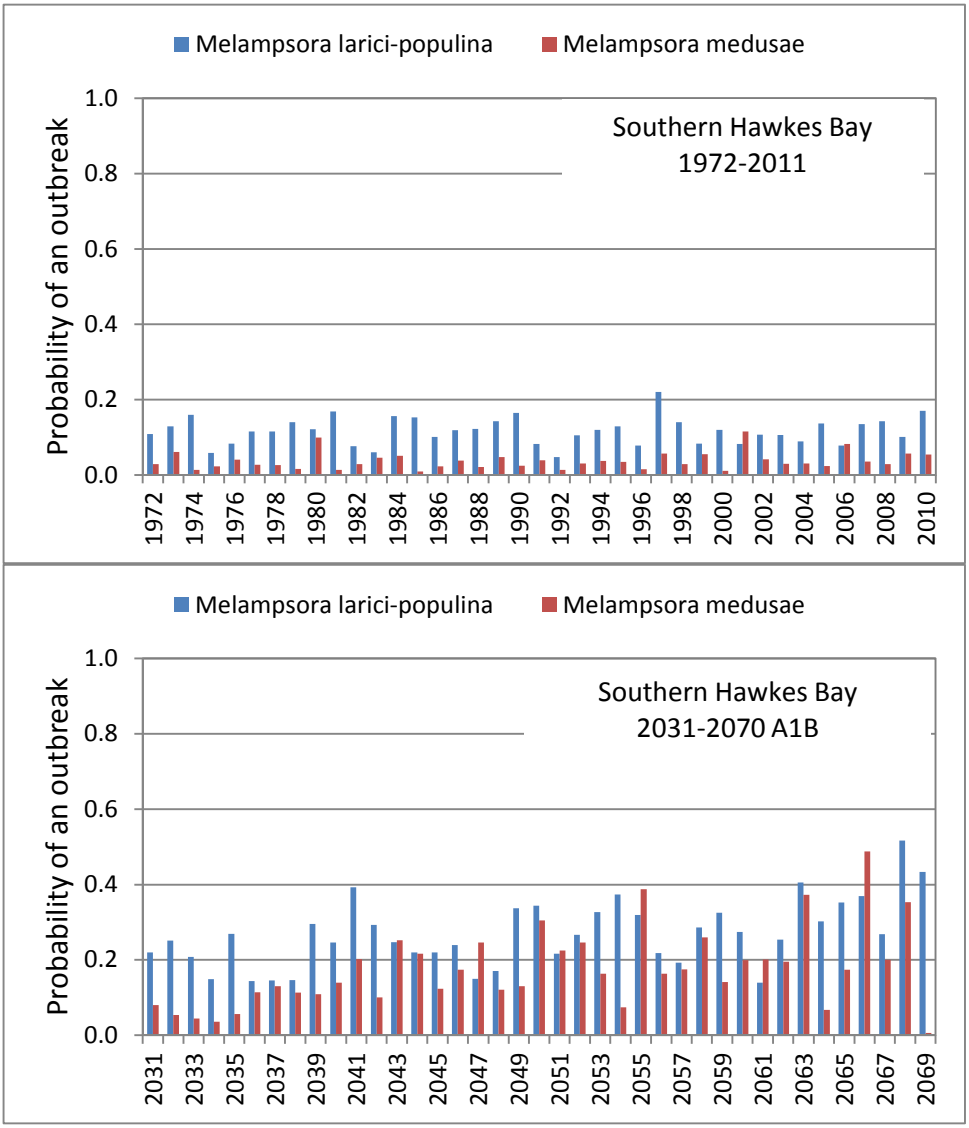

Figure 1.6.4. Model outputs used to assess the risk of occurrence of an outbreak of *Melampsora* rust on poplar trees growing in the Southern Hawke's Bay region under the current (1972–2010) and future (2031–2070 A1B) climate change scenarios.

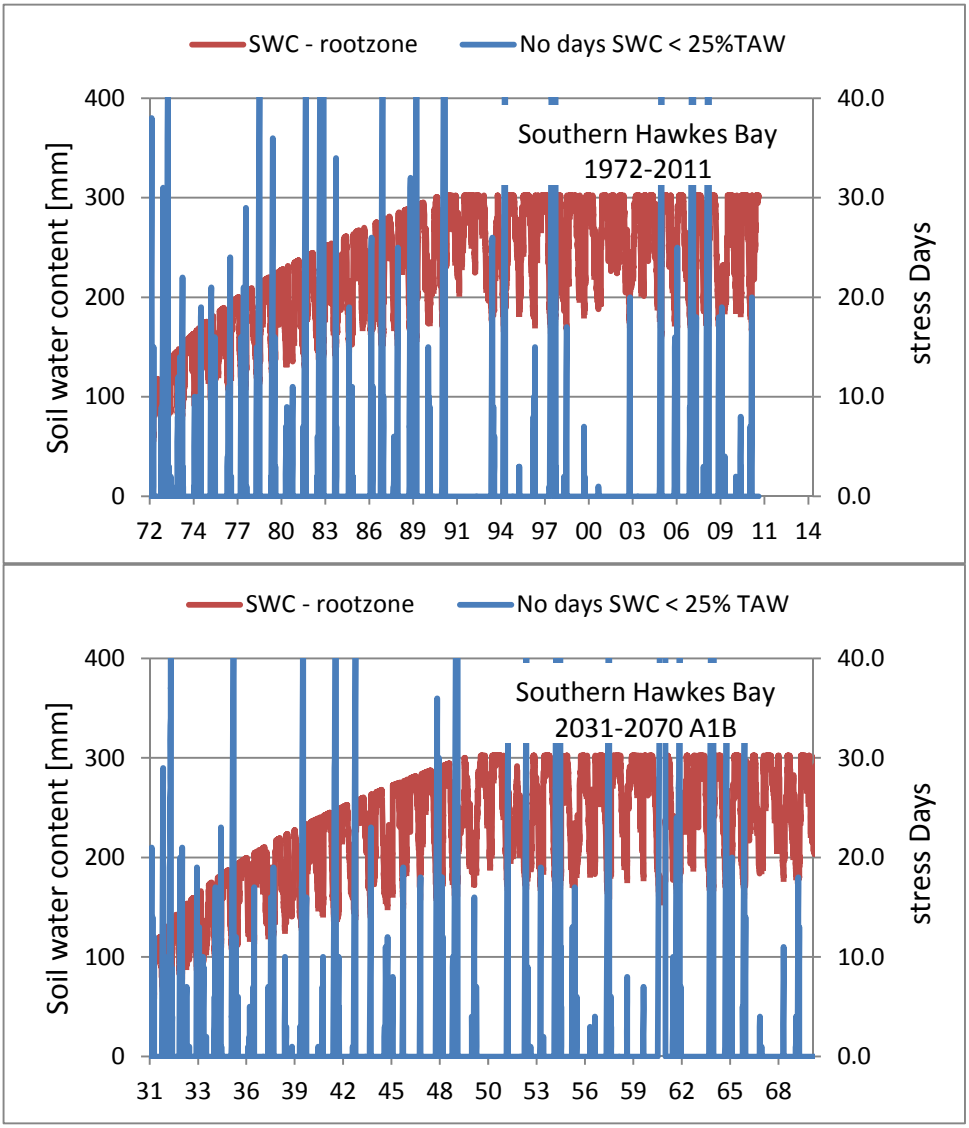

Figure 1.6.5. Model outputs for poplar trees growing under current (1972–2013) and future (2030–2070 A1B) climate change scenarios in the Southern Hawke's Bay region. These results depict the changing pattern of soil water content in the root zone (red line) and the corresponding cumulative number of mild-stress days (SWC < 25%TAW) that occur during each growing season.

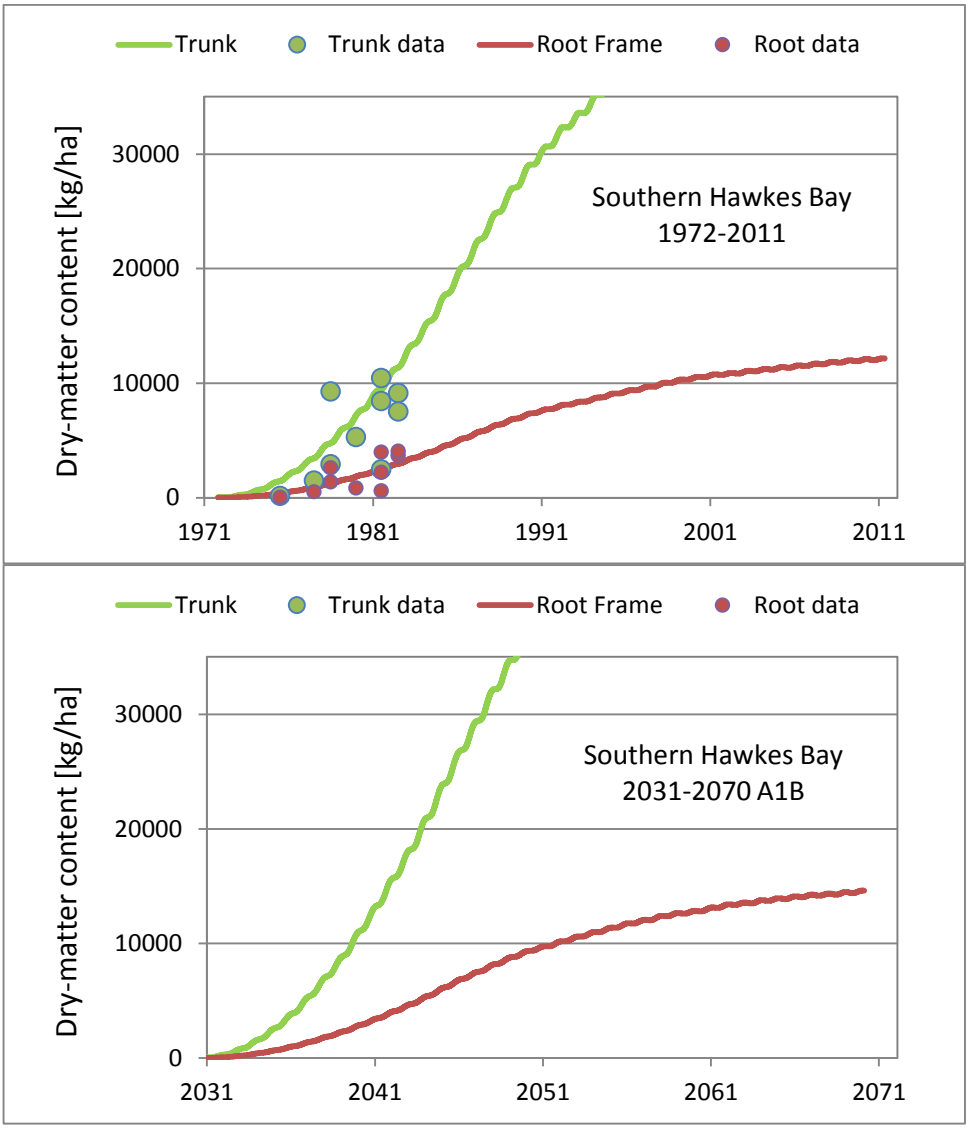

Figure 1.6.6. Model outputs for the dry-matter accumulation (i.e. growth) of poplar trees growing under current (1972–2013) and future (2030–2070 A1B) climate change scenarios in the Southern Hawke's Bay region. Data are from field trials near Woodville.

Table 1.6.1. A statistical analysis of model outputs used to assess survivability and disease risk of poplar poles growing in the Southern Hawke's Bay under current (1972–2011) and future (2031–2070 A1B) climate change scenarios. Here we have assumed a fixed root-zone depth of 0.40 m.

Southern Hawkes Bay (1972–2011)	statistic	no. moderate stress days	no. critical stress days	Disease risk *M. larici-populina*	Disease risk *M. medusae*
	mean	30	5	0.12	0.04
	stdev	19	6	0.04	0.02
	PE20	45	10	0.15	0.06
	Prob (NSD>7)	0.91	0.29	-	-
Southern Hawkes Bay (2031–2070 A1B)	**statistic**	**no. moderate stress days**	**no. critical stress days**	**Disease risk *M. larici-populina***	**Disease risk *M. medusae***
	mean	27	5	0.27	0.18
	stdev	19	6	0.09	0.10
	PE20	43	9	0.34	0.26
	Prob (NSD>7)	0.96	0.29	-	-

Table 1.6.2. A statistical analysis of model outputs used to assess survivability and disease risk of poplar trees growing in the Southern Hawke's Bay region under current (1972–2011) and future (2031–2070 A1B) climate change scenarios. Trees have been 'grown' from poles planted at the start of the simulation period.

Southern Hawkes Bay (1972–2011)	statistic	no. moderate stress days	no. critical stress days	Disease risk *M. larici-populina*	Disease risk *M. medusae*
	mean	30	2	0.16	0.04
	stdev	24	4	0.06	0.02
	PE20	50	4	0.20	0.06
	Prob (NSD>7)	0.83	0.09	-	-
Southern Hawkes Bay (2031–2070) A1B	**statistic**	**no. moderate stress days**	**no. critical stress days**	**Disease risk *M. larici-populina***	**Disease risk *M. medusae***
	mean	31	1	0.26	0.10
	stdev	30	3	0.09	0.06
	PE20	55	3	0.33	0.15
	Prob (NSD>7)	0.86	0.06	-	-

Table 1.6.3. Model outputs for the dry-matter accumulation (i.e. growth) of poplar trees growing under current (1972–2013) and future (2030–2070 A1B) climate change scenarios in the Southern Hawke's Bay. $T_{50\%}$ and $T_{90\%}$ represent the amount of time (years) to reach 50% and 90% of the final value, respectively.

Southern Hawke's Bay	(1972–2011)		Southern Hawke's Bay A1B	(2031–2070)	
age	tree biomass [kg/ha]		age	tree biomass [kg/ha]	
	above ground	below ground		above ground	below ground
0	93	28	0	93	28
5	3136	868	5	3632	1006
10	10920	2935	10	13013	3463
15	22186	5831	15	26857	6945
25	39643	9880	25	48106	11981
39	52378	12427	39	63657	14922
$T_{50\%}$	17	16	$T_{50\%}$	17	16
$T_{90\%}$	32	31	$T_{90\%}$	32	31

6.6.7 Model Outputs: Southern Wairarapa

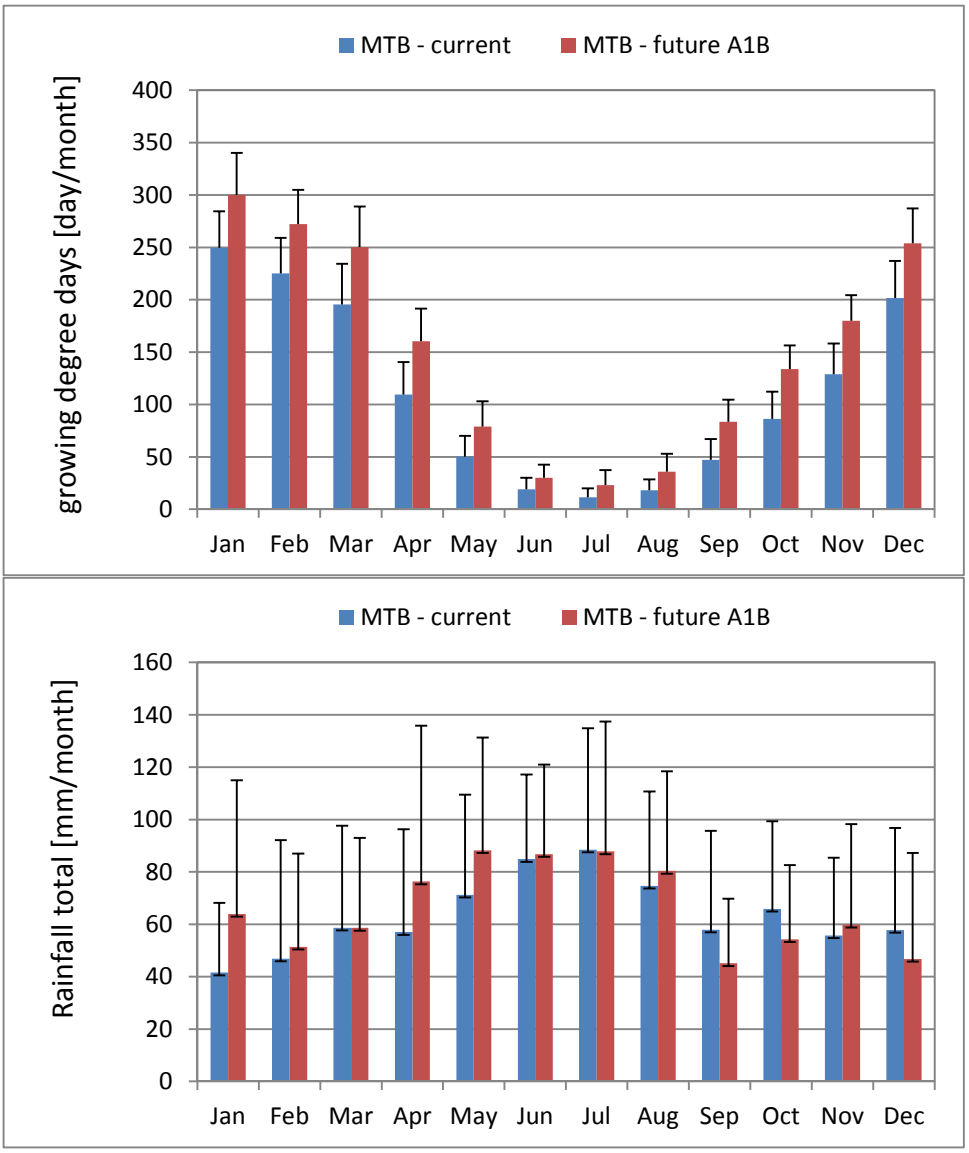

Figure 1.7.1. Summary of seasonal climate data for the Southern Wairarapa (MTB, near Martinborough) as represented by the number growing-degree days (base 10ºC) and monthly rainfall under current (1972–2013) and future (2031–2070 A1B) climate change simulations.

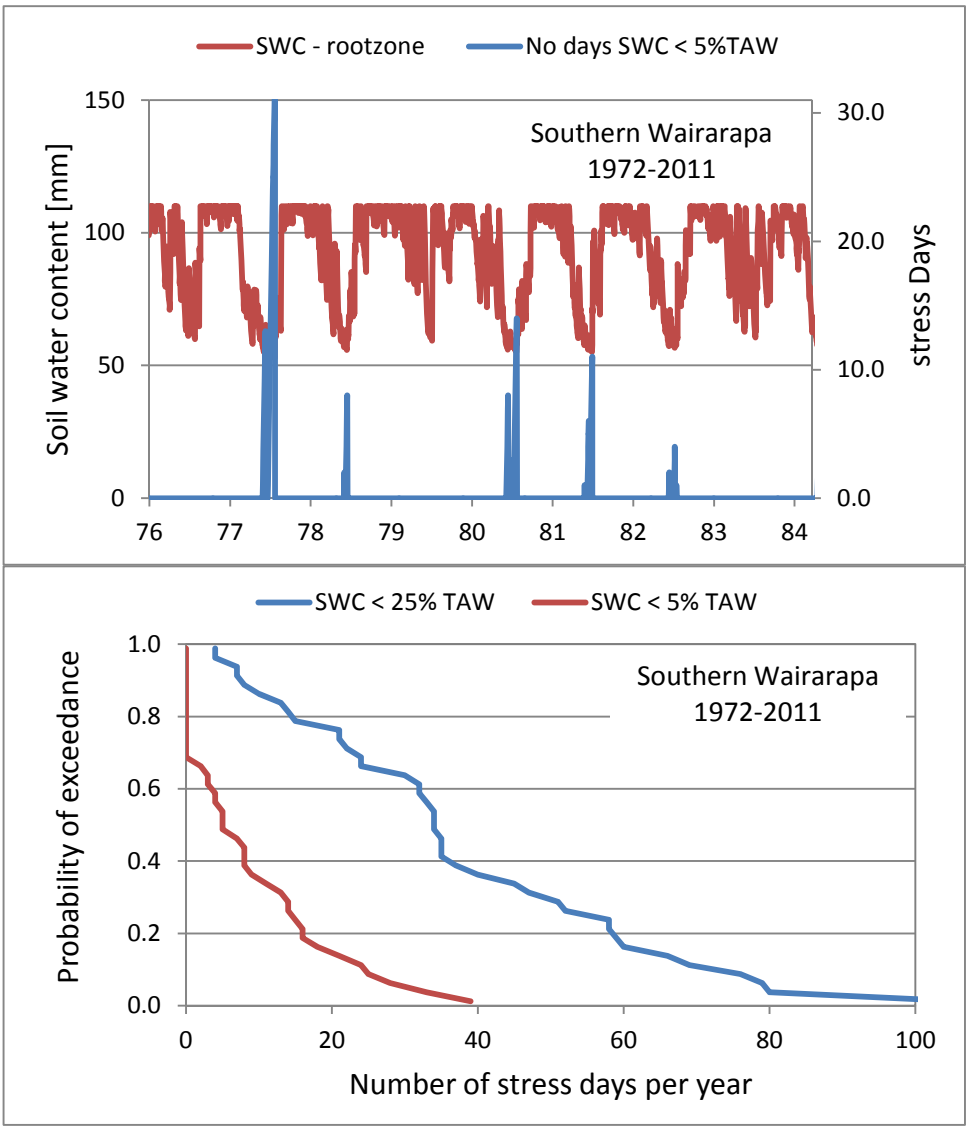

Figure 1.7.2. Model outputs used to assess the survivability of planted poplar poles growing under a current climate scenario (1972–2013) in the Southern Wairarapa. The top panel shows a time series of soil water content (SWC) in the top 40 cm of the root-zone soil, and the cumulative number of high-stress days where SWC < 5% of total available water (TAW). The bottom panel shows the probabilities of exceedance associated with cumulative of high stress days (SWC<5%TAW) and mild-stress days (SWC < 25%TAW) that occur during each growing season.

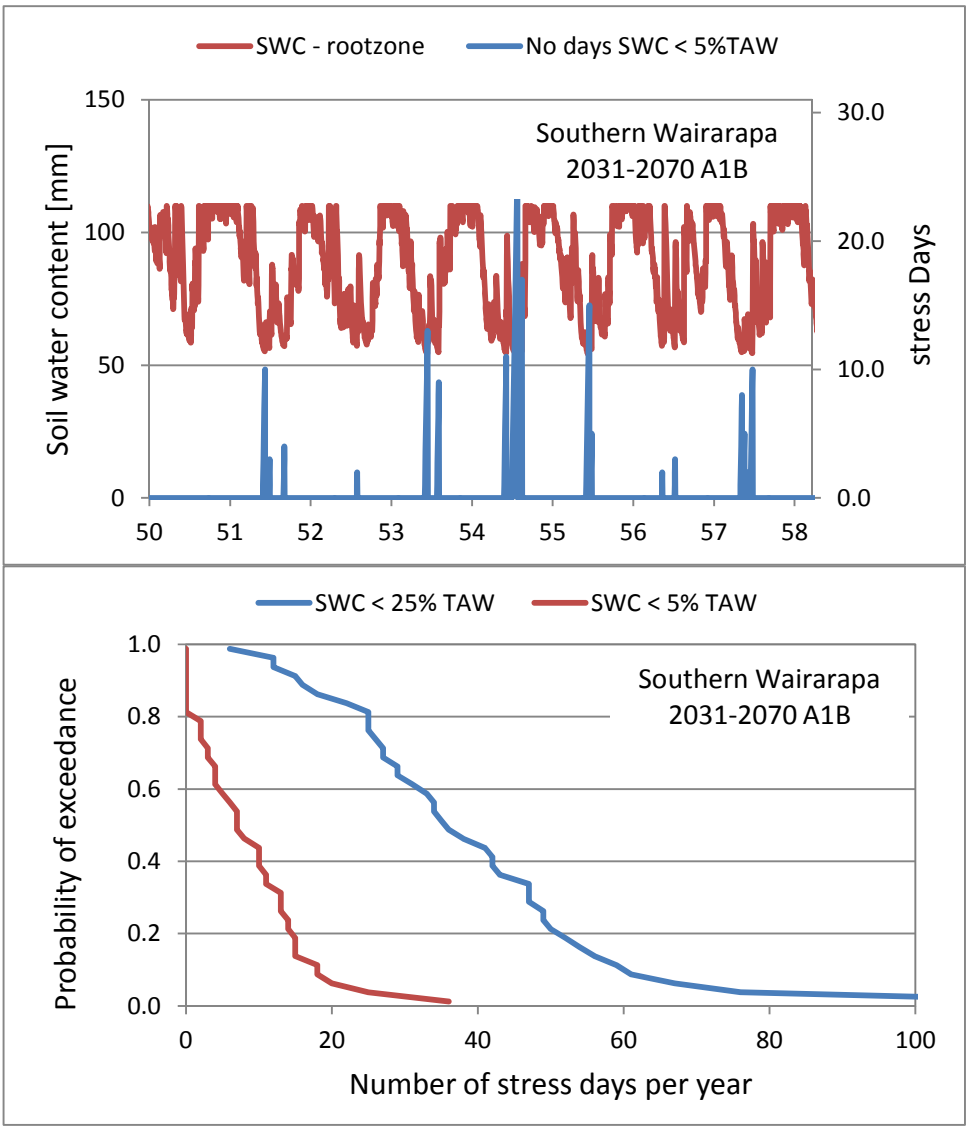

Figure 1.7.3. Model outputs used to assess the survivability of planted poplar poles growing under a future climate scenario (2031–2070 A1B) in the Southern Wairarapa. The top panel shows a time series of soil water content (SWC) in the top 40 cm of the root-zone soil, and the cumulative number of high-stress days where SWC < 5% of total available water (TAW). The bottom panel shows the probabilities of exceedance associated with cumulative of high stress days (SWC<5%TAW) and mild-stress days (SWC < 25%TAW) that occur during each growing season.

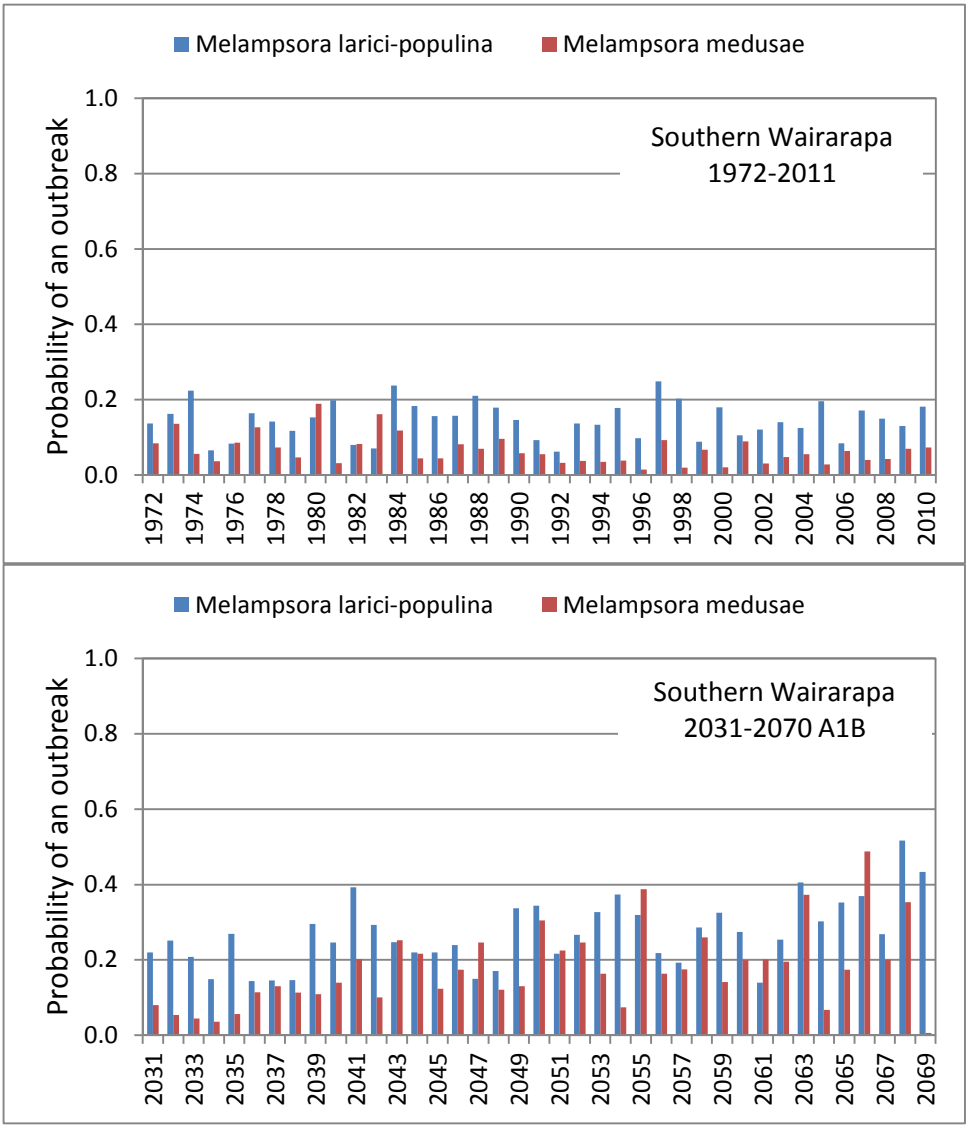

Figure 1.7.4. Model outputs used to assess the risk of occurrence of an outbreak of *Melampsora* rust on poplar trees growing in the Southern Wairarapa under the current (1972–2010) and future (2031–2070 A1B) climate change scenarios.

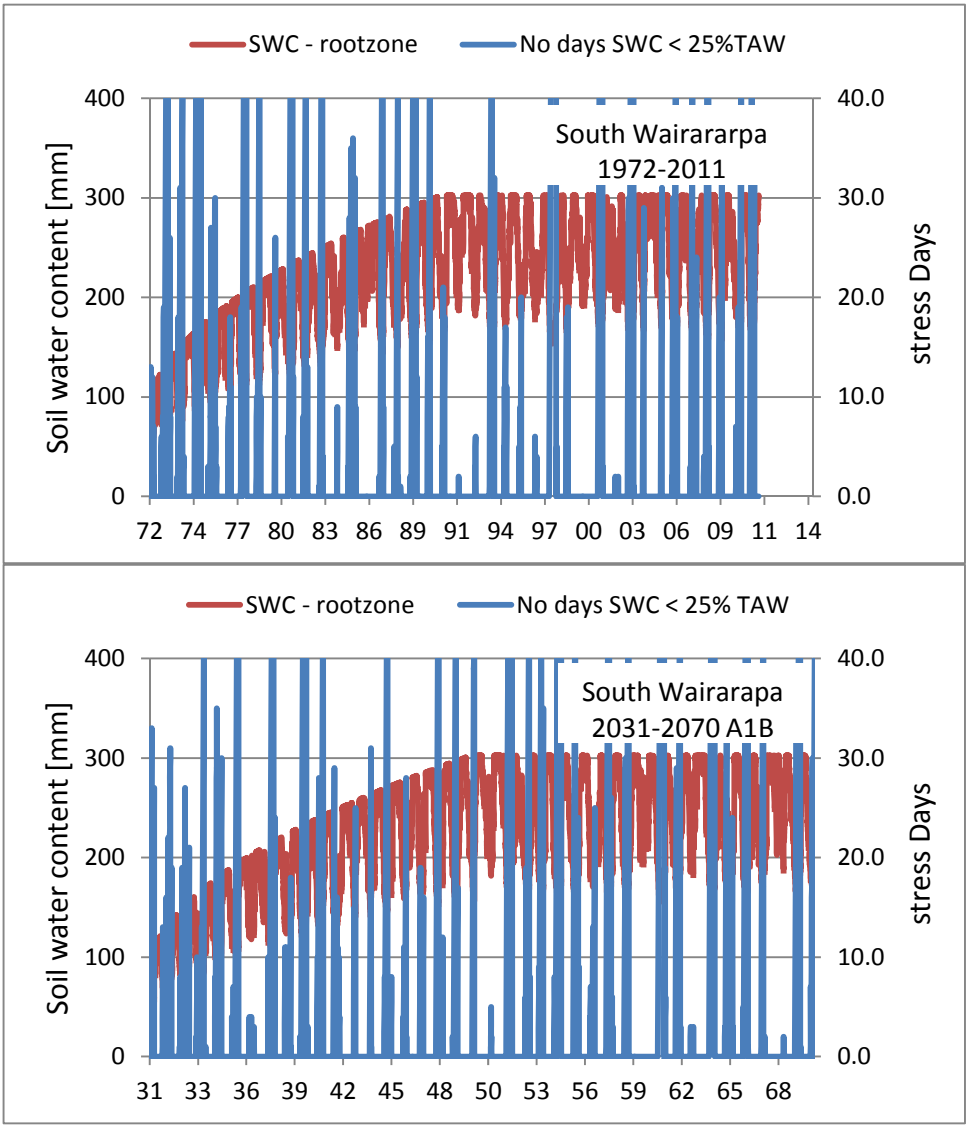

Figure 1.7.5. Model outputs for poplar trees growing under current (1972–2013) and future (2030–2070 A1B) climate change scenarios in the Southern Wairarapa. These results depict the changing pattern of soil water content in the root zone (red line) and the corresponding cumulative number of mild-stress days (SWC < 25%TAW) that occur during each growing season.

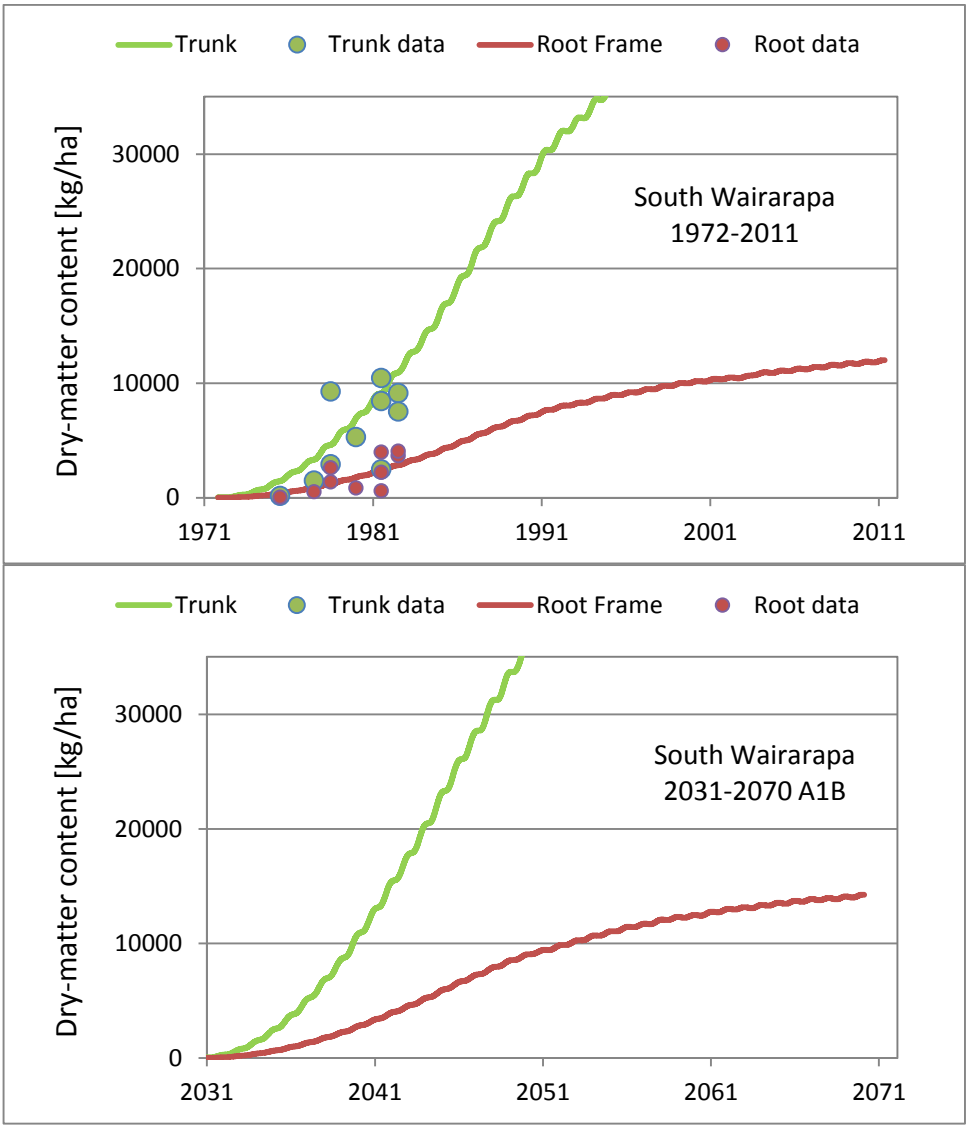

Figure 1.7.6. Model outputs for the dry-matter accumulation (i.e. growth) of poplar trees growing under current (1972–2013) and future (2030–2070 A1B) climate change scenarios in the Southern Wairarapa. Data are from field trials near Woodville.

Table 1.7.1. A statistical analysis of model outputs used to assess survivability and disease risk of poplar poles growing in the Southern Wairarapa under current (1972–2011) and future (2031–2070 A1B) climate change scenarios. Here we have assumed a fixed root-zone depth of 0.40 m.

Southern Wairarrapa (1972–2011)	statistic	no. moderate stress days	no. critical stress days	Disease risk *M. larici-populina*	Disease risk *M. medusae*
	mean	38	9	0.15	0.07
	stdev	24	10	0.05	0.04
	PE20	58	17	0.19	0.10
	Prob (NSD>7)	0.91	0.46	-	-
Southern Wairarapa (2031–2070 A1B)	**statistic**	**no. moderate stress days**	**no. critical stress days**	**Disease risk *M. larici-populina***	**Disease risk *M. medusae***
	mean	39	9	0.27	0.18
	stdev	21	8	0.09	0.10
	PE20	56	15	0.34	0.26
	Prob (NSD>7)	0.99	0.49	-	-

Table 1.7.2. A statistical analysis of model outputs used to assess survivability and disease risk of poplar trees growing in the Southern Wairarapa under current (1972–2011) and future (2031–2070 A1B) climate change scenarios. Trees have been 'grown' from poles planted at the start of the simulation period.

South Wairarapa (1972–2011)	statistic	no. moderate stress days	no. critical stress days	Disease risk *M. larici-populina*	Disease risk *M. medusae*
	mean	47	4	0.20	0.07
	stdev	37	9	0.07	0.04
	PE20	78	11	0.26	0.10
	Prob (NSD>7)	0.86	0.22	-	-
South Wairarapa (2031–2070) A1B	**statistic**	**no. moderate stress days**	**no. critical stress days**	**Disease risk *M. larici-populina***	**Disease risk *M. medusae***
	mean	47	3	0.35	0.18
	stdev	31	5	0.12	0.10
	PE20	73	7	0.45	0.26
	Prob (NSD>7)	0.88	0.19	-	-

Table 1.7.3. Model outputs for the dry-matter accumulation (i.e. growth) of poplar trees growing under current (1972–2013) and future (2030–2070 A1B) climate change scenarios in the Southern Wairarapa. $T_{50\%}$ and $T_{90\%}$ represent the amount of time (years) to reach 50% and 90% of the final value, respectively.

South Wairarapa (1972–2011)			South Wairarapa (2031–2070) A1B		
age	tree biomass [kg/ha]		age	tree biomass [kg/ha]	
	above ground	below ground		above ground	below ground
0	93	28	0	93	28
5	3048	842	5	3535	979
10	10502	2824	10	12690	3412
15	21406	5632	15	25911	6741
25	38800	9665	25	46651	11656
39	51353	12246	39	61170	14538
$T_{50\%}$	17	16	$T_{50\%}$	17	16
$T_{90\%}$	33	32	$T_{90\%}$	32	31

6.6.8 Model outputs: Horowhenua District

Table 1.8.1. A statistical analysis of model outputs used to assess survivability and disease risk of poplar poles growing in the Horowhenua District under current (1972–2011) and future (2031–2070 A1B) climate change scenarios. Here we have assumed a fixed root-zone depth of 0.40 m.

	statistic	no. moderate stress days	no. critical stress days	Disease risk *M. larici-populina*	Disease risk *M. medusae*
Horowhenua District (1972–2011)	mean	13	1	0.11	0.11
	stdev	15	3	0.04	0.06
	PE20	25	4	0.14	0.16
	Prob (NSD>7)	0.64	0.06	-	-
Horowhenua District (1972–2011)	statistic	no. moderate stress days	no. critical stress days	Disease risk *M. larici-populina*	Disease risk *M. medusae*
	mean	20	3	0.21	0.32
	stdev	15	5	0.08	0.17
	PE20	32	7	0.28	0.46
	Prob (NSD>14)	0.61	0.06	na	na

Table 1.8.2. Statistical analysis of model outputs used to assess survivability and disease risk of poplar trees growing in the Horowhenua District under current (1972–2011) and future (2031–2070 A1B) climate scenarios. Trees have been 'grown' from poles planted at the start of the simulation period.

	statistic	no. moderate stress days	no. critical stress days	Disease risk *M. larici-populina*	Disease risk *M. medusae*
Horowhenua District (1972–2011)	mean	9	1	0.13	0.11
	stdev	16	2	0.05	0.06
	PE20	22	2	0.17	0.16
	Prob (NSD>7)	0.37	0.06	-	-
Horowhenua District (2031–2070) A1B	statistic	no. moderate stress days	no. critical stress days	Disease risk *M. larici-populina*	Disease risk *M. medusae*
	mean	17	1	0.25	0.32
	stdev	21	3	0.10	0.17
	PE20	34	3	0.33	0.46
	Prob (NSD>7)	0.78	0.01	-	-

Table 1.8.3. Model outputs for the dry-matter accumulation (i.e. growth) of poplar trees growing under current (1972–2013) and future (2030–2070 A1B) climate change scenarios in the Horowhenua District. $T_{50\%}$ and $T_{90\%}$ represent the amount of time (years) to reach 50% and 90% of the final value, respectively.

Horowhenua District (1972–2011)			Horowhenua District (2031–2070) A1B		
age	tree biomass [kg/ha]		age	tree biomass [kg/ha]	
	above ground	below ground		above ground	below ground
0	93	28	0	93	28
5	3227	892	5	3396	937
10	10667	2852	10	12070	3218
15	20915	5463	15	24443	6289
25	36325	9010	25	44295	10974
39	48494	11474	39	57753	13666
$T_{50\%}$	17	16	$T_{50\%}$	17	16
$T_{90\%}$	33	31	$T_{90\%}$	32	30

6.6.9 Model Outputs: Tasman District

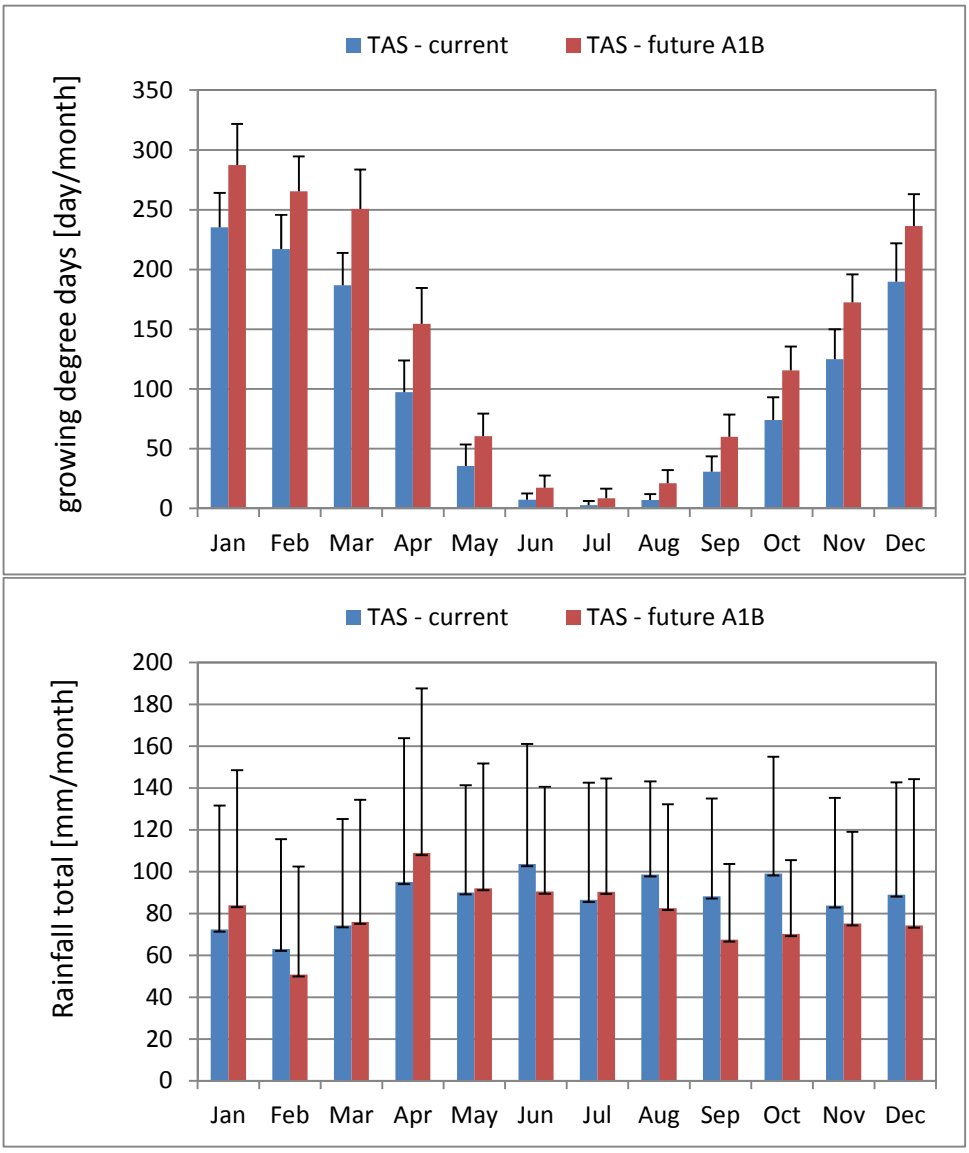

Figure 1.9.1. Summary of seasonal climate data for the Tasman District (TAS) as represented by the number growing-degree days (base 10ºC) and monthly rainfall under current (1972–2013) and future (2031–2070 A1B) climate change simulations.

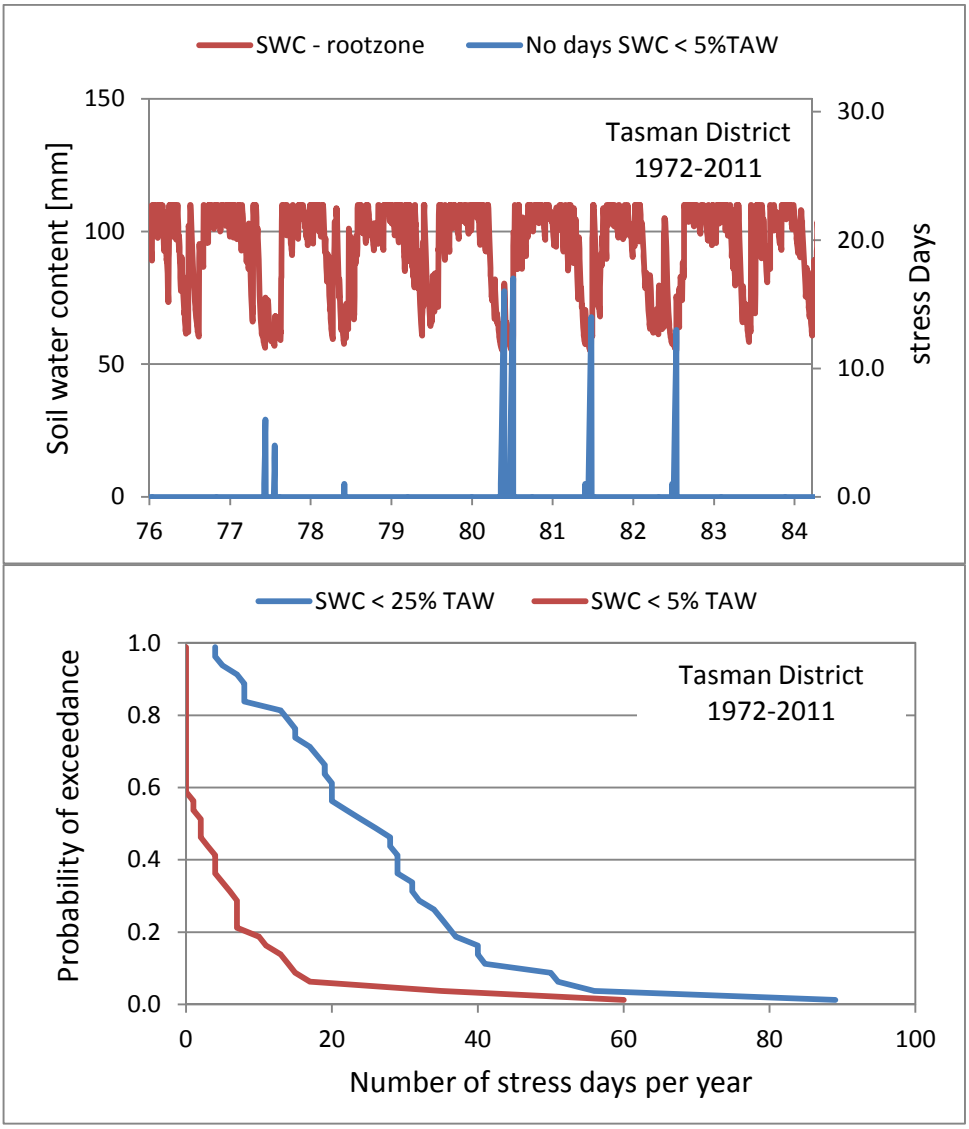

Figure 1.9.2. Model outputs used to assess the survivability of planted poplar poles growing under a current climate scenario (1972–2013) in the Tasman District. The top panel shows a time series of soil water content (SWC) in the top 40 cm of the root-zone soil, and the cumulative number of high-stress days where SWC < 5% of total available water (TAW). The bottom panel shows the probabilities of exceedance associated with cumulative of high stress days (SWC<5%TAW) and mild-stress days (SWC < 25%TAW) that occur during each growing season.

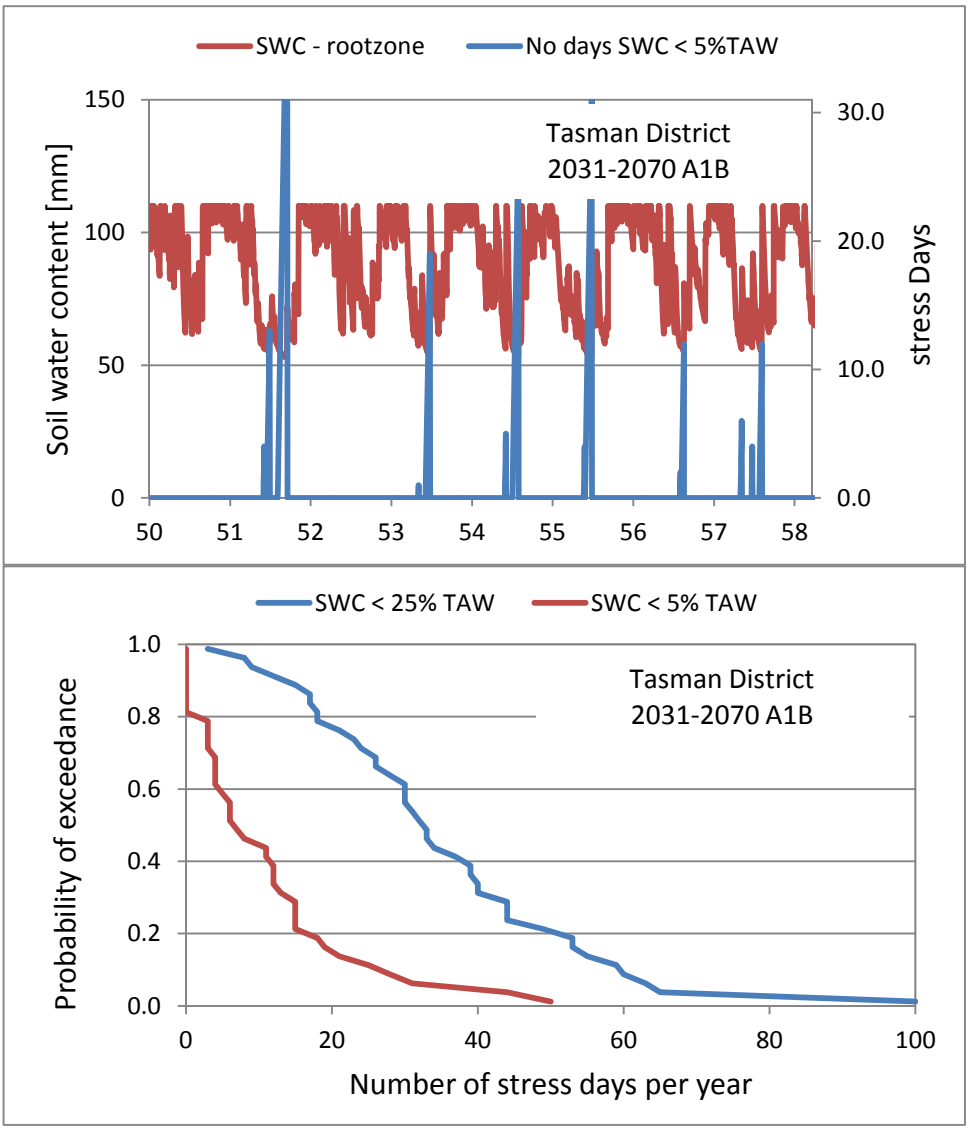

Figure 1.9.3. Model outputs used to assess the survivability of planted poplar poles growing under a future climate scenario (2031–2070 A1B) in the Tasman District. The top panel shows a time series of soil water content (SWC) in the top 40 cm of the root-zone soil, and the cumulative number of high-stress days where SWC < 5% of total available water (TAW). The bottom panel shows the probabilities of exceedance associated with cumulative of high stress days (SWC<5%TAW) and mild-stress days (SWC < 25%TAW) that occur during each growing season.

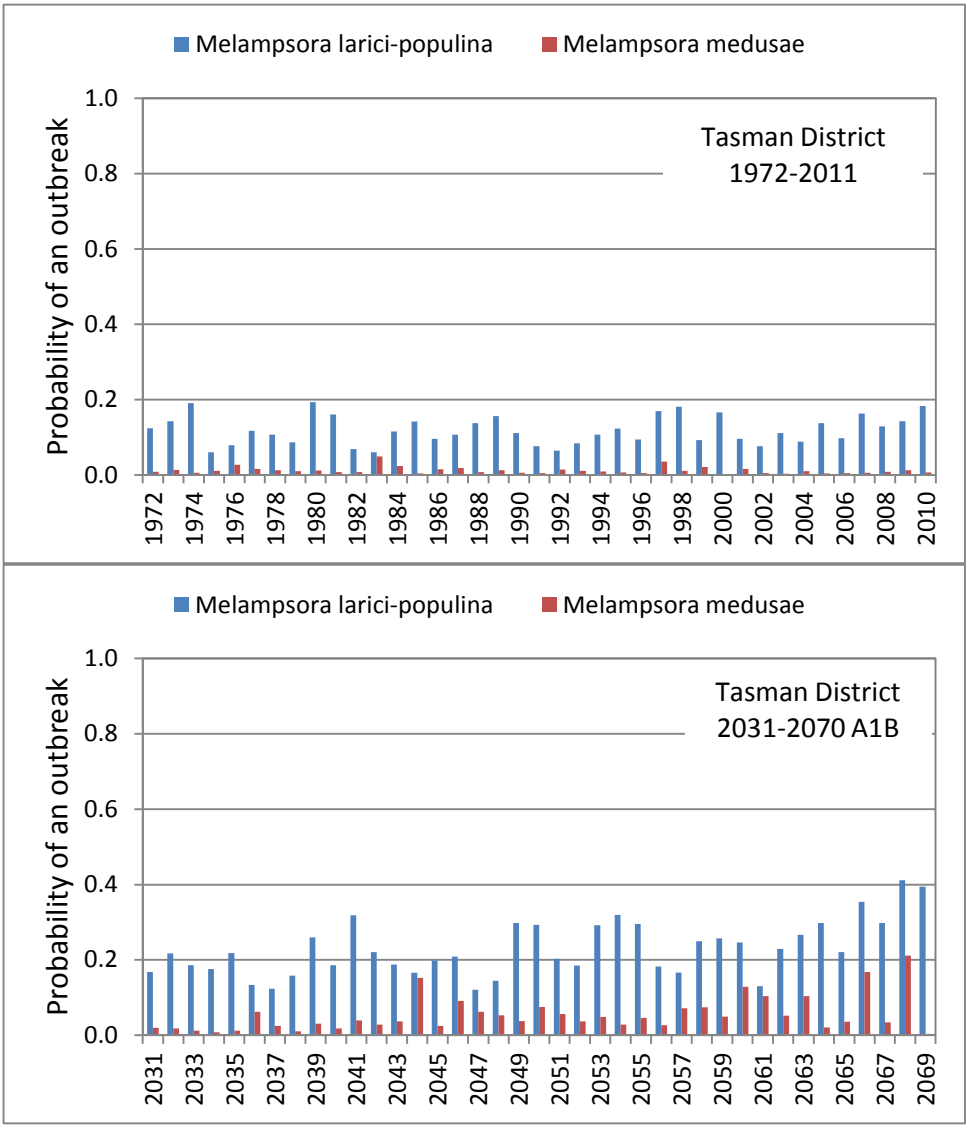

Figure 1.9.4. Model outputs used to assess the risk of occurrence of an outbreak of *Melampsora* rust on poplar trees growing in the Tasman District under the current (1972–2010) and future (2031–2070 A1B) climate change scenarios.

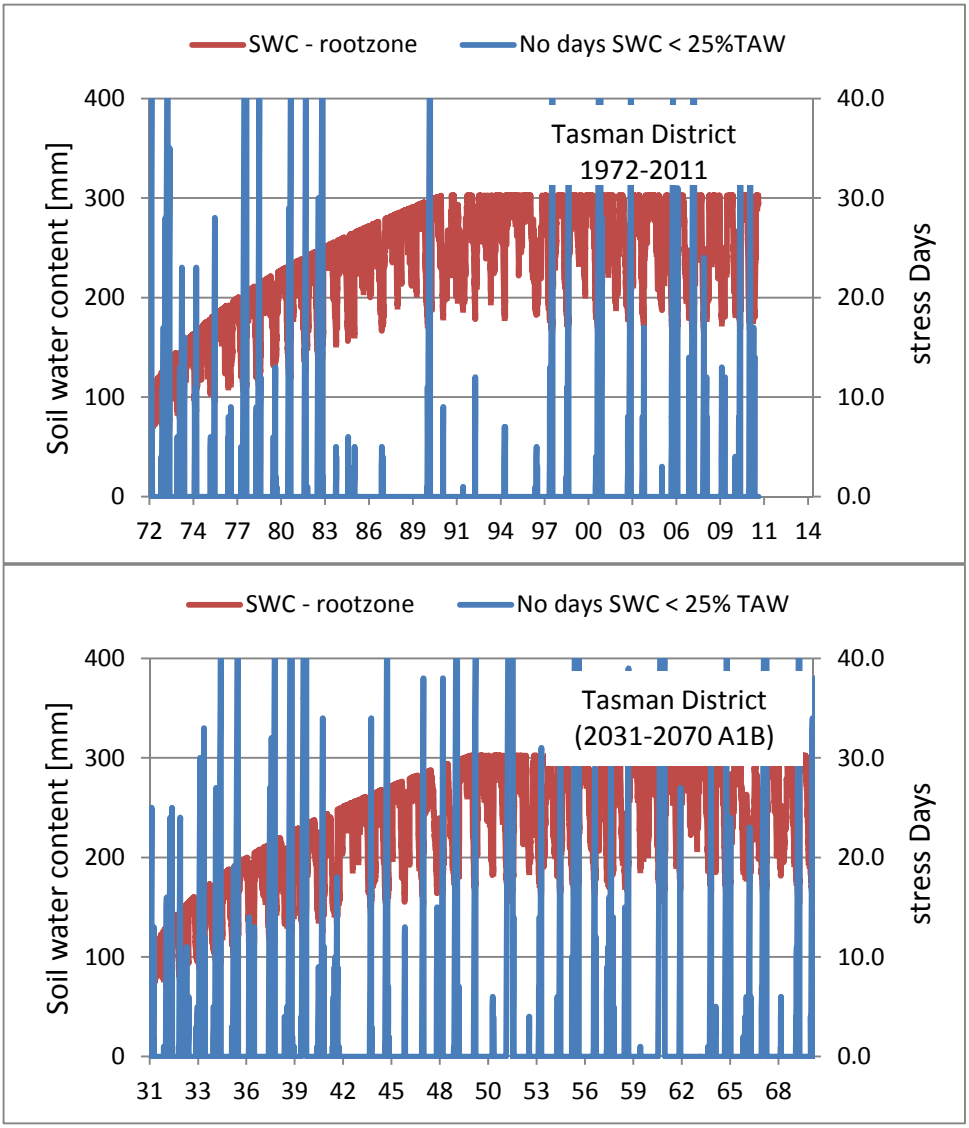

Figure 1.9.5. Model outputs for poplar trees growing under current (1972–2013) and future (2030–2070 A1B) climate change scenarios in the Tasman District. These results depict the changing pattern of soil water content in the root zone (red line) and the corresponding cumulative number of mild-stress days (SWC < 25%TAW) that occur during each growing season.

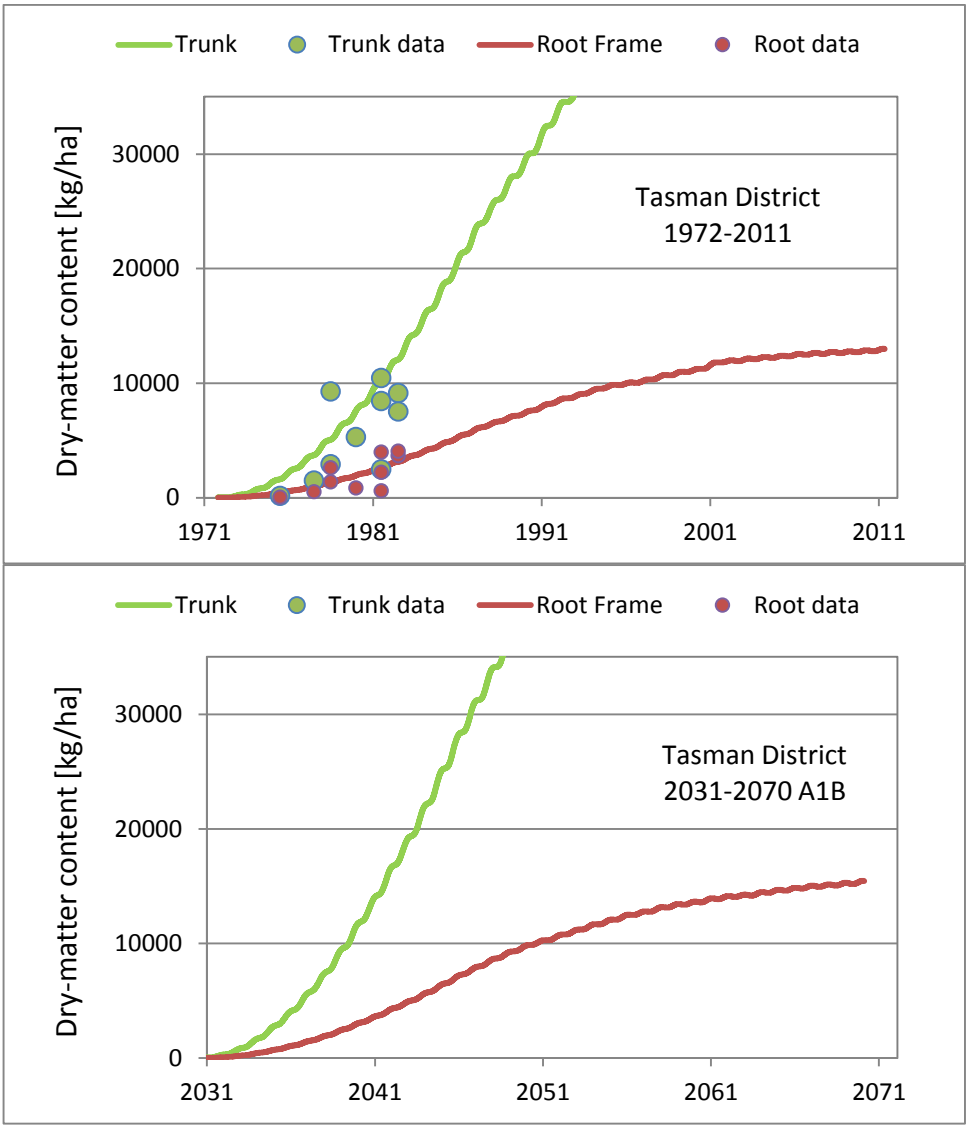

Figure 1.9.6. Model outputs for the dry-matter accumulation (i.e. growth) of poplar trees growing under current (1972–2013) and future (2030–2070 A1B) climate change scenarios in the Tasman District. Data are from field trials near Woodville.

Table 1.9.1. A statistical analysis of model outputs used to assess survivability and disease risk of poplar poles growing in the Tasman District under current (1972–2011) and future (2031–2070 A1B) climate change scenarios. Here we have assumed a fixed root-zone depth of 0.40 m.

	statistic	no. moderate stress days	no. critical stress days	Disease risk *M. larici-populina*	Disease risk *M. medusae*
Tasman District (1972–2011)	mean	26	6	0.12	0.01
	stdev	17	11	0.04	0.01
	PE20	40	15	0.15	0.02
	Prob (NSD>7)	0.91	0.21	-	-
	statistic	no. moderate stress days	no. critical stress days	Disease risk *M. larici-populina*	Disease risk *M. medusae*
Tasman District (2031–2070 A1B)	mean	35	11	0.23	0.05
	stdev	19	12	0.07	0.05
	PE20	51	20	0.29	0.09
	Prob (NSD>7)	0.99	0.49	-	-

Table 1.9.2. A statistical analysis of model outputs used to assess survivability and disease risk of poplar trees growing in the Tasman District under current (1972–2011) and future (2031–2070 A1B) climate change scenarios. Trees have been 'grown' from poles planted at the start of the simulation period.

	statistic	no. moderate stress days	no. critical stress days	Disease risk *M. larici-populina*	Disease risk *M. medusae*
Tasman District (1972–2011)	mean	25	2	0.15	0.01
	stdev	25	7	0.06	0.01
	PE20	46	8	0.20	0.02
	Prob (NSD>7)	0.65	0.09	na	na
	statistic	no. moderate stress days	no. critical stress days	Disease risk *M. larici-populina*	Disease risk *M. medusae*
Tasman District (2031–2070) A1B	mean	42	3	0.29	0.05
	stdev	35	7	0.10	0.05
	PE20	71	9	0.38	0.09
	Prob (NSD>7)	0.86	0.14	-	-

Table 1.9.3. Model outputs for the dry-matter accumulation (i.e. growth) of poplar trees growing under current (1972–2013) and future (2030–2070 A1B) climate change scenarios in the Tasman District. $T_{50\%}$ and $T_{90\%}$ represent the amount of time (years) to reach 50% and 90% of the final value, respectively.

Tasman District (1972–2011)			Tasman District (2031–2070) A1B		
age	tree biomass [kg/ha]		age	tree biomass [kg/ha]	
	above ground	below ground		above ground	below ground
0	93	28	0	93	28
5	3407	941	5	3884	1074
10	11625	3114	10	13779	3690
15	23726	6182	15	28442	7331
25	42268	10522	25	50828	12732
39	55977	13258	39	66450	15772
$T_{50\%}$	17	16	$T_{50\%}$	17	16
$T_{90\%}$	31	29	$T_{90\%}$	32	31

6.6.10 Model outputs: Marlborough

Table 1.10.1. A statistical analysis of model outputs used to assess survivability and disease risk of poplar poles growing in the Marlborough District under current (1972–2011) and future (2031–2070 A1B) climate change scenarios. Here we have assumed a fixed root-zone depth of 0.40 m.

Marlborough District (1972–2011)	statistic	no. moderate stress days	no. critical stress days	Disease risk *M. larici-populina*	Disease risk *M. medusae*
	mean	42	14	0.14	0.01
	stdev	26	14	0.05	0.01
	PE20	63	25	0.18	0.02
	Prob (NSD>7)	0.99	0.54	-	-
Marlborough District (2031–2070 A1B)	**statistic**	**no. moderate stress days**	**no. critical stress days**	**Disease risk *M. larici-populina***	**Disease risk *M. medusae***
	mean	43	17	0.24	0.08
	stdev	20	14	0.07	0.07
	PE20	60	29	0.30	0.13
	Prob (NSD>7)	0.96	0.76	-	-

Table 1.10.2. A statistical analysis of model outputs used to assess survivability and disease risk of poplar trees growing in the Marlborough District under current (1972–2011) and future (2031–2070 A1B) climate scenarios. Trees have been 'grown' from poles planted at the start of the simulation period.

Marlborough District (1972–2011)	statistic	no. moderate stress days	no. critical stress days	Disease risk *M. larici-populina*	Disease risk *M. medusae*
	mean	56	8	0.20	0.01
	stdev	40	16	0.07	0.01
	PE20	89	21	0.26	0.02
	Prob (NSD>7)	0.99	0.29	-	-
Marlborough District (2031–2070) A1B	**statistic**	**no. moderate stress days**	**no. critical stress days**	**Disease risk *M. larici-populina***	**Disease risk *M. medusae***
	mean	61	8	0.32	0.08
	stdev	39	12	0.10	0.07
	PE20	94	18	0.41	0.13
	Prob (NSD>7)	0.78	0.01	na	na

Table 1.10.3. Model outputs for the dry-matter accumulation (i.e. growth) of poplar trees growing under current (1972-2013) and future (2030-2070 A1B) climate change scenarios in the Marlborough District. $T_{50\%}$ and $T_{90\%}$ represent the amount of time (years) to reach 50% and 90% of the final value, respectively.

Marlborough District	(1972–2011)		Marlborough District	(2031–2070) A1B	
age	tree biomass [kg/ha]		age	tree biomass [kg/ha]	
	above ground	below ground		above ground	below ground
0	93	28	0	93	28
5	3237	896	5	3729	1032
10	11044	2968	10	13130	3530
15	22432	5895	15	26733	6966
25	41376	10313	25	48372	12134
39	53621	12722	39	63178	15050
$T_{50\%}$	17	16	$T_{50\%}$	17	16
$T_{90\%}$	32	31	$T_{90\%}$	32	31

6.6.11 Model Outputs: Canterbury district

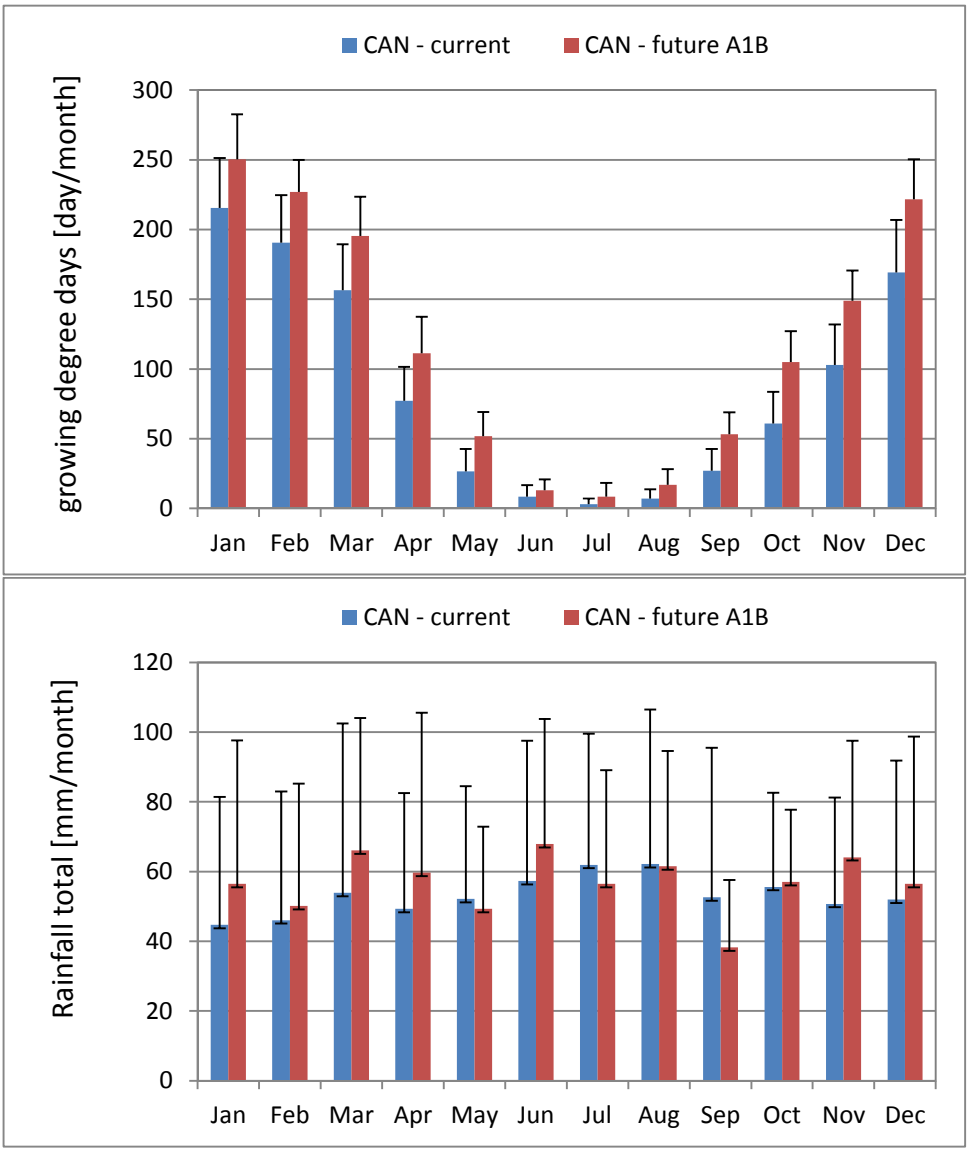

Figure 1.11.1. Summary of seasonal climate data for the Canterbury Region (CAN) as represented by the number growing-degree days (base 10ºC) and monthly rainfall under current (1972–2013) and future (2031–2070 A1B) climate change simulations.

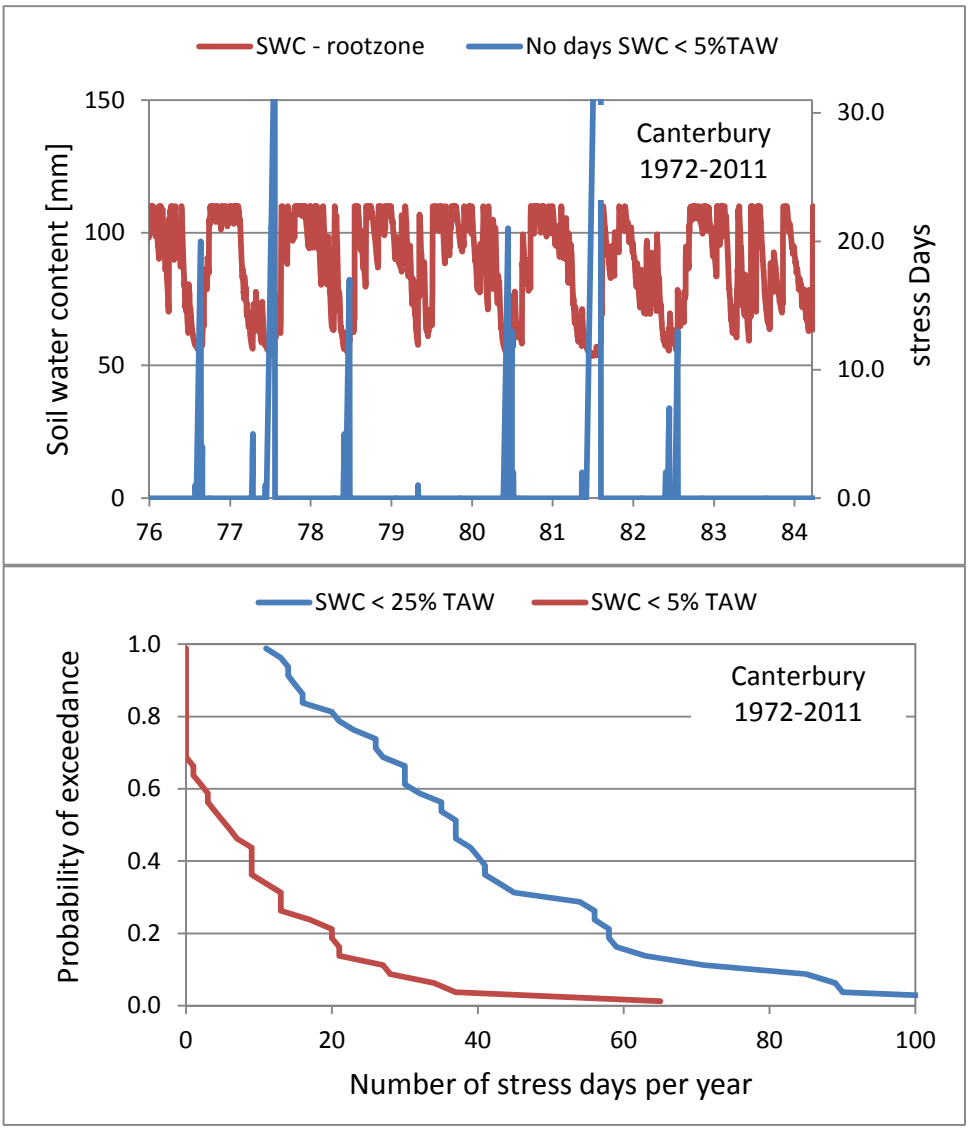

Figure 1.11.2. Model outputs used to assess the survivability of planted poplar poles growing under a current climate scenario (1972–2013) in the Canterbury Region. The top panel shows a time series of soil water content (SWC) in the top 40 cm of the root-zone soil, and the cumulative number of high-stress days where SWC < 5% of total available water (TAW). The bottom panel shows the probabilities of exceedance associated with cumulative of high stress days (SWC<5%TAW) and mild-stress days (SWC < 25%TAW) that occur during each growing season.

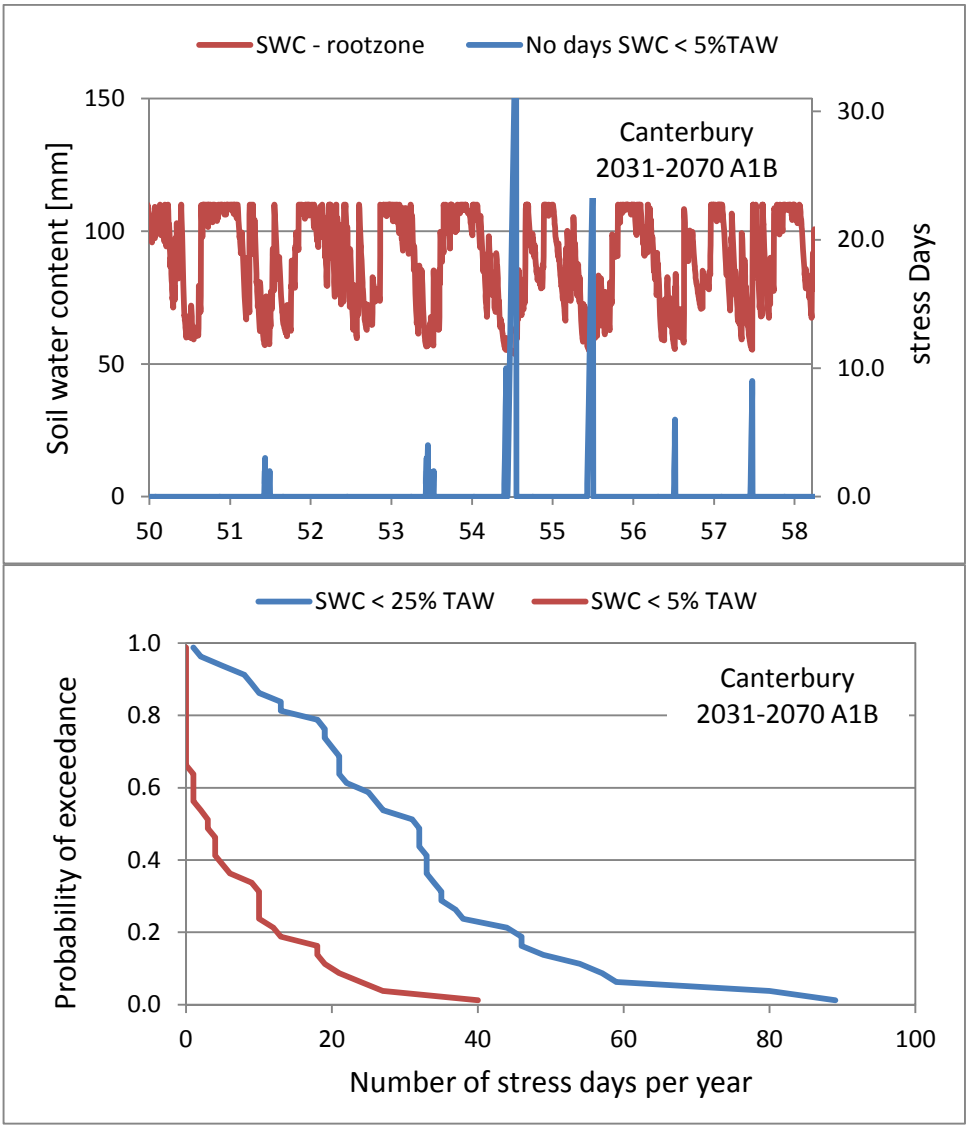

Figure 1.11.3. Model outputs used to assess the survivability of planted poplar poles growing under a future climate scenario (2031–2070 A1B) in the Canterbury Region. The top panel shows a time series of soil water content (SWC) in the top 40 cm of the root-zone soil, and the cumulative number of high-stress days where SWC < 5% of total available water (TAW). The bottom panel shows the probabilities of exceedance associated with cumulative of high stress days (SWC<5%TAW) and mild-stress days (SWC < 25%TAW) that occur during each growing season.

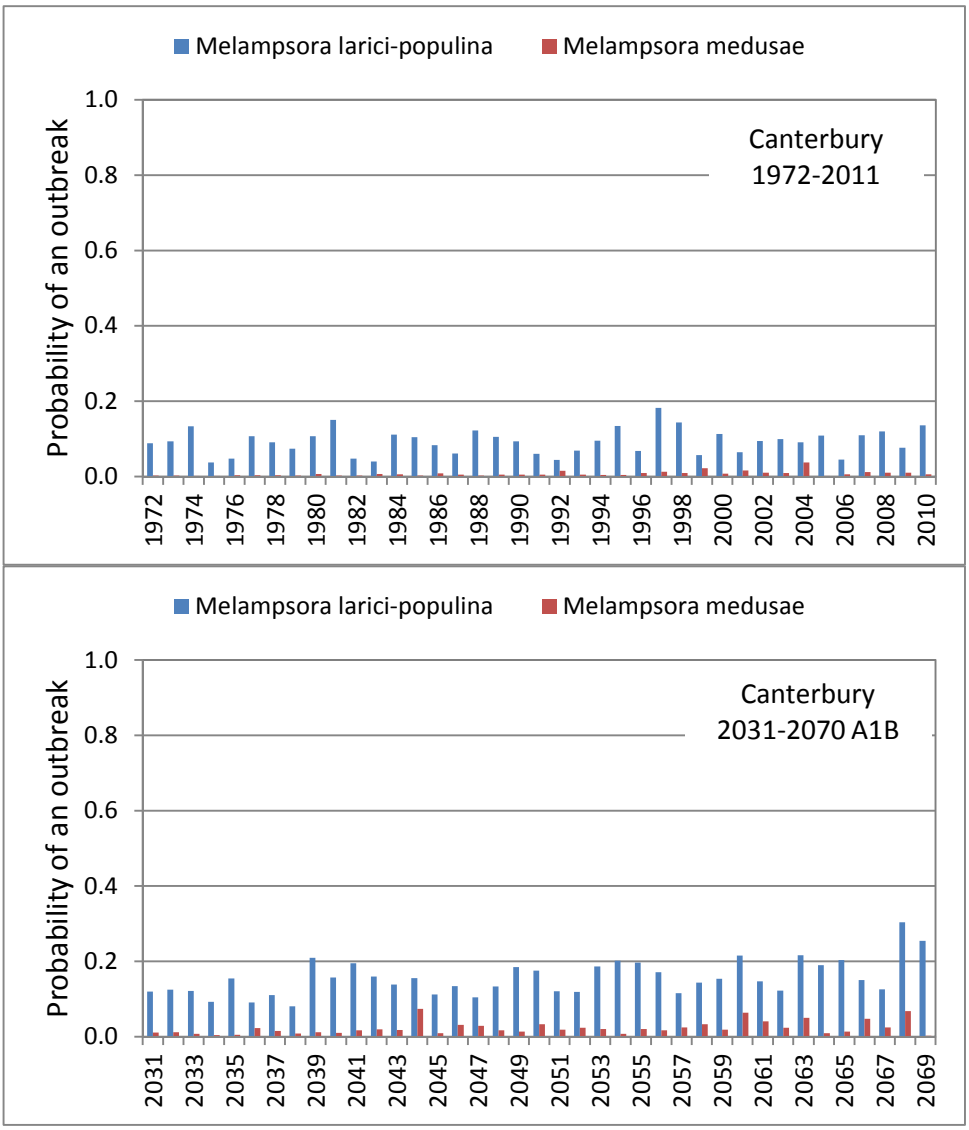

Figure 1.11.4. Model outputs used to assess the risk of occurrence of an outbreak of *Melampsora* rust on poplar trees growing in the Canterbury Region under the current (1972–2010) and future (2031–2070 A1B) climate change scenarios.

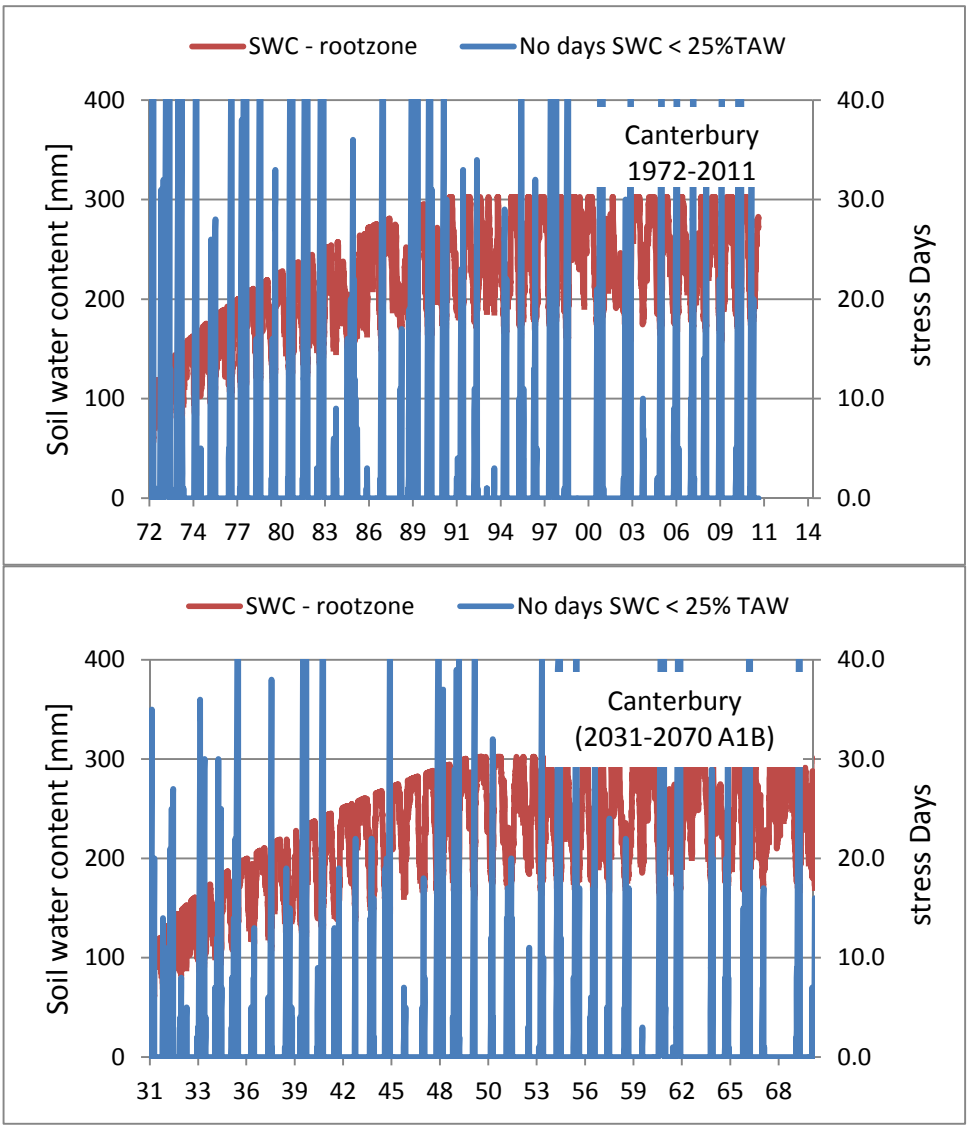

Figure 1.11.5. Model outputs for poplar trees growing under current (1972–2013) and future (2030–2070 A1B) climate change scenarios in the Canterbury Region. These results depict the changing pattern of soil water content in the root zone (red line) and the corresponding cumulative number of mild-stress days (SWC < 25%TAW) that occur during each growing season.

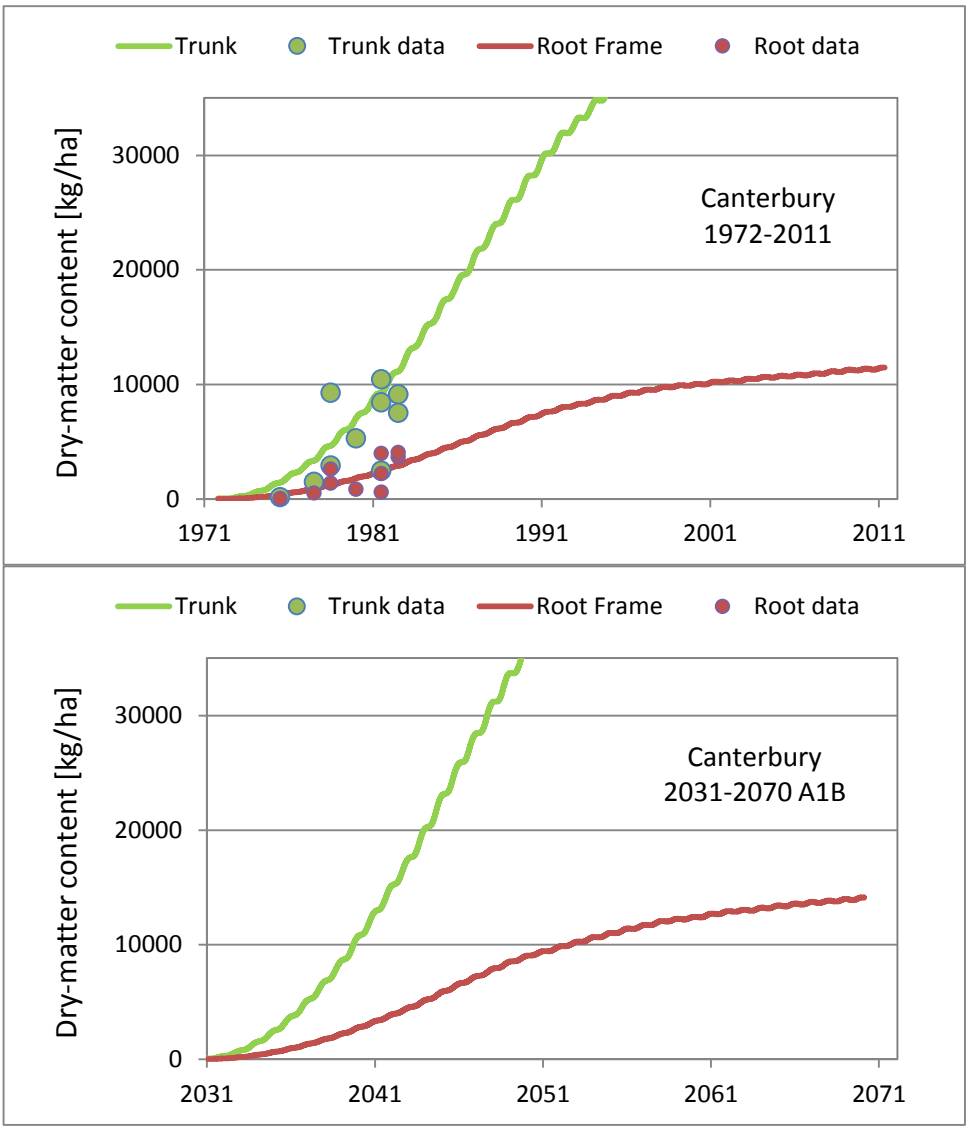

Figure 1.11.6. Model outputs for the dry-matter accumulation (i.e. growth) of poplar trees growing under current (1972–2013) and future (2030–2070 A1B) climate change scenarios in the Canterbury Region. Data are from field trials near Woodville.

Table 1.11.1. A statistical analysis of model outputs used to assess survivability and disease risk of poplar poles growing in the Canterbury Region under current (1972–2011) and future (2031–2070 A1B) climate change scenarios. Here we have assumed a fixed root-zone depth of 0.40 m.

	statistic	no. moderate stress days	no. critical stress days	Disease risk *M. larici-populina*	Disease risk *M. medusae*
Canterbury (1972–2011)	mean	41	10	0.09	0.01
	stdev	24	14	0.03	0.01
	PE20	61	21	0.12	0.01
	Prob (NSD>7)	>0.99	0.46	-	-
	statistic	no. moderate stress days	no. critical stress days	Disease risk *M. larici-populina*	Disease risk *M. medusae*
Canterbury (2031–2070 A1B)	mean	31	7	0.16	0.02
	stdev	19	9	0.05	0.02
	PE20	46	14	0.20	0.04
	Prob (NSD>7)	0.94	0.36	-	-

Table 1.11.2. A statistical analysis of model outputs used to assess survivability and disease risk of poplar trees growing in the Canterbury Region under current (1972–2011) and future (2031–2070 A1B) climate change scenarios. Trees have been 'grown' from poles planted at the start of the simulation period.

	statistic	no. moderate stress days	no. critical stress days	Disease risk *M. larici-populina*	Disease risk *M. medusae*
Canterbury (1972–2011)	mean	55	6	0.13	0.01
	stdev	37	13	0.06	0.01
	PE20	85	17	0.18	0.01
	Prob (NSD>7)	0.91	0.24	-	-
	statistic	no. moderate stress days	no. critical stress days	Disease risk *M. larici-populina*	Disease risk *M. medusae*
Canterbury (2031–2070) A1B	mean	37	2	0.21	0.02
	stdev	27	5	0.07	0.02
	PE20	59	6	0.28	0.04
	Prob (NSD>7)	0.91	0.09	-	-

Table 1.11.3. Model outputs for the dry-matter accumulation (i.e. growth) of poplar trees growing under current (1972–2013) and future (2030–2070 A1B) climate change scenarios in the Canterbury Region. $T_{50\%}$ and $T_{90\%}$ represent the amount of time (years) to reach 50% and 90% of the final value, respectively.

Canterbury	(1972–2011)		Canterbury	(2031–2070) A1B	
age	tree biomass [kg/ha]		age	tree biomass [kg/ha]	
	above ground	below ground		above ground	below ground
0	93	28	0	93	28
5	3070	849	5	3522	977
10	10687	2878	10	12585	3383
15	21452	5635	15	25832	6702
25	38951	9735	25	46515	11618
39	49344	11717	39	61082	14417
$T_{50\%}$	17	16	$T_{50\%}$	17	16
$T_{90\%}$	32	30	$T_{90\%}$	32	31

6.6.12 Model outputs: Central Otago

Table 1.12.1. A statistical analysis of model outputs used to assess survivability and disease risk of poplar poles growing in Central Otago under current (1972–2011) and future (2031–2070 A1B) climate change scenarios. Here we have assumed a fixed root-zone depth of 0.40 m.

	statistic	no. moderate stress days	no. critical stress days	Disease risk *M. larici-populina*	Disease risk *M. medusae*
Central Otago (1972–2011)	mean	60	13	0.13	0.00
	stdev	27	12	0.05	0.00
	PE20	82	23	0.16	0.00
	Prob (NSD>7)	>0.99	0.64	-	-
	statistic	no. moderate stress days	no. critical stress days	Disease risk *M. larici-populina*	Disease risk *M. medusae*
Central Otago (2031–2070 A1B)	mean	60	19	0.23	0.00
	stdev	29	15	0.08	0.00
	PE20	84	32	0.29	0.00
	Prob (NSD>7)	>0.99	0.81	-	-

Table 1.12.2. A statistical analysis of model outputs used to assess survivability and disease risk of poplar trees growing in Central Otago under current (1972–2011) and future (2031–2070 A1B) climate change scenarios. Trees have been 'grown' from poles planted at the start of the simulation period.

	statistic	no. moderate stress days	no. critical stress days	Disease risk *M. larici-populina*	Disease risk *M. medusae*
Central Otago (1972–2011)	mean	120	7	0.19	0.00
	stdev	67	12	0.07	0.00
	PE20	176	17	0.25	0.00
	Prob (NSD>7)	>0.99	0.29	-	-
	statistic	no. moderate stress days	no. critical stress days	Disease risk *M. larici-populina*	Disease risk *M. medusae*
Central Otago (2031–2070) A1B	mean	96	12	0.32	0.00
	stdev	47	14	0.11	0.00
	PE20	136	23	0.41	0.00
	Prob (NSD>7)	>0.99	0.50	-	-

Table 1.12.3. Model outputs for the dry-matter accumulation (i.e. growth) of poplar trees growing under current (1972–2013) and future (2030–2070 A1B) climate change scenarios in Central Otago. $T_{50\%}$ and $T_{90\%}$ represent the amount of time (years) to reach 50% and 90% of the final value, respectively.

Otago Region (1972–2011)			Central Otago (2031–2070) A1B		
age	tree biomass [kg/ha]		age	tree biomass [kg/ha]	
	above ground	below ground		above ground	below ground
0	93	28	0	93	28
5	3009	834	5	3476	966
10	9897	2668	10	12357	3336
15	20209	5344	15	24724	6476
25	37755	9484	25	45053	11282
39	49169	11716	39	58551	13959
$T_{50\%}$	18	16	$T_{50\%}$	17	16
$T_{90\%}$	32	30	$T_{90\%}$	32	31

7 COMMUNICATIONS TO STAKEHOLDERS

These communications are condensed from full reports found earlier in this report and are intended to be read and distributed by land management officers, river engineers, trustees of the New Zealand Poplar & Willow Research Trust, staff from Beef & Lamb NZ, other stakeholders.

Key messages and recommendations are included in the communications.

SHORT COMMUNICATIONS TO STAKEHOLDERS

7.1 Status of poplar rust in New Zealand –national survey report 2014

Ian McIvor and Duncan Hedderley, Plant & Food Research. (ian.mcivor@plantandfood.co.nz)

Key messages

The most significant poplar diseases in New Zealand are caused by the poplar leaf rust *Melampsora larici-populina* and the leaf spot or anthracnose fungus *Marssonina brunnea*. Both of these leaf diseases thrive in our cool, moist environments and cause early defoliation, reduced root and stem growth, and dieback in susceptible cultivars. The poplar leaf rust *Melampsora medusa* is less significant nationally because of its limited range as determined from previous national rust surveys (Sivakumaran & McIvor 2010). Rust fungi have complex life cycles involving up to five different spore stages, and often require two unrelated host plants to complete their life cycle (Sivakumaran & McIvor 2010). The secondary host in New Zealand for *M. larici-populina* is larch (*Larix* sp.).

Incorporating resistance to leaf rusts is included as an objective in the national poplar and willow breeding programme carried out at Plant & Food Research. National monitoring is carried out as part of this breeding objective. Genetic diversity of *Melampsora* is recognised as contributing to a reduction in rust resistance in poplar clones (Borassa et al. 2007). For this reason it is important that a poplar breeding program is continually evaluating any changes in the rust resistance of its current stable of clones through field and nursery observations of the degree of *Melampsora* rust infection, while at the same time measuring the genetic diversity of *Melampsora* across its range.

Leaf samples bearing a variable rust load were collected from a range of infected poplar clones during March–April 2014 from the national rust indicator sites. Identification of the rust species was made microscopic study of urediniospores from 24 separate samples of infected poplar leaves. The urediniospores had a mean spore length of 27.0±1.8 mm and a mean spore diameter of 12.8±1.1 mm with an apex devoid of spines. All were identified as belonging to *Melampsora larici-populina*.

Urediniospore dimensions varied with poplar clones and location, but still fitted within published data for spore size in *Melampsora larici-populina.* There was no new evidence of hybridisation or species evolution based on the urediniospore appearance.

7.2 Climate change and growth of poplar and willow clones

Ian McIvor and Jonathan Crawford, Plant & Food Research. (ian.mcivor@plantandfood.co.nz)

Key messages

Future climate scenarios for New Zealand (http://www.niwa.co.nz/our-science/climate/information-and-resources/clivar/scenarios) depict a climate with elevated temperature (~2.5°C annual mean increase by 2090) and atmospheric CO_2 (550 ppm). In summer and autumn, the North Island and northwest of the South Island are predicted to show the greatest warming, whereas in winter the South Island will have the greatest warming. These scenarios further predict that eastern parts of New Zealand will experience more frequent and more intense droughts.

An experiment was carried out in a controlled environment to evaluate the growth response of selected willow and poplar clones to future climate change (550 ppm CO_2 and day/night temperature of 25.5°C/16.5°C) under normal and drought conditions. Since these environmental changes are predicted to rise together and are recognised as being interdependent, the experiment did not separate the effect of temperature from the effect of CO_2.

Willows and poplars increased above-ground biomass production in response to higher CO_2 and temperature when water was not limiting.

Drought reduced above-ground biomass production in willows and poplars but the reduction was possibly less severe, but not significantly, in an environment with higher CO_2 and temperature.

Drought significantly offsets enhanced CO_2 and temperature in its effect on willow and poplar growth. Of all the parameters measured the root biomass was the least affected by the imposition of drought conditions, and the net reduction in root growth in response to drought was less severe under the enhanced conditions than under the normal conditions.

The combined effect of increased atmospheric CO_2 and increased mean day/night temperature is expected to result in an increase in biomass production. Under future climate change responses are likely to vary between clones in both poplar and willow and the interim period should be used to evaluate the relative responses to drought stress in the range of commercial poplar and willow clones being currently used or in the developmental stage.

A full report is given in Plant & Food Research Report No. 9387 Confidential report for Ministry for Primary Industries January 2014.

7.3 Response to water stress and drought tolerance of novel poplars

Trevor Jones, Ian McIvor, Plant & Food Research, Michael McManus, Massey University. (trevor.jones@plantandfood.co.nz)

Key messages

The soil water deficits that occur in drought conditions are a major factor limiting the survival and growth of poplar trees for soil conservation in New Zealand. Poplars are among the fastest growing trees under temperate latitudes, but their high productivity is associated with a dependency on water availability. There is wide variability in the water-use efficiency and drought tolerance of poplar species and hybrids, and potential for the selection of poplar clones with improved adaptability to drought conditions.

The physiological response of four experimental hybrid poplar clones and the 'Veronese' poplar clone to soil water deficits was evaluated in a greenhouse pot trial, with well-watered, moderate and severe (90, 60 and 40% of field capacity) soil water deficit treatments. The biomass growth and water-use efficiency of the poplar trees, leaf stomatal conductance and water potential, and leaf chlorophyll content and antioxidant enzyme activity were measured to determine the drought tolerance of the poplar clones.

Poplar clones	Female parent	Male parent
'Veronese'	*Populus deltoides*	*P. nigra*
MT103 - 07-05-103	*P. maximowiczii* 87-007-04	*P. trichocarpa*
MT304 - 07-02-304	*P. maximowiczii* 87-007-01	*P. trichocarpa*
TN008 - 07-03-008	*P. trichocarpa*	*P. nigra* PN866 PG22
TN014 - 07-06-014	*P. trichocarpa*	*P. nigra* PN874 Blanc de Garonne

The four experimental hybrid poplar clones were not as drought-tolerant as the 'Veronese' poplar clone, showing a less conservative response to the soil water deficits, and lower antioxidant enzyme activity in the leaves, but they had the advantage of better biomass growth and water-use efficiency under drought conditions.

The 'Veronese' clone appears well adapted for drought-prone areas, where the survival of the trees during periods of severe soil water deficits is a constraint. In contrast, the new hybrid poplar clones appear better adapted to moderately drought-prone areas, where there is an advantage in combining high productivity and high water-use efficiency to better utilise the available water during the growing season.

These findings need to be complemented by information on performance aspects, particularly survival, gathered from field trials of the clones in regions with high current and future drought risk. National field trials of these novel clones are currently underway in different climatic zones.

A full report can be found in Plant & Food Research Report No. 10154 sent to Regional Councils in June 2014.

7.4 Response to water stress and drought tolerance of novel willows

Trevor Jones, Ian McIvor, Plant & Food Research, Michael McManus, Massey University. (trevor.jones@plantandfood.co.nz)

Key messages

Drought conditions and extreme rainfall events are likely to increase in both frequency and severity in New Zealand, in response to a warming climate during the 21st century. Large areas of the eastern lowlands are likely to have less soil moisture, while more frequent and intense storms could lead to erosion becoming a bigger problem on pastoral hill country. Willow trees are widely used for soil conservation in New Zealand, and are effective in reducing the occurrence of shallow landslides during rain events, and maintaining the productive capacity of pastoral hill country farms. Currently, willow clones of *Salix matsudana* and *S. matsudana* x *S. alba* are used, but a wider range of hybrid willow clones have been bred at Plant & Food Research to broaden the genetic base of willow clones available for planting.

The physiological responses to soil water deficits of four new experimental hybrid willow clones of *Salix matsudana*, *S. lasiandra*, and *S. pentandra*, and the *S. matsudana* x *S. alba* 'Tangoio' willow clone that is widely used for soil conservation in New Zealand, were evaluated in a greenhouse pot trial, with well-watered, moderate and severe (90, 60 and 40% of field capacity) soil water deficit treatments. The biomass growth and water-use efficiency of the willow trees, and leaf stomatal conductance, water potential, and photosynthesis were measured to determine the drought tolerance of the willow clones.

Willow clones	Female parent	Male parent
'Tangoio'	*Salix matsudana* PN 227 'Kew'	*S. alba* I4/59
ML089 - 07-01-089	*S. matsudana* PN 227 'Kew'	*S. lasiandra* 000/0-15
ML022 - 03-004-022	*S. matsudana* PN 227 'Kew'	*S. lasiandra* 113/1-13
MP002 - 03-012-002	*S. matsudana* PN 227 'Kew'	*S. pentandra* PN 670 'Dark French'
LP026 - 03-001-026	*S. lasiandra*	*S. pentandra* PN 670 'Dark French'

The four new experimental hybrid willow clones were not as drought tolerant as the 'Tangoio' willow clone, but the two willow clones of *S. matsudana* x *S. lasiandra* were able to achieve biomass growth that was similar to the 'Tangoio' willow clone under moderate and severe soil water deficits. The drought tolerance varied among the willow clones, and was associated with higher water-use efficiency, lower stomata conductance, and the ability to minimise leaf senescence at the onset of drought conditions.

The *'Tangoio' and S. matsudana x S. lasiandra* clones, and the slower growing *S. lasiandra x S. pentandra* clone, appeared to be adapted for drought-prone locations, but the fast-growing *S. matsudana x S. pentandra* clone was less tolerant of drought and better suited for higher rainfall and well-watered locations.

A full report can be found in Plant & Food Research Report No. 11676 sent to Regional Councils in June 2015.

7.5 Modelling survival, growth and disease risk of poplars under current and future climate

Steve Green and Ian McIvor, Plant & Food Research. (ian.mcivor@plantandfood.co.nz)

Key messages

Future climate as predicted by A1B scenario climate change is expected to deliver greater drought length and severity in eastern regions of New Zealand, higher rainfall in western regions, a small rise in temperature, and greater uncertainty around significant weather events the frequency of which is predicted to increase across all regions. Severe rainstorms generate serious soil erosion in pastoral hill country in all regions of the country, generating large costs for landowners, local authorities and society in general. Soil erosion reduces primary productivity and impacts adversely on water quality and management of waterways.

The growth model based on SPASMO (Soil Plant Atmosphere Model) utilised long-term weather and poplar growth data to model current survivability and disease risk of poplar poles, survivability and disease risk of poplar trees, and risk of occurrence of an outbreak of *Melampsora* rust on poplar trees. We then applied future predicted climate data to predict how survivability, growth and disease risk will change under A1B climate scenario in each of 12 regions/districts of New Zealand. Regions not included in the model outputs had insufficient or unsuitable long term weather data, and the predictions for those regions should approximate that in other regions with similar predicted climate. For example, we consider that information presented for Tasman and Horowhenua districts represents the likely scenario for Taranaki, parts of southern Waikato and western districts in Horizons region.

Survivability and establishment of poplar poles is predicted to decrease in regions with increased susceptibility to prolonged drought, and remain unchanged in western regions where summer rainfall is predicted to increase.

While all regions are likely to experience drought periods, these will be more severe in the eastern regions and poplar poles (and all trees) will become increasingly harder to establish in the first 1–3 years. This makes it imperative to increase effort to plant erosion-prone pastoral hill country with urgency if the detrimental effects of climate change are to be mitigated.

Growth of established trees is predicted to change little from present rates.

Disease risk from poplar fungal rusts is predicted to rise in all regions. Poplar clones bred in future should be selected for rust resistance and options for drought tolerance need to be part of the clonal mix available to landowners.

DISCOVER. INNOVATE. GROW.